The photochemistry of $M(CO)_6$ and (η^6-pyridine)$Cr(CO)_3$ (M = Cr, Mo, or W) and related systems.

This thesis is presented to Dublin City University

for the degree, Doctor of Philosophy, by

Ciara Breheny BSc

Supervisor Dr Conor Long

School of Chemical Sciences,

Dublin City University

1996

Declaration

This thesis has not been submitted as an exercise for a degree at this or at any other university. Except as otherwise stated, this work has been carried out by the author alone.

Signed CIARA Breheny

Ciara Breheny.

Dedication

This thesis is dedicated to my family, Mum, Dad, Conor, and Saibh

Acknowledgements

I would like to say a most sincere thank you to all the following people, Dr Conor Long, for his constant support, help, and advice over the past few years All members past and present of the CLRG, namely Irene, Mick, Maureen, Celia, Mary, Siobhan, and Deirdre Everyone in AG07 who made the past few years enjoyable and unforgettable All members of the chemistry department, especially the technicians, who were always at hand to help when a problem arose (as it invariably did)

A word of thanks to my friends outside DCU without whom the past few years would not have been the same, namely, Marie, Ger, Siobhan, Orla, Greg, Ciaran, Shivaun, Ciara, Teresa, Monica, Susan, Bronagh, Anna, Dawn, and Fiona Also a special thanks to Paul for his support over the past year

Finally, to my family for their never-ending patience with the seemingly endless student life I have undertaken Without their love and support these past few years would have been a lot more difficult

A special thanks to anyone else I have forgotten

Abstract

The reaction of $M(CO)_5$(solvent) with CO has been investigated in a range of alkane solvents, where M = Cr, Mo, or W The kinetic and activation parameters have been determined for Reaction 1

$$M(CO)_5(S) + CO \rightarrow M(CO)_6 \qquad \textit{Reaction 1}$$

For chromium hexacarbonyl the $\Delta H^{\neq}$ is constant (22 ± 2 kJ mol^{-1}), the rate of Reaction 1 increases with the lengthening as the alkane chain, this is reflected in the $\Delta S^{\neq}$ term, which becomes less negative as the alkane chain length increases For the larger metals the variation in the kinetic and activation parameters is less significant The kinetic and activation parameters indicate that solvent displacement by CO involves an interchange mechanism for the $Cr(CO)_6$ system, while for the $Mo(CO)_6$ and $W(CO)_6$ systems the mechanism is more associative in character

The photochemistry of $(\eta^6\text{-}2,6\text{-}X_2C_5H_3N)Cr(CO)_3$ was investigated both in low-temperature matrices (X = H, $(CH_3)_3Si$) and in room temperature solution (X = H, CH_3, or $(CH_3)_3Si$) Room temperature photolysis ($\lambda_{exc} > 410$ nm) of $(\eta^6$-pyridine$)Cr(CO)_3$ in CO saturated methanol yielded $(\eta^1$-pyridine$)Cr(CO)_5$ which subsequently formed $Cr(CO)_6$ in a secondary photochemical process The efficiency of this reaction is reduced in cyclohexane, or when X = CH_3 rather than X = H Photolysis in low temperature matrices resulted in an η^6 to η^1 haptotropic rearrangement of pyridine (λ_{exc} = 460 nm, X = H) Visible irradiation in a CO-doped methane matrix produced $(\eta^1$-pyridine$)Cr(CO)_5$ while in N_2 matrix *fac*-$(\eta^1$-pyridine$)(N_2)_2Cr(CO)_3$ is formed Irradiation with λ_{exc} =

308 nm produced both the ring-slip product and also the CO-loss product (η^6-pyridine)$Cr(CO)_2$ Time resolved infrared spectroscopy in cyclohexane revealed only the CO-loss product (λ_{exc} = 308 nm, X = H) The apparent difference in room-temperature and low-temperature photochemistry is explained by the rapid regeneration of the parent species from the η^1-intermediate This explanation is supported by the laser flash photolysis experiments (λ_{exc} = 355 nm) in CO-saturated cyclohexane (S), where the recovery of the (η^6-pyridine)$Cr(CO)_3$ absorption follows a biphasic time profile, whereby the faster process was assigned to the η^1 to η^6 rearrangement and the slower to the reaction of (η^6-pyridine)$Cr(CO)_2$(S) with CO When the matrix photochemistry was investigated in a CO-doped matrix, where X = $(CH_3)_3Si$, no pentacarbonyl or hexacarbonyl species were obtained Both the ring-slip and the CO-loss product were formed following irradiation with λ_{exc} = 308 nm, and both were sensitive to photoreversal with white light, which may explain the lack of photoproducts following long wavelength photolysis

Crystals of (η^6-2,6-$X_2C_5H_3N$)$Cr(CO)_3$ (X = H, CH_3, or $(CH_3)_3Si$) were characterised by X-Ray diffraction When X = H or CH_3 an eclipsed conformation is adopted, where the carbonyl ligands eclipse the carbon atoms When X = $(CH_3)_3Si$ the more common conformation where the carbonyl groups are in a staggered conformation and eclipse the ring bond centres is adopted In all the compounds the chromium atom is located directly below the arene ring, which is essentially planar

TABLE OF CONTENTS

INTRODUCTION: PAGE 1

CHAPTER 1: PAGE 25

CHAPTER 2: PAGE 72

CHAPTER 3: PAGE 141

CHAPTER 4: PAGE 162

INTRODUCTION

This introduction attempts to provide an overview of the relevant chemistry and techniques which are explored in this thesis It is not an extensive review of the relevant literature, this is provided at the beginning of the each chapter

(i) A brief history of organometallic chemistry

The history of organometallic chemistry can be described as one of unexpected discoveries The oldest compound in the history of organometallic chemistry was prepared and characterised by Zeise in 1827 [1] The compound was called Zeise's salt and was formulated as $PtCl_2(C_2H_4)KCl\,H_2O$ When it was first reported by Zeise his assignment was attacked by contemporary chemists and the compound was condemned as a fantasy [2]

In 1848 Bunsen correctly identified, the mixture of Me_2As-$As\,Me_2$ and $(Me_2As)_2O$, that had been prepared many years previously The following year Frankland synthesised the first alkylzinc compound These compounds were used extensively as alkylating agents, before being replaced by Grignard reagents (1900), which were easier to prepare and to handle

The period between 1870 and 1950 was dominated by the investigation of σ-bonded organometallic derivatives of non-transition metals These investigations concentrated on synthesis and the applications of these compounds as reagents in organic preparations During this period the chemistry of the metal carbonyls were also investigated Nickel and iron carbonyls were first to be discovered by Mond in 1890,[3]

who readily identified the industrial importance of metal carbonyl compounds Further investigations were carried out by Hieber after 1930

The turning point in organometallic chemistry, that led to the near exponential growth in the last 46 years can be attributed to the discovery of ferrocene in 1951 by, Kealy and Pauson,[4] Miller, Tebboth and Tremaine [5] Wilkinson and Fischer[6] proposed and confirmed the now familiar structure of ferrocene, depicted in Figure 1 The discovery and recognition of this new type of bond between the metal and organic unsaturated molecules prompted the enormous interest in these compounds

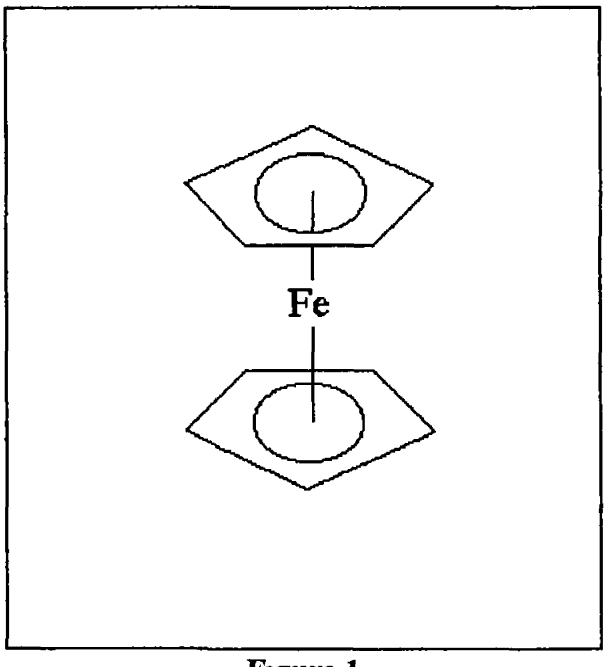

Figure 1

(Sandwich structure of ferrocene)

With the discovery of ferrocene, the classical period of organometallic chemistry drew to a close, and the modern era began This was facilitated by the

introduction of physical methods of investigation which afforded detailed information about the structure and bonding in organometallic compounds and made possible the understanding of their behaviour The development of the organometalhc chemistry of the non-transition elements contmued as well, but the modern period is dominated by the interest m transition metal derivatives

Only two years after the discovery of ferrocene, a revolutionary new process for converting ethylene into polyethylene by a catalyst composed of $TiCl_4$ and $AlEt_3$ was invented by Ziegler and his group at the Max-Planck Institute for Coal Research [7] This process was then passed on to Natta's group in Italy where its utility was quickly expanded to polymerise a variety of other monomers This is a good example of how basic research on organometallic compounds, which were regarded as curiosities at the time, suddenly produced a world-wide industrial process, thus justifying the interest that these compounds provoked

(ii) Definition of an organometallic compound

Organometallic compounds are organic compounds that contain at least one direct metal - carbon bond Accordingly, organometallic compounds can be classified as derivatives of main group elements (involving only *s*- and *p*-orbitals and electrons in bonding) and transition metal derivatives (involving *d*- and possibly *f*-orbitals) The most common type of bond for the main group elements is a σ-covalent bond, however the alkali and alkaline earths form mainly ionic compounds Electron deficient structures are

formed by elements like Li, Be, Mg, B and Al The transition metals generally form π-complexes involving dative bonds, but they can just as equally form normal σ-metal-carbon bonds

(iii) Organometallic bonds encountered in this study

Bonds between transition metal atoms and unsaturated organic molecules are formed by electron donation in two opposite directions, from the ligand to the metal (direct donation) and from the metal to the ligand (backbonding) In order to participate in this type of bonding, the metal should have a partially filled *d*-shell and should have a low oxidation state, preferably 0 ± 1 The unsaturated organic molecule must possess vacant orbitals of suitable symmetry to interact with the filled *d*-orbitals on the metal

(a) Carbon monoxide as a ligand

Compounds containing the carbonyl ligand (CO) are amongst the most widely and intensively investigated species in organometallic photochemistry Figure 2 depicts the bonding interactions of CO with transition metals Empty anti-bonding orbitals on the CO have suitable symmetry for bonding with transition metals The ligand has a lone pair of electrons that are located on the carbon atom and can be donated to the metal, forming a σ-bond interaction of the donor-acceptor nature The metal can then donate electron density from the occupied *d*-orbital to the vacant anti-bonding orbitals thus forming a π-bond Therefore the bond between the metal and ligand is actually a double

bond, resulting from the superposition of the σ interaction (ligand to metal) and the π-bond (metal to ligand) This back donation reduces the electron density at the metal centre and strengthens the metal to carbon bond The strengthening of this bond affects the carbon to oxygen bond, as the carbon monoxide has accepted electrons into its anti-bonding orbital Therefore this decrease in the bond order results in a decrease in bond strength This decrease in the bond order is reflected in the decrease in the frequency of the C-O absorption bands in the infrared spectrum Metal complexes exhibit shifts of hundreds of wavenumbers to lower energy for their ν(CO) bands compared to free CO, consistent with the weakening of the CO bond, ($Cr(CO)_6$ = ~2000 cm^{-1}, CO = 2149 cm^{-1})

The number of CO ligands that are bonded to a metal is generally dictated by the 18 electron rule This rule requires that the metals achieve an "effective atomic number" equal to that of the following noble gas Metals that possess an odd atomic order dimerize through metal to metal bond formation in order to satisfy this rule, or alternatively form compounds with other single electron donor ligands Relating this theory to a simple metal carbonyl compound demonstrates the rule clearly Chromium = [Ar] $4s^2 3d^4 4p^0$ (*i e* six valence electrons), therefore six CO ligands all donating two electrons are necessary to satisfy the rule

Cr	=	6 electrons
6CO	=	12 electrons
$Cr(CO)_6$	=	18 electrons

When one of these CO ligands is removed, employing UV photolysis for instance, the resulting moiety is a 16 electron intermediate, which is exceptionally reactive

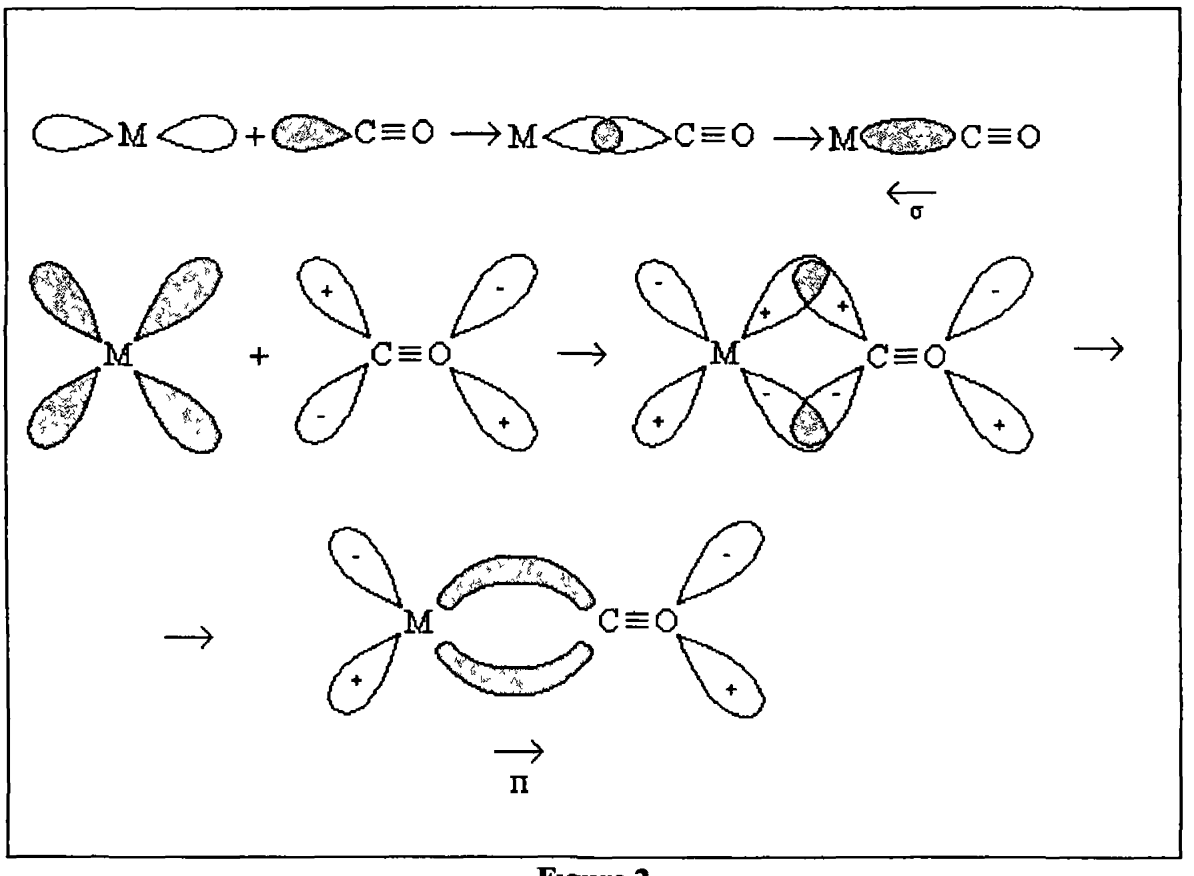

Figure 2

(Bonding interactions of CO with transition metals)

(b) Arene ligands

Arene ligands are extensively employed in organometallic chemistry and will form a significant part of this thesis, the normal type of bonding for this type of ligand is where the planar ligand lies above the metal, forming a perpendicular bond between the metal and the arene ring Taking benzene as an example of an arene ligand (benzene's π

orbitals are depicted in Figure 3), the following can describe the interaction between the metal and the arene ring If the *z* direction is assigned to the axis from the metal to the centre of the arene ligand, the d_z^2 orbital should have the correct symmetry to interact with the a_{2u} orbital However this interaction results in very little overlap as the d_z^2 orbital points at the hole in the benzene ring The next two degenerate orbitals e_{1ga} and e_{1gb} on the ligand donate electrons *via* a π interaction to the d_{xz} and d_{yz} and in this instance the

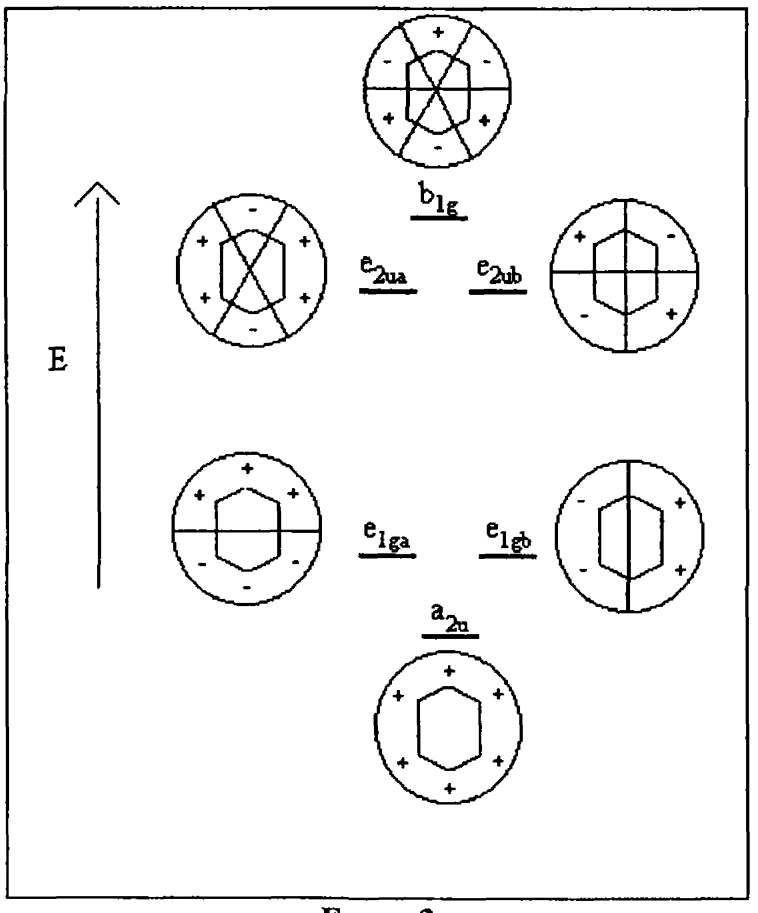

Figure 3

(Benzene π-molecular orbitals, the + and - signs designate the signs of the molecular orbitals above the plane of the paper)

spatial overlap is large The e_{2u} orbital set on the ligand does not have the correct symmetry to interact with any of the metal orbitals, except for a weak interaction with the d_{xy} and $d_{x^2-y^2}$ orbitals Figure 4 depicts an interaction diagram for the construction of the orbitals of $M(CO)_3$ and $M(C_6H_6)$ from the metal orbitals that are presented in the centre of the diagram [8]

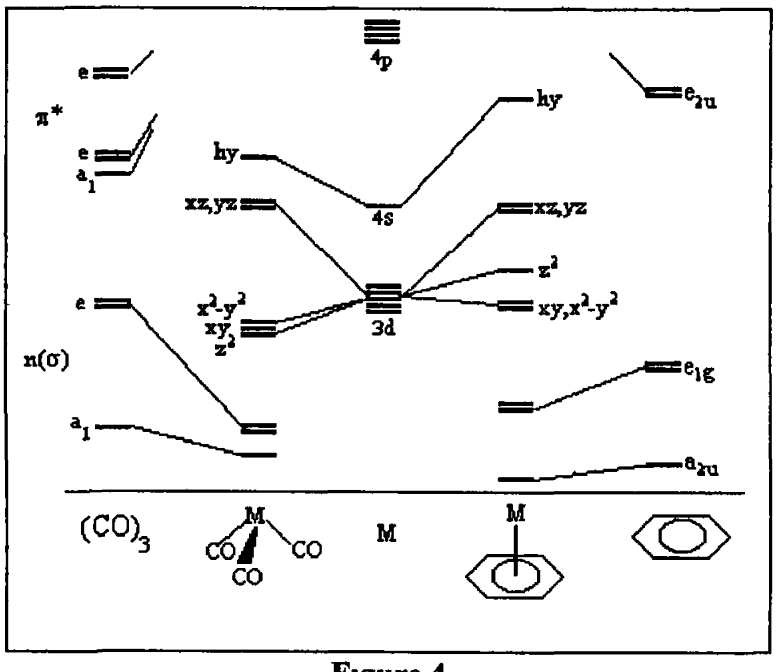

Figure 4

(An orbital interaction diagram for the formation of $M(CO)_3$ and $M(\eta^6$-benzene))

Thus, benzene and other ligands are good electron donors but poor electron acceptors The electronic properties can be altered by varying the nature of the arene substituents, or indeed as will be outlined in this thesis by varying the nature of the arene

(iv) Excited states encountered in this study

The photochemistry of organometallic compounds has been an area of intense interest over the past few decades [9] This is as a result of the discovery that the irradiation of organometallic compounds can lead to catalytically and synthetically useful transformations

Organometallic complexes can have a variety of low lying excited states, meaning states that can be populated by optical irradiation in the near-infrared, visible or ultraviolet region (*i e* 200-1100 nm) $M(CO)_6$ complexes (where M = Cr, Mo, or W) have ligand field (LF) transitions at ~333 nm This transition corresponds to electronic transitions between the "*d*-like" orbitals on the metal Such transitions are also known as "d-d" transitions, or "metal centred" transitions However, as organometallic compounds are highly covalent they actually have considerable ligand character, which can result in the relaxation of the selection rules for the transition, resulting in the high extinction coefficients observed for these transitions The transition is from a filled t_{2g} orbital of π symmetry, that is π bonding with respect to the M-CO bond, to the empty e_g orbital that is of σ symmetry and strongly σ anti-bonding with respect to the M-CO bond This transition results in substantial labilisation of the M-CO bond, which is as a result of both the depopulation of the π bonding levels and population of the σ anti-bonding orbital, the latter appearing to be the most consequential

The $M(CO)_6$ complexes also have metal to ligand charge transfer (MLCT) transitions, observed at ~286 nm This transition originates in a metal-centred orbital and

terminates in a ligand localised orbital In its most extreme case it can be viewed as oxidation of the metal and reduction of the ligand Therefore an easily oxidised metal centre and a ligand that has low lying acceptor orbitals should exhibit easily accessible MLCT transitions Organometallic compounds generally satisfy these requirements, and thus MLCT transitions are commonplace These transitions may make the M-L bond more photochemically inert, as a result of the population of a ligand localised orbital, that does not substantially influence the metal to ligand bond Such transitions may be valuable as the introduction of a similar ligand with a lower lying acceptor orbital, to a complex, will interfere with a LF transition, creating an inert complex with respect to photosubstitution or *vice-versa*, thus enabling the photochemical behaviour to be "tuned" for particular applications

(v) USES OF ORGANOMETALLIC COMPOUNDS

Transition metal complexes have been extensively used in industrial and laboratory processes to catalyse a variety of chemical reactions A catalyst acts by producing an alternative low energy pathway, which speeds up the reaction without losing its chemical identity Inhibitors, catalysts that reduce the rate of reaction are also of great practical importance (e g inhibitors of oxidation, anti-corrosion or anti-knocking additives) The catalyst must have carefully balanced bonding properties such that it has the ability to discriminate between the desired ligand and an alternative but nonreactive ligand Homogenous transition metal catalysts, consisting of discrete molecules in

solution, have the advantage that a great number of spectroscopic methods may be used in their investigation and thus detailed information about the nature of the catalytically active transition metal complexes may be obtained

A vacant coordination site is perhaps the single most important property of an homogeneous catalyst [10] Organometallic compounds generally have high quantum yields for the ejection of a ligand (e g 0 67 for the photochemical ejection of a CO ligand from $Cr(CO)_6$ in cyclohexane[11]), resulting in a coordinately unsaturated species, possessing the required vacant coordination site Vacant coordination sites are not only necessary to activate a substrate by bringing it into the coordination sphere, but coordinatively unsaturated complexes are especially active in oxidative addition and reductive elimination reactions The action of CO, phosphines and sulphur compounds as "poisons" in catalytic systems can be attributed to the tenacity with which these ligands bind to the vacant coordination sites on the metal Induction periods and the requirement of thermal or photochemical stimulation are usually indications that the active catalyst is formed by the expulsion of a ligand

Hydrogenation of 1,3 dienes has been known for a number of years to be catalysed by $Cr(CO)_6$ This reaction is photoassisted, and photoexpulsion of a CO ligand is essential High yields and selectivities are obtained from this process [12] It was also found that the chromium hexacarbonyl catalysed watergas shift reaction, was accelerated by UV irradiation [13] Organometalhc compounds can also act as thermal catalysts, e g η^6-(arene)$Cr(CO)_3$ thermally catalyses 1,3, dienes very selectively and in high yields,[14] however this catalyst requires both elevated temperatures and high H_2 pressure As most

of the catalysis involving (η^6-arene)$Cr(CO)_3$ and $Cr(CO)_6$ involves ligand loss, thus forming a sixteen electron intermediate, the structure and reactivity of such intermediates are of great interest

(vi) The nature of the interaction between solvents and metal centres

In Chapter 1 the interaction between $M(CO)_5$ species (where M = Cr, Mo or W) and the solvent environment will be discussed Saillard and Hoffmann[15] investigated the activation of the C-H bond upon coordination of the methane and hydrogen to a sixteen electron intermediate There are two possible orientations that the C-H could assume with respect to the metal Firstly it could bond in a perpendicular fashion where the C-H is collinear with the metal (1), and the second is where the C-H approaches the metal in such a manner that the metal to carbon, and metal to hydrogen distances are the same (2), as depicted in Figure 4 Mode 2 was found to be more energetically favourable for a H-H interaction with a metal centre The interaction with methane was investigated, but the results could also be applied to long chain alkanes It was found that mode 1 was the more favourable type of interaction for methane, as mode 2 resulted in an overlap between the filled metal d_{xz} and the occupied C-H σ orbital This repulsive effect dominated, causing the d_{xz} orbital to be raised in energy, thus diminishing the stabilisation that was observed for H-H interaction

Figure 4

(Possible modes of bonding for M-C-H interaction)

(vii) Techniques employed for studying organometallic transient species

In studying organometallic systems it is important to understand the structures of the intermediates formed during any reaction This information can lead to a greater understanding of the reactivities of certain systems and generates a clearer picture of pathways involved Conventional X-Ray diffraction techniques are not suitable for characterising transient species, therefore a variety of techniques are employed to elucidate the structures of these short lived intermediates

(a) Low temperature techniques

Matrix isolation is a useful tool for determining the structures of intermediates that would not be observed at room temperature The technique is based on the trapping of a parent species in a large excess of an inert solid (the matrix) and then irradiating it to generate unstable fragments These are then trapped in the cold matrix

and can then be studied at leisure The matrix is generally a solid gas or frozen hydrocarbons (e g noble gases or CH_4 at 10-30 K) A more recent advance in this area is to use cast polymer films, this technique and isolation in a frozen hydrocarbon have the advantage of a greater temperature range There are a great number of spectroscopic techniques that can then be employed to study the trapped intermediate, of these UV/vis and IR are the most common Matrix isolation with IR detection has been extremely successful in studying mononuclear metal carbonyl compounds mainly because of the very narrow IR absorptions with many structure-specific features that are characteristic of these compounds However this technique does have limitations, it is not easy to use with charged species, very little kinetic information is available as a result of the restricted temperature range and limited diffusion Also the matrix cage may prevent some reaction pathways by preventing the reactant species escaping, thus promotmg recombination processes The intermediates are studied in a low temperature rigid environment Direct comparison with the solution phase therefore is not possible However the results can be used to assist the interpretation of the solution behaviour

Low temperature solutions have also been employed to study metal carbonyl fragments The studies in liquefied noble gases have a particular advantage over other techniques because of the total lack of IR absorptions of these solvents, which when combined with Fourier transform infrared (FTIR) allows the weak bands of the coordinated ligands to be observed, as well as the more intense carbonyl bands The species is also being studied in a liquid environment, which makes it possible to obtain

kinetic data by varying the temperature This information can not be obtained from matrix experiments

(b) Flash photolysis of metal carbonyls

(1) UV/visible detection

Flash photolysis is a method for the initiation and study of the primary photochemical processes Light absorption occurs very rapidly (10^{-14}s) but the decay processes subsequent to this absorption cover a much wider range of times from picoseconds to seconds Conventional flash photolysis was developed by Norrish and Porter in the 1950's for which they received the Nobel prize in 1967 [16]

When a sudden flash of high-intensity light is absorbed by a reactant, a relatively high concentration of excited molecules or photoproducts are formed and can be observed by UV/vis absorption spectroscopy A complete absorption spectrum over the complete wavelength range can be recorded at one time Alternatively, a single selected wavelength can be monitored over time and thus the kinetics information can be obtained Time resolution of flash photolysis experiments is determined by the duration of the flash, which is usually a few microseconds in the case of plasma flash lamps but can be as short as picoseconds or even femtoseconds with pulsed lasers

Flash photolysis techniques involving UV/vis detection have several advantages

- generally metal carbonyl intermediates are easy to detect in solution,

- quantum yields for their formation are high and their UV/vis absorptions are intense,
- also the high sensitivity of this technique allows the study of very small concentrations of reactive intermediates,
- identification of intermediates can be facilitated if their spectra are characteristic and well resolved from the absorption of the parent,
- it is possible to undertake investigations in the picosecond and even the femtosecond time domain,
- it is also very useful that most solvents do not absorb in the visible to near UV region

However the technique does have a number of disadvantages, namely

- the sample must be optically clear to the monitoring light, therefore the presence of scattering particles must be avoided,
- if the reactive intermediates possess low molecular extinction coefficients, they may not be detected,
- analysis of complicated spectra may be difficult if the absorption bands overlap each other,
- it is also impossible to obtain any structural information from this technique,
- reaction rates can be fast, therefore good time resolution is also essential

This technique is effective in establishing the broad outlines of the photochemistry of a particular system Nasielski *et al*[17] pioneered flash photolysis coupled with UV/vis detection on metal carbonyl systems with their work on the photochemistry of $Cr(CO)_6$ A number of factors, such as moderate solubility in non-polar

solvents, large UV/vis extinction coefficients and high quantum yields for photochemical reactions (*vide supra)* contribute to the suitability of metal carbonyl complexes for flash photolysis with UV/vis detection

(2) Time Resolved IR Spectroscopy

It has long been recognised that vibrational spectra offer more structural information than the spectra in the UV-vis regions Unfortunately, largely because of detector response problems, fast time resolved infrared (TRIR) is in practise much more difficult technologically than the corresponding UV/vis experiments [18] With the development of solid-state detectors, and the fact that the ν(CO) bands of metal carbonyls are extremely intense, it has been possible to obtain TRIR data at room temperature for the $M(CO)_5$ species in cyclohexane [19] A conventional flashlamp was used as the photolysis source A globar, monochromator and fast IR detector were employed as a detection system Later systems employed lasers as the photolysis source and an IR laser as detector probe Detection in this technique is based on a "point by point" approach For each UV flash, kinetic measurements are made at one IR wavelength The monitoring wavelength is then changed and the photolysis source is triggered again Thus, using a number of flashes, data can be accumulated for wavelengths across the spectral region of interest These data can then be used to construct "point by point" spectra corresponding to any particular time delay after the flash Therefore the essential requirements for such measurements are a monochromatic IR beam, a pulsed UV light source and an IR detector Most spectrometers that are arranged to monitor organometallic compounds

only measure changes in IR absorptions Therefore the parent bands, that are being destroyed, appear as negative peaks, and the bands assigned to the photoproducts appear as positive absorptions Static IR bands, (e g solvent bands) do not appear in the spectra because their IR absorptions do not vary

The photochemistry of $[CpFe(CO)_2]_2$ ($Cp = \eta^5$-C_5H_5) provides an illustration of the use of TRIR techniques Flash photolysis with UV/vis detection had indicated that the compound dissociated *via* two pathways,[20] depicted in Reactions

$[CpFe(CO)_2]_2 \rightarrow Cp_2Fe_2(CO)_3$ (long lived) + CO	*Reaction 1*
$[CpFe(CO)_2]_2 \rightarrow 2CpFe(CO)_2$ (short lived)	*Reaction 2*

1 and 2 However, matrix isolation studies found $Cp_2Fe_2(CO)_3$ to be the sole product [21,22] Employing ^{13}CO isotopes, Rest *et al* [21] showed that this compound had the unusual structure $CpFe(\mu\text{-}CO)_3FeCp$, with three bridging carbonyl groups arranged symmetrically around the Fe-Fe bond This intermediate was unexpectedly stable Undoubtedly UV photolysis also generated the species observed in Reaction 2, but in the enclosed matrix "cage", this species readily recombined so as not to appear in the IR spectra, thus illustrating one limitation of the matrix technique Room temperature flash photolysis coupled with IR detection clearly showed that both of the species were present following UV photolysis [23] $CpFe(CO)_2$ was the first coordinatively unsaturated species to be identified by TRIR without previous matrix isolation data being available

Thus TRIR allows structural information to be obtained without the loss of kinetic data Even though it may not always provide a complete solution to every problem, when it is combined with other techniques it becomes a very powerful tool for elucidating the structures of organometallic intermediates

(c) Gas phase

Studies carried out in the gas phase have a number of advantages over the solution phase work Firstly it is possible to study truly "naked" coordinatively unsaturated species, as there is no environment with which to interact, unlike the interactions present between the solvent and the "naked" species in solution phase work In kinetic studies, reactions in solution will, in general, be displacement reactions rather than addition reactions Thus, these reactions may not probe the rate of reaction of the "naked" species Coordination of the solvent can also affect the structure of the species being observed since the coordinated solvent molecule can distort the structure of the "naked" coordinatively unsaturated species The insidious feature of this effect is that it is not clear how large an effect solvent coordination will have on the structure and it is difficult to be sure that any solvent is totally uncoordinating

Gas phase work may also result in a greater number of photolysis products from the absorption of a single photon As observed in the photolysis of $Cr(CO)_6$, where $Cr(CO)_5$ and $Cr(CO)_4$ were produced [24] Therefore more than one CO ligand may be ejected with one photon However, almost universally in the solution phase only one

ligand is ejected This difference is attributed to the relaxation of the internal vibration-rotation energy by collision with the solvent environment, dissipating the excess energy of the photon, preventing the ejection of a second ligand in solution Such a relaxation is not efficient in the gas phase, therefore the excess energy is available to eject a further ligand The kinetic parameters in the gas phase are usually one or two orders of magnitude faster than the corresponding diffusion controlled reactions in solution Consequently such studies require fast detection systems

(d) Time resolved photoacoustic calorimetry (PAC)

Pulsed, time-resolved photoacoustic calorimetry is a technique which has been used to determine the reaction enthalpy for photoinitiated reactions generating either stable products or transient intermediates Because PAC measures thermal relaxation processes, reaction pathways involving intermediates without easily-monitored chromophores can be detected In PAC the amplitude of an acoustic wave after photolysis is dependent on the amount of heat liberated from chemical and physical processes It was found that all "fast" processes (<1 ns) gave the same signal on the transducer, and all "slow" processes (>1 ms) were ignored [25] In between the fast and slow domains, there exists an intermediate regime in which the transducer response tracks the profile of heat deposition

To state any reaction enthalpy with certainty, it is necessary to know precisely the quantum yields for the formation of the product [26] The quantum yield is only necessary to obtain thermodynamic information, the reaction kinetics, once initiated, are independent of the quantum yield for photoinitiation

REFERENCES

(Introduction)

[1] Zeise W C , *Pogg Ann* , 1827, **9**, 632

[2] Liebig J , *Ann* , 1837, **23**, 12

[3] Mond L , Langer C , Quincke F , *J Chem Soc* , 1890, **57**, 749

[4] Kealy T J , Pauson P L , *Nature*, 1951, **168**, 1039

[5] Miller S A , Tebboth J A , Tremaine J F , *J Chem Soc* , 1952, 632

[6] (a) Wilkinson G , Rosemblum M , Whiting M C , Woodward R B ,

J Am Chem Soc 1952, **74**, 2125

(b) Fischer E O , Pfab W , *Z Naturforsch Teil B*, 1952, **7**, 377

[7] Ziegler K , Holtzkampf E , Breil H , Martin H , *Angew Chem* , 1955, **67**, 543

[8] Elian M , Chen M M L , Mingos D M P , Hoffmann R , *Inorg Chem* , 1976, **15**, 1149

[9] Geoffroy G L , Wrighton M S , *Organometallic Photochemistry*

Academic Press, New York, 1979

[10] Collman J P , *Acc of Chem Res* , 1968, **1**, 136

[11] Nasielski J , Colas A , *J Organomet Chem* , 1975, **101**, 215

[12] (a) Wrighton M , Schroeder M A , *J Am Chem Soc* 1973, **95**, 5764

(b) Platbrood G , Wilputte-Steinert L , *Bull Soc Chim Belg* , 1973, **82**, 733

[13] Nagorski H , Mirbach M J , Mirbach M F , *J Organomet Chem* , 1985, **297**, 171

[14] Cais M , Frankel E N , Rejoan A , *Tetrahedron Letters*, 1968, 1919

[15] Saillard J Y , Hoffmann R , *J Am Chem Soc* , 1984, **106**, 2006

[16] Avery H E , *Basic Reaction Kinetics and Mechanisms*, Macmillan, 1974

[17] Nasielski J , Kirsch P , Wilputte-Steinert L , *J Organomet Chem* , 1971, **29**, 269

[18] Poliakoff M , Weitz E , *Adv Organomet Chem* , 1986, **25**, 277

[19] Hermann H , Grevels F-W , Henne A , Schnaffer K , *J Phys Chem* , 1982, **86**, 5151

[20] Casper J V , Meyer T J , *J Am Chem Soc* , 1980, **102**, 7794

[21] Hooker R H , Mahmoud K A , Rest A J , *J Chem Soc , Chem Commun* , 1983, 1022

[22] Hepp A F , Blaha J P , Lewis C , Wrighton M S , *Organometallics*, 1984, **3**, 174

[23] Moore B D , Simpson M B , Poliakoff M , Turner J J , *J Chem Soc , Chem Commun* , 1984, 972

[24] Ishikawa Y , Brown C E , Hackett P A , Raynor D M , *J Phys Chem* , 1990, **94**, 2404

[25] Rothberg L J , Simon J D , Bernstein M , Peters K S , *J Am Chem Soc* , 1983, **105**, 3464

[26] Bernstein M , Simon J D , Peters K S , *Chem Phys Lett* , 1983, **100**, 241

CHAPTER 1

1.1 LITERATURE SURVEY

The photochemistry of group six hexacarbonyls has been of great interest over the past thirty years They are of considerable interest because of the role they play as catalysts, as already discussed in the introduction They are ideal systems to study both in the UV and the IR, because of their characteristic spectra

1 1 1 Early low temperature studies of the photochemistry of $M(CO)_6$

Most of the initial work in this field was involved in identifying the species that was formed upon photolysis of $M(CO)_6$ (where M = Cr, Mo or W) [1,2] Initial suggestions,[1] that a pentacarbonyl was the species formed, was confirmed by Stolz *et al* [2] Photolysis of $W(CO)_6$ in a 1 4 methylcyclohexane isopentane glass at 77K, produced a photoproduct Infrared peaks characteristic of a square pyramid of five carbonyl groups around a metal centre were observed, after melting the glass The possibility of a charged species being produced was discounted because of its solubility in non-polar solvents Also extensive electron spin resonance studies were carried out, indicating no evidence for the existence of unpaired electrons Stolz *et al* [3] further investigated the metal hexacarbonyls in glasses Because of improvements in technology, monitoring at 77 K was possible and spectroscopy confirmed the C_{4v} structure previously assigned However when the temperature was raised for the molybdenum system, the band pattern of three ν_{co}

bands changed to two bands of equal intensity, which they assigned to the metal pentacarbonyl with D_{3h} symmetry However Braterman *et al* [4], disagreed with this assignment and proposed that the spectral changes were as a result of polymer formation This was later confirmed by Turner *et al* [5] who observed peaks that were assigned to this polymeric species upon photolysis of the $M(CO)_6$ (M = Cr, Mo or W) in an argon matrix, but much weaker than the dominant $M(CO)_5$ (C_{4v}) and $M(CO)_4$ bands It was also observed that the peaks were dilution dependent, thus suggesting that the peaks could have been a result of the combination of the $M(CO)_6$ and the $M(CO)_5$ fragments

Previous matrix isolation work[6] had shown a variation of the position of the visible band of the $Cr(CO)_5$ species, depending on the nature of the matrix Turner *et al* [5] examined the difference in the spectroscopic behaviour of $Cr(CO)_6$ in a methane matrix, compared with the previously reported argon matrix [6] The UV/visible spectra of $Cr(CO)_6$ in both matrices were practically identical, however there was a shift in the visible band assigned to $Cr(CO)_5$, produced upon photolysis of the parent compound To explain these shifts it was suggested that there was an interaction between the C_{4v} $Cr(CO)_5$ and the environment that surrounded it, *via* the "hole" in the C_{4v} structure

1 1 2 Room temperature studies of the photochemistry of $M(CO)_6$

Contemporary investigations in room temperature solutions were carried out at this time Kelly *et al* [7] studied the photochemistry of $Cr(CO)_6$ in (extensively purified) cyclohexane and observed a species immediately following the flash This

species had a broad band situated at 503 nm ± 5 nm and a lifetime of greater than 200 ms This species decayed away to form other species that were assigned as the interaction of the $Cr(CO)_5$ with impurities The possibility that this second band being assigned to a dinuclear species formed by the interaction of the pentacarboyl with the parent compound was disregarded, because a change in the concentration of $Cr(CO)_6$ had no effect on the concentration of this second species The impurities were found to affect the lifetime of the pentacarbonyl with CO It was therefore suggested that a highly reactive species was formed within 50 ns of the excitation of $Cr(CO)_6$, which was assigned to the $Cr(CO)_5$ species

Koerner von Gustorf *et al* [8] examined the rates of reaction of the $Cr(CO)_5$ moiety with a variety of solvents Again it was noted that the preparation of the sample solution was extremely important, as any trace amount of impurity was liable to be complexed to the photoproduct Incorporating the results obtained by Turner *et al*,[5] which indicated there was an interaction between the $Cr(CO)_5$ moiety and a hydrocarbon matrix, it was proposed that the $Cr(CO)_5$ species was not completely free, but was "readily available", as it could be expected to weakly interact with the cyclohexane solvent With addition of other solvents to cyclohexane, such as acetone, acetonitrile or benzene, the photogenerated $Cr(CO)_5$ reacted to form the $Cr(CO)_5L$ species (L = solvent) Again a dependence of the visible bands on L was observed, the relevant $Cr(CO)_5L$ band was seen to grow in at the same rate as the $Cr(CO)_5$ decayed, confirming first order kinetics

1 1 3 An in depth study of the photochemistry in the matrix

However useful in obtaining kinetic data, UV/vis monitored flash photolysis is unable to provide structural data The ideal tool for obtaining structural information involves infrared detection Turner *et al* [9] carried out an in depth study of the group six metal hexacarbonyls in a variety of matrices, employing both UV\visible and infrared detection When $Cr(CO)_6$ was photolysed in a methane matrix, a new IR spectrum was produced, that was indicative of a $Cr(CO)_5$ species with C_{4v} symmetry as already indicated *(vide ante)* A visible band was also observed that grew in at the same rate, clearly this band was also due to the C_{4v} $Cr(CO)_5$ With all the hexacarbonyls in a variety of matrices it was possible to regenerate the parent by longer wavelength photolysis into the visible band This visible band was found to be extremely sensitive to the matrix, varying from 624 nm in Ne to 489 nm in methane, this extreme sensitivity to the matrix environment was not observed with IR detection, where variations in the ν_{co} bands were not as pronounced It was then necessary to determine if this variation was a the result of stereospecific interaction between the $Cr(CO)_5$ and the matrix or alternatively a general solvent effect To clarify this mixed matrices were employed These experiments were based on the principle that if the effect was a general solvent one, there should be one visible peak with a λ_{max} at a wavelength within the extremes of the individual matrices However this was not observed, when the experiment was carried out in a Ne/2%Xe matrix two peaks were observed, which corresponded closely to those reported for the pure matrices Further evidence for a stereospecific interaction was

obtained by using the "tail photolysis" method Irradiation of $Cr(CO)_5$ in its visible band in pure matrices was known to give $Cr(CO)_6$[6(b)], therefore removal of each component of the mixed matrix spectrum in turn, by selective photolysis into one of the bands, should have been possible A reversible photosubstitution reaction was observed, where photolysis into one of the bands produced the other band as well as $Cr(CO)_6$, and the reverse reaction could also be seen, which is depicted in Figure 1 1 This interconversion could be repeated several times, until the intensities of both photoproducts had decreased because of the production of $Cr(CO)_6$

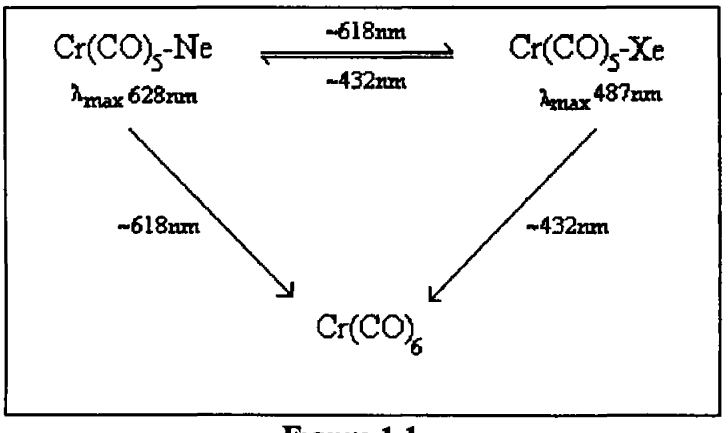

Figure 1.1

(Tail photolysis in a mixed matrix[9])

Infrared detection was also employed to observe the $Cr(CO)_5$ fragment in the matrix Comparison of spectral behaviour in a variety of matrices demonstrated that the positions of the ν_{co} bands were sensitive to the matrix environment, however both the metal hexacarbonyls and the metal pentacarbonyls were similarly affected The constancy of these separations indicated that most of the perturbing effect of the matrix was a

general solvent one Calculations carried out demonstrated that the change in intensity of the high frequency A_1 band from $Cr(CO)_5$-Ar to $Cr(CO)_5$-Xe was caused by a decrease in the axial-radial bond angle of about 4° Any change in this angle has a dramatic affect on the energies of the molecular orbitals, particularly the one with a_1 symmetry (Figure 1 2) As the angle θ increases, the energy of the e orbital rises slightly, while the energy of the a_1 orbital falls dramatically [10] Therefore a small increase of the axial-radial bond angle can generate a significant drop in the $e \rightarrow a_1$ transition energy Also possible is an interaction between the matrix and the a_1 orbital of the $Cr(CO)_5$ moiety It was concluded that the sensitivity of the visible band position is a combination of these two effects

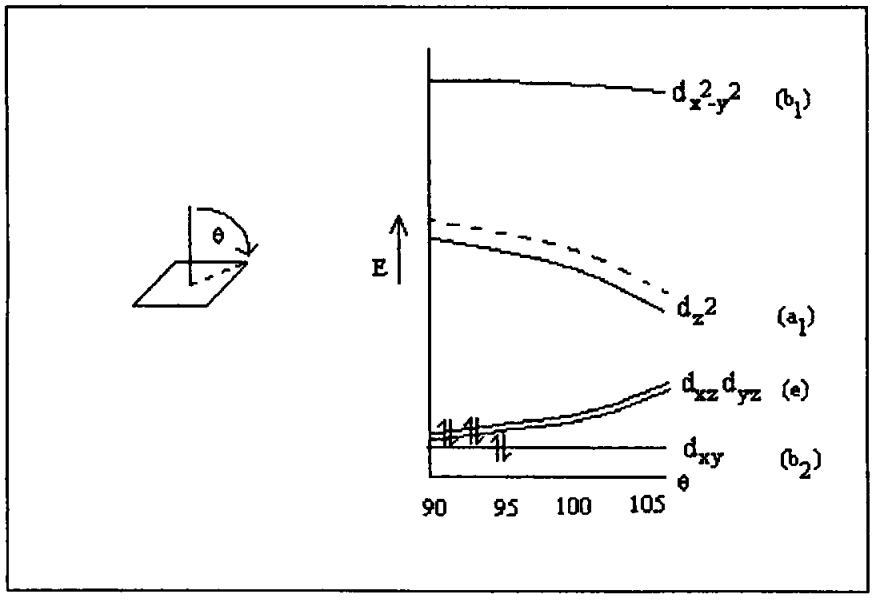

Figure 1.2

(Relationship between the axial-radial bond angle and the energies of the molecular orbitals)

The ability to interconvert $Cr(CO)_5$ - Ne and $Cr(CO)_5$ - Xe in the matrix indicated that there was some mobility of the $Cr(CO)_5$ fragment in the matrix Conclusive evidence for this came from matrix experiments, using plane polarised light [11] The principle of this method is that if a molecule, held rigid by the matrix, is photolysed with plane polarised light only those molecules that are orientated in a specific manner will absorb the light, resulting in dichroic photodepletion The products of this photochemistry will have also a specific orientation, dichroic photoproduction However if dichroic photodepletion is observed without dichroic photoproduction, this would indicate that some intermediate species is mobile during the photochemical act, thus resulting in some random orientation of the product A mixture of $Mo(CO)_5$-Ar and $Mo(CO)_5$-N_2 was generated by unpolarised photolysis, in a mixed Ar/N_2 matrix This led to the production of two randomly orientated species However, upon polarised photolysis into the $Mo(CO)_5$-N_2 band (367 nm), this band became specifically orientated, which was expected because of the theory of dichroic photodepletion The band assigned to $Mo(CO)_5$-Ar was seen to increase in intensity, but it remained randomly orientated, therefore not displaying dichroic photoproduction, demonstrating that there must have been some motion during the reaction, in order to randomize the orientation of the photoproduct

Another phenomenon that is possible with plane polarised light, is called photoreorientation This occurs when the starting material rotates following absorption but does not react This phenomenon was observed when $Cr(CO)_6$ was photolysed in a pure matrix of N_2, Ar or methane It was found that linear dichroism developed upon polarised photolysis, photolysis with polarised light produced an increase in the intensity

of the molecules orientated in the opposite direction was observed This orientation was reversible upon rotating the polarization of the irradiating beam by 90^{o}, indicating that in theory it could have been possible to interconvert the orientations This indicated that the molecules were being orientated to positions of lower probability of absorbing the incident radiation, resulting in a bleaching of the particular orientation

Previous studies had been carried out employing the $Cr(CO)_5$-CS species which mirrored the reactions of $Cr(CO)_6$ [12] The elegance of this system was the fact that the CS group could act as a "labelled" CO group, making it possible to follow otherwise unobservable processes Burdett *et al* [11] carried out further experiments involving the $Cr(CO)_5$-CS species, to determine if the reorientation observed was a simple rotation or a specific intramolecular rearrangement The visible absorption band of the $Cr(CO)_4CS$-Ar species depended on the relative position of the CS group and Ar This species was generated by UV photolysis and showed wavelength dependent isomerisation The isomerisation was explained by a reorientation of the $Cr(CO)_4CS$ species via a trigonal bipyramidal intermediate, in a manner analogous to the reorientation of the $Cr(CO)_5$ species Incorporating all the above information the authors then proposed a complete account of the photochemical behaviour of the $M(CO)_6$ molecule in the matrix, their conclusions are depicted in Figure 1 3

From Figure 1 3 when the parent hexacarbonyl is isolated in a mixed matrix of X and Y, UV irradiation results in the loss of one CO, to form a C_{4v} $Cr(CO)_5$ (spy) molecule This initially generated excited state is not stable in this geometry and therefore

distorts to a trigonal bipyramid (tbp) intermediate The tbp can then relax to three different ground state spy species, with equal probability Each of these three ground state

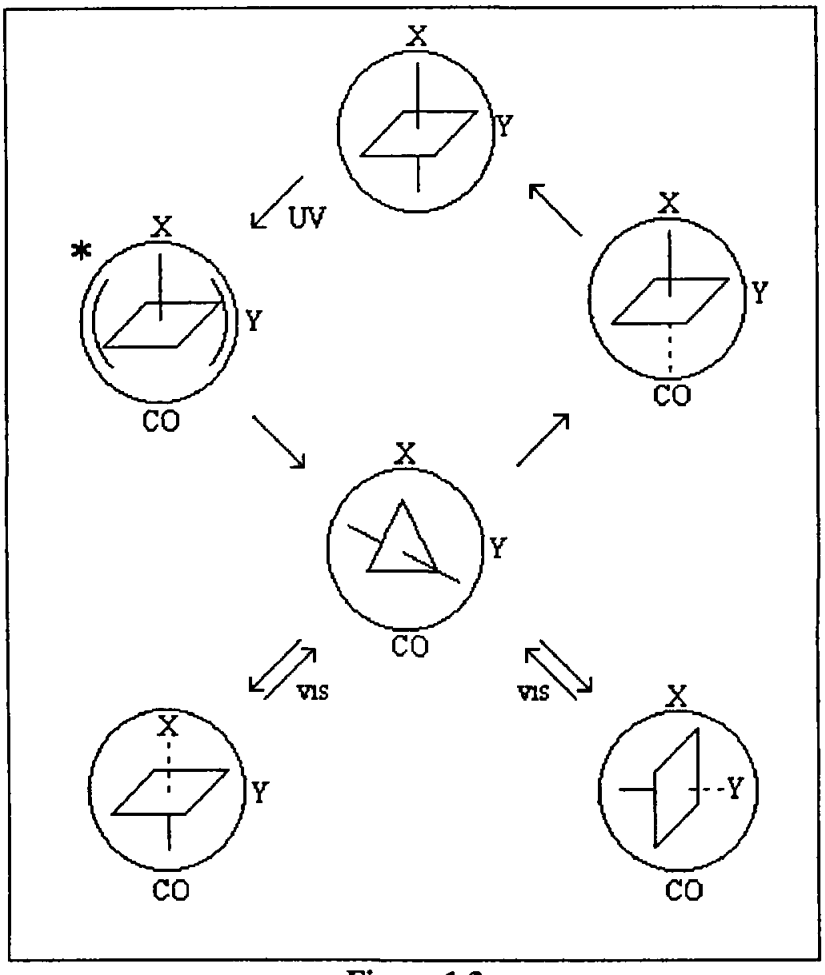

Figure 1.3

(Photochemical behaviour of $M(CO)_5$ in a mixed matrix X,Y)

spy molecules has a vacant site in a different orientation There is an equal chance of the pentacarbonyl fragment interacting with X, Y or recombining with the ejected CO This mechanism for CO loss from a hexacarbonyl, explains how the CO molecule manages to escape the vacant site Hay[13] confirmed that the visible absorption in these complexes

could be assigned to the e $\rightarrow$ a_1 transition and found that the ground state $M(CO)_5$ (spy) species was at lower energy than the tbp species

Therefore by employing matrices and a variety of different physical, photochemical and chemical methods, it was possible to elucidate the photochemical behaviour of $M(CO)_6$, including a characterisation of the intermediates, which could not have been possible in solution at that time

1 1 4 Solution phase photochemistry in weakly coordinating solvents

Kelly *et al* [14] used perfluorocarbon solvents, to investigate the photochemistry of chromium hexacarbonyl They observed that the λ_{max} of the visible absorption of the $Cr(CO)_5$ in this solvent was ~620 nm This is very close to the λ_{max} of $Cr(CO)_5$-Ne in a Ne matrix (624 nm) Therefore it was concluded that the perfluoro solvent interacted only very weakly, if at all, with the pentacarbonyl fragment This intermediate reacted with N_2, CO and cyclohexane at about the diffusion controlled limit for this solvent (6 6 $\times 10^9$ dm^3 mol^{-1} s^{-1}) [8] The diffusion controlled limit is where there is no barrier to activation for the reaction The only parameter that is controlling the rate, is the diffusion of the two molecules so that they are close enough to interact This study confirmed that the $Cr(CO)_5$ species was formed within 50 ns of the excitation of the hexacarbonyl and demonstrated that the species was formed in cyclohexane, within the 5 ns excitation pulse

Further work with $W(CO)_6$ or $Mo(CO)_6$ was conducted in perfluoro solvents [15] The production of a $Cr(CO)_5$-$Cr(CO)_6$ species was also reported and the reaction of this species with CO was investigated It was found that this compound decayed with a biphasic profile The first fast decay was assigned to the recombination of the species with CO and the longer decay time was assigned to the reaction with impurities This species however was formed by the reaction of the $Cr(CO)_5$ fragment with the parent $Cr(CO)_6$ complex and was only observed with a relatively high concentration of $Cr(CO)_6$, therefore it was thought that it should not play an important role in reactions in dilute solutions

1 1 5 The photochemistry of $M(CO)_6$ in liquefied noble gases

In a low temperature solvent it is likely that moderately stable species will be stabilised sufficiently to permit study with conventional techniques Perhaps the most revealing spectroscopic technique for transient organometallic species has been infrared The most appropriate solvents would therefore be inert and transparent to IR radiation, of which liquid noble gases are a perfect example This method thus permits the study of novel photogenerated species, and as the species are being studied in a liquid environment it is possible to monitor kinetics, and by measuring kinetic change with temperature, to extract thermodynamic information

A series of studies were undertaken investigating the photochemistry of $M(CO)_6$ in liquefied noble gases A long lived species was observed upon UV photolysis

of $Cr(CO)_6$ in liquefied xenon or krypton in the presence of di-nitrogen, that was identified as $Cr(CO)_5N_2$ [16] The identification of $Cr(CO)_5$-Xe, formed following photolysis of $Cr(CO)_6$ in Xe, or Kr doped with Xe, indicated the extreme reactivity of the $Cr(CO)_5$ fragment [17] Noble gases have no absorptions in the IR, therefore allowing the observation of IR bands associated with η^2-H_2, η^2-HD, or η^2-D_2, which would normally be very difficult to observe It was possible to characterise $M(CO)_5(H_2)$ (M = Cr, Mo and W) and *cis*-$Cr(CO)_4(H_2)_2$ Also *cis*-$Cr(CO)_4(N_2)_2$ was exclusively formed upon exchange of *cis*-$Cr(CO)_4(H_2)_2$ with N_2 [18] Therefore liquefied noble gases provided a general route to characterise whole groups of unstable organometallic compounds and investigate their thermal stability

1 1 6 Investigation of the dynamics of solvation employing picosecond and femtosecond flash photolysis

The, by now, well established interaction between the photolytically produced $Cr(CO)_5$ and solvent environment, which previously was considered inert, prompted a number of workers to investigate picosecond and femtosecond time-resolved spectroscopy of $Cr(CO)_6$, to investigate the initial solvent co-ordination with the ground state C_{4v} $Cr(CO)_5$ fragment Simon *et al* [19] investigated $Cr(CO)_6$ in cyclohexane containing THF, employing picosecond absorption spectroscopy Both $Cr(CO)_5$-cyclohexane and $Cr(CO)_5$-THF were formed following the excitation of $Cr(CO)_6$ In a relatively high concentration of THF (5M) nearly all of the $Cr(CO)_5$-cyclohexane

converted to the THF coordinated species within 25 ps Again using mixed solvent systems, Simon *et al* [20] examined the dynamics of the formation of Cr(CO)-S, (S = cyclohexane or methanol) and found that the cyclohexane analogue was formed within the time resolution of the equipment (0 8 ps), however the rise time of the $Cr(CO)_5$-methanol species was 2 5 ps This longer rise time was thought to reflect a greater barrier to solvent reorganisation leading to the co-ordination of the solvent molecule to the vacant site of the reactive $Cr(CO)_5$ intermediate

The dynamics of solvation were then examined in pentanol [21] It was anticipated that it should be possible to observe the reorganisation of the solvent interaction from the less thermodynamically stable, M-alkyl group, to the more favourable M-OH group A difference in the visible absorption band was observed The $Cr(CO)_5$-alkyl species had an absorption at λ_{max} = 520 nm, while the $Cr(CO)_5$-hydroxyl species absorbed at 460 nm These results are as expected, in that the alkyl interaction is weaker than the M-OH interaction Immediately upon photolysis, both species were formed, but the alkane complexes were seen to rearrange, with time, to the more thermodynamically stable hydroxyl complexes This interchange could be followed by transient absorption spectroscopy, the band at 520 nm decayed away concurrently with the increased absorption of the 460 nm band There are three plausible mechanisms for this rearrangement Firstly the mechanism could have been dissociative Secondly, it could involve an associative substitution, or finally a unimolecular process, where reorientation of the solvent coordinated to the pentacarbonyl fragment takes place In order to clarify the exact mechanism for this rearrangement, photolysis of $Cr(CO)_6$ was carried out in 1-

propanol and 2-propanol [22] On a macroscopic level the two solvents have similar properties, therefore the rate for the rearrangement in both solvents should be approximately the same However the initially formed alkane complex disappeared faster in 2-proponol solvent than the 1-proponol The rate of the rearrangement was 3 orders of magnitude faster than that expected for a dissociative mechanism This led to the conclusion that the mechanism was unimolecular for the 2-proponol solvent The solvation in ethanol was also assigned a unimolecular mechanism, as it portrayed similar kinetic behaviour

Simon *et al* [20] had already shown that the formation of $Cr(CO)_5(MeOH)$ occurred within the first 2 5 ps, Joly and Nelson[23] employed femtosecond absorption spectroscopy to study this system and found that the "bare" $Cr(CO)_5$ complex was formed within 500 fs They also noted that there was a 1 6 ps rise time for the formation of $Cr(CO)_5$-methanol Similar results were obtained for both the tungsten and molybdenum analogues Simon *et al* [24] carried out a series of experiments involving the solvation of $Cr(CO)_5$ with a series of linear alcohols, and found that the initial co-ordination of the solvent molecule to the $Cr(CO)_5$ fragment occurs in a random fashion

Using 266 nm excitation of $Cr(CO)_6$ in cyclohexane, Wang *et al* [25] claimed to have observed "naked" $Cr(CO)_5$ using picosecond IR transient absorption spectroscopy They also postulated that the excited $Cr(CO)_5$ fragment decayed to both C_{4v} and D_{3h} and that the D_{3h} species decayed 2 3 times faster than the C_{4v} species They also examined the dynamics of the solvation of $Cr(CO)_5$ in THF[26] and confirmed that the initial co-ordination of the solvent to the $Cr(CO)_5$ occurred randomly, but then the

$Cr(CO)_5(THF)$ species, bound to C-H group on the THF, rearranges to the $Cr(CO)_5(O\text{-}C_4H_8)$ species Like the cyclohexane work they identified two states that led to products, again they found that the D_{3h} species reacted faster than the C_{4v} species (D_{3h} species reacts 7 times faster than the C_{4v} species for co-ordination at the O site)

Simon and Xie[27] presented data that contradicted the above results The photochemistry of $Cr(CO)_6$ in THF was investigated, but picosecond absorption spectroscopy was used Under these conditions $Cr(CO)_6$ underwent photodissociation and solvation within the time resolution of the experiment and the dynamics of the solvent rearrangement were similar to that reported for the solvation of $Cr(CO)_5$ with the linear alcohols The time scale for solvent migration was found to be at least an order of magnitude faster in these experiments than those reported from the transient IR study The fact that a 266 nm pump beam was employed in the IR experiments was a possible reason for the observation of both the C_{4v} and the D_{3h} states The high energy of the 266 nm laser beam could have resulted in the formation of different initial species, consequently, the dynamics studied may not have been those of the $Cr(CO)_5$ species Lee and Harris[28] carried out picosecond pump-probe (295 nm) measurements in the visible region with 1 ps time resolution, in order to investigate the solvation dynamics A rise time for the $Cr(CO)_5$(cyclohexane) species was measured (17 ps) that was between that of Wang *et al*[25] (100 ps) and Simon *et al*[20] (< 1 ps) The red tail of the absorption spectrum of the $Cr(CO)_5$ solvated species was monitored (622 nm in cyclohexane) This region in the spectrum corresponds to the vibrationally hot species, and it was found that this species decayed away with a lifetime of 21 ps, which is very close to the rise time

observed at 500 nm Therefore the rise time for the $Cr(CO)_5$(cyclohexane) species was postulated to be as a result of vibrational relaxation

Joly and Nelson[29] conducted a femtosecond transient absorption study into the photodissociation of $M(CO)_6$ (M = Cr, Mo, or W) in a variety of linear alcohols, in order to determine the role of the solvent on the initial CO dissociation event The CO dissociation appeared to be independent of the solvent, implying that the dissociating fragment felt no significant influence from the solvent neighbours The dissociation time did not vary with the substitution of tungsten for chromium, indicating that the triplet state plays no role in the reaction For all three metal hexacarbonyls, photoejection of the initial CO was found to occur within 500 fs, complexation of the solvent to the $Cr(CO)_5$ fragment was complete within the next several picoseconds The results also suggested that the solvent had no influence over which of the six CO's dissociated, but the initial solvent configuration did determine which part of the solvent coordinated with the $Cr(CO)_5$ species

1 1 7 The photochemistry of $M(CO)_6$ in the gas phase

Coordinately unsaturated metal carbonyls have also been studied in the gas phase This method of investigation has a number of advantages over the solution phase A comprehensive review of the subject has been published [30] However considering the importance of solution phase chemistry, it may be argued that solution studies are more important, not withstanding the added complications of the solution phase Firstly, as

already shown, these coordinately unsaturated species form interactions with the solvent environment within the picosecond time scale, therefore any kinetic measurements will actually be displacement reactions rather than addition reactions Therefore in solution these reactions may not probe the interaction of the "naked" species with the incoming ligand Secondly, coordination of the solvent may influence the structure of the species being studied, thus making it difficult to unambiguously assign the structure of the "naked" fragment The gas phase is not affected by solvent co-ordination therefore it is a valuable tool to further investigate the photochemistry of these species

The gas phase differs from the solution phase in that multiple coordinately unsaturated species are formed following the absorption of one single UV photon, these species are only formed in condensed phases upon photolysis of initially produced coordinately unsaturated species This fragmentation of the parent species results from the sequential loss of CO coupled to a high degree of internal energy retention in the remaining metal carbonyl fragment In the gas phase a high degree of internal energy retention results in the eventual ejection of successive CO ligands in order to dissipate the excess energy This was demonstrated by Yardly *et al* [31] who studied the $Fe(CO)_5$ system and employed large excesses of PF_3 as a trapping agent to coordinate to the "naked" species, formed following excitation of the parent $Fe(CO)_5$ species It was also demonstrated that upon increasing the photolysis wavelength, a higher number of the CO ligands were ejected from the $Fe(CO)_5$ molecule Multiple CO loss processes were also observed upon photolysis of $Cr(CO)_6$ [32] Only 107 kJ mol^{-1} of energy is required to break one Cr-CO bond, photon excitation energy of 481 kJ mol^{-1} was employed in the gas phase

experiments, therefore sufficient energy was available to potentially break four bonds This did not occur in condensed media, as rapid dissipation of excess energy to the surrounding environment was possible This explains the difference between the gas phase and condensed phase results

A pulsed laser pyrolysis technique was employed by Smith *et al* [33] to study the gas phase thermal decomposition of $Fe(CO)_5$ and $M(CO)_6$ (M = Cr, Mo, or W) These results provided first bond dissociation energies for $Fe(CO)_5$ = 171 8 kJ mol^{-1}, $Cr(CO)_6$ = 155 kJ mol^{-1}, $Mo(CO)_6$ = 167 6 kJ mol^{-1}, and $W(CO)_6$ = 192 7 kJ mol^{-1} $Cr(CO)_6$ decomposed via a different mechanism from the other hexacarbonyls, as the rate determining step was not the first bond scission, but a subsequent bond scission, which had a 167 6 kJ mol^{-1} activation energy

Weitz *et al* [34] employed time-resolved infrared spectroscopy (TRIR) to study the gas phase photofragmentation of $Cr(CO)_6$ These results confirmed that the "naked" $Cr(CO)_5$ fragment had a square pyramidal structure, only $Cr(CO)_5$ and $Cr(CO)_4$ were observed upon photolysis at 351 nm (343 6 kJ mol^{-1}), as there was only enough energy to eject two CO ligands Breckenridge and Stewart[35] again employed transient absorption spectroscopy to study the photofragmentation of $Cr(CO)_6$ in the gas phase The hexacarbonyl was photolysed at 355 nm, again this was just sufficient energy to remove two CO ligands The uncomplexed $Cr(CO)_5$ was observed with a λ_{max} at 620 nm This is consistent with the values obtained from the solution work in perfluoro solvents[15] or in rare gas matrices [9]

Weitz *et al*[36] varied the excitation wavelength (193 nm, 248 nm, 351 nm) and monitored the different fragments produced by TRIR The results indicated that the gas-phase structures of the $Cr(CO)_x$ (x = 5, 4, 3, and 2) species were similar to those observed in condensed phase media [6(b),9] Variable wavelength excitation of $W(CO)_6$, demonstrated that more energy was required to remove two CO ligands, than for $Cr(CO)_6$ analogue[37] Using an Eximer laser 351 nm (XeF) and 308 nm (XeCl) excitation produced $W(CO)_5$ However when more energy was employed 248 nm (KrF) $W(CO)_4$ was the main product The $W(CO)_5$ fragment was assigned a C_{4v} symmetry, again consistent with the matrix work [9]

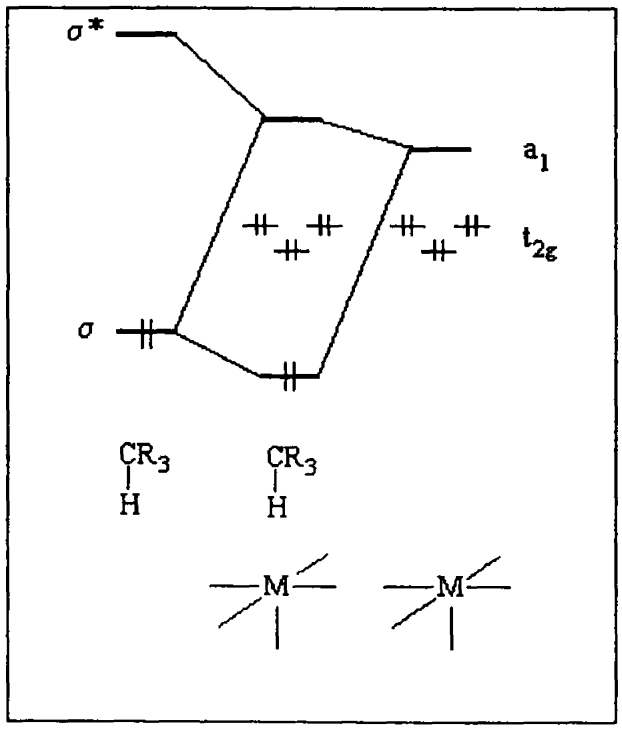

Figure 1.4

(Interaction diagram for the perpendicular approach of a C-H bond to $M(CO)_5$)

Brown *et al* [38] studied the interaction of alkanes with $W(CO)_5$ in the gas phase, employing TRIR as the detection system The results demonstrated that the binding energy increased as the length of the alkane chain increased, no binding energy for the interaction of methane with the $W(CO)_5$ fragment was observed It was concluded that the binding energy was less than 21 kJ mol^{-1} Photoelectron spectroscopy demonstrated that the C-H σ molecular orbital (MO) in alkanes rose in energy, with increasing alkane size The largest change in alkane MO could be observed between CH_4 and C_2H_6 and this correlated with the largest change in alkane binding energy (from <21 kJ mol^{-1} to 31 kJ mol^{-1}) Therefore as the C-H σ MO increased to match the energy of the a_1 orbital of the metal (Figure 1 4) the binding energy was found to increase accordingly, as was expected for a $\sigma \rightarrow$ metal bonding mechanism

1 1 8 Time resolved photoacoustic calorimetry experiments

Time resolved photoacoustic calorimetry (PAC) has been employed to measure the strength of bonds to coordinately unsaturated species This method uses the amplitude of an acoustic wave produced following photolysis Yang *et al* [39] measured the strength of the $Cr(CO)_5$-L bonds in heptane, where L is a variety of ligands including CO Comparing these results to the Cr-CO bond dissociation energy in the gas phase, it was concluded that co-ordination of heptane leads to a 42 kJ mol^{-1} stabilisation of the $Cr(CO)_5$ fragment To examine steric effects, the workers carried out a study where the incoming ligands contained a number of methyl groups, for instance pyridine, 2-picoline, 2,6-

lutidine [40] It was found that the enthalpy for the dissociation of heptane from $Cr(CO)_5$(heptane) was exothermic for all the ligands, but decreased in magnitude by about 9 7 kJ mol^{-1} upon successive methylation of the ligand This was not surprising due to the increasing steric hindrance about the nitrogen with the extra methyl groups The metal-heptane bond strength is approximately 42 kJ mol^{1}, and as the $\Delta H^{\neq}$ for the two ligands are 21 or 31 kJ mol^{-1} the transition state must be associative for the incoming ligand Also as the $\Delta S^{\neq}$ values for both systems are close to zero, it was suggested that the there is a high degree of heptane-metal bond lengthening concurrent with the association of the incoming ligand, indicative of an interchange mechanism

Burkey *et al* [41] used PAC to determine the enthalpies for CO dissociation from $Cr(CO)_6$ in pentane, heptane, isooctane or cyclohexane and values of 116 8, 112 6, 108 4 and 100 1 kJ mol^{1} respectively, were obtained These values obtained depended on the quantum yield (Φ) for CO dissociation from $Cr(CO)_6$, it was assumed that Φ was independent of the solvent, Wieland and van Eldik[42] showed that this was not the case The solvated intermediate was trapped with a variety of ligands and it was found that the Φ for the ligand substitution, did not depend on the entering ligand or its concentration, it only depended on the solvent employed, indicating a dependency of the Φ on the solvent

Burkey *et al* [41] calculated the $M(CO)_5$(heptane) bond strengths (M = Cr, Mo or W) by subtracting the M-CO bond energies[33] from the enthalpies of CO dissociation in heptane *(vide supra)* The values obtained for ΔH_{m-s} were $Cr(CO)_5$(heptane) = 37 1 kJ mol^{-1}, $Mo(CO)_5$(heptane) = 36 3 kJ mol^{-1} and

$W(CO)_5$(heptane) = 55 9 kJ mol ^{1}, these bond energies were used to explain the differences in the gas phase and the solution phase activation enthalpies for $Mo(CO)_6$ and $W(CO)_6$ (33 5 kJ mol ^{1} and 25 kJ mol^{-1} respectively) [33,44]

Burkey and Nayak[43] investigated the low quantum yield for CO loss from $Cr(CO)_6$ observed in fluorocarbon solvents, employing PAC They concluded that a more efficient cage recombination of CO was occurred in one solvent and this was primarily responsible for the low Φ obtained Φ is independent of excitation wavelength, thus indicating that the low Φ was not as a result of more efficient vibrational relaxation It could therefore be concluded that the relative strong coordination of cyclohexane to the $M(CO)_5$ fragment inhibited the recombination of the CO in the solvent cage and led to its expulsion

1 1 9 Mechanistic information obtained from solution phase experiments

Infrared and ultraviolet detection have also been used to determine the reaction kinetics of the intermediate that was produced by laser pulse photolysis of $M(CO)_6$ Graham and Angelici[44] employed IR detection to measure the substitution reactions of $M(CO)_6$, they proposed that the initial ejection of the CO ligand occurred via a dissociative mechanism, positive values for entropy of activation supported this proposition Addition of the ligand was then proposed to occur via an associative process again supported by entropy values, in this case negative The enthalpy of activation of CO dissociation was found to be nearly the same for $Cr(CO)_6$ and $W(CO)_6$, however the value

was lower for the $Mo(CO)_6$ analogue It was also noted that as the Mo and W metals were larger than the Cr, they had a greater tendency to undergo associative substitution reactions, on steric grounds

Earlier work had shown that $Cr(CO)_5$ was liable to coordinate to an impurity at room temperature even in rigorously purified cyclohexane [8,45] Church *et al* [46] characterised the trace product formed following photolysis of $Cr(CO)_6$ in cyclohexane, as the $Cr(CO)_5(H_2O)$ species and investigated the kinetic effect of water in these systems Activation parameters for the decay of this species allowed an estimate of 75 ± 15 kJ mol^{-1} for the dissociation of the H_2O ligand It was also found that $Cr(CO)_5(C_6H_{12})$ reacted 13 times faster with water than with CO, demonstrating the importance of impurities in the overall investigation of the photochemistry of $Cr(CO)_6$ Lees and Adamson[47] obtained a kinetic estimate of tungsten to methylcyclohexane bond energy to be <13 3 kJ mol^{1}, employing a UV detection system

A mechanistic study of the substitution reactions of $M(CO)_5(THF)$ by a variety of ligands was carried out using conventional and high pressure stopped flow analysis [48] As M changed from Cr to Mo to W, the $\Delta V^{\neq}$ values exhibited a trend towards negative values and this was interpreted as a gradual change over from a dissociative pathway to a more associative mechanism The activation parameters for the displacement of cyclohexane or n-heptane from $W(CO)_5$ by 1-hexene were estimated to be within experimental error of each other ($\Delta H^{\neq}$ = 34 2 and 35 kJ mol^{-1} respectively) [49] The observed entropies of activation were suggestive of some residual C-H-W bonding in the

transition states leading to the W-alkane bond breaking, $W(CO)_5$(n-heptane) $\Delta S^{\neq} = 7.5$ J K^{-1} mol^{-1} and $W(CO)_5$(cyclohexane) = $\Delta S^{\neq} = -15.5$ J K^{-1} mol^{-1} Mechanisms for the displacement of fluorobenzene, chlorobenzene and n-heptane from $Cr(CO)_5$ by 1-hexene and piperidine were investigated [50] The enthalpies of activation for these reactions were compared with the bond energies obtained by the PAC studies, and it was found that the PAC results were some 21-29 kJ mol^{-1} greater The more dissociative mechanisms appeared to correlate better with the PAC results, however for benzene, where an agostic interaction was inferred prior to bond dissociation, a difference of 23.4 kJ mol^{-1} was observed between the two methods The PAC results depended on the quantum yield for CO dissociation and as already shown,[41,51] the quantum yield varied with alkane solvent, therefore their values were viewed with caution

1.1.10 Photochemistry of $M(CO)_6$ in the presence of bidentate ligands

Photolysis of group 6 metal hexacarbonyls in the presence of a variety of potentially bidentate ligands, has also been investigated [52-62] It was found that the ligand initially photosubstituted one CO ligand, ultimately leading to the bidentate chelate complex The ligands employed were a variety of substituted diimine type ligands (1,4 diazabutadienes, 2,2'-bipyridines and 1,10 phenanthrolines) Oishi *et al* [52] observed that the bidentate $M(CO)_4$(1,10-phenanthroline) was formed faster when M = W and Mo than for Cr, this was attributed to the M to CO bond length, in chromium, being shorter than

that of the other two metals, thus the electronic interaction between the adjacent nitrogen and the metal must be stronger for W and Mo Further work investigated the activation parameters for this process and found that the both the entropies and volumes of activation for Mo and W were negative, supporting an interchange mechanism for the ejection of the second CO [53] For chromium however the entropy of activation was negative and the volume of activation was positive, this could indicate a lengthening of the CO bond rather than the Cr-N bond shortening as the rigid chelating ring adjusts into the transition state An unexpected precursor to the formation of the tetracarbonyl has also been observed, when the ligand, 4,4-Dimethyl-2,2'-bipyridine was employed with the aim of generating a monodentate $Cr(CO)_5L$ It was found that the ligand bound to two $Cr(CO)_5$ units, rather than one [54]

The pressure dependence of the quantum yield for photosubstitution of CO in $M(CO)_4$ (1,10- phenanthroline), where M = Cr, Mo and W has been investigated at different excitation wavelengths It was found that upon photolysis in the UV region, a positive value for the volumes of activation was observed, thus indicating that ligand field photolysis resulted in dissociative substitution mechanism If low lying MLCT states are populated at longer wavelengths, so that the energy of the gap to the lowest LF state increases and thermal back population becomes less important, the residual quantum yield could then be interpreted in terms of the MLCT states Therefore photolysis into the metal to ligand charge transfer state (MLCT) (546 nm) resulted in negative values for Mo and W, which was taken as strong evidence for an associative mechanism The Cr values

for volume of activation were slightly positive and this was interpreted as a dissociative process from the MLCT state for the smaller Cr analogue [55,56]

1.2 RESULTS AND DISCUSSION

As already discussed coordinatively unsaturated metal complexes are sufficiently reactive to form complexes with alkane solvents A stereospecific interaction exists between the metal centre and the alkane solvents [63] This interaction may play a role in C-H insertion, β-elimination, ligand exchange and hence catalytic reactions, therefore a thorough investigation into the solvent to metal interaction is essential

In order to investigate the reactivity of the metal to solvent bond, the desolvation process of the $M(CO)_5$(Solvent) species (Reaction 1 1) was investigated, where M = Cr, Mo, and W The incoming ligand was CO and the solvents were a variety of straight chain and cyclic alkanes

$$M(CO)_6 \xrightarrow{S} M(CO)_5(S) + CO \qquad \textit{Reaction 1 1}$$

1 2 1 Possible mechanisms for solvent dissociation

There are three possible mechanisms for the dissociation of the solvent molecule from $M(CO)_5$(Sol) These are represented in Figure 1 5 The first involves a dissociation of the solvent, with subsequent coordination of the CO to reform the $M(CO)_6$ molecule The $\Delta H^{\neq}$ for this possibility should equal to the bond dissociation energy for the respective system, as dissociation of the ligand must occur prior to reaction with CO The second occurs when the CO enters the reaction sphere before the solvent is

dissociated and forms a 20 electron transition state, before ejection of the solvent The final possibility is the interchange mechanism in which the CO is being coordinated as the solvent is dissociating in a concerted process

The activation enthalpy required for a dissociative reaction should be close to the M-solvent bond strength, because the bond is largely broken in going to the transition state The bond strengths have been obtained for the coordination of heptane

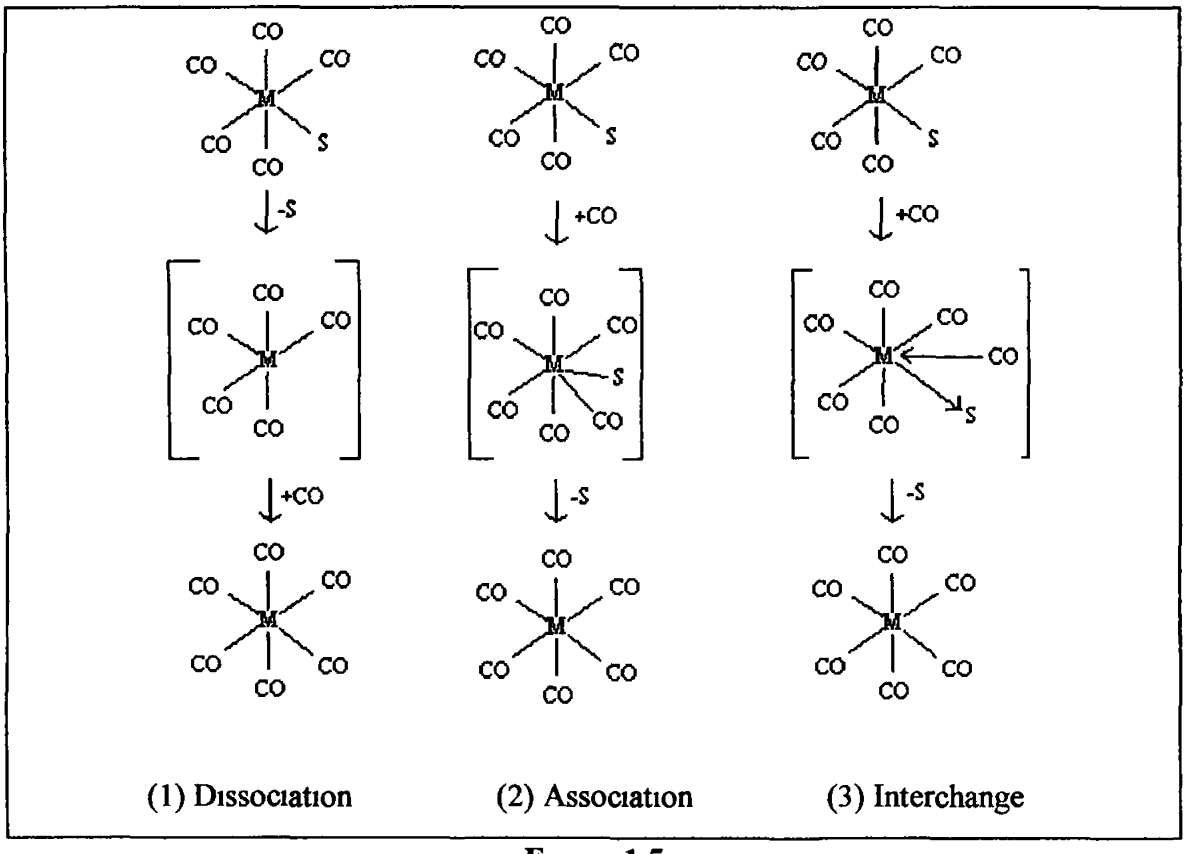

Figure 1.5

(Possible mechanisms for solvent displacement by CO)

with $M(CO)_5$ they were reported to be 42, 38 or 55 kJ mol^{-1} for Cr, Mo or W respectively [41] Figure 1 6 depicts the enthalpies of activation that would be necessary for

a dissociate type of mechanism for $Cr(CO)_5(S)$ and the enthalpies of activation obtained in this study

A dissociative process would result a near zero or positive entropy of activation, as expected as the transition state is less ordered An associative mechanism would have a negative value of ~ -100 $J K^{-1} mol^{-1}$ or less, resulting from the more ordered transition state As a result it can be seen that an interchange mechanism would have a $\Delta S^{\neq}$ value in between the above possibilities

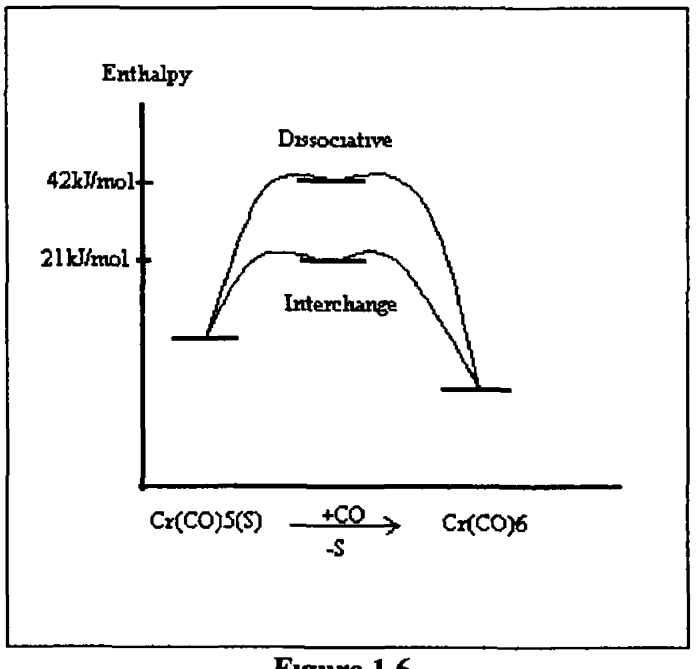

Figure 1 6

(Scheme depicting the differences in $\Delta H^{\neq}$ for solvent dissociation)

1 2 2 SPECTROSCOPIC INFORMATION

The $M(CO)_6$ complexes exhibit a number of intense ($\varepsilon > 10^2$) transitions in the UV-visible region of the spectrum Figure 1 7 shows the ground state absorption

spectra for $M(CO)_6$ (M = Cr, Mo or W) in cyclohexane The lowest energy absorption is found at ~333 nm (30,000 cm^{-1}) for all three metals and is assigned as the $^1A_{1g} \rightarrow {}^1T_{1g}$ ligand field (LF) transition This band is a shoulder on the more intense $M \rightarrow \pi^*$ CO charge transfer transition, found at ~286 nm (~35,000 cm^{-1}) A second LF band $^1A_{1g} \rightarrow {}^1T_{2g}$ is observed at 266 nm (37,500 cm^{-1}) and the most intense transition at 233 nm (43,000 cm^{-1}) is assigned as the second component of the $M \rightarrow \pi^*$ CO CT transition An extra band is observed for Mo and W, at an energy lower than the $^1A_{1g} \rightarrow {}^1T_{1g}$ ligand field (LF) transition, which has a higher ε for W than Mo This band was assigned to the lowest LF spin forbidden singlet $\rightarrow$ triplet transition, $^1A_{1g} \rightarrow {}^3T_{1g}$ This transition was allowed because of spin-orbit coupling, which is applicable in the case of tungsten However the band is also observed for the $Mo(CO)_6$ and this metal is not large enough for spin orbit coupling to have an affect, this transition would therefore not be allowed, thus casting some doubt over this assignment The intensities of the LF bands are uncommonly large because of the high degree of covalence in these molecules, which means that the molecular orbitals have substantial contribution from both the metal and ligand atomic orbitals, thus tending to remove restrictions associated with the intensity of LF transitions

The relevant spectroscopic data, obtained in cyclohexane, for the three compounds employed in this study, are presented in Table 1 1, the experimental details are presented in Appendix IA

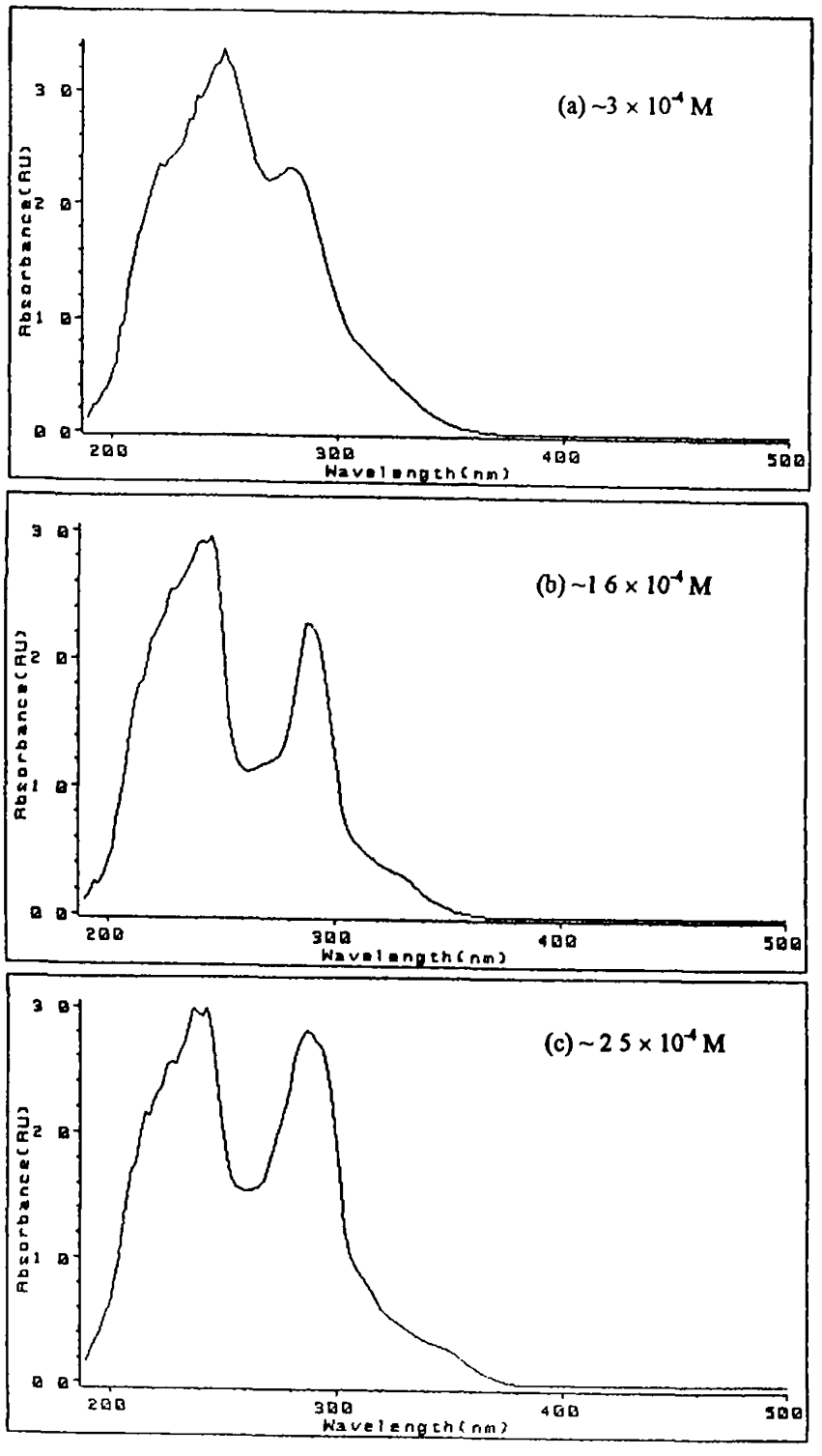

Figure 1.7

(UV-visible spectra of (a) $Cr(CO)_6$ (b) $Mo(CO)_6$ (c) $W(CO)_6$ in cyclohexane)

Compound	υ_{CO} (cm^{-1})	λ_{max} (nm)	ε @ 354 nm
$Cr(CO)_6$	1985	280	2.0×10^2
$Mo(CO)_6$	1985	298	2.6×10^2
$W(CO)_6$	1981	298	8.4×10^2

Table 1.1

(Spectroscopic data for $M(CO)_6$ in cyclohexane)

1.2.3 Measurement of rate constants

The $M(CO)_5$(solvent) species was formed by excitation, of the respective hexacarbonyl, at 355 nm. The λ_{max} for the $M(CO)_5$(solvent) species were found to be, $Cr(CO)_5(S)$ = ~500 nm, $Mo(CO)_5(S)$ = ~420 nm and $W(CO)_5(S)$ = ~450 nm. Figure 1.8 displays a typical two dimensional spectrum for the $Cr(CO)_5$(Cyclohexane) species. It can be seen that following excitation at 355 nm, the transient species is formed within 10 μs (from the literature it is clear that the transient species has been formed well before 10 μs[20,25]), and it has nearly decayed back to baseline after 150 μs. As the solvated complex decays back to the baseline, as can be seen in Figure 1.9, it indicates that there is an efficient back reaction with CO to reform the parent $M(CO)_6$ species. Any impurities (X) in the solvent would result in the production of a side product $M(CO)_5(X)$, hindering efficient back reaction with CO, thus resulting in the trace not returning completely to the baseline. The λ_{max} for the species was observed at ~500 nm, as this value does not vary greatly between the solvents the kinetics were measured at this wavelength for all the solvents.

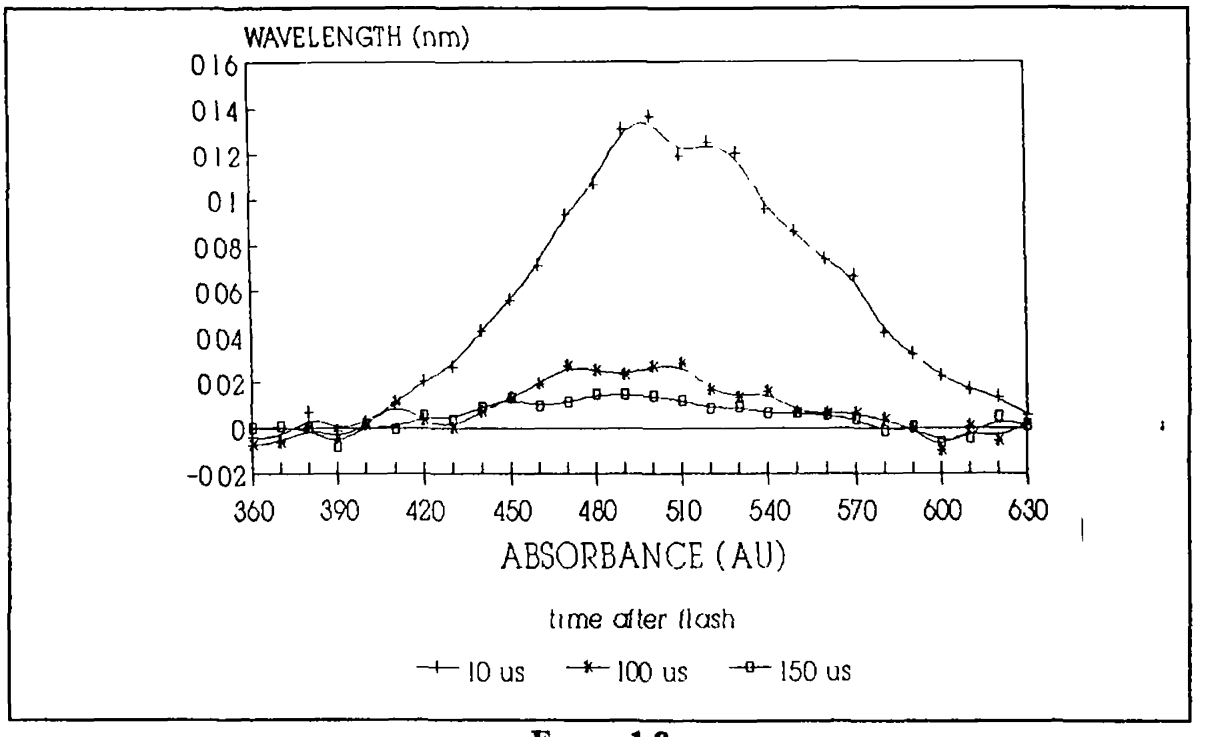

Figure 1.8

(UV/vis spectrum of $Cr(CO)_5$(Solvent) in Cyclohexane at different time intervals following excitation with λ_{exc}= 355 nm)

It has already been proven that the formation of the $M(CO)_5(S)$ species is a single photon process [51] This was done by varying the power of the laser and measuring the absorbance of the product It was found that the absorbance of the product increased as the voltage of the laser was increased The relationship between the two was linear, thus indicating a single photon process

The observed rate constant (k_{obs}) for the reaction of $M(CO)_5(Sol)$ with CO was measured at 298 K Pseudo first order conditions were maintained for the three systems, as the concentration of CO was always much larger than the concentration of the $M(CO)_5(S)$ species The k_{obs} was then obtained from the plots of $\ln(A_\infty-A_0)/(A_\infty-A_t)$ vs time, an example of the decay observed is shown in Figure 1 9 The second order rate

constant (k_2) was then obtained by dividing k_{obs} by the concentration of CO^{64} in the respective solvent

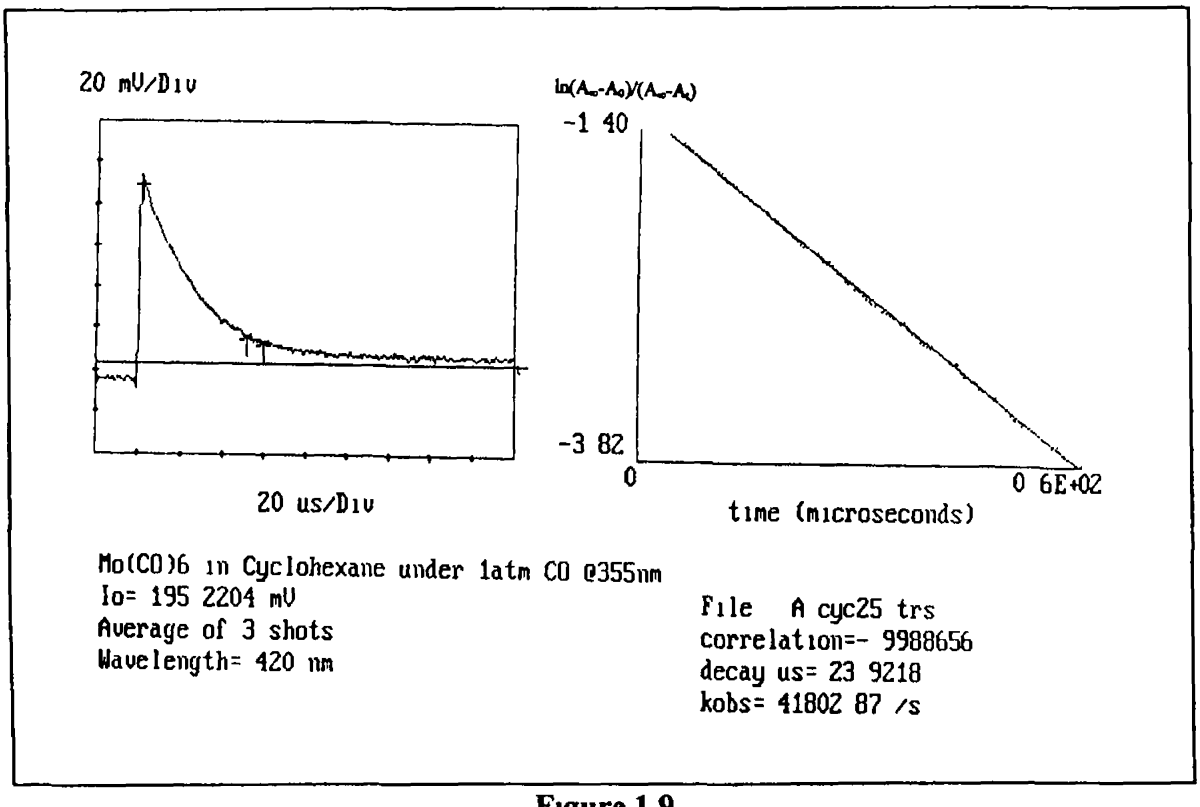

Figure 1.9

(Decay of $Mo(CO)_5$(Cyclohexane) monitored at 420 nm)

1 2 4 Activation parameters

The activation parameters the k_{obs} were obtained by measuring over a temperate range of 279-310 K and Eyring and Arrhenius plots were then constructed This assumed a zero intercept in the plot of k_{obs} vs [CO] From these plots it was possible to obtain the activation parameters for the reaction of $M(CO)_5(S)$ with CO, all the experimental data are in Appendix IB Figure 1 10 shows an Arrhenius and Eyring plot for $W(CO)_6$ in Cyclohexane

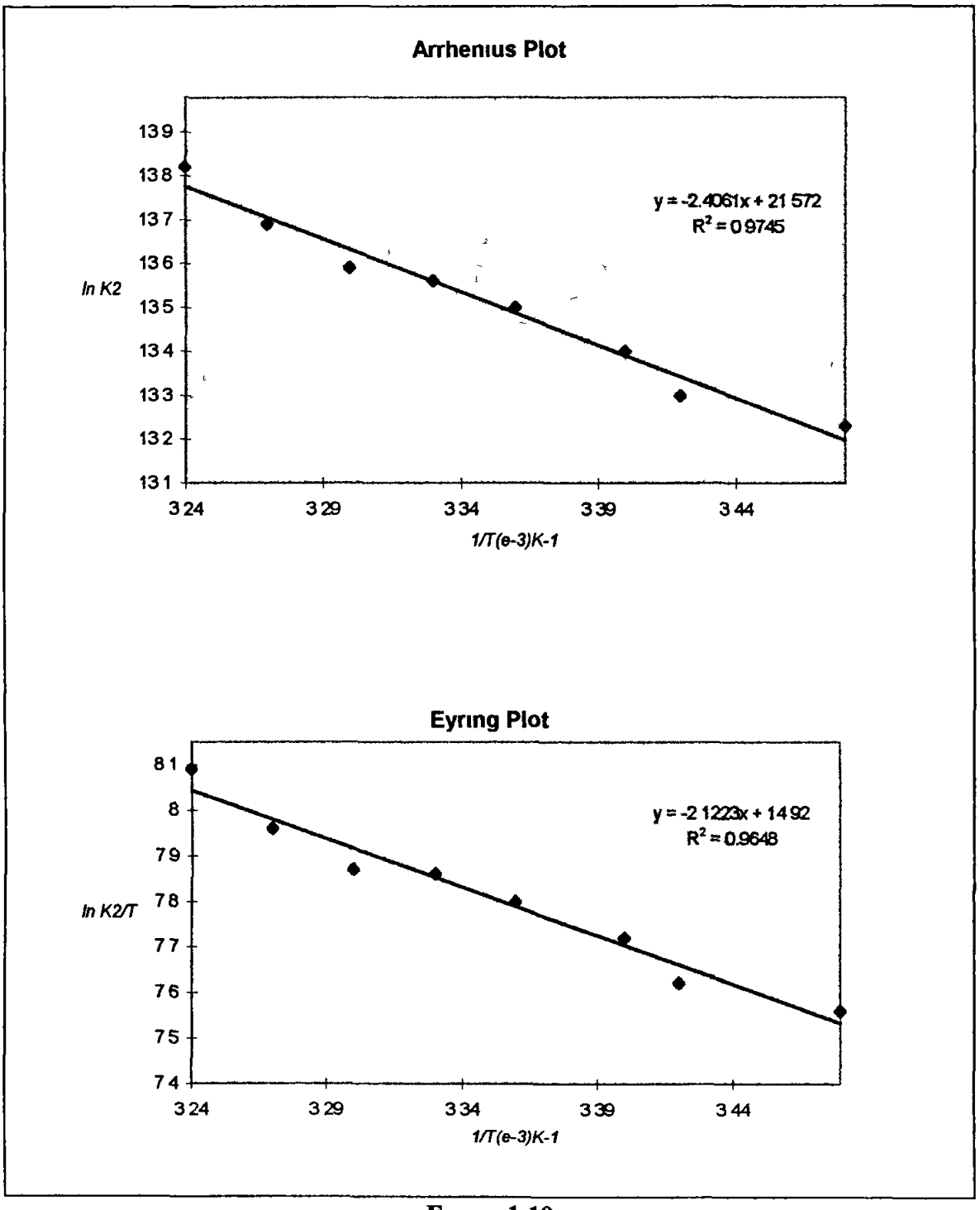

Figure 1.10

(Arrhenius and Eyring plots for Reaction 1.1 (M = W), in Cyclohexane)

The second order rate constants and the activation parameters obtained in these studies are presented in Table 1.2

	Solvent	k_2[a]	[b]$Ea^{\neq}$	[c]$\Delta H^{\neq}$	[d]$\Delta S^{\neq}$	[e]$\Delta G^{\neq}$
$Cr(CO)_5(S)$	[f]Cyclo	$2\,3 \times 10^6$	25	22	-46	35
	[g]Mecyclo	$3\,5 \times 10^6$	26	24	-40	35
	Heptane	$9\,3 \times 10^6$	23	21	-42	33
	Decane	$1\,2 \times 10^7$	26	23	-30	33
	Dodecane	$2\,4 \times 10^7$	26	24	-24	31

	Solvent	k_2	$Ea^{\neq}$	$\Delta H^{\neq}$	$\Delta S^{\neq}$	$\Delta G^{\neq}$
$Mo(CO)_5(S)$	[f]Cyclo	$4\,7 \times 10^6$	22	21	-48	35
	[g]Mecyclo	$5\,8 \times 10^6$	23	21	-45	34
	Heptane	$7\,8 \times 10^6$	24	21	-41	34
	Decane	$8\,8 \times 10^6$	23	21	-42	33
	Dodecane	$4\,9 \times 10^7$	20	19	-35	29

	Solvent	k_2	$Ea^{\neq}$	$\Delta H^{\neq}$	$\Delta S^{\neq}$	$\Delta G^{\neq}$
$W(CO)_5(S)$	[f]Cyclo	$7\,2 \times 10^5$	20	18	-73	40
	[g]Mecyclo	$2\,1 \times 10^6$	22	20	-58	37
	Heptane	$1\,8 \times 10^6$	23	20	-58	37
	Decane	$1\,1 \times 10^6$	23	21	-59	38
	Dodecane	$1\,7 \times 10^6$	22	20	-60	38

[a] @ 298 ± 2 K, ($dm^3\ mol^{-1}\ s^{-1}$), [b] ±2 kJ mol^{-1}, [c] ±2 kJ mol^{-1}, [d] ±4 J K^{-1} mol^{-1}, [e] ±2 kJ mol^{-1},

[f]Cyclo = Cyclohexane, [g]Mecyclo = Methylcyclohexane

Table 1 2

(Second Order Rate constants and activation parameters for $M(CO)_5(S)$)

1 2 6 Discussion

There are a number of trends that can be observed from the data presented in Table 1 2 Investigating the $Cr(CO)_6$ results first it can be seen that there is an obvious increase in the k_2 value in going from cyclohexane to dodecane This increase in the rate of reaction is not reflected in the $\Delta H^{\neq}$ values, which are found to be the same, within experimental error (22 ± 2 kJ mol^{-1}) As the reactions of the "naked" $Cr(CO)_5$ with alkanes are close to the diffusion controlled limit ($6\ 6 \times 10^9$ dm^3 mol^{-1} s^{-1}, for cyclohexane with $Cr(CO)_5$)[8], the $\Delta H^{\neq}$ term for the reaction of $Cr(CO)_5$(sol) with CO should approximate the bond energy of the metal to solvent bond The binding energy for Cyclohexane, 52 kJ mol^{-1}, obtained from photoacoustic calorimetry (PAC) measurements, is nearly twice the value obtained in this study However similar studies carried out on the $W(CO)_6$ system, employing PAC, yielded higher values for the binding energies, than $\Delta H^{\neq}$ values obtained from kinetic studies [48] A dissociative mechanism for the Reaction 1 2 would require a $\Delta H^{\neq}$ value approximating the interaction energy obtained in the PAC

$$Cr(CO)_5(S) + CO \rightarrow Cr(CO)_6 + S \qquad \textit{Reaction 1 2}$$

measurements As the $\Delta H^{\neq}$ values obtained in this study are half the interaction energy it would appear that a dissociative mechanism is precluded The $\Delta H^{\neq}$ values required for a

dissociative mechanism compared to values obtained in this study as depicted in Figure 16

As there is no correlation between the $\Delta H^{\neq}$ values and the rate of Reaction 12, the variation in the rates must be reflected in the $\Delta S^{\neq}$ term. The $\Delta S^{\neq}$ term becomes less negative as the solvent changes from cyclohexane to dodecane, varying from -46 J K^{-1} mol^{-1} to -24 J K^{-1} mol^{-1} respectively. The $\Delta S^{\neq}$ values would be expected to be closer to zero, if not positive, for a dissociative mechanism and an associative mechanism should result in more negative values than those obtained, *i e* there would be a significant decrease in the entropy of the reaction at the transition state. Therefore the $\Delta S^{\neq}$ values appear to indicate that the mechanism for the displacement of the solvent from $Cr(CO)_5$ occurs *via* an interchange process. An interchange mechanism has also been postulated for the displacement of cyclohexane and methylcyclohexane from $W(CO)_5$ by 4-Acetylpyridine[65] and the displacement of solvent (S) from (η^6- arene)$Cr(CO)_2$(S) by CO[66]. Yang *et al*[40] concluded that there was considerable lengthening of the Cr to heptane bond concurrent with the association of either pyridine and 2-picoline as the incoming ligand. It was reported that the $\Delta H^{\neq}$ value was ~21 kJ mol^{-1} for the replacement of heptane by pyridine, which is lower than the reported Cr-heptane interaction energy, therefore indicating that this reaction also was not a dissociative mechanism, but in fact an interchange mechanism. Pyridine as a nucleophile is very similar to CO, except that it possesses reduced π^* accepting ability.

The $\Delta S^{\neq}$ values reflect the differences in the k_2 values, the reason for this could be as a result of the motional freedom attained by the solvents upon desolvation When an alkane solvent forms an agostic bond with the $Cr(CO)_5$ moiety its motional freedom is restricted, this is more evident for the longer chain alkanes Therefore the rate of displacement would be faster for the longer chain alkanes as the removal of the restriction leads to a more favourable orientation for the solvent

Investigating the effect of increasing the atomic mass of the metal, it can be seen from Table 1 2 that the change of solvent does not have as significant an effect as for the chromium system The rates for solvent displacement from $W(CO)_5$ for the straight chain alkanes show very little variation and this is reflected in the $\Delta S^{\neq}$ values The $\Delta S^{\neq}$ values are smaller than those reported for the chromium system, this is a reflection of the size of the metal, as the larger metal leads to less steric hindrance Seven coordinate chemistry is extensive for Mo and W, however it is not for the Cr system The fact that there is not the same steric hindrance around the tungsten is also reflected in the slower rates of reaction, as the motional freedom of the solvent is not as restricted as for the chromium system The rate of displacement of cyclohexane from the $W(CO)_5$ moiety does appear to be slower than the other solvents, this difference in rate is reflected in the $\Delta S^{\neq}$ value which is slightly more negative, thus indicating that cyclohexane is not as restricted upon coordination to tungsten

The $\Delta S^{\neq}$ values again support an interchange mechanism for $Mo(CO)_6$, as the metal is larger than chromium, the steric hindrance is not as pronounced, therefore it can be seen that there is no variation between heptane and decane, within experimental

error Dodecane does have a faster rate of reaction, this is reflected in the slightly more negative value for the $\Delta S^{\neq}$, indicating the restriction placed on the solvent upon coordination and the subsequent freedom of rotation achieved upon desolvation

1 2 7 Conclusions

In this study, any variation for the rate reaction from the $M(CO)_5(S)$ species is only reflected in the values for the entropy of activation The values for the enthalpy of activation remain constant This is also reflected in the similarity in the position of the $M(CO)_5(S)$ peaks in the UV/visible spectra for the various solvents The relationship between the $\Delta S^{\neq}$ values and the k_2 values can be explained in terms of the liberation of motional freedom attained upon desolvation, which influences the kinetics of the reaction

The activation parameters obtained for the Reaction 1 3, (where M = Cr, Mo or W) can be interpreted as evidence for a gradual changeover from an interchange mechanism to a more associative type mechanism along the series Cr, Mo to W This trend along the series, towards a more associative mechanism has been observed

$$M(CO)_5(S) + CO \rightarrow M(CO)_6 + S \qquad \textit{Reaction 1 3}$$

previously [47,67] The fact that the variation in rates is not as apparent for the Mo and W systems could be as a result of the larger size of these metals compared to the chromium system The solvents will therefore not be as restricted upon coordination to the larger metals Therefore alkane chain length does not play as significant a role in the kinetics of the larger metals, as the impetus to attain motional freedom upon desolvation is not as pronounced

REFERENCES

(Chapter 1)

[1] (a) Orgel L E *Nature*, 1961, **191**, 1387

(b) Dobson G R., El Sayad M A , Stolz I W , *Inorg Chem* , 1962, **1**, 526

(c) Strohmeier W , *Chem Ber* , 1961, **94**, 3337

[2] Stolz I W , Dobson G R , Sheline R K , *J Am Chem Soc* , 1962, **84**, 3589-3599

[3] Stolz I W , Dobson G R , Sheline R K , *J Am Chem Soc* , 1963, **85**, 1013-1014

[4] Boylan M J , Braterman P S , Fullarton A , *J Organometal Chem* , 1971, **31**, C29

[5] Graham M A , Perutz R N , Poliakoff M , Turner J J , *J Organometal Chem* , 1972, **34**, C34

[6] (a) Graham M A , Rest A J , Turner J J , *J Organometal Chem* , 1970, **24**, C54

(b) Graham M A., Poliakoff M , Turner J J , *J Chem Soc A*, 1971, 2939

[7] Kelly J M , Hermann H , Koerner von Gustorf E , *J Chem Soc , Chem Commun* 1973, 105

[8] Kelly J M , Bent D V , Hermann H , Schulte-Frohlinde E , Koerner von Gustorf E , *J Organometal Chem* , 1974, **69**, 259

[9] Perutz R N , Turner J J , *J Am Chem Soc* , 1975, **97**, 4791

[10] Burdett J K , *J Chem Soc , Faraday Trans II*, 1974, **70**, 1599

[11] Burdett J K , Grzybowski J M , Perutz R N , Poliakoff M , Turner J J , Turner R F , *Inorg Chem* 1978, **17**, 147

[12] (a) Poliakoff M , *Inorg Chem* , 1976, **15**, 2022

(b) Poliakoff M , *Inorg Chem* , 1976, **15**, 2892

[13] Hay P J , *J Am Chem Soc* , 1978, **100**, 2411

[14] Bonneau R., Kelly J M , *J Am Chem Soc* , 1980, **102**, 1220

[15] Kelly J M , Long C , Bonneau R., *J Phys Chem* , 1983, **87**, 3344

[16] (a) Maier II W B , Poliakoff M , Simpson M B , Turner J J , *J Chem Soc* , *Chem Commun* , 1980, 587

(b) Maier II W B , Poliakoff M , Simpson M B , Turner J J , *Inorg Chem* , 1983, **22**, 911

[17] Simpson M B , Poliakoff M , Turner J J , Maier II W B , McLaughlin J G , *J Chem Soc , Chem Commun* , 1983, 1355

[18] (a) Upmacis R K , Poliakoff M , Turner J J , *J Am Chem Soc* , 1986, **108**, 3645

(b) Jackson S A , Upmacis R K , Poliakoff M , Turner J J , Burdett J K , Grevels F W , *J Chem Soc , Chem Commun* , 1987, 678

[19] Simon J D , Peters K S , *Chem Phys Lett* , 1983, **98**, 53

[20] Simon J D , Xie X , *J Phys Chem* , 1986, **90**, 6751

[21] Simon J D , Xie X , *J Phys Chem* , 1987, **91**, 5538

[22] Simon J D , Xie X , *J Phys Chem* , 1989, **93**, 291

[23] Joly A G , Nelson K A , *J Phys Chem* , 1989, **93**, 2876

[24] Simon J D , Xie X , *J Am Chem Soc* , 1990, **112**, 1130

[25] Wang L , Zhu X , Spears K G , *J Am Chem Soc* , 1988, **110**, 8695

[26] Wang L , Zhu X , Spears K G , *J Phys Chem* , 1989, **93**, 2

[27] Xie X , Simon J D , *J Phys Chem* , 1989, **93**, 4401

[28] Lee M , Harris C B , *J Am Chem Soc* , 1989, **111**, 8963

[29] Joly A G , Nelson K A , *Chem Phys* , 1991, **152**, 69

[30] Weitz E , *J Chem Phys* , 1987, **91**, 3945

[31] (a) Nathanson G , Gitlan B , Rosan A M , Yardly J T , *J Chem Phys* , 1981, **74**, 361

(b) Yardly J T , Gitlan B , Nathanson G , Rosan A.M , *J Chem Phys* , 1981, **74**, 370

[32] Tumas W , Gitlan B , Rosan A M , Yardly J T , *J Am Chem Soc* , 1982, **104**, 55

[33] Lewis K E , Golden D M , Smith G P *J Am Chem Soc* , 1984, **106**, 3905

[34] Seder T A , Church S P , Ouderkirk A J , Weitz E , *J Am Chem Soc* ,
1985, **107**, 1432

[35] BreckenridgeW H , Stewart G M , *J Am Chem Soc*, 1986, **108**, 364

[36] Seder T A , Church S P , Weitz E *J Am Chem Soc*, 1986, **108**, 4721

[37] Ishikawa Y , Hackett P A , Raynor D M , *J Phys Chem* , 1988, **92**, 3863

[38] (a) Ishikawa Y , Brown C E , Hackett P A , Raynor D M , *Chem Phys Lett* 1988,
150, 506

(b) Brown C E , Ishikawa Y , Hackett P A , Raynor D M , *J Am Chem Soc*,
1990, **112**, 2530

[39] Yang G K , Peters K S , Vaida V , *Chem Phys Lett* , 1986, **125**, 566

[40] Yang G K , Vaida V , Peters K S , *Polyhedron*, 1988, 7, 1619

[41] Morse J M , Parker G H , Burkey T J , *Organometallics*, 1989, **8**, 2471

[42] Wieland S , van Eldik R , *J Phys Chem* , 1990, **94**, 5865

[43] Nayak S K , Burkey T J , *Organometallics*, 1991, **10**, 3745

[44] Graham J R , Angelici R J , *Inorg Chem* 1967, **6**, 2082

[45] Hermann H , Grevels F -W , Henne A., Schnaffer K , *J Phys Chem* , 1982, **86**, 5151

[46] Church S P , Grevels F W , Hermann H , Schaffner K , *Inorg Chem* 1985, **24**, 418

[47] Lees A , Adamson A W , *Inorg Chem* 1981, **20**, 4381

[48] Wieland S , van Eldik R , *Organometallics*, 1991, **10**, 3110

[49] Dobson G R , Asali K J , Cate C D , Cate C W , *Inorg Chem* 1991, **30**, 4471

[50] Zhang S , Dobson G R , *Organometallics*, 1992, **11**, 2447

[51] Walsh M M , PhD Thesis at Dublin City University 1993

[52] Oishi S , *Organometallics*, 1988, 7, 1237

[53] Zhang S , Zang V , Dobson G R , van Eldik R , *Inorg Chem* 1991, **30**, 355

[54] Creaven B S , Grevels F W , Long C , *Inorg Chem* 1989, **28**, 2231

[55] Wieland S , van Eldik R , *J Chem Soc , Chem Commun* , 1989, 367

[56] Wieland S , Reddy K B , van Eldik R , *Organometallics* 1990, **9**, 1802

[57] Schadt M J , Gresalfi N J , Lees A J , *Inorg Chem* 1985, **24**, 2942

[58] Schadt M J , Lees A J , *Inorg Chem* 1986, **25**, 672

[59] Kalyanasundaram K , *J Phys Chem* 1988, **92**, 2219

[60] Zhang S , Dobson G R , *Inorg Chem* 1990, **29**, 598

[61] Lindsay E , Vlcek Jnr A , Langford C , *Inorg Chem* 1993, **32**, 2269

[62] Grevels F W , Kayran C , Ozkar S , *Organometallics* 1994, **13**, 2937

[63] Brookhart M , Green M L H , *J Organomet Chem* 1983 **250** 395

[64] Makranczy J , Megyery-Balog K , Rosz L , Patyt D , *Hungarian J Indust Chem* , 1976, **4**, 169

[65] Dobson G R , Spradling M D , *Inorg Chem* , 1990, **29**, 880

[66] Creaven B S , George M W , Ginzberg A G , Hughes C , Kelly J M , Long C , McGrath I M , Pryce M T , *Organometallics,* 1993, **12**, 3127

[67] (a) Zhang S , Dobson G R , Bajaj H C , Zang V , van Eldik R , *Inorg Chem* , 1990, **29**, 3477

(b) Zhang S , Zang V , Bajaj H C , Dobson G R , van Eldik R , *J Organomet Chem* , 1990, **397**, 279

CHAPTER 2

2.1 LITERATURE SURVEY

2 1 1 Photochemistry of (η^6-arene)M(CO)$_3$ complexes

Early reports on the chemistry of (η^6-arene)M(CO)$_3$ complexes claimed that both arene exchange[1] (Reaction 2 1) and CO loss[2] (Reaction 2 2) were general photoreactions

$$(\eta^6\text{-arene})M(CO)_3 \xrightarrow[\text{arene*}]{h\nu} (\eta^6\text{-arene*})M(CO)_3 + \text{arene} \qquad \textit{Reaction 2 1}$$

$$(\eta^6\text{-arene})M(CO)_3 \xrightarrow[L]{h\nu} (\eta^6\text{-arene})M(CO)_2L + CO \qquad \textit{Reaction 2 2}$$

When M = Cr the quantum yield (Φ) for Reaction 2 2 is high and many (η^6-arene)Cr(CO)$_2$L complexes can be synthesised by photochemical methods Reaction 2 2 was also observed for the Mo analogue[3] however the W species was found to be photoinert This was a curiosity given the similarities in the photochemistry of the M(CO)$_6$ system (M = Cr, Mo, or W) Wrighton *et al*[4] reported that the Φ for the formation of (η^6-arene)Cr(CO)$_2$(pyridine) was 0 72, (where arene = benzene or mesitylene) following photolysis of (η^6-arene)Cr(CO)$_3$ in the presence of pyridine This

was later confirmed by Gilbert *et al* [5] and the efficiency of the arene exchange was given as approximately a sixth of this value Reaction 2 1 was found to be suppressed by the addition of CO and this reaction was only a minor component in the overall photochemistry These results were consistent with dissociative loss of CO as the primary excited state decay process of (η^6-arene)Cr(CO)$_3$ A relatively high Φ was reported for the displacement of CO from (η^6-mesitylene)Cr(CO)$_3$ by *N*-dodecylmaleimide in benzene of 0 9,[6] no benzene - mesitylene exchange was observed in these experiments

Continuous photolysis of (η^6-arene)Cr(CO)$_3$ complexes produces both the arene ring and Cr(CO)$_6$ [7] Bamford *et al* [8] observed that upon addition of CCl_4 the rate of arene generation increased, while in the absence of CCl_4, CO suppresses the reaction as a result of recombination with the (η^6-arene)Cr(CO)$_2$ species

Oxidative addition of a trisubstituted silane to (η^6-arene)Cr(CO)$_2$ had been established to result from irradiation of the tricarbonyl species in solution, producing the coordinatively unsaturated (η^6-arene)Cr(CO)$_2$ species As a result of the high efficiency of the CO loss from these compounds, even at low temperatures,[9] these compounds were studied in order to elucidate the quantitative data regarding oxidative addition, as the CO dissociation could be induced faster than the thermal oxidative reaction [10] Trisubstituted silanes underwent oxidative addition to a number of photochemically generated (η^6-arene)Cr(CO)$_2$ species The reactions of silanes with transition metal carbonyl complexes are of interest because hydrosilation is a reaction of considerable importance Beyond this, however, the reactions of silanes serve as readily studied analogues of C-H bond activation

CO loss from (η^6-arene)M(CO)$_3$ has also been observed in the gas phase, the ejection of one CO was the predominant process upon 355 nm excitation, while the production of (η^6-arene)M(CO) and (η^6-arene)M(CO)$_2$ in a ration of 5 2 was observed upon 266 nm excitation [11] The extreme reactivities of these coordinatively unsaturated species was again demonstrated by the observation of addition of N_2 and H_2 to (η^6-C_6H_6)Cr(CO)$_2$ in the gas phase [12] Kubas *et al* [13] had observed and isolated products with an M-η^2 H_2 non classical type of interaction Zheng *et al* [12] concluded that the dihydrogen complexes formed in the gas phase were "non-classical" molecular hydrogen complexes, as the CO frequencies did not shift to the higher wavenumbers as would be expected for bonding in a classical dihydride, because of the oxidation of the metal centre

2 1 2 Thermal chemistry of (η^6-arene)M(CO)$_3$ complexes

Although CO loss from the excited state of (η^6-arene)M(CO)$_3$ appears to be the most efficient process, arene exchange reactions dominate the ground state (*i e* thermal) reactions Arene exchange between free arene and an (η^6-arene)M(CO)$_3$ complex generally requires elevated temperatures if the solvent is either an aromatic hydrocarbon or a non-coordinatmg solvent Arene exchange can occur by a number of mechanisms Firstly, it can proceed by an intramolecular dissociative process, which involves either complete arene dissociation or possibly a multistepped ligand dissociation [for (η^6-arene)ML$_3$ species] prior to the new ligand coordinatmg Secondly, intramolecular arene associative processes are possible, which results from a rearrangement prior to the association of the new arene Finally an intermolecular process

is possible, where the high energy species are stabilised by interaction with the parent complex, either *via* a M-L-M (if L is an effective bridging molecule) or a M-arene-M type bond [14]

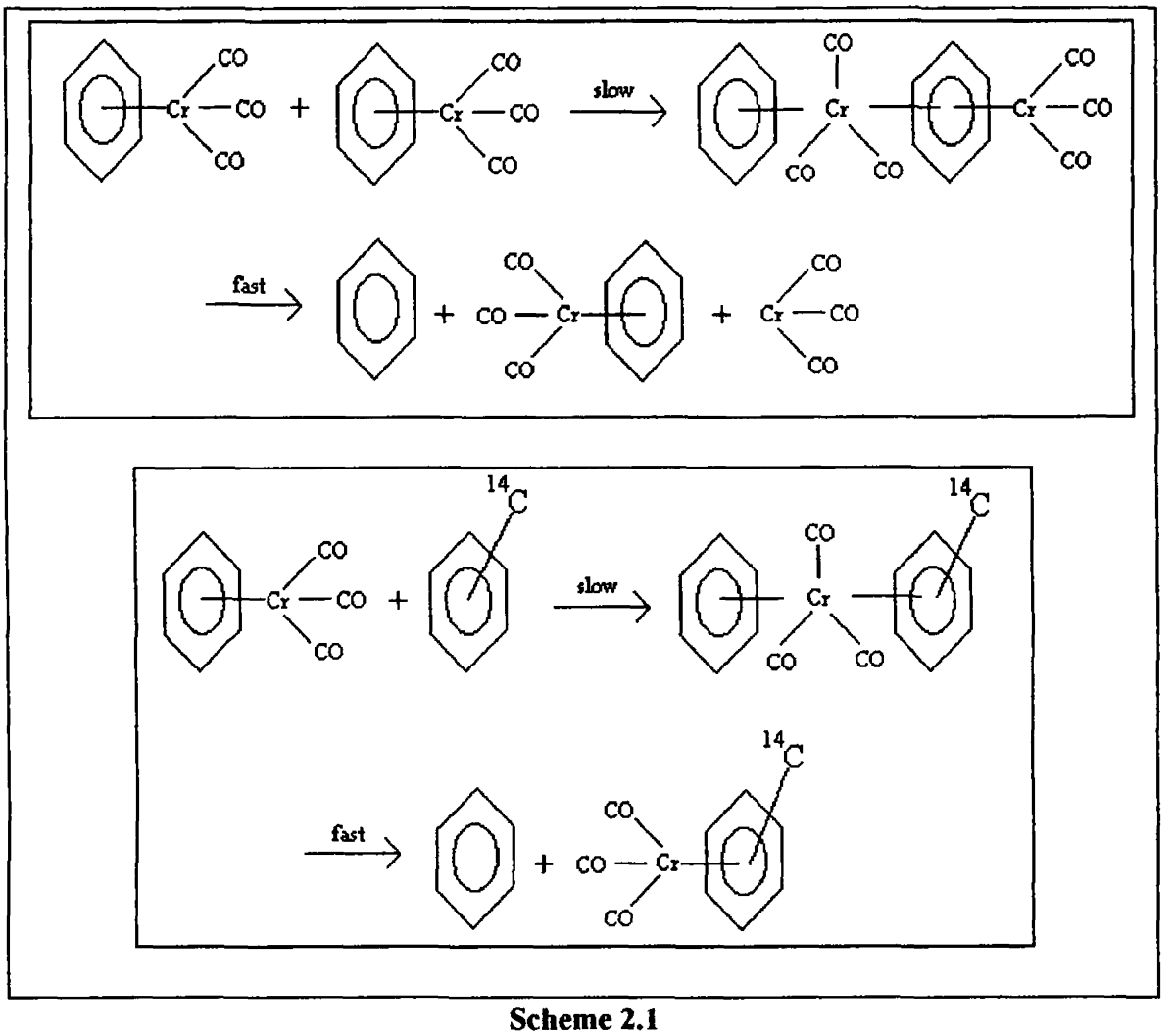

Scheme 2.1

(Proposed mechanism for arene displacement indicating simultaneous exchange of two complex molecules[15])

Strohmeier *et al* [15] reported that a major component of arene exchange reactions in heptane (or heptane/THF mixtures) follows second order kinetics, the rate

constant was independent of arene concentrations This led to the mechanism presented in Scheme 2 1

However this mechanism was not compatible with the observation of Jackson *et al* [16] that *cis-* or *trans-* complexes of 1- or 2-methylindane failed to isomerize on heating in the absence of the free arene Catalysis of arene exchange by donor solvents was demonstrated by Mahaffy and Pauson[17] thus indicating that the solvents initiated partial arene displacement from the metal (Scheme 2 2) Moreover, Zimmerman *et al* [18] also reported the presence of a, presumably solvent stabilised, $Cr(CO)_3$ fragment Therefore stressing the more specific role that donors played in promoting the arene displacement reaction than previously assumed [15]

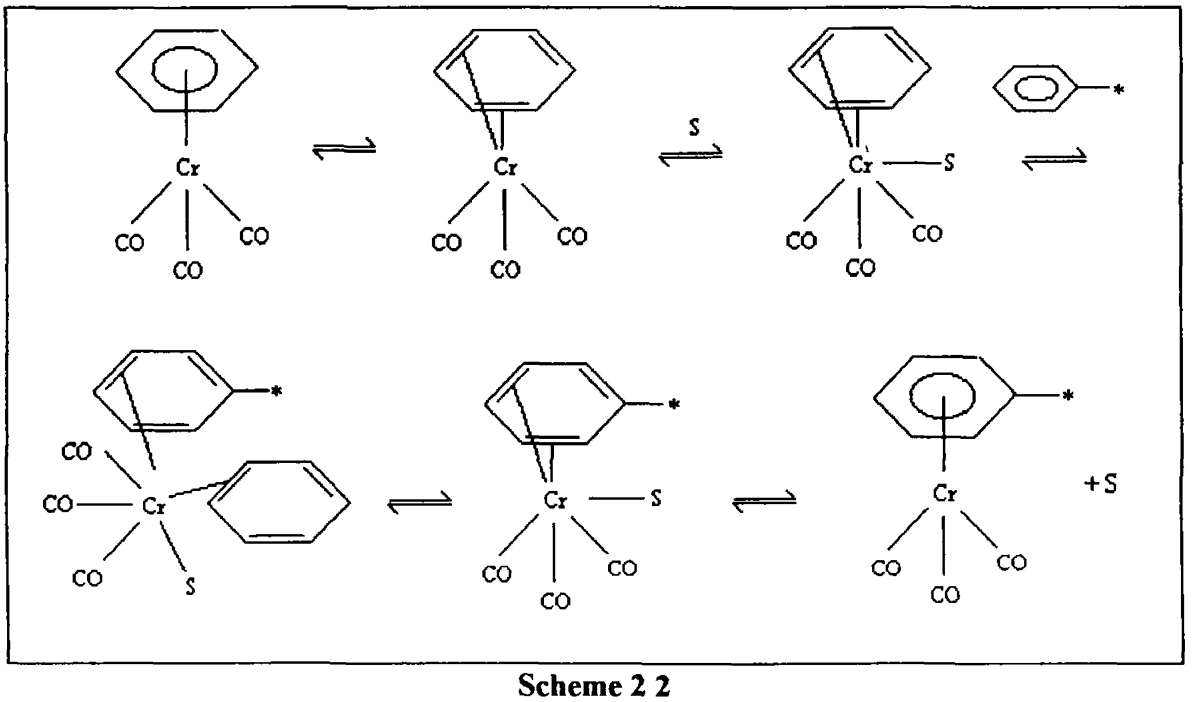

Scheme 2 2

(Solvent initiated arene displacement [17])

A thorough investigation was conducted by Traylor, Stewart and Goldberg[19] into the mechanisms for arene exchange in these systems It was reported that the CO ligand can act as a nucleophilic catalyst,[19(a)-(c)] resulting in CO redistribution between the two complexes As the CO ligand was known to be capable of acting as a bridging ligand the possibility of a bridged complex was also considered The π system of the arene ring was then extended and the neighbouring group participation was investigated, these results confirmed the possibility that the coordination of the arene ring could be "unzipped" from η^6 to η^4 to η^2 Although no direct evidence for such a process was obtained

2 1 3 Haptotropic rearrangements

The term haptotropic rearrangements refers to cases where an ML_n unit changes its connectivity (hapto number) with some ligand possessing multicoordinate site possibilities In the majority of cases the ligand is a polyene, as a result the coordination site changes from one coordination site to another in a bicyclic polyene Albright *et al*[20] conducted theoretical investigation of the minimum energy pathways for shifting an ML_n group from one ring to another in a bicyclic polyene Howell *et al*[21] calculated the dynamics of ring slippage, employing extended Huckel molecular orbital calculations to investigate the energetics of the proposed haptotropic rearrangements A potential energy surface was created for the slippage of an MnCp group in benzene-MnCp This provides a good model for the $Cr(CO)_3$ group in the analogous group 6 system Figure 2 1 depicts the potential energy surface for the slipping of the MnCp group in benzene-MnCp

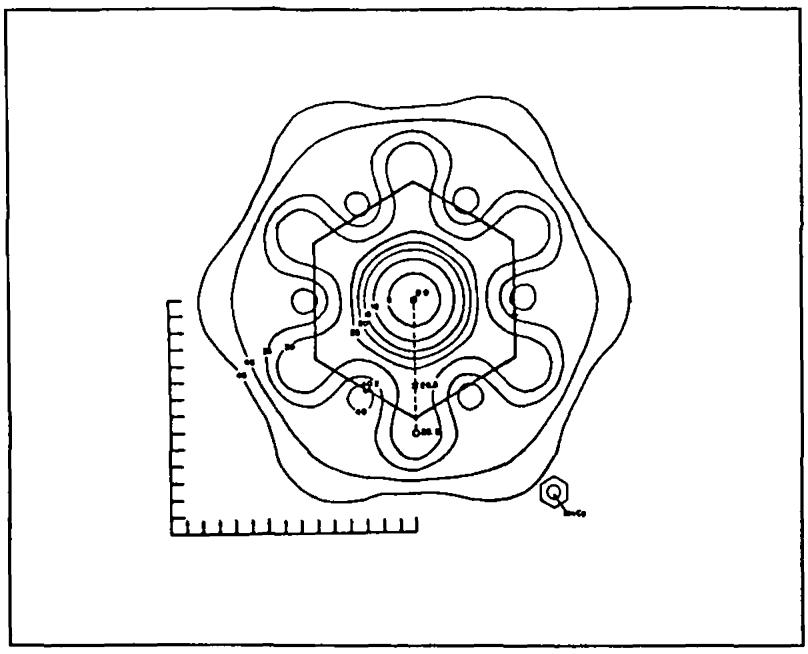

Figure 2.1

(The distance scale on the lower left is plotted in 0 2 Å intervals, the energy contours are in kcals mol[-1] The ground state is given by the large solid circle, a minimum by an open circle, and a transition state by a cross The energies of these points relative to the ground state are explicitly given [21])

It was found that the potential surface around the η^6 ground state is nearly circular and quite steep until the MnCp group reaches the periphery of the benzene ring There was no evidence for the intervention of a discrete η^4 intermediate The potential was found to rise as the coordination moved towards an η^1 intermediate until it reached a transition state, then continuing along the reaction path leading to an intermediate that could have been labelled as the η^1 species, however there was still substantial bonding from the neighbouring carbons The orbital interactions for (η^6benzene)$Cr(CO)_3$ have been discussed in the introduction It can be seen that there is not a great deal of interaction lost between the d_z^2 and the a_{2u} orbital upon slipping towards the η^1 configuration, thus the energy of this orbital remains nearly constant The interaction

between the e_{1gb} and the d_{yz} is affected slightly more than the e_{1ga} to the d_{xz} interaction Given this rise in energy there is still a significant stabilisation of the benzene ring orbitals upon coordination to the $Cr(CO)_3$ unit, this stabilisation persists in the η^1 configuration The filled orbitals on the metal, which could be viewed as three lone pairs that are directed between the CO ligands, are destabilised along the reaction path as a result of repulsion between them and the benzene σ orbitals This destabilisation results in mixing of the filled molecular orbital and the empty receptor orbitals on the metal, which causes the orbital to become stabilised and could explain the shallow minimum depicted in the potential energy surface presented in Figure 2 1

The haptotropic rearrangement was also examined for (η^6-2,6-dimethylpyridine)$Cr(CO)_3$, it was found that arene exchange reactions were faster for this compound, compared even to the naphthalene analogue The binding energy was found to be the very close for the two compounds, and this was estimated to be 183 kJ mol^{-1} for the (η^6 pyridine)$Cr(CO)_3$ compound By comparison the addition of two methyl groups, at the 2 and 6 positions on the pyridine ring, raised the energy by 8-13 kJ mol^{-1} Slippage of the ring to the C_3 in the 2,6-dimethylpyridine was said to be more favourable than the analogous slippage in the benzene, as there is intermixing of the π and the π^* orbitals in the pyridine this leads to more electron density on the C_3 and the C_5, making this reaction path more favourable Replacement of the CH group in the benzene by the more electronegative N atom leads to splitting of the degenerate e_{1gb} and e_{1ga} orbitals, with the e_{1gb} orbital being lowered in energy Therefore its stabilisation by the d_{xz} orbital on the metal is decreased, as a result of which the η^6- η^1 reaction path is more favoured

2 1 4 Molecular orbitals for η^6 pyridine vs η^1 pyridine

The interaction of the benzene ring with a $Cr(CO)_3$ unit has been discussed in the introduction and is depicted in Figure 4 In this study the arene employed was pyridine and, as indicated, the substitution of a carbon in the benzene ring for a nitrogen does affect the energy levels of the molecular orbitals Figure 2 2 depicts the changes in the molecular orbitals from benzene to pyridine The intermixing of the π and the π^* orbitals in the pyridine redistributes the electron density From the perturbations in the molecular orbitals on the pyridine ring it can be seen that the interaction with the e_{1gb} and the d_{yz} should not be greatly different from the benzene analogue However the lowering of the energy of the e_{1ga} leads to the destabilisation of its interaction with the d_{xz} orbital on the metal [22] Therefore pyridine should be a poorer π-donor ligand and a better π-acceptor to a metal centre than benzene

When the nitrogen binds to the metal in an η^1 mode, the $\pi \rightarrow \pi^*$ transitions of the pyridine ring are not affected because the bonding is directly through the lone pair The transition from the $n \rightarrow \pi^*$ level on the ring is significantly altered and the $n\pi^*$ state becomes obscured by often energetically similar energy levels

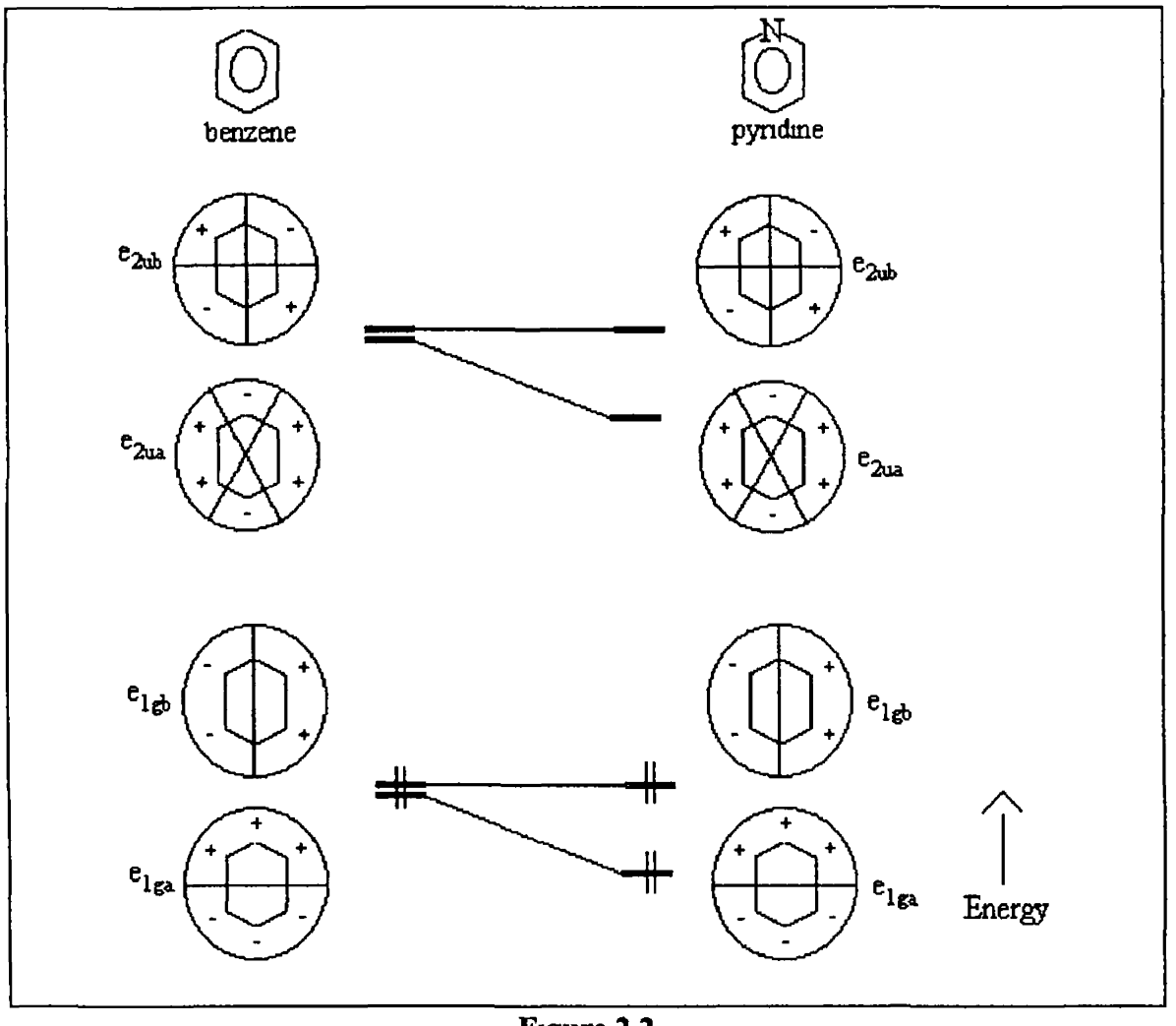

Figure 2.2

(Molecular perturbations of the HOMO and LUMO levels in benzene and pyridine)

The differences between σ and π bonding have also been observed in chemisorbed pyridine on Ni(001) [23] The π bonded species was observed at low coverages and when the temperature was raised to room temperature It was found that the $\pi \rightarrow \pi^*$ transitions were not observed for the π bonded species in the electron energy loss study A strong metal to ligand charge transfer was observed for the σ bonded species, which is consistent with a low lying π^* acceptor orbital on the pyridine

2 1 5 Pyridine as a η^6 ligand

There have been very few reported π pyridine metal complexes in the literature until recently [24] The earliest type of complex was synthesised by Timms P L [25] using the cocondensation reaction of "hot" chromium atoms with pyridine and trifluorophosphine (PF_3), to form (η^6-pyridine)$Cr(PF_3)_3$ The yield was very low and the main products of the reaction was the σ bonded complex (σ-pyridine)$Cr(PF_3)_5$ A number π complexes were reported employing substituted pyridine rings, where the nitrogen was sterically protected by methyl groups[26] and were produced by direct complexation of chromium hexacarbonyl in dioxan Employing the same strategy of sterically blocking the nitrogen, bis(η^6-2,6-dimethylpyridine)chromium was also synthesised [27] In order to prevent bonding *via* the nitrogen Fischer *et al* [28] used *N*-methyldihydropyridine ligands, resulting in the formation of (1-methyl-1,2,-dihydropyridine)$Cr(CO)_3$, which is complexed *via* an η^2-alkenyl and an η^3- 4 electron vinylamine system

Formation of an η^6 pyridine complex $Mo(PMePh_2)_3$(η^6 pyridine) from a σ bonded pyridine in $Mo(N_2)_2(NC_5H_5)(PMePh_2)_3$ was reported [29] Pyridine has also been reported to act as an η^6 ligand when bonded to ruthenium [30] The polymeric complex $[Cp^*RuCl]_n$ (where $Cp^* = \eta^5$-C_5Me_5), was employed as a precursor for the production of [Cp*Ru(η^6 pyridine)]Cl [29(a)] The compound $Ru(Cp)(CH_3CN)_2$(2,methylpyridine) was reported[29(b)] to thermally rearrange to Ru(Cp)(2,methylpyridine)$^+$

When Elschenbroich *et al* [31] reported the synthesis of bis(η^6-pyridine)Cr in 1988, interest was renewed for the synthesis of other η^6-pyridine complexes The

observed from the W species was therefore considered to be LF in character and the emission lifetimes were in the range expected for heavy-metal complexes exhibiting emission which has spin forbidden character

Luminescence assigned as originating in a low lying MLCT excited state has been reported from complexes of the general formulae $M(CO)_5L$ and $M(CO)_4L_2$, where M = W, Mo, and L = an electron donor ligand, in low temperature glasses[35] or matrices [36] The failure of group 6 metal carbonyl complexes to luminesce in solution was attributed to the relatively high photoreactivities and efficient nonradiative decay of the excited states of these complexes However, Lees[37] reported electronic absorption, emission and excitation spectra obtained from a series of $Mo(CO)_5L$ species (where L was a series of 4-substituted pyridine ligands) in room temperature solution In the electronic spectra of each of the complexes the position and the intensity of a shoulder (430 - 450 nm), observed on the more intense LF transition, was found to be dependent on the nature of the solvent This band was assigned to an MLCT transition, and the strongly electron withdrawing substituents yielded substantially lower energy MLCT absorptions Broad, unstructured emission with quantum yields in the order of 10^{-4}-10^{-3} was reported from these complexes, following excitation at 436 nm, in room temperature benzene This emission was assigned to be from the low lying MLCT excited state Importantly, for $Mo(CO)_5$(pyridine) in which the lowest lying excited state is LF in character,[36] no emission at room temperature was observed Therefore investigating a wide variety of $M(CO)_5L$ complexes enables the formulation of a theoretical model which embodies the

excited state characteristics of these species and provides the possibility of excited state tuning

Room temperature emission was also observed from $M(CO)_4L_2$ complexes (L = pyridine or a substituted pyridine) [38] Again the emission was found to originate from the low energy MLCT excited state For complexes of the general formula $M(CO)_4L$ (M = Cr, Mo or W and L = diimine ligand) the variation in energy of the MLCT state is one of the largest known among inorganic or organometallic species [39] When L is 2,2-bipyridine or 1,10-phenanthroline the low lying MLCT states are well separated from the higher energy LF states that they offer an opportunity to study the photophysical and photochemical properties of the MLCT excited state exclusively

2.2 RESULTS AND DISCUSSION

Early photochemical studies on the $(\eta^6\text{-arene})Cr(CO)_3$ system found that the quantum yield for the CO loss reaction (Reaction 2 3) was 0 72[6] and the quantum yield for the arene exchange reaction (Reaction 2 4) was approximately one sixth of this value

$$(\eta^6\text{-arene})Cr(CO)_3 \xrightarrow[L]{h\nu} (\eta^6\text{-arene})Cr(CO)_2L + CO \qquad \textit{Reaction 2 3}$$

$$(\eta^6\text{-arene})Cr(CO)_3 \xrightarrow[\text{arene*}]{h\nu} (\eta^6\text{-arene*})Cr(CO)_3 + \text{arene} \qquad \textit{Reaction 2 4}$$

Consequently Reaction 2 3 was studied in some detail, and the possibility that the arene exchange reaction was photoassisted, was largely overlooked Some indirect evidence of a second photoproduct, possibly one involving a ring-slip process, was obtained in earlier UV/vis monitored flash photolysis experiments of $(\eta^6$-benzene$)Cr(CO)_3$ [40] Additional transient signals were observed following flash photolysis, which could not be assigned to the known photoproduct $(\eta^6$-benzene$)Cr(CO)_2$(solvent), or any species formed by a subsequent reaction of this intermediate It was reasoned that if there was a functionality on the arene ring that could

"trap" the ring slippage, prior to the loss of the arene, it would give conclusive evidence for the existence of this pathway and a handle with which to study this reaction path The obvious choice was therefore the pyridine ring, as the metal to ligand bond is very similar to the (η^6-benzene)$Cr(CO)_3$ system, however pyridine also possesses the lone pair on the nitrogen, which is widely known to bond to the transition metals in an η^1 fashion It was the ease with which the nitrogen bonded to the metals in the η^1 fashion that precluded earlier studies of this system, as no synthetic method had been developed to prevent this mode of interaction Consequently the photochemistry of (η^6-pyridine)$Cr(CO)_3$ and its 2,6-disubstituted derivatives was investigated, by matrix isolation and time resolved spectroscopic techniques, in the hope of detecting haptotropic changes at the heteroarene ligand

2 2 1 Spectroscopic information

In this investigation (η^6-pyridine)$Cr(CO)_3$ **(1)** was studied in most detail Comparison was made with systems containing bulky groups at the 2 and 6 positions on the pyridine ring, for example (η^6-2,6-dimethylpyridine)$Cr(CO)_3$ [(η^6-2,6-lutidine)$Cr(CO)_3$] **(2)** and (η^6-2,6-bis(trimethylsilyl)pyridine)$Cr(CO)_3$ **(3)**

Table 2 1 summarises the spectroscopic information obtained for the three compounds and compares them to the literature values Three absorptions of almost equal intensities are observed in the IR spectrum of compound **1**, which has C_s symmetry The UV spectrum contains a valley at 280 nm through which it is possible to observe transient species in the UV flash photolysis experiments While it is thought that the band with the

λ_{max} represents the chromium to pyridine charge transfer transition, by comparison with the UV/vis spectra of the other (η^6-arene)$Cr(CO)_3$ compounds Complexes of the general formula (η^6-arene)$Cr(CO)_3$ exhibit a number of LF and MLCT transitions, which are

Compound **1** *(η^6-pyridine)$Cr(CO)_3$*					
ν_{co} (cm^{-1})		^{1}H NMR (p p m)[b]		λ_{max} (nm)[a]	ε[a] at λ_{max}
A[a](± 1cm^{-1})	Ref 33[c]	A (400MHz)	*Ref 33*	A (± 2nm)	A[⊕]
1997 1938 9 1926 8	1985 1920	6 57 (m,2H) 5 64 (m,1H) 5 25 (m,2H)	6 56 (m,2H) 5 65 (m,1H) 5 26 (m,2H)	316	8 81 × 10^3
Compound **2** *(η^6-2,6-dimethylpyridine)$Cr(CO)_3$*					
ν_{co} (cm^{-1})		^{1}H NMR (p p m)		λ_{max} (nm)[a]	ε[a] at λ_{max}
A[a](± 1cm^{-1})	Ref 26(a)[d]	A[b](400MHz)	*Ref 26(a)*[e]	A (± 2nm)	A[⊕]
1987 1926 1916 8	1986 1925 1913	5 65 (t,1H) 5 12 (d,2H) 2 41 (s,6H)	4 75 (t,1H) 4 15 (d,2H) 2 00 (s,6H)	318	6 02 × 10^3
Compound **3** *(η^6-2,6-bis(trimethylsilyl)pyridine)$Cr(CO)_3$*					
ν_{co} (cm^{-1})[a]		^{1}H NMR (p p m)[b]		λ_{max} (nm)[a]	ε[a] at λ_{max}
A(± 1cm^{-1})	Ref 33[c]	A (400MHz)	*Ref 33*	A (± 2nm)	A[⊕]
1984 1919 1924*	1980 1905	5 48 (d,2H) 5 28 (t,1H) 0 32 (s,18H)	5 48 (d,2H) 5 29 (t,1H) 0 33 (s,18H)	324	7 85 × 10^3

Table 2 1

*([a] in cyclohexane, [b] in $CDCl_3$, [c] in chloroform, [d] in n-hexane, [e] in C_6D_6, *shoulder, [⊕] ± 1% L mol^{-1} cm^{-1} A = data obtained in this study*

Data in full presented in Appendix 2A)

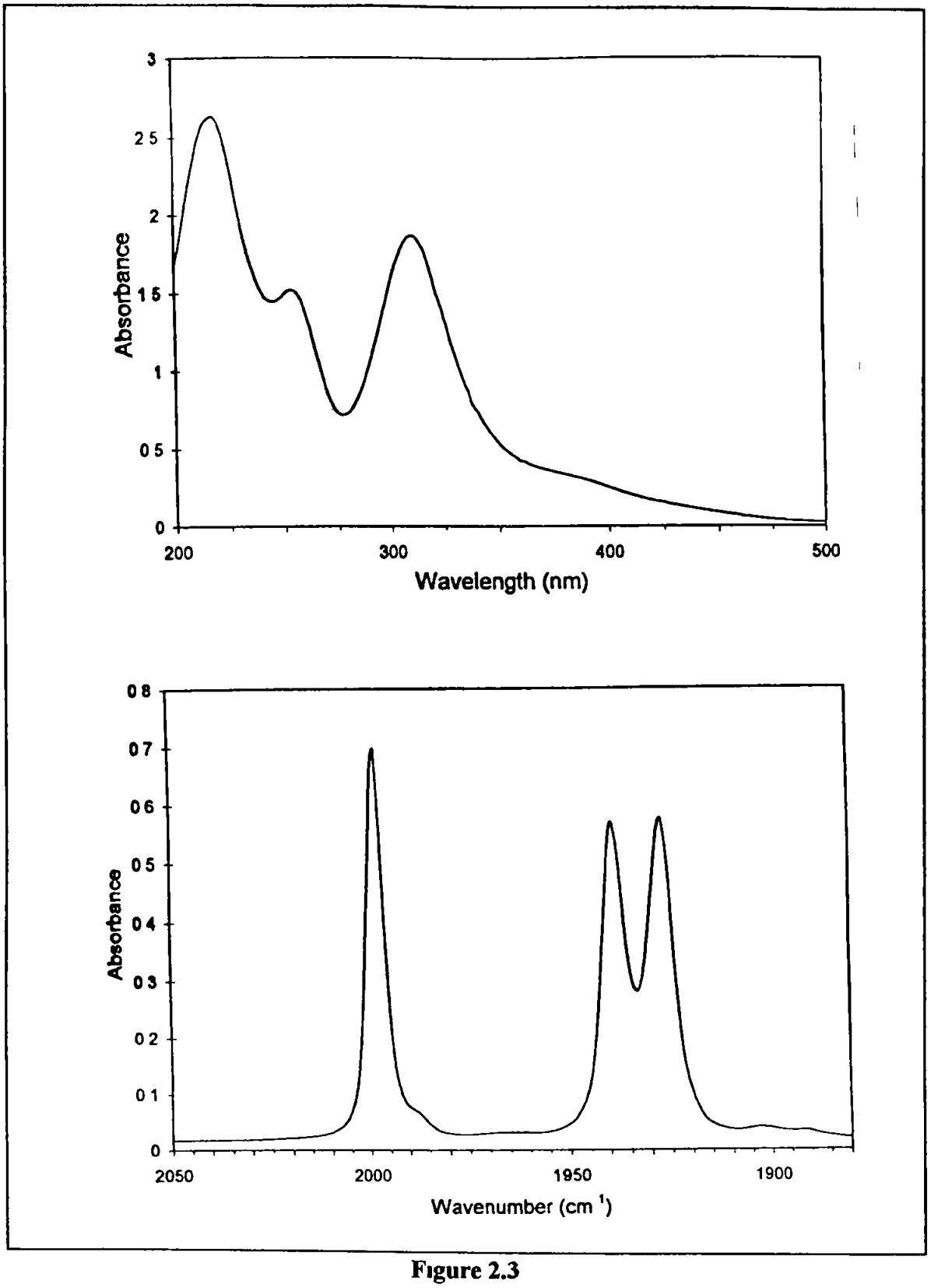

Figure 2.3

(Ground state absorption spectrum and IR spectrum of compound 1 in cyclohexane)

present in the ground state absorption spectrum of compound **1** Figure 2 3 contains both a ground state absorption spectrum and an IR spectrum of compound **1** in cyclohexane The ^{1}H NMR data indicates the presence of two sets of equivalent hydrogens and one unique hydrogen, the peaks are all shifted upfield with respect to free pyridine The ^{13}C NMR spectrum was also obtained (Appendix 2A), it indicated the presence of four unique carbon atoms in the molecule

The lack of symmetry makes spectral interpretation easy, as the number of ν_{co} absorption bands exhibited by a particular photofragment will equal the number of carbonyl ligands in the fragment A decrease in the ν_{co} frequency of the CO bands is observed upon methylation of the pyridine ring (compound **2**) This is as a result of increased electron density at the metal, resulting in donation to the antibonding orbitals of the CO ligand, thus decreasing the C-O bond order A further decrease is observed for compound **3**, indicating the increased electron donating ability of the trimethylsilyl substituents

The UV absorption spectra of the three compounds are similar to other (η^6-arene)$Cr(CO)_3$ complexes This is illustrated in Figure 2 4, where ground state absorption spectra are presented of (η^6-benzene)$Cr(CO)_3$ and (η^6-2,6-dimethylpyridine)$Cr(CO)_3$ ($\sim 1\ 4 \times 10^{-4}$M) are presented The spectra are very similar, the shoulder on the 318 nm absorption is at a slightly lower energy for the (η^6-2,6-dimethylpyridine)$Cr(CO)_3$ compound

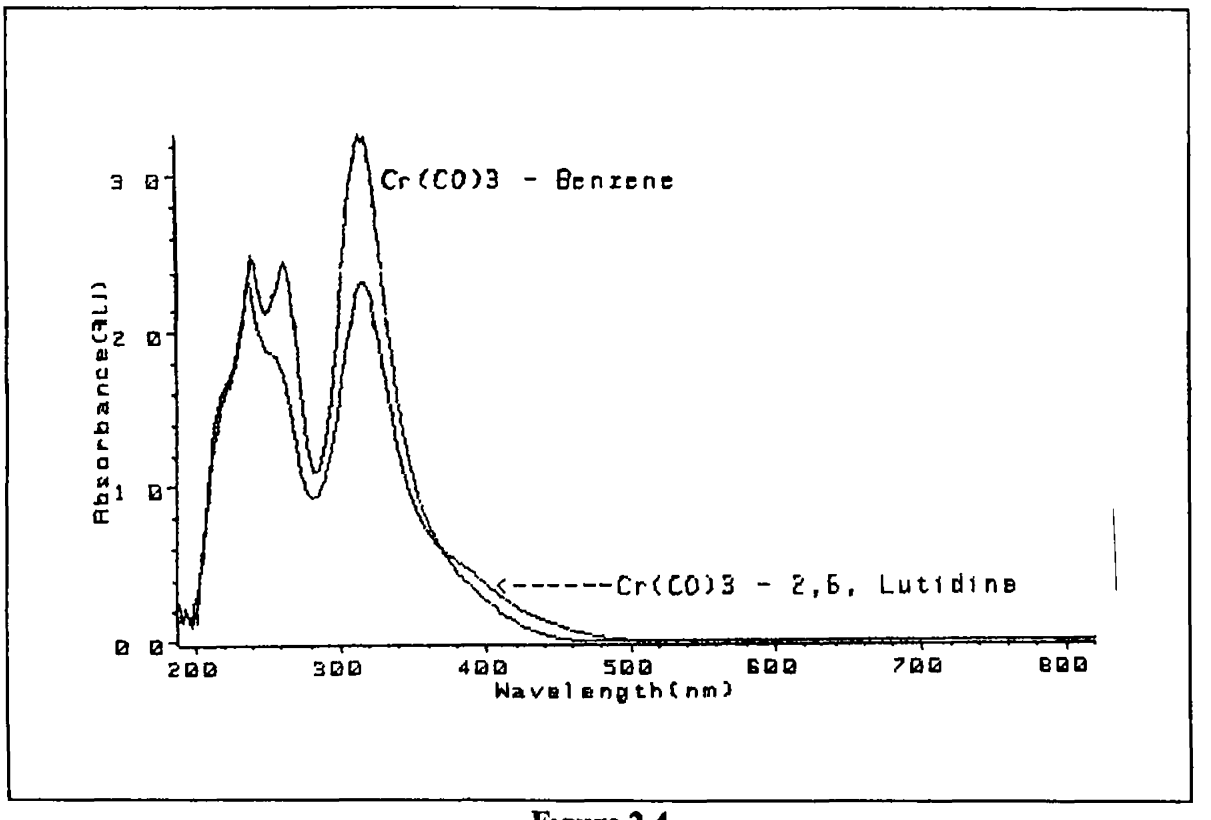

Figure 2.4

(Ground state absorption spectra for (η^6-benzene)Cr(CO)$_3$ and **2** *(~1 4 x 10^{-4}M) in cyclohexane)*

2 2 2 Steady state photolysis of (η^6-pyridine)Cr(CO)$_3$

The photochemistry of (η^6-pyridine)Cr(CO)$_3$ was investigated in either CO saturated C_6D_6, CD_3CN, CD_3OD, or DMSO-d_6 and was followed by ^{1}H NMR spectroscopy (λ_{exc} > 410 nm) All the samples were degassed by three "freeze pump thaw" cycles (see experimental section) before addition of CO, at 1 atm pressure The samples were protected from the light during this procedure

The initial spectra of the aromatic region for (η^6-pyridine)Cr(CO)$_3$ in C_6D_6 and CD_3CN are presented in Figure 2 5 and Figure 2 6 respectively Only the parent

(a) *Time zero*

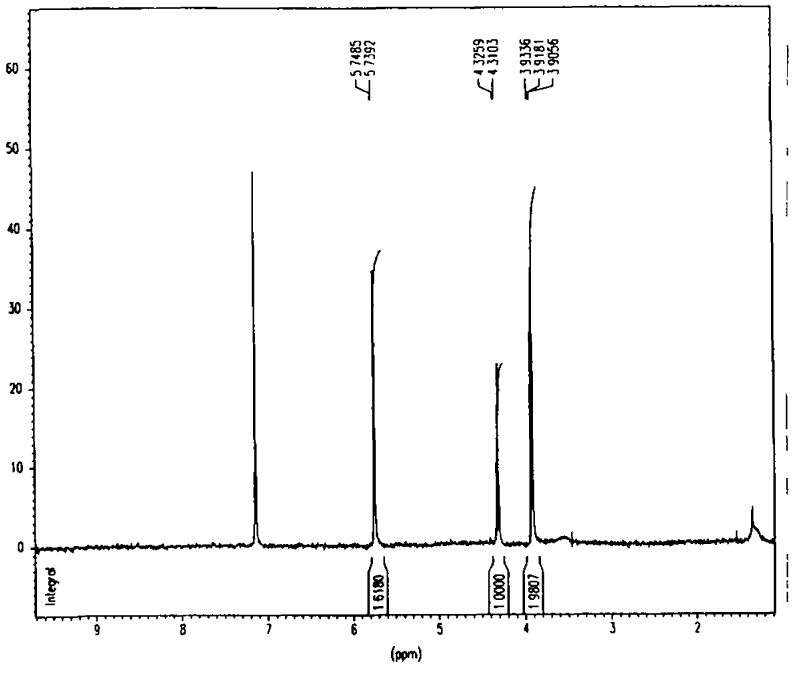

(b) *Time 50 minutes*

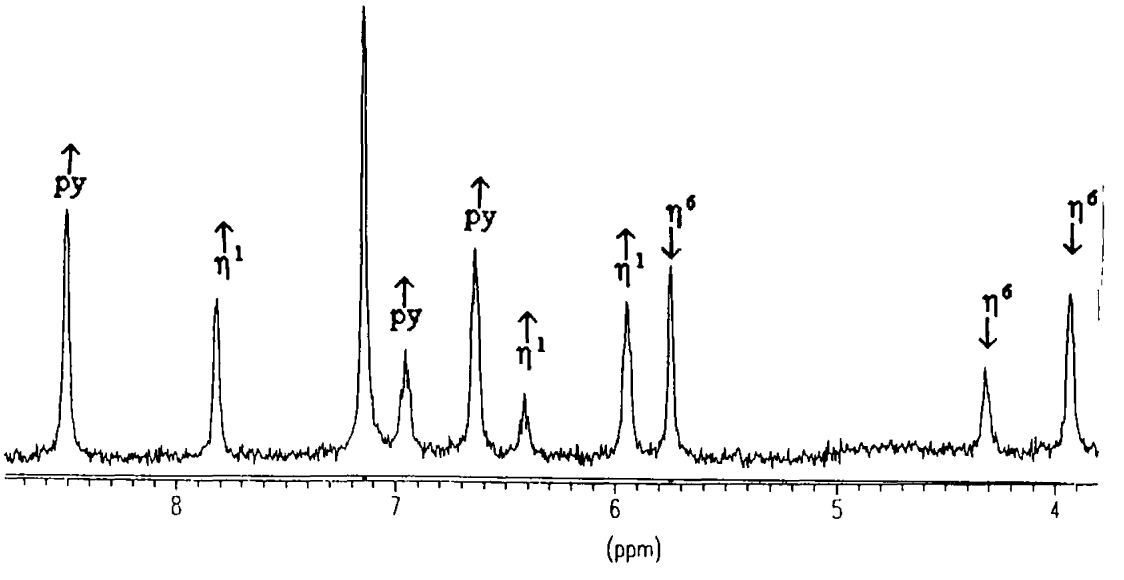

Figure 2.5

(Steady state photolysis of ***(1)*** *in C_6D_6, $\lambda_{exc} > 410$ nm)*

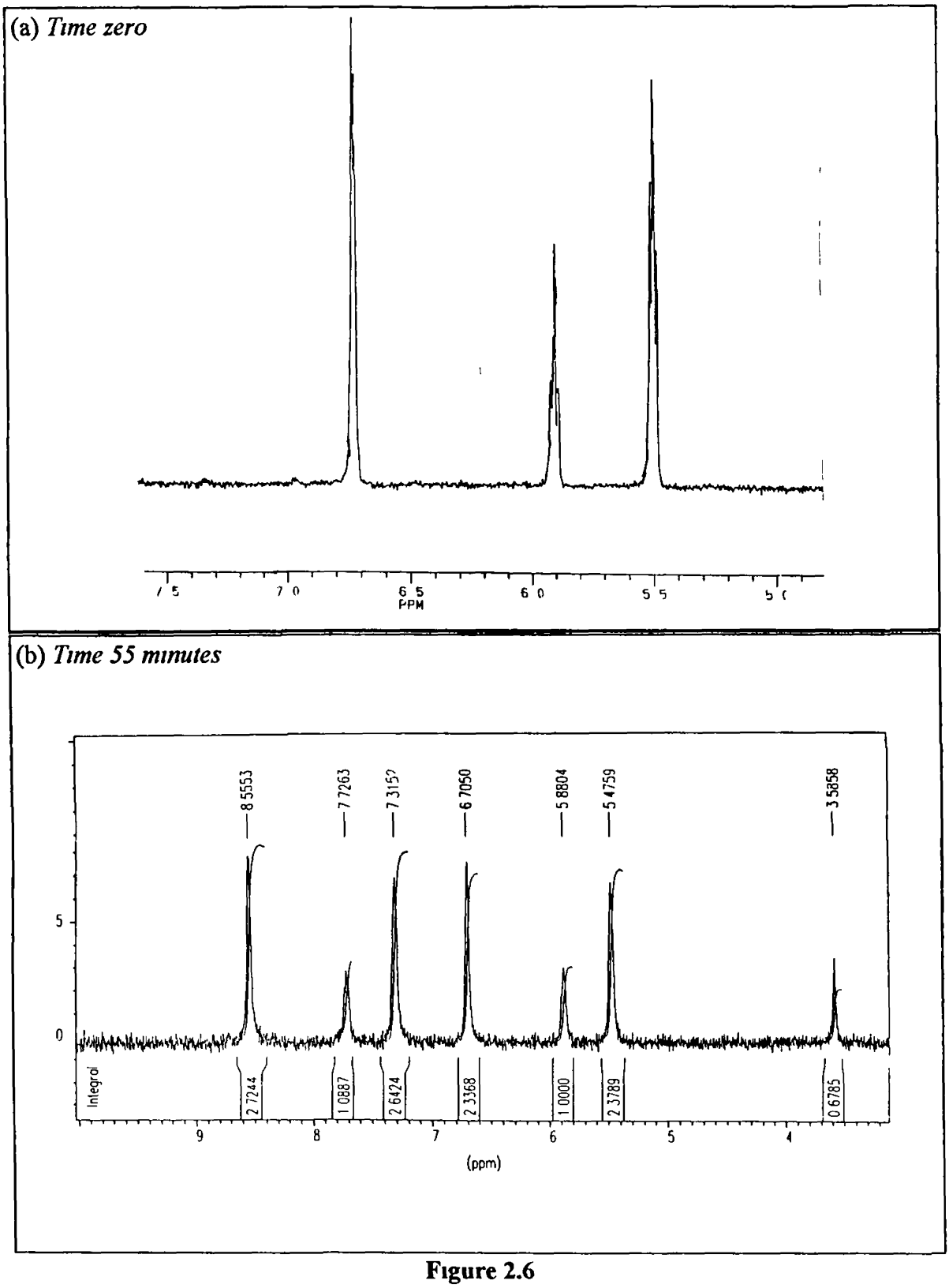

Figure 2.6

(Steady state photolysis of (1) in CD_3CN, $\lambda_{exc} > 410$ nm)

bands are present before photolysis in these solvents A reduction in intensity of these bands are observed upon excitation at $\lambda > 410$ nm (275 watt, xenon arc lamp), with concomitant formation of bands assigned to (η^1–pyridine)$Cr(CO)_5$ and free pyridine These assignments were confirmed by comparison with authentic samples of the relevant compounds either prepared independently, or obtained from suppliers Table 2 2 contains all the band positions of (η^6-pyridine)$Cr(CO)_3$, (η^1–pyridine)$Cr(CO)_5$, and pyridine in the deuterated solvents employed in this study It is important to note that the band positions for pyridine and (η^1–pyridine)$Cr(CO)_5$ in CD_3CN are very similar This explains why there appears to be only one product in Figure 2 6

Solvent	(η^6-pyridine)$Cr(CO)_3$ (ppm)	(η^1–pyridine)$Cr(CO)_5$ (ppm)	pyridine (ppm)
C_6D_6	5 74, 4 32, 3 91	7 83, 6 42, 5 95	8 56, 7 15, 6 82
CD_3CN	6 70, 5 88, 5 48	8 62, 7 81, 7 32	8 60, 7 68, 7 31
CD_3OD	6 67, 5 91, 5 50	8 66, 7 84, 7 32	8 56, 7 81, 7 40
DMSO-d_6	6 93, 6 13, 5 74	8 66, 7 91, 7 43	8 58, 7 72, 7 33

Table 2.2

(^{1}H NMR band positions in various solvents at 400 MHz)

IR analysis of the final solution confirmed the presence of the pentacarbonyl species, as a band at ~2070 cm^{-1} was observed Unfortunately, the other two bands for this species (at lower wavenumbers), were obscured by the parent absorption The characteristic band of chromium hexacarbonyl was also observed at 1984 cm^{-1}, inferring that the ring-slip process had occurred Therefore photolysis of (η^6-pyridine)$Cr(CO)_3$, at $\lambda > 410$ nm for

~50 minutes in C_6D_6 or CD_3CN results in the depletion of the parent with the production of the (η^1–pyridine)$Cr(CO)_5$, which in turn is photolysed to produce free pyridine and $Cr(CO)_6$ The overall reaction sequence is outlined in Scheme 2 3

$$(\eta^6\text{-pyridine})Cr(CO)_3 \xrightarrow[2CO]{h\nu} (\eta^1\text{–pyridine})Cr(CO)_5 \xrightarrow[CO]{h\nu} Cr(CO)_6 + \text{pyridine}$$

Scheme 2 3

In these experiments the initial spectra in CD_3OD or DMSO-d_6 before photolysis, shows that the parent complex is not the only species present This demonstrates the efficiency of these solvents in "trapping" the intermediates Every care was taken to prevent any stray light photolysis prior to the initial spectrum However, because of the lengthy degassing procedures employed it is impossible to ensure that the solution was kept in the dark at all times This is a possible explanation why the photoproducts are observed prior to photolysis, as can be seen in Figure 2 7 for photolysis in CD_3OD (however a thermal process cannot be excluded) In this solvent, both free pyridine and (η^1–pyridine)$Cr(CO)_5$ possess a peak at ~7 84 ppm (*vide supra)*, however there is sufficient resolution between the other two peaks to observe the subsequent photolysis of the (η^1–pyridine)$Cr(CO)_5$ complex to form the free pyridine Following 15 minutes of photolysis, at $\lambda_{exc} > 410$ nm, in CD_3OD, a higher percentage of the parent species is depleted, than was observed following ~50 minutes photolysis in either C_6D_6 or CD_3CN Further photolysis of the CD_3OD solution resulted in noisy spectra as a result of the production of a precipitate

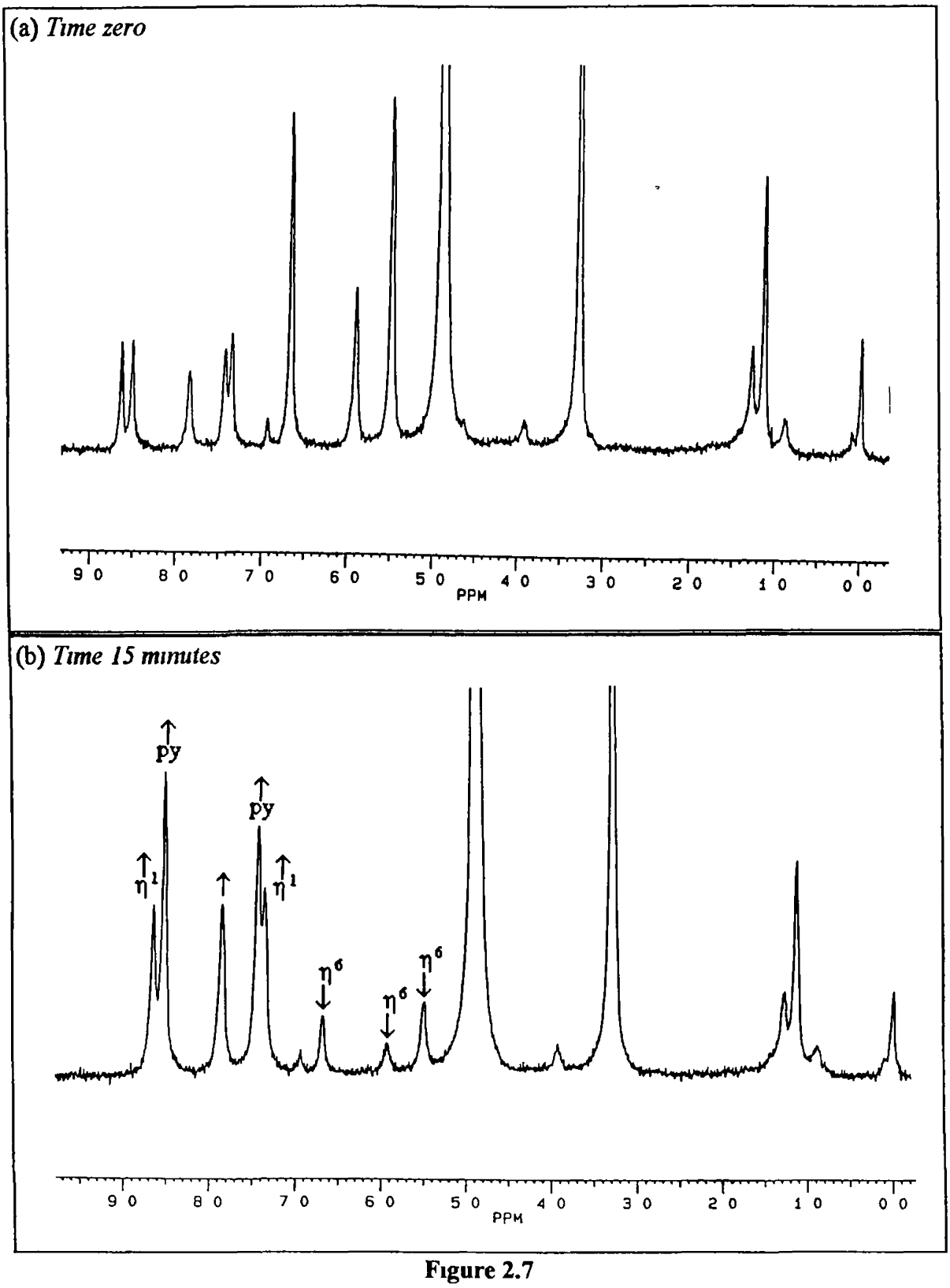

Figure 2.7

(Steady state photolysis of (1) in CD_3OD, $\lambda_{exc} > 410$ nm)

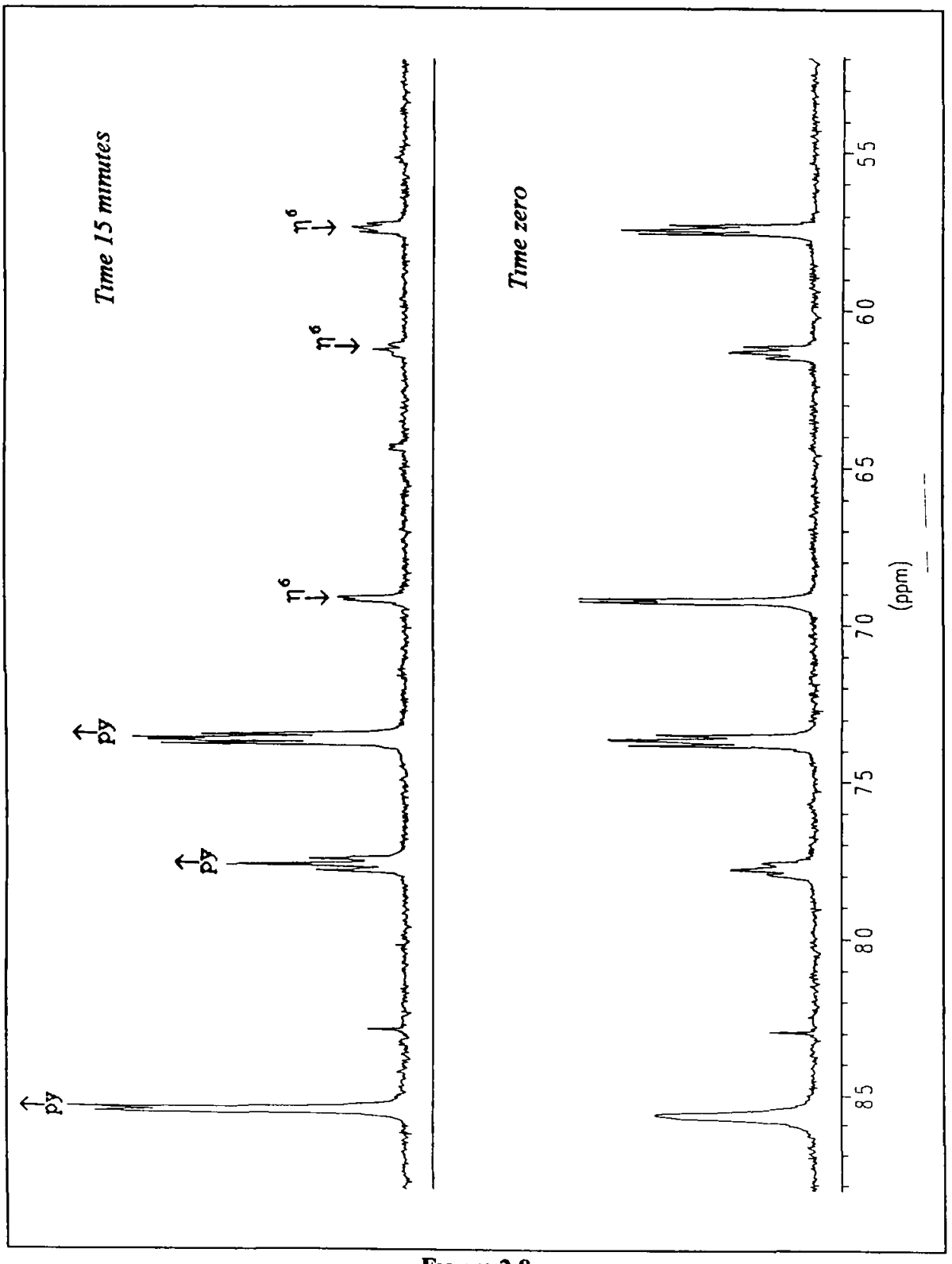

Figure 2 8

(Steady state photolysis of (1) in DMSO-d_6 λ_{exc} > 410 nm)

Figure 2 8 depicts the spectra for the photolysis of (η^6-pyridine)$Cr(CO)_3$ in DMSO-d_6 The initial spectrum contains practically the same amount of photoproduct as parent, demonstrating the capability of the DMSO-d_6 to act as a donating solvent, thus efficiently "trapping" the ring slip process This efficiency may also be reflected in the absence of the pentacarbonyl species in the spectrum As with photolysis in CD_3OD, nearly all of the parent is depleted after 15 minutes

The relative quantum efficiency for the disappearance of the parent depends on the solvent employed and on the substituents on the pyridine ring in the 2,6-positions, as measured by UV/vis spectroscopy Absorbances were measured at the λ_{max} for the parent species, in CO-saturated solvent The samples were then photolysed at λ_{exc} > 410 nm, and the decrease in absorbance was measured over the same time period

Compound	Solvent	O D difference after 10 s photolysis[a]	Relative quantum efficiency (CH_3OH C_6H_{12})
(η^6-pyridine)$Cr(CO)_3$	CH_3OH	0 0376	2 3 1
	C_6H_{12}	0 01664	
(η^6-2,6-lutidine)$Cr(CO)_3$	CH_3OH	0 03072	3 3 1
	C_6H_{12}	0 00932	

Table 2.3

(Relative quantum efficiencies for the photochemical depletion of compounds 1 and 2

[a] *average of first two absorbance differences)*

Table 2 3 gives the relative quantum efficiencies in the two solvents It can be clearly seen that the process is more efficient in the methanol solvent, confirming what

has been observed in the NMR experiments The effect of the substituents at the 2 and 6 positions on the pyridine ring could also be obtained from these experiments Depletion of the parent in cyclohexane is approximately twice as efficient for (η^6-pyridine)$Cr(CO)_3$ when compared with (η^6-2,6-lutidine)$Cr(CO)_3$ Figure 2 9 shows the photochemical depletion of (η^6-2,6-lutidine)$Cr(CO)_3$ in cyclohexane, compared to methanol

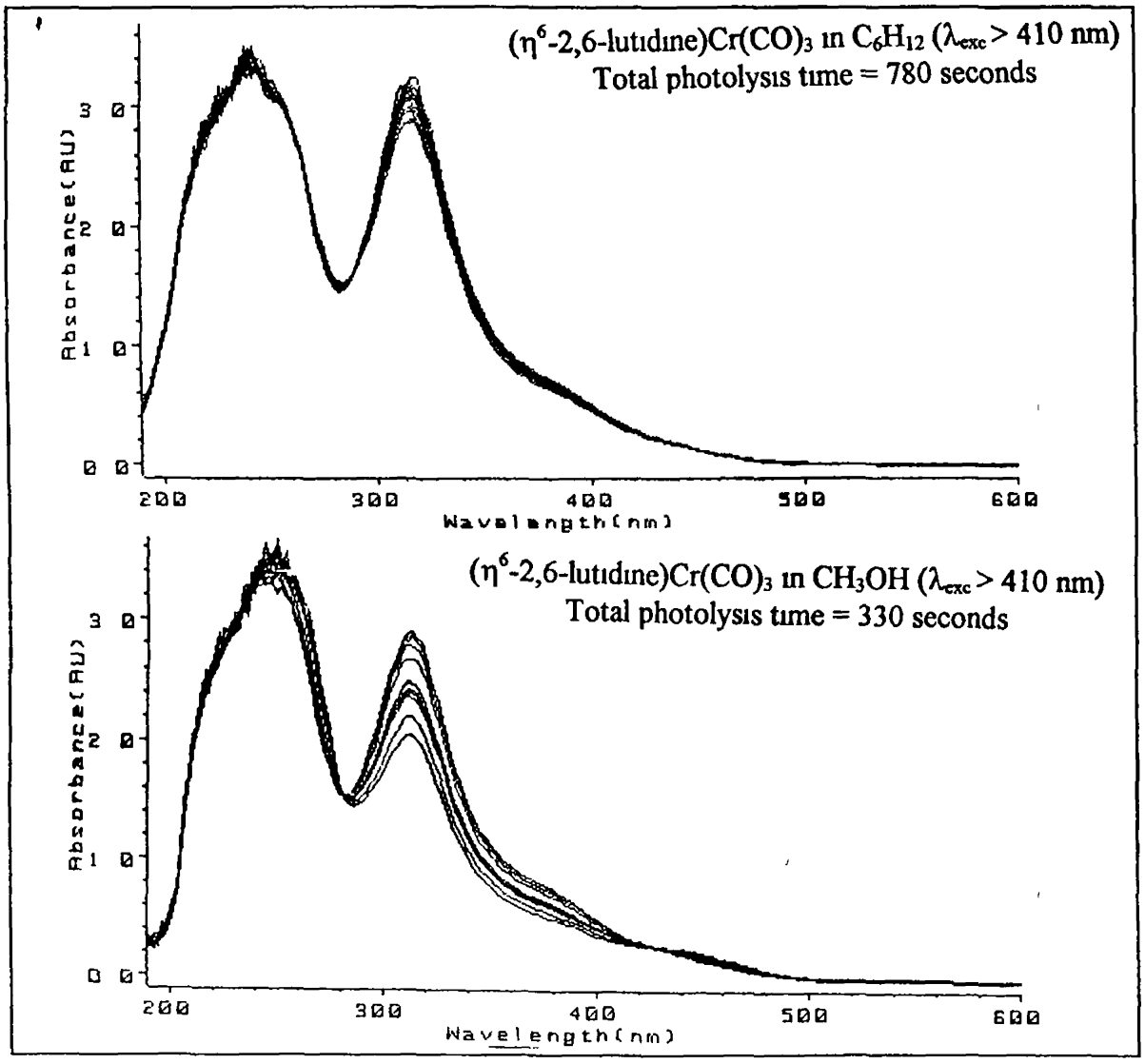

Figure 2.9

(Photochemical depletion of 2 (λ_{exc} > 410 nm) in C_6H_{12} or CH_3OH)

In methanol the total photolysis time is only 330 seconds, however in cyclohexane the compound was photolysed for a total of 780 seconds The efficiency of photodepletion of the (η^6-2,6-bis(trimethylsilyl)pyridine)$Cr(CO)_3$ compound in cyclohexane is essentially zero

2 2 3 Matrix Isolation Experiments

(a) The photochemistry of (η^6-pyridine)$Cr(CO)_3$

The photochemistry of (η^6-pyridine)$Cr(CO)_3$ was investigated in a number of different matrices The photochemistry was investigated in a methane matrix at 12 K at two different excitation wavelengths At longer excitation wavelength (460 nm) depletion of the parent bands (1999, 1939, and 1924 cm^{-1}) was observed with concomitant formation of three bands (1957, 1841, and 1833 cm^{-1}) This is depicted as a difference spectrum (Figure 2 10(a)), where the depletion of the parent bands are shown as negative peaks and the product bands as positive peaks As discussed previously, the number of CO bands for this system is related to the number carbonyl groups present in the photofragment provided additional symmetry is not introduced Therefore as there are three bands present in the product upon excitation at 460 nm, CO-loss has not occurred from this species This photofragment was assigned to a heteroarene ring slip product (η^x-pyridine)$Cr(CO)_3$ ($x < 6$) Confirmation that CO-loss is insignificant under these conditions is obtained by the failure to observe free CO in the matrix

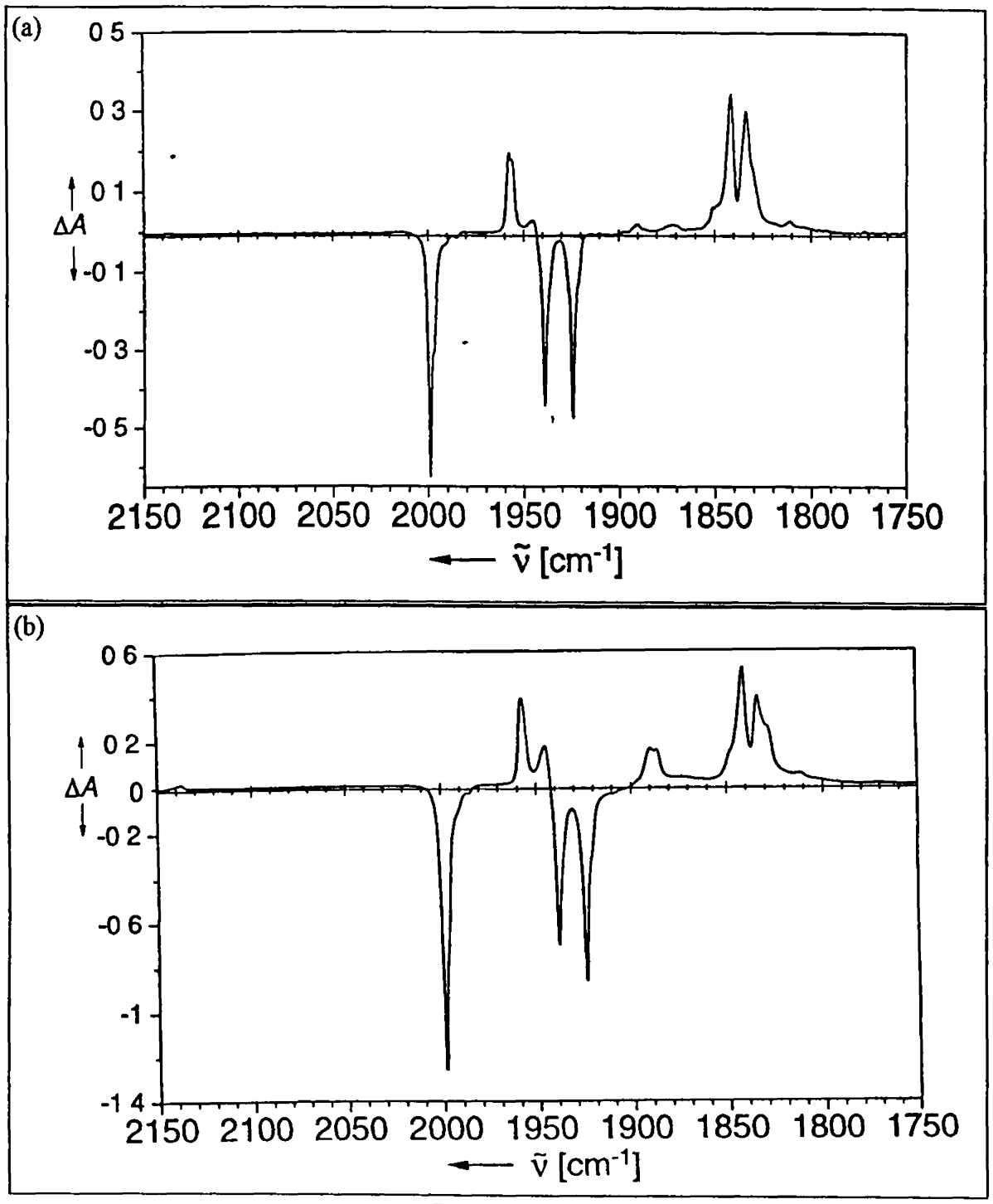

Figure 2 10

(Difference Spectra obtained after irradiation of a CH_4 matrix at 12 K containing (η^6-pyridine)$Cr(CO)_3$ (a) λ_{exc}= 460 nm (b) λ_{exc}= 308 nm)

At shorter wavelength excitation (308 nm), two bands are observed (the low-energy band is subject to matrix splitting) in addition to the bands of the ring slip product The two bands (1945 and 1888 cm^{-1}) can be observed in Figure 2 10(b) and are assigned as the CO loss product, (η^6-pyridine)$Cr(CO)_2$ for a number of reasons Firstly free CO is observed in matrix, at 2137 cm^{-1} Secondly, the high energy band is shifted by 56 cm^{-1} relative to the equivalent parent absorption This wavenumber shift is identical to that observed for the (η^6-benzene)$Cr(CO)_3$ system (1983 to 1927 cm^{-1}) [41] Averaging the two low energy absorptions of the parent (1931 cm^{-1}) a shift of 44 cm^{-1} is observed which compares to the shift of 38 cm^{-1} observed in the (η^6-benzene)$Cr(CO)_3$ system, (1915 to 1877 cm^{-1})

These results had shown that a ring slip process did occur following long wavelength irradiation, but the extent of the haptotropic rearrangement could not be determined Therefore experiments were conducted in N_2 or CO-doped matrices in order to obtain more information about the ring slip process

Irradiation in a N_2 matrix (λ_{exc} = 460 nm) produced three bands (1967, 1987, and 1884 cm^{-1}) confirming the conservation of the $Cr(CO)_3$ moiety (Figure 2 11(a)) Two bands of similar intensity were also observed in the $\nu_{N\,N}$ region (2221 and 2188cm^{-1}), indicative of two *cis*-coordinated N_2 ligands The wavenumber difference between the $\nu_{N\text{-}N}$ antisymmetric and symmetric vibrational modes (33 cm^{-1}) is similar to the differences observed for (η^5-C_5H_5)$Nb(CO)_2(N_2)_2$ in liquid xenon (39 cm^{-1}),

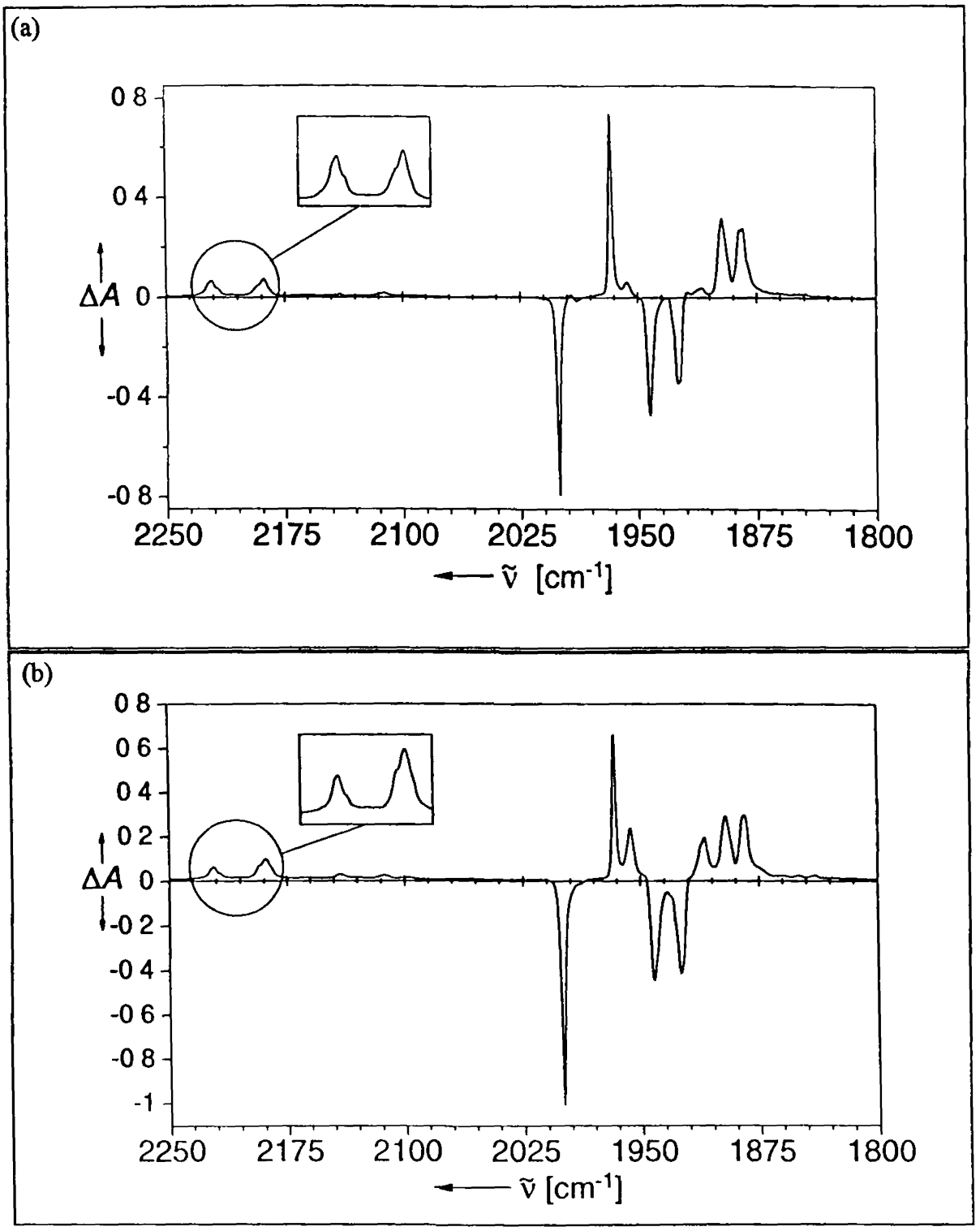

Figure 2.11

(Difference Spectra obtained after irradiation of a N_2 matrix containing $(\eta^6$-pyridine)$Cr(CO)_3$ (a) λ_{exc}= 460 nm (b) λ_{exc}= 308 nm)

and (η^5-C_5H_5)V(CO)$_2$(N_2)$_2$ in a N_2 matrix (32 cm^{-1}) [42] Therefore 460 nm irradiation of (η^6-pyridine)Cr(CO)$_3$ in N_2 matrix produces *fac*-(η^1-pyridine)(N_2)$_2$Cr(CO)$_3$

Irradiation of a N_2 matrix containing (η^6-pyridine)Cr(CO)$_3$ with λ_{exc} = 308 nm, resulted in additional bands at 1957 cm^{-1} and 1910 cm^{-1} (Figure 2 11(b)) This two band pattern is assigned as the CO loss product, as the absorption of free CO is observed following photolysis (Appendix 2B(i)) Therefore both the ring slip product and the CO loss product are formed simultaneously in the N_2 matrix In this case however, the $\nu_{N\text{-}N}$ bands observed following 308 nm irradiation are of different relative intensities (cf insets in Figure 2 11) An explanation for this is that the (η^6-pyridine)Cr(CO)$_2$(N_2) species, possesses a $\nu_{N\text{-}N}$ band that overlaps with the low-energy $\nu_{N\,N}$ band of the *fac*-(η^1-pyridine)(N_2)$_2$Cr(CO)$_3$ species

Photolysis of (η^6-pyridine)Cr(CO)$_3$ in a CH_4 CO (10 1) matrix with a λ_{exc} of 460 nm resulted in a three band pattern (marked *, 2070, 1937, and 1916 cm^{-1}) characteristic of the (η^1-pyridine)Cr(CO)$_5$ species with local C_{4v} symmetry (Figure 2 12) Also present is a band at 1983 cm^{-1} which is assigned to Cr(CO)$_6$, which is probably formed by subsequent photolysis of the pentacarbonyl photoproduct If the matrix is further photolysed with λ_{exc}= 250 nm, bands at 2030, 1909, and 1870 cm^{-1} are formed which have been assigned to a tetracarbonyl species that is produced by CO-loss from (η^1-pyridine)Cr(CO)$_5$ Also formed with λ_{exc}= 250 nm is a peak at 1956 cm^{-1} (Figure 2 12), which has tentatively been assigned as one of the bands for the Cr(CO)$_5$(CH_4) species (2088, 1961, and 1932 cm^{-1}) [43] The band at 1961 cm^{-1} was found to be relatively more intense than the other two bands, which may explain why they were not observed This

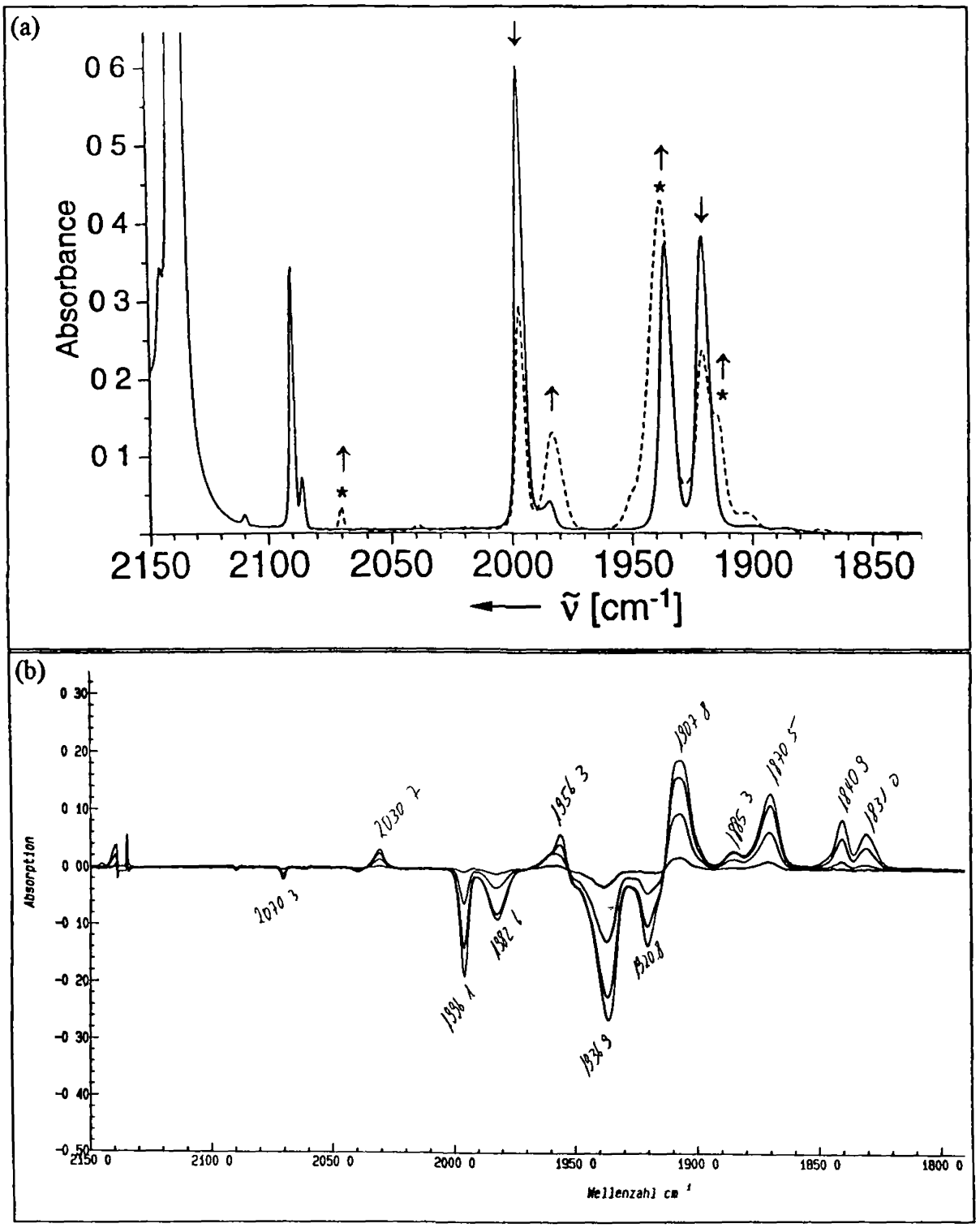

Figure 2 12

(Spectra obtained after irradiation of a CH_4 CO (10 1) matrix containing

(η^6-pyridine)$Cr(CO)_3$ (a) λ_{exc}= 460 nm (b) subsequent λ_{exc}= 250 nm)

pentacarbonyl species could be produced by either irradiation of $Cr(CO)_6$ or (η^1-pyridine)$Cr(CO)_5$

Subsequent long wavelength photolysis (λ_{exc} = 530 nm) of the tetracarbonyl species regenerated the (η^1-pyridine)$Cr(CO)_5$ complex (Appendix 2B(ii)) When an excitation wavelength of 370 nm was employed, $Cr(CO)_6$ was formed and possibly the $Cr(CO)_5(CH_4)$ species (Appendix 2B(iii)) The results obtained when the (η^6-pyridine)$Cr(CO)_3$ compound underwent long wavelength photolysis in a methane matrix indicated that a ring slip process occurred The extent of this haptotropic rearrangement was not determined until photolysis of the compound was carried out in a CO doped and a N_2 matrix The results obtained from irradiation of (η^6-pyridine)$Cr(CO)_3$ in both a N_2 and a CO doped matrix are consistent with an η^6 to an η^1 haptotropic rearrangement following long wavelength photolysis

(b) The photochemistry of (η^6-2,6-bis(trimethylsilyl)pyridine)$Cr(CO)_3$

The matrix photochemistry of (η^6-2,6-bis(trimethylsilyl)pyridine)$Cr(CO)_3$ was investigated, in order to observe the effect of the bulky substituents on the resulting photochemistry When the compound was photolysed at λ_{exc} = 460 nm, in an Ar matrix containing 10% CO, no photochemical change was observed When an excitation wavelength of 250 nm was employed depletion of the parent was observed with concomitant growth of two bands assigned to the dicarbonyl species (1942 and 1890cm^{-1}) This can be observed in Figure 2 13(a), where the two bands can be seen to grow in following the 250 nm excitation Subsequent photolysis with λ_{exc} = 313 nm results in an

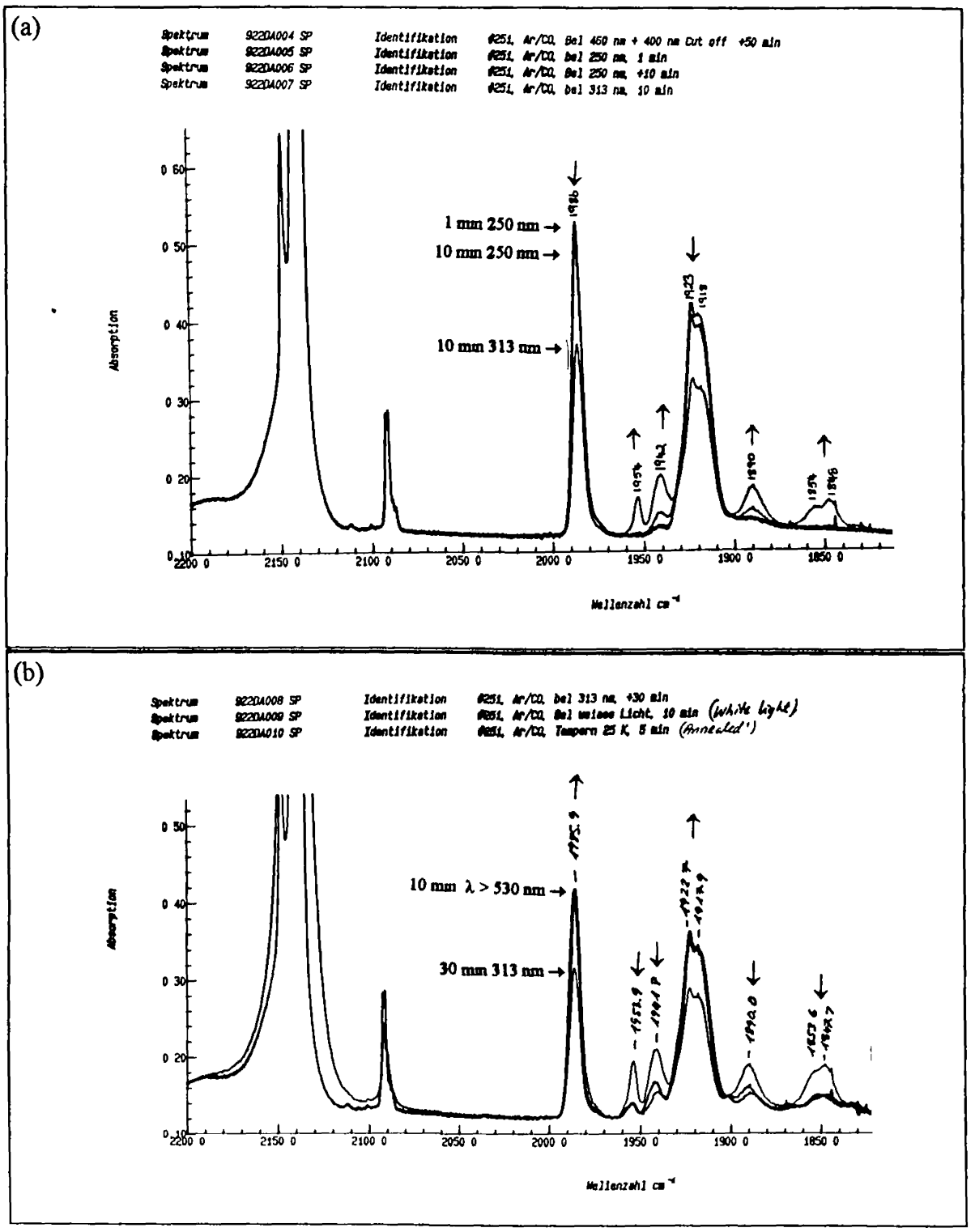

Figure 2.13

(Spectra obtained after irradiation of an Ar CO (10 1) matrix containing (η^6-2,6-(TMS)pyridine)Cr(CO)$_3$ (a) λ_{exc}= 250 nm, 313 nm (b) λ_{exc}= 313 nm, λ_{exc}>530 nm)

increase in the bands assigned to the dicarbonyl species, but new bands are also observed at 1954, 1854, and 1845 cm^{-1} These new bands are assigned to the (η^1-2,6-bis(trimethylsilyl)pyridine)$Cr(CO)_3$ species by comparison with the photochemistry of the (η^6-pyridine)$Cr(CO)_3$ in a methane matrix

Figure 2 13(b) shows the photoreversibility of the η^1 and the dicarbonyl species Following photolysis at 313 nm, (producing both the photoproducts), if the matrix is irradiated with white light, a depletion of these bands is observed with concomitant regeneration of the parent bands

The photochemistry of (η^6-2,6-bis(trimethylsilyl)pyridine)$Cr(CO)_3$ was also investigated in a N_2 matrix (Figure 2 14) Photolysis at 460 nm results in the production of a ν_{N-N} band at 2180 cm^{-1} and two ν_{co} bands at 1947 and 1904 cm^{-1} which are assigned

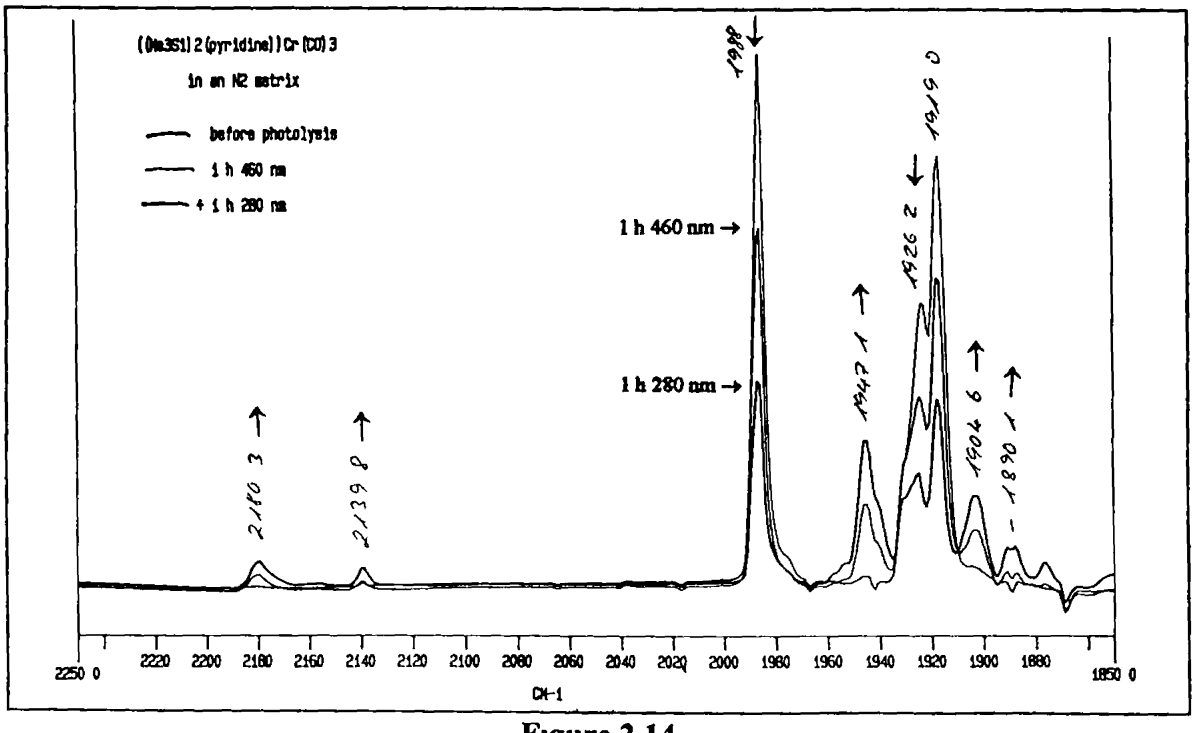

Figure 2 14

(Spectra obtained after irradiation of a N_2 matrix containing (η^6-2,6-(TMS)pyridine)$Cr(CO)_3$ λ_{exc}= 460 nm, 280 nm)

as the dicarbonyl species (η^6-2,6-bis(trimethylsilyl)pyridine)$Cr(CO)_2(N_2)$ Confirming this assignment is the presence of free CO in the matrix following photolysis This process is not very efficient, a small amount of the ring slip product can also be observed Following photolysis at 280 nm slightly more of the ring slip product can be observed, however the bands are still weak and it proved impossible to determine if the photoproduct interacts with the matrix environment

2 2 4 Time Resolved Infrared Spectroscopy Experiments

The photochemistry of (η^6-pyridine)$Cr(CO)_3$ was investigated in CO saturated cyclohexane solution and was monitored by TRIR spectroscopy The concentration of CO in the cyclohexane solution was $9\ 0 \times 10^{-3}$ M [44] Figure 2 15 represents the difference spectrum, obtained 1 μs after excitation with a laser pulse (λ_{exc} = 308 nm) The negative peaks observed at 1999, 1940, and 1930 cm^{-1} correspond to depletion of the parent compound The positive peaks at 1950 and 1890 cm^{-1} are assigned to the photoproduct (η^6-pyridine)$Cr(CO)_2(C_6H_{12})$ because they are at wavelengths similar to the bands observed for the dicarbonyl species in a CH_4 matrix (*vide ultra)*
Examination of the negative lower frequency bands of the parent, shows that the 1940 cm^{-1} band is not of the same intensity as the 1930 cm^{-1} band The initial spectrum of the compound exhibits two bands of nearly equal intensity The could be a result of overlap with the 1950 cm^{-1} band of the photoproduct

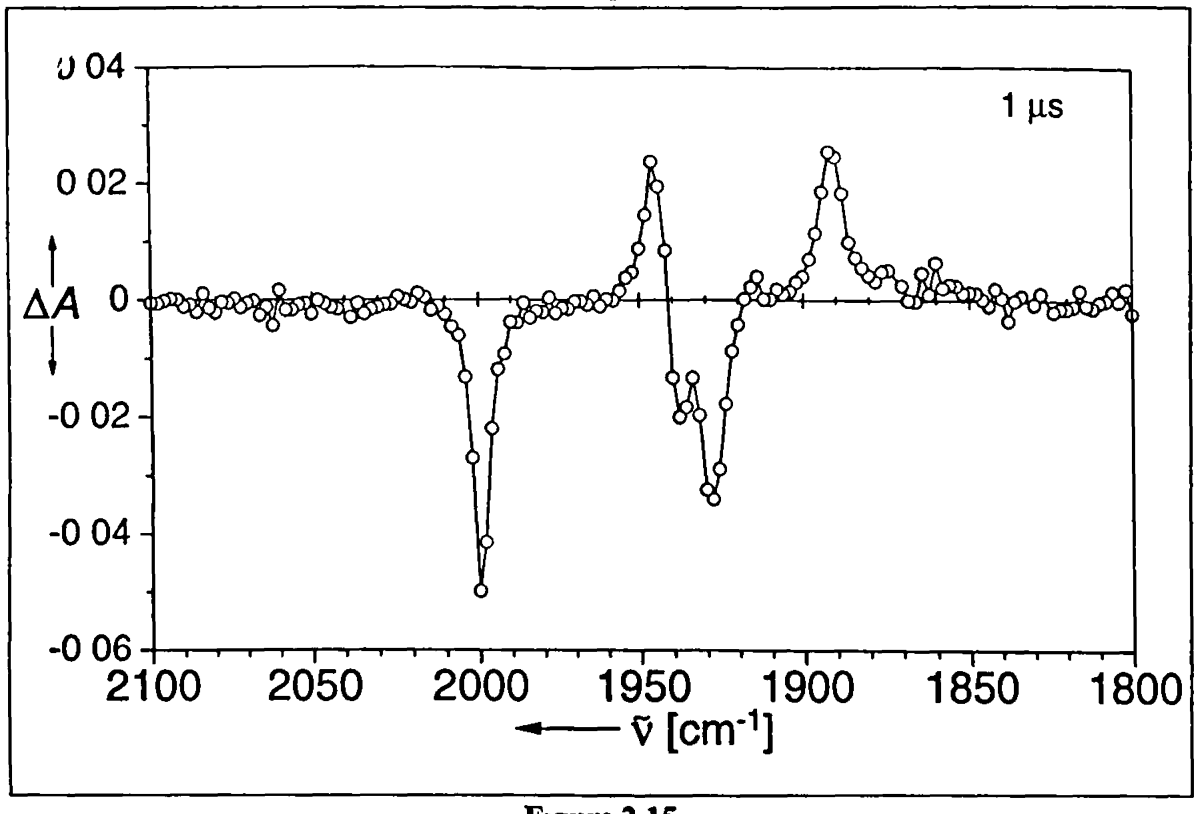

Figure 2.15

(The TRIR spectrum obtained in room temperature CO-saturated C_6H_{12},

1 μs after excitation (λ_{exc} = 308 nm) of (η^6-pyridine)Cr(CO)$_3$)

Following ~16 μs a very weak band at 2066 cm^{-1} can be observed, also at this time a band at ~1916 cm^{-1} (overlapping with the parent depletion) is present, these bands are assigned as the pentacarbonyl species These results indicate, that unlike the matrix results, the CO loss process is more efficient in solution compared to the ring slip process

The photoproducts were observed to decay over ~50 μs regenerating the parent, although not quantitatively, according to Reaction 2 5 The rate constant for this reaction was determined by subtracting the k_{obs} in the absence of CO from that in the presence of 9 mM CO and dividing by 9 mM, and was found to be 1 4 × 10^7 dm^3 M^{-1}s^{-1}

$$(\eta^6\text{-pyridine})Cr(CO)_2(C_6H_{12}) + CO \xrightarrow{k_2} (\eta^6\text{-pyridine})Cr(CO)_3 + C_6H_{12} \qquad \textit{Reaction 2 5}$$

2 2 5 Ultraviolet/visible Flash Photolysis Experiments

A series of UV/vis flash photolysis experiments were undertaken in a variety of solvents and under different gasses The effect of changing the solvent media was examined for the three complexes under investigation in this study

(a) The photochemistry of (η^6-pyridine)Cr(CO)$_3$

(1) Cyclohexane

The photochemistry of (η^6-pyridine)Cr(CO)$_3$ was investigated by UV/vis flash photolysis with λ_{exc} = 355 nm in CO saturated cyclohexane Figure 2 16 depicts a difference spectrum obtained 5 μs after the laser pulse The negative peak observed at ~330 nm represents the depletion of the parent compound The photoproducts absorb in the valley of the parent absorption (290 nm) and a weaker absorption is present at ~500 nm Analysis of the kinetic parameters associated with the absorption at 290 nm indicates that this species reacts with CO with identical k_2, within experimental error, to that obtained from TRIR experiments (1 4 × 10^7 $dm^3 M^{-1}s^{-1}$)

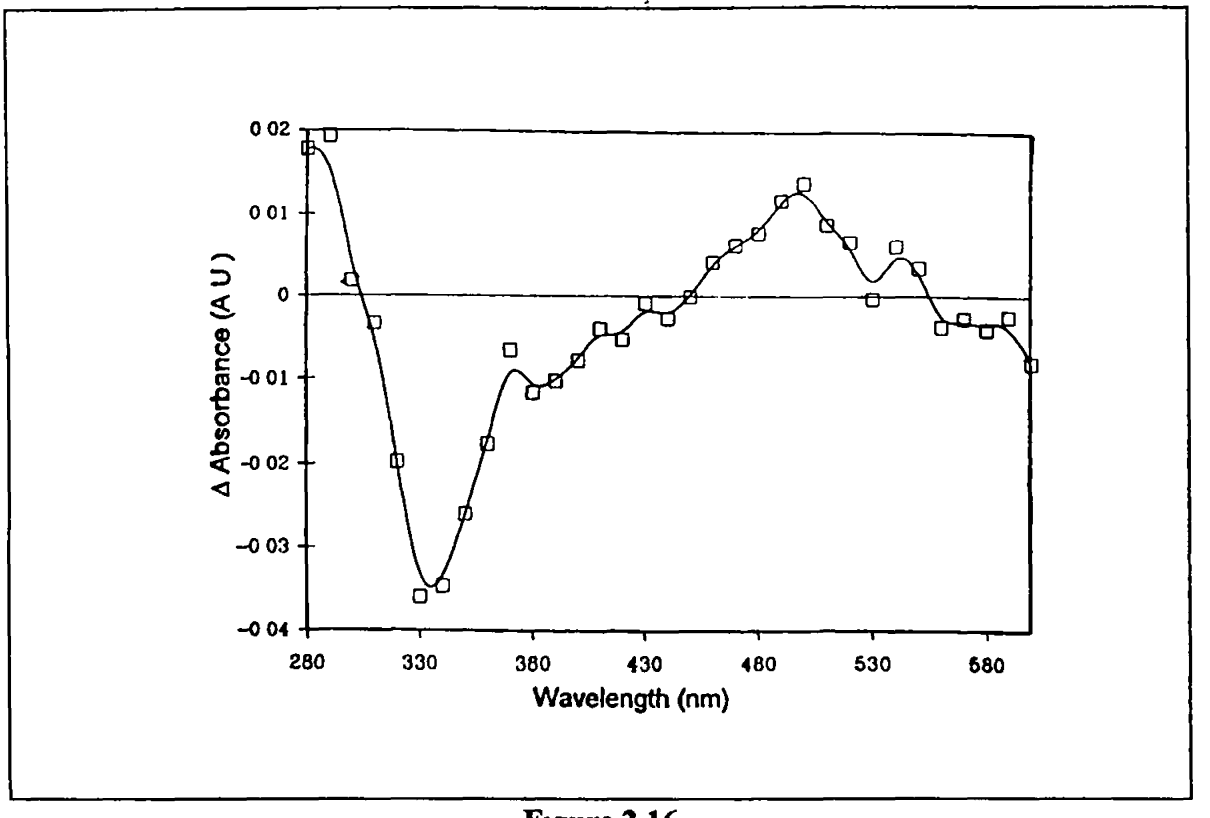

Figure 2.16

(UV/vis difference spectrum obtained in room temperature CO saturated C_6H_{12}, 5 μs after excitation (λ_{exc} = 355 nm) of (η^6-pyridine)Cr(CO)$_3$)

The k_2 values were obtained from different CO concentrations When the experiment is repeated under an Ar atmosphere, no depletion of the photoproduct, that absorbs at 290 nm, was observed This indicates that the decay of this species has a dependence on CO Therefore this absorption could be assigned to the CO loss product, or possibly to the formation of a dinuclear species formed in the absence of CO

Under a CO atmosphere the parent absorption that is monitored at 330 nm recovers by two temporally resolved processes The slower process, *i e* that occurring after the time indicated by the arrow in Figure 2 17, corresponds to the reformation of the

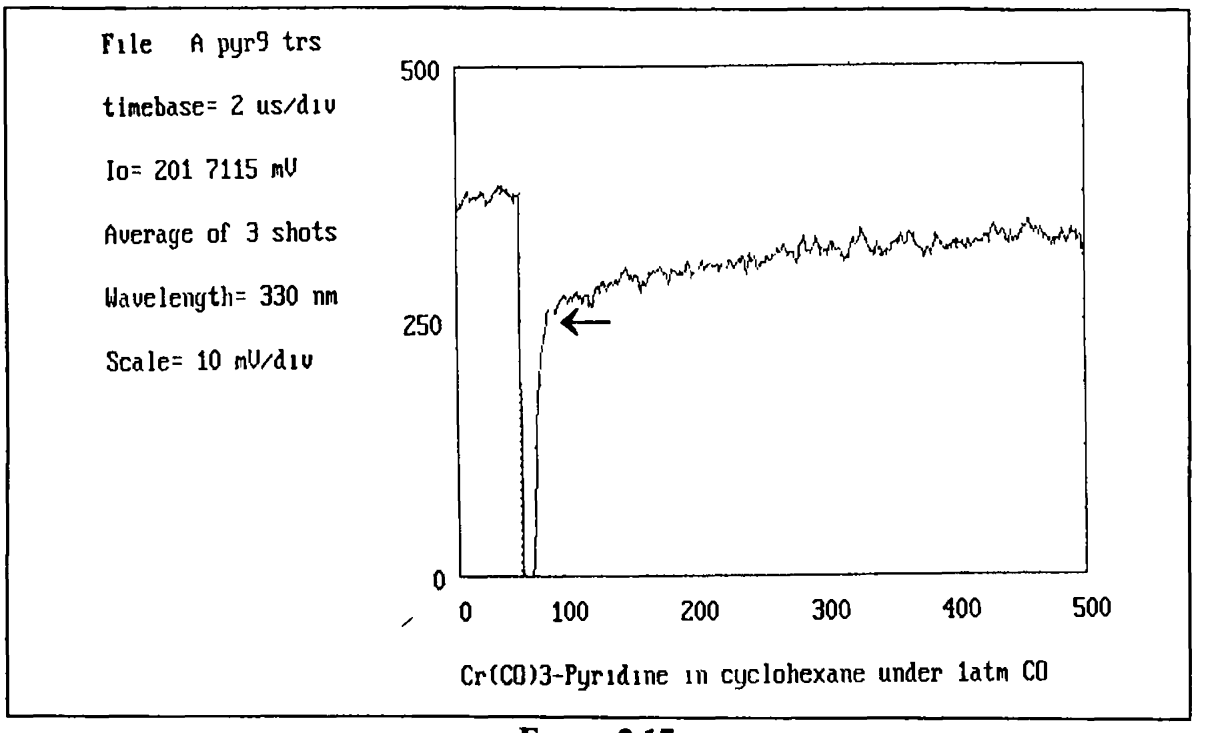

Figure 2.17

(The transient signal obtained following photolysis (λ_{exc} = 355 nm) of (η^6-pyridine)Cr(CO)$_3$ in room temperature, CO saturated, C_6H_{12}, monitored at 330 nm)

(η^6-pyridine)Cr(CO)$_3$ species *via* the reaction depicted in Reaction 2 5 The value for k_2 for this reaction is 1 1 × 10^7 dm^3 M^{-1}s^{-1} when the concentration of CO is 9 0 × 10^{-3} M, as presented in Table 2 4 This k_2 value is not identical to the value obtained at 280 nm although it is within experimental error, however the transients at 330 nm are noisier, possibly explaining the difference observed When the concentration is decreased by half, to 4 5 × 10^{-3} M, the rate is similarly affected dropping to 6 3 × 10^6 dm^3 M^{-1}s^{1} Therefore confirming the assignment of this process as the recombination of the dicarbonyl species with CO reforming the parent Examination of the transients indicate that the process is not fully reversible

[CO] (M)	k_{obs} (s^{-1})
9.0×10^{-3}	1.1×10^{7}
4.5×10^{-3}	6.3×10^{6}

Table 2.4

(k_{obs} for Reaction 2.5 at different concentrations of CO)

The faster process, up to the time indicated by the arrow in Figure 2.17, is completed within the rise time of the current equipment (~40 ns). This process has been assigned to the recovery of (η^6-pyridine)$Cr(CO)_3$ from the (η^1-pyridine)$Cr(CO)_3$ intermediate.

(2) Acetonitrile

The photochemistry of (η^6-pyridine)$Cr(CO)_3$ was investigated by UV/vis flash photolysis with λ_{exc} = 355 nm in CO saturated acetonitrile. Acetonitrile is a better coordinating solvent than cyclohexane, because of the lone pair on the nitrogen. Formation of a band with λ_{max} at 500 nm was observed, which did not decay within the time scale of this experiment. The fast process assigned as the reversal of the ring slip process could be observed at 310 nm (Figure 2.18). A photoproduct was found to absorb in the same region as the parent species, the formation of this photoproduct could be observed, again not decaying within the timescale of the experiment. This photoproduct could possibly have been the (η^6-pyridine)$Cr(CO)_2(CH_3CN)$ species.

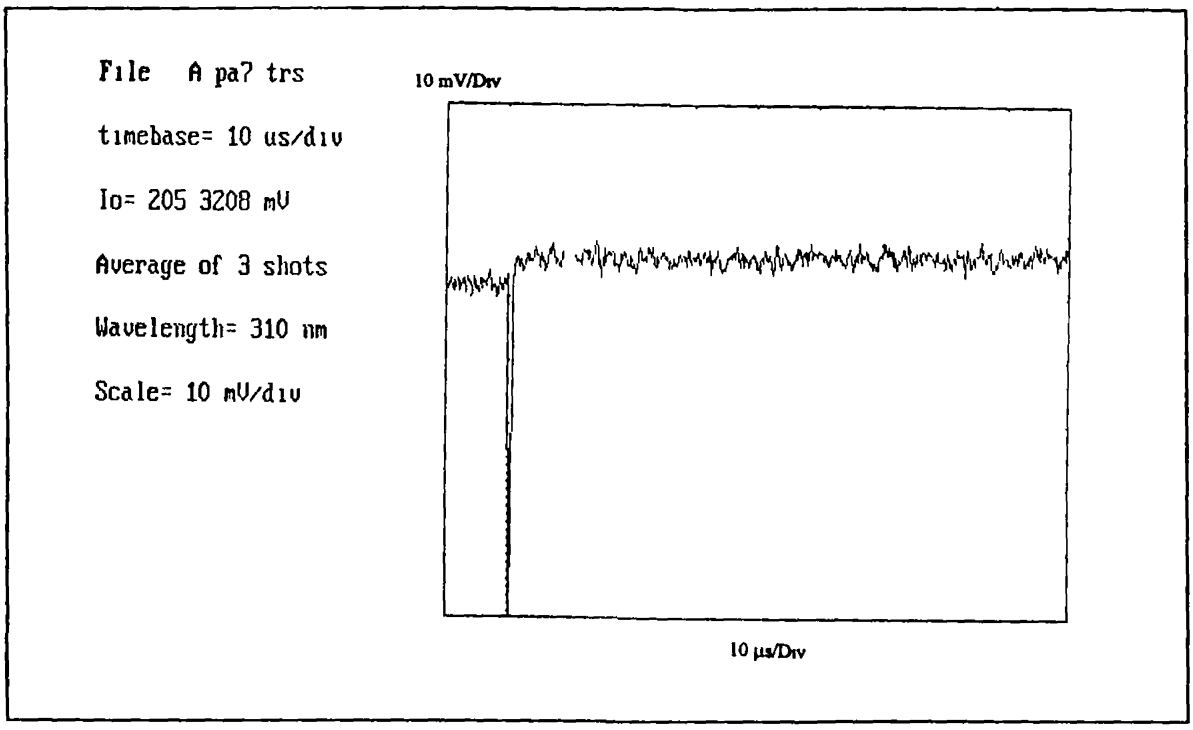

Figure 2.18

((The transient signal obtained following photolysis (λ_{exc} = 355 nm) of (η^6-pyridine)Cr(CO)$_3$ in room temperature, CO saturated, CH_3CN, monitored at 310 nm)

The ground state UV/vis spectrum, obtained during the flash photolysis experiment, reveals some information about the spectrum of this photoproduct Examination of the spectrum (Figure 2 19) reveals that a band is produced at ~410 nm This band is assigned as a pentacarbonyl species, which could be the (η^1-pyridine)Cr(CO)$_5$ or the Cr(CO)$_5$(CH_3CN) compound The spectrum of the (η^1-pyridine)Cr(CO)$_5$ compound in acetonitrile is similar to the photoproduct formed following photolysis A band can also be observed growing in at ~500 nm, this absorption is assigned to the relatively stable species (η^6-pyridine)Cr(CO)$_2$($NCCH_3$) (*vide ultra)* The depletion of the parent band can also be observed at 330 nm

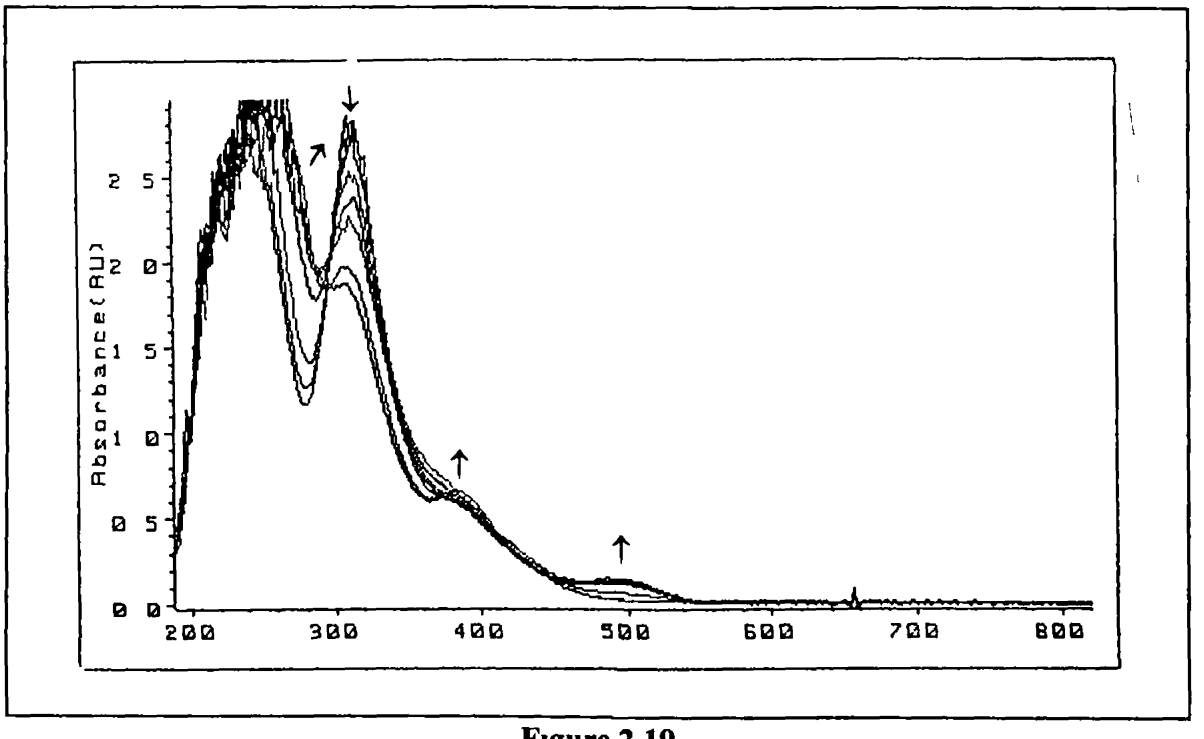

Figure 2.19

(Ground state absorption spectrum of (η^6-pyridine)Cr(CO)$_3$ following photolysis (λ_{exc} = 355 nm) in room temperature, CO saturated, acetonitrile)

An infrared spectrum obtained of the solution after the experiment confirms the presence of a pentacarbonyl species and also indicates the presence of $Cr(CO)_6$ The bands are broad as would be expected in acetonitrile The characteristic band of $Cr(CO)_6$ can be observed at 1984 cm^{-1} The two lower absorption bands of the pentacarbonyl compound are overlapping with the parent, but broadening of the parent bands are observed, indicating the presence of some other species The proof for the existence of this pentacarbonyl species in the solution comes from the presence of the distinctive a_1 band observed at 2071 cm^{-1} A spectrum was obtained of (η^1-pyridine)$Cr(CO)_5$ in

acetonitrile and the positions of the bands were identical with those found in this experiment

(b) The photochemistry of (η^6-2,6-lutidine)Cr(CO)$_3$

(1) Cyclohexane

The photochemistry of (η^6-2,6-lutidine)Cr(CO)$_3$ was also investigated by UV/vis flash photolysis with λ_{exc} = 355 nm in CO saturated cyclohexane Photoproducts were observed at similar wavelengths to those seen for the (η^6-pyridine)Cr(CO)$_3$ system Figure 2 20 depicts the transients observed at two different wavelengths The first transient observed at 280 nm corresponds to the formation of the dicarbonyl species and its subsequent recombination with CO The second represents the depletion of the parent absorption (330 nm), followed by its biphasic recovery, which corresponds to the fast reversal of the ring slip product and the slower recombination of the dicarbonyl species with CO Examination of the kinetic parameters of the recombination of the dicarbonyl species with CO, according to Reaction 2 6 (S = cyclohexane), yields a k_2 value of 1 5 × 10^7 dm^3 M^{-1}s^{-1} (at 280 nm)

$$(\eta^6\text{-2,6-lutidine})Cr(CO)_2(S) + CO \xrightarrow{k_2} (\eta^6\text{-2,6-lutidine})Cr(CO)_3 + S \qquad \textit{Reaction 2 6}$$

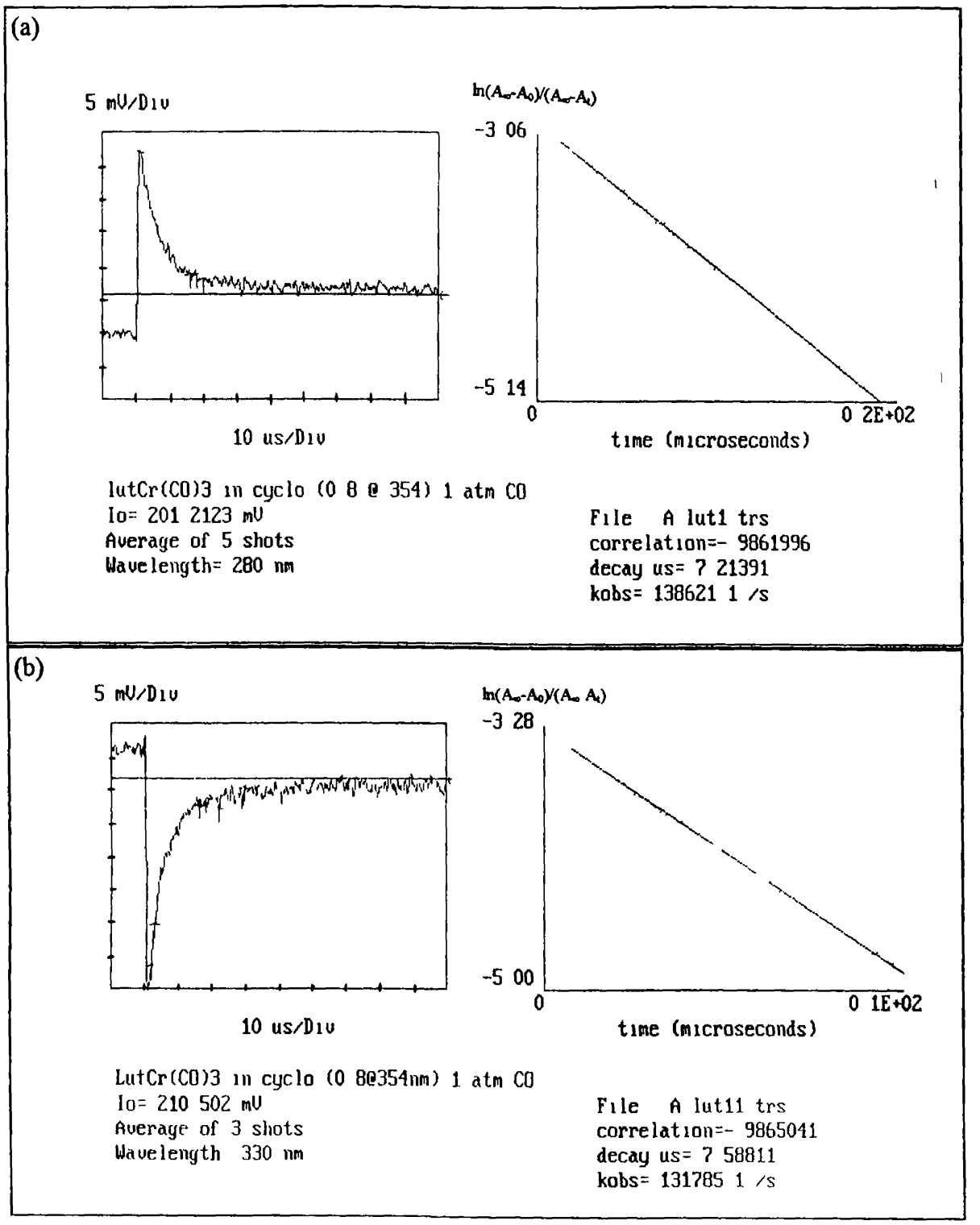

Figure 2.20

(The transient signals obtained following photolysis, (λ_{exc}=355 nm) of

(η^6-2,6-lutidine)Cr(CO)$_3$ in C_6H_{12}(CO), monitored at (a)280 nm, (b) 330 nm)

In Figure 2 20 the k_{obs} obtained for the recombination with CO are shown, the k_2 values can then be found by, dividing this value by the concentration of CO ($9\ 0 \times 10^{-3}$ M)

The ground state absorption spectra obtained during the flash photolysis experiment exhibits a sharp isosbestic point at ~298 nm The parent absorption decreases during the experiment, which agrees with the results of the flash photolysis experiments observed in Figure 2 20 The transient signals indicate that Reaction 2 6 in not totally reversible, and that the parent depletion does not fully recover on the finite-scale of this experiment, which would explain the decrease in the parent absorption

When the experiment is repeated under an Ar atmosphere, depletion of the parent absorption is observed at 330 nm, but this time no recovery is observed The transient at 280 nm shows the formation of the dicarbonyl species, this species does not decay in the time scale of the experiment (100 μs) Ground state UV/vis absorption spectra obtained during the experiment are similar to those obtained under a CO atmosphere This indicates the isosbestic points, observed in both spectra, could be a result of the formation of the (η^6-2,6-lutidine)$Cr(CO)_2(C_6H_{12})$ species However under the Ar atmosphere the presence of a dinuclear species cannot be discounted

(2) Acetonitrile

The photochemistry of (η^6-2,6-lutidine)$Cr(CO)_3$ was investigated by UV/vis flash photolysis with $\lambda_{exc} = 355$ nm in CO saturated acetonitrile A transient signal was observed at 280 nm assigned to the dicarbonyl species, (η^6-2,6-lutidine)$Cr(CO)_2(S)$, where S is acetonitrile This species was not observed to react with CO No transient

signal was observed at 500 nm in this experiment, unlike the (η^6-pyridine)$Cr(CO)_3$ experiments The ground state absorption spectra obtained during the flash photolysis experiment exhibits an isosbestic point at ~300 nm A band can be observed growing at ~500 nm, corresponding to the (η^6-2,6-lutidine)$Cr(CO)_2(S)$ species (Figure 2 21) Another weak band can be observed at ~400 nm, which could possibly be a pentacarbonyl species, either (η^1-2,6-lutidine)$Cr(CO)_5$ or $Cr(CO)_5(CH_3CN)$ This is confirmed by an IR

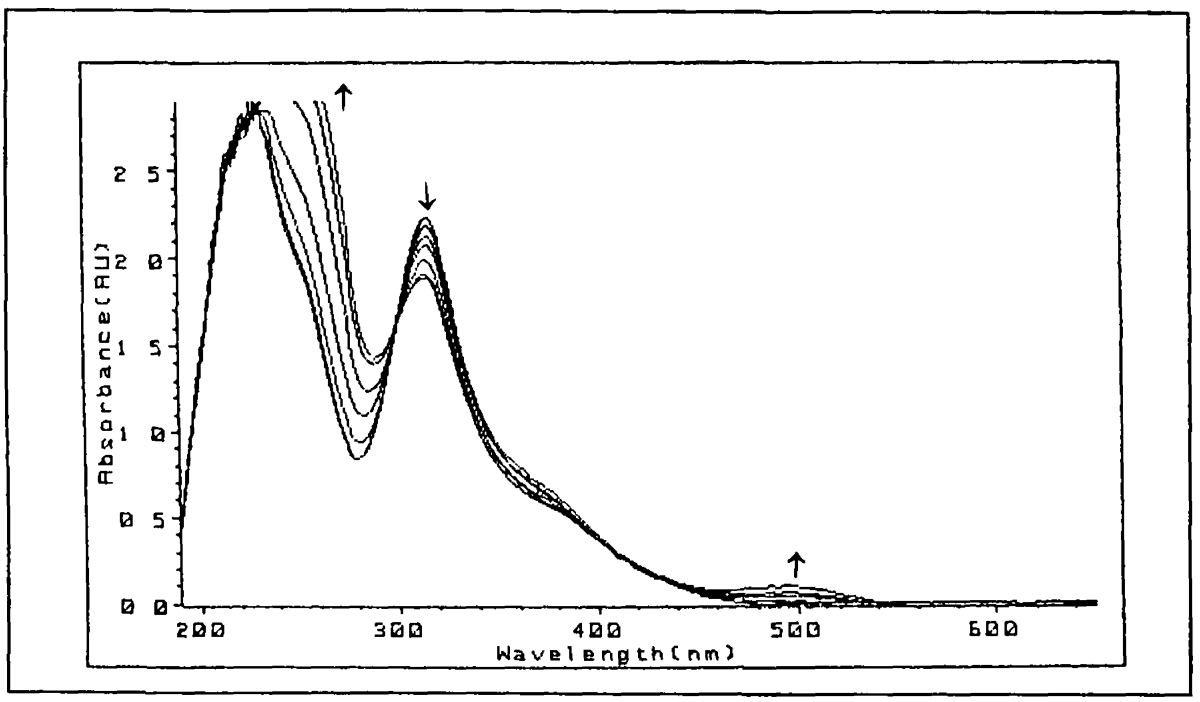

Figure 2.18

(Ground state absorption spectrum of (η^6-2,6-lutidine)$Cr(CO)_3$ (~1 3 x 10^{-4}M) following photolysis (λ_{exc} = 355 nm) in room temperature, CO saturated, acetonitrile)

spectrum obtained of the final solution, again exhibiting the distinctive 2074 cm^{-1} band of the pentacarbonyl species (Figure 2 22) Two bands are assigned to the dicarbonyl species (η^6-2,6-lutidine)$Cr(CO)_2(CH_3CN)$, because of their similarity to the bands observed in the

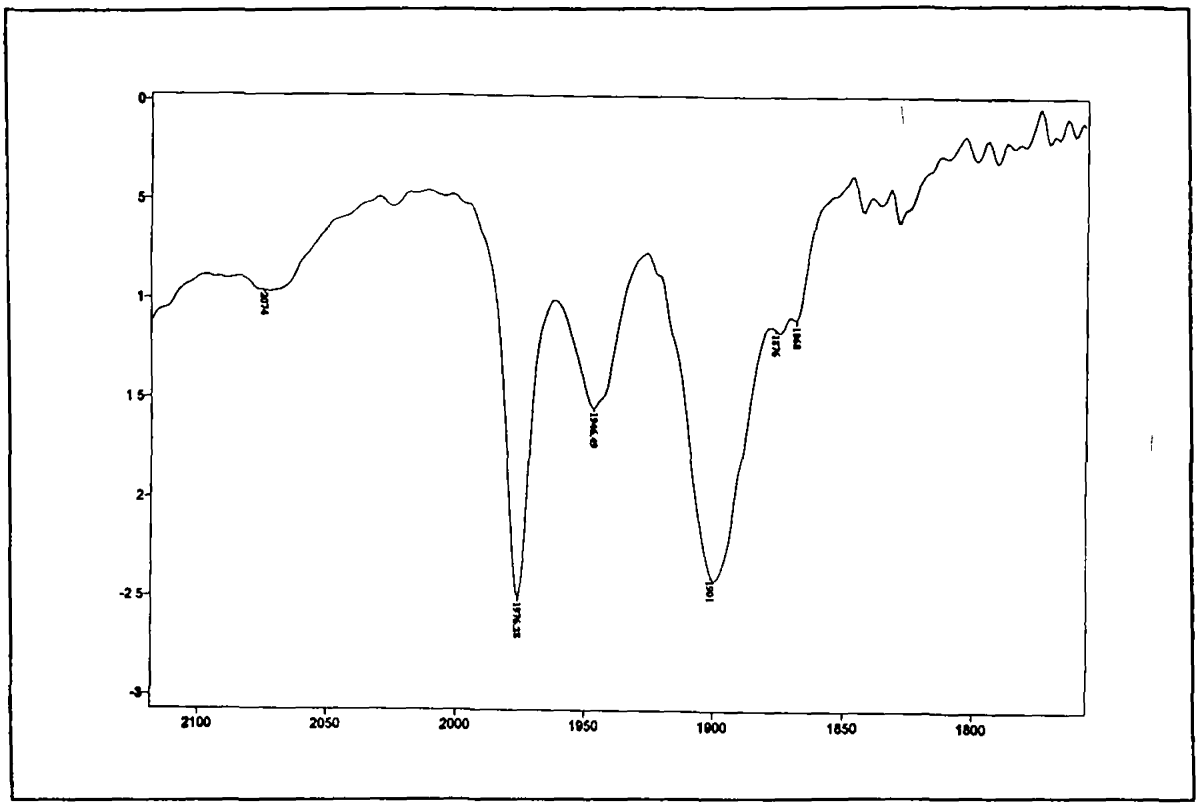

Figure 2.22

(IR spectrum of the solution obtained following photolysis of (η^6-2,6-lutidine)Cr(CO)$_3$ (λ_{exc} = 355 nm) in room temperature, CO saturated, acetonitrile)

methane matrix for the (η^6-pyridine)Cr(CO)$_2$(CH$_4$) species (1945 and 1888 cm^{-1}) No Cr(CO)$_6$ was observed in this experiment, the Cr(CO)$_6$ is presumably formed by the photolysis of the pentacarbonyl species The photolysis time in this experiment was shorter than the corresponding experiment conducted with the (η^6-pyridine)Cr(CO)$_3$ compound This could possibly result in an insufficient amount of the pentacarbonyl species being formed, hence preventing the production of Cr(CO)$_6$

(c) The photochemistry of (η^6-2,6-bis(trimethylsilyl)pyridine)Cr(CO)$_3$

(1) Cyclohexane

The photochemistry of (η^6-2,6-bis(trimethylsilyl)pyridine)Cr(CO)$_3$ was investigated by UV/vis flash photolysis, with λ_{exc} = 355 nm in CO saturated cyclohexane A transient absorption was observed at 280 nm, and this species reacted with CO with a k_2 value 1 6 × 10^8 dm^3 M^{-1} s^{-1} according to Reaction 2 7, (where TMS = 2,6-bis(trimethylsilyl) and S = cyclohexane) This k_2 value was obtained by dividing the k_{obs} by the concentration of CO at 1 atm of CO

$$(\eta^6\text{-(TMS)pyridine})Cr(CO)_2(S) + CO \xrightarrow{k_2} (\eta^6\text{-(TMS)pyridine})Cr(CO)_3 + S \quad \textit{Reaction 2 7}$$

The transient signal observed at 280 nm is shown in Figure 2 23(a) From this it can be seen that the species responsible for the absorption decays fully to regenerate the parent complex At 330 nm both the very fast reaction assigned to the reversal of the ring slip process and the recombination with CO is observed (not illustrated) No transient species is observed at 500 nm

The ground state absorption spectra obtained during the flash photolysis experiment shows no change, which is consistent with the reversibility observed for the transient species Consequently the IR spectrum of the final solution also shows no photoproducts

Figure 2 23(b) shows the transient signal observed at 280 nm under an Ar

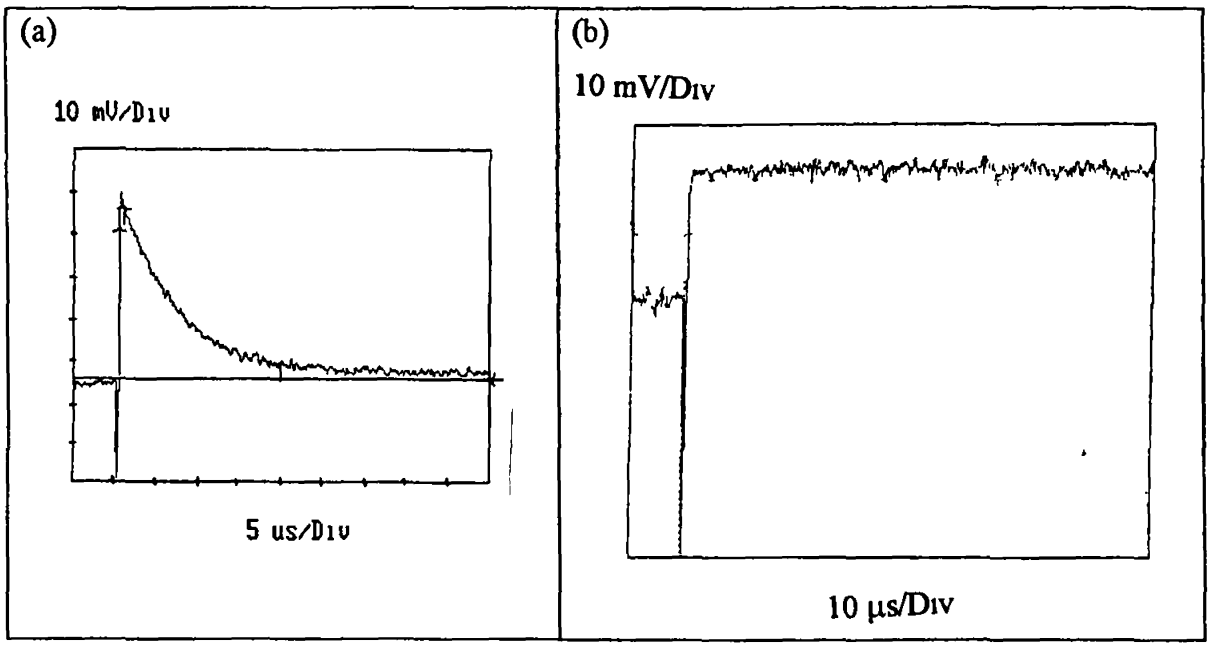

Figure 2.23

(The transient signals obtained following photolysis, (λ_{exc} = 355 nm) of (η^6-2,6-(TMS)pyridine)Cr(CO)$_3$ in C_6H_{12} monitored at 280 nm (a) CO (b) Ar)

atmosphere, in cyclohexane This could be the (η^6-2,6-(TMS)pyridine)Cr(CO)$_2$(S) species or possibly a dinuclear species not involving the arene ring, as the substituents would probably hinder this interaction This transient signal did not decay on the timescale of the experiment

The ground state absorption spectrum monitored during the experiment in the absence of CO, exhibits depletion of the parent complex with concomitant growth of bands at ~ 260 nm and 280 nm and a weak broad band in the visible region (440 to 520 nm) The IR spectrum of the final solution shows the production of bands at ~1870 cm^{-1} and a shoulder on the parent band ~1934 cm^{-1} similar to the bands observed for the

dicarbonyl species in an Ar CO matrix (1890 and 1942 cm^{-1}), supporting the assignment of this species as the (η^6-2,6-(TMS)pyridine)$Cr(CO)_2$(S) complex

(2) Acetonitrile

The photochemistry of (η^6-2,6-bis(trimethylsilyl)pyridine)$Cr(CO)_3$ was investigated by UV/vis flash photolysis with λ_{exc} = 355 nm in CO saturated acetonitrile The formation of the dicarbonyl species, (η^6-2,6-(TMS)pyridine)$Cr(CO)_2$(S), is observed at 280 nm, which does not decay within the timescale of the experiment No transient signals were observed at 500 nm The ground state absorption spectrum depicted in Figure 2 24 shows the growth of two bands assigned to (η^6-2,6-(TMS)pyridine) $Cr(CO)_2(CH_3CN)$ at ~ 260 and ~ 500 nm Unlike the (η^6-pyridine)$Cr(CO)_3$ and

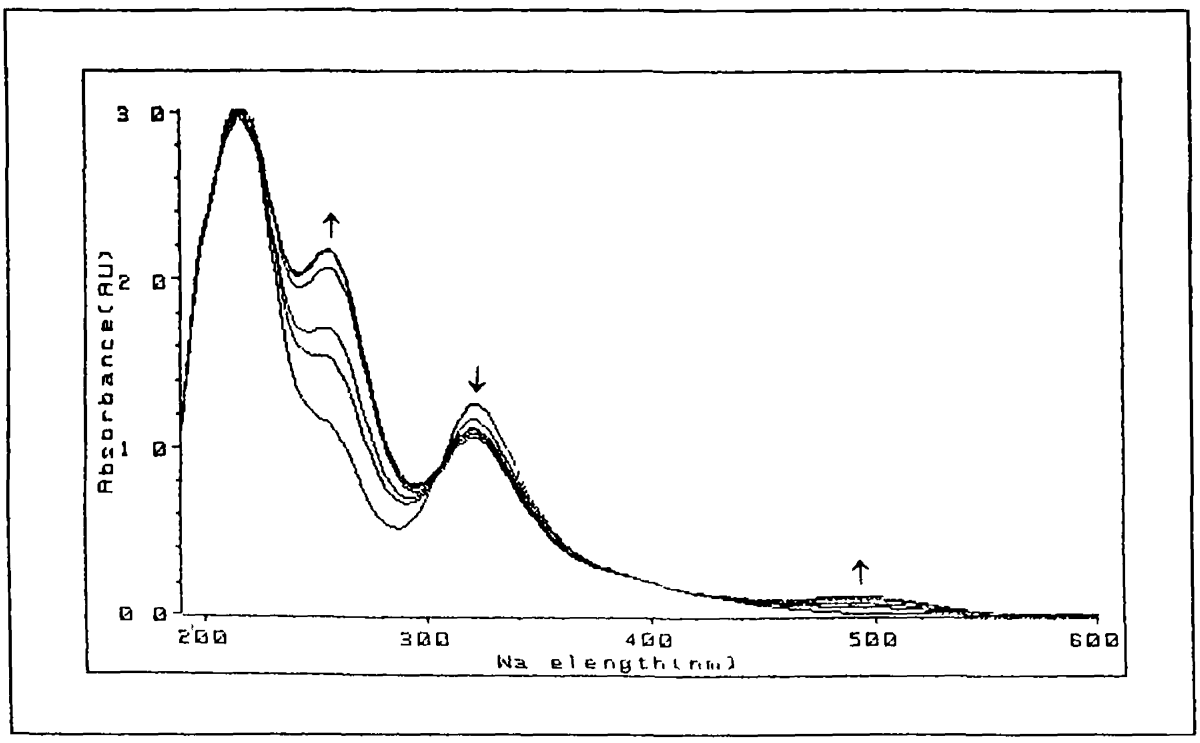

Figure 2 24

(Ground state absorption spectrum of (η^6-2,6-(TMS)pyridine)$Cr(CO)_3$ following photolysis (λ_{exc} = 355 nm) in room temperature, CO saturated acetonitrile)

(η^6-2,6-lutidine)$Cr(CO)_3$ systems no band at ~ 400 nm is observed, indicating that no (η^1-2,6-(TMS)pyridine)$Cr(CO)_5$ or $Cr(CO)_5(CH_3CN)$ is formed This is confirmed by the IR spectrum, the only photoproducts observed are assigned to the dicarbonyl species, (1945 and 1870 cm^{-1}) (η^6-2,6-(TMS)pyridine)$Cr(CO)_2(CH_3CN)$

2 2 6 Discussion

The formation of (η^1-pyridine)$Cr(CO)_5$ and ultimately $Cr(CO)_6$ as a result of the photolysis of (η^6-pyridine)$Cr(CO)_3$ in the presence of CO, demonstrates that CO-loss is not the only photochemical route accessible to this complex If this were the case, then no photochemical change would be apparent under these conditions The efficiency of this photochemical process is dependent on the nature of the solvent and the substituents α-to the nitrogen on the pyridine ring From the steady state experiments (Section 2 2 2) it can be seen that photolysis in solvents with a Lewis base character (e g methanol or dimethylsulphoxide) results in a more efficient formation of the pentacarbonyl species and the free pyridine, than photolysis in cyclohexane, benzene, or acetonitrile This suggests that solvents play a role in stabilising the intermediate formed from the haptotropic rearrangement of the pyridine ring The UV/vis flash photolysis experiments (Section 2 2 5) of the three compounds, demonstrate the effect of the substituents α-to the nitrogen on the pyridine ring When hydrogen atoms are present at the 2 and 6 positions the pentacarbonyl species is formed However, bulky trimethylsilyl groups appear to hinder the production of the pentacarbonyl species The matrix isolation experiments

prove to be valuable in determining the nature of the intermediate formed *via* the ring slip process

The photochemistry of (η^6-pyridine)$Cr(CO)_3$, isolated in a range of low temperature matrices exhibited a wavelength dependency Long wavelength irradiation (λ_{exc} = 460 nm) results in an haptotropic change of the pyridine ring coordination This was observed in a methane matrix, where the photoproduct possessed a three band pattern in the ν_{co} region which corresponds to the number of CO ligands present Therefore no CO loss occurred, further supported by the absence of a band associated with free CO in the matrix, and the only photochemistry involved an hapticity change of the pyridine coordination The photochemistry of (η^6-pyridine)$Cr(CO)_3$ was investigated in a nitrogen matrix to elucidate the extent of this hapticity change The results suggested that an η^6 to η^1 haptotropic rearrangement occurred producing the 14 electron, doubly coordinatively unsaturated, (η^1-pyridine)$Cr(CO)_3$, which subsequently coordinates to two N_2 molecules This species, *fac*-(η^1-pyridine)$(N_2)_2Cr(CO)_3$ has two absorption bands in the $\nu_{N\text{-}N}$ region Following long wavelength irradiation (λ_{exc} = 460 nm) in a CO rich matrix (η^1-pyridine)$Cr(CO)_5$ is predominantly formed, the tetracarbonyl compound is only produced following subsequent photolysis of the pentacarbonyl species (λ_{exc} = 250 nm) Regeneration of the pentacarbonyl species occurs following white light photolysis of the tetracarbonyl photoproduct Therefore the results from these two matrix environments suggests, that absorption of a visible photon, generates two vacant coordination sites on the metal, as a result of the η^6 to η^1 haptotropic rearrangement of the pyridine ring as depicted in Scheme 2 4

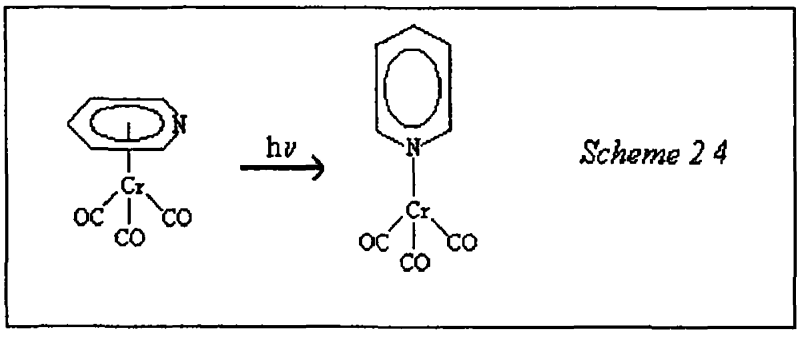

Scheme 2 4

Shorter wavelength irradiation (308 nm) of (η^6-pyridine)$Cr(CO)_3$ isolated in a CH_4 matrix produced two photoproducts Again the (η^1-pyridine)$Cr(CO)_3$ species was observed, and also further bands at 1945 and 1888 cm^{-1} In these experiments a band assigned to free CO was also observed These bands were assigned to the CO loss product, because of the presence of free CO in the matrix Confirmation of this assignment was attained by a comparison of the shifts in the band positions, between the parent to the photoproduct, relative to the shifts observed for the (η^6-benzene)$Cr(CO)_3$ system The high energy band of the photoproduct is shifted by 56 cm^{1} compared to the parent compound in both the (η^6-benzene)$Cr(CO)_3$ and the (η^6-pyridine)$Cr(CO)_3$ systems Averaging the lower energy absorptions, results in a shift of 44 cm^{1} for the (η^6-pyridine)$Cr(CO)_3$ system, this is similar to the shift observed for the (η^6-benzene)$Cr(CO)_3$ system (38 cm^{-1}) Therefore the photochemistry of (η^6-pyridine)$Cr(CO)_3$ exhibited a wavelength dependence when isolated in a range of matrices Long wavelength photolysis resulted in an haptotropic rearrangement of the pyridine ring, without any CO-loss, (which is the most common photoproduct observed upon photolysis of (η^6-arene)$Cr(CO)_3$ compounds), whereas shorter wavelength photolysis produced both (η^6-pyridine)$Cr(CO)_2$(S) and also the ring slip product

The matrix photochemistry of (η^6-2,6-bis(trimethylsilyl)pyridine)$Cr(CO)_3$ was examined to investigate the effect of the bulky substituents on the photochemistry of this system In contrast to the photochemistry of the unsubstituted analogue described above, no evidence for the production of a pentacarbonyl or hexacarbonyl species was obtained, following photolysis of the TMS derivative In fact when the compound was photolysed with an excitation wavelength of 460 nm, no photoproducts were observed in the IR spectrum Irradiation with λ_{exc} = 313 nm produced both the ring-slip and CO-loss species, although the absorption bands of the ring slip product were weak The

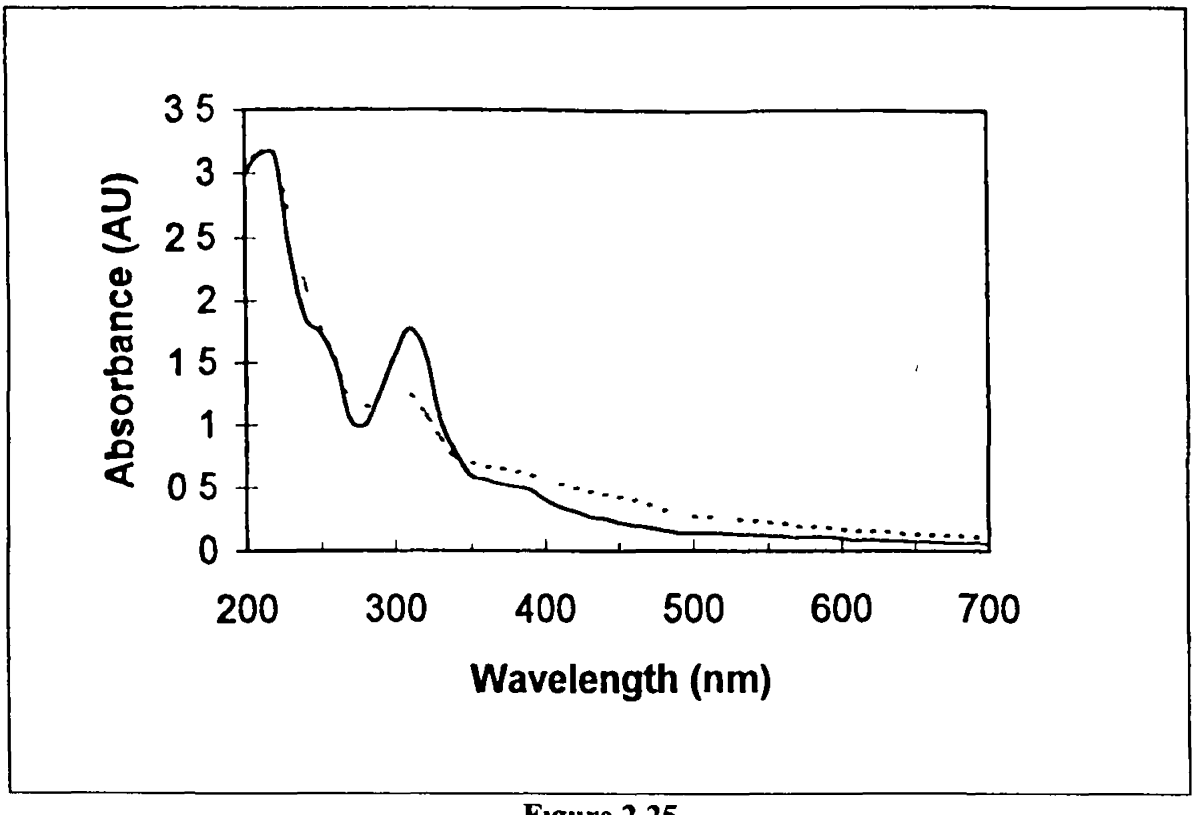

Figure 2 25

(The UV/vis spectrum of (η^6-pyridine)$Cr(CO)_3$ in a CH_4 matrix at 12K (—), and the same matrix following irradiation 60 s with λ_{exc} = 308 nm (----) These spectra are not corrected for matrix scatter)

photoproducts underwent photoreversal upon white light photolysis, this may explain the lack of photoproducts observed following 460 nm irradiation, which may simply reflect an efficient photoreversal of the ring-slip product Figure 2 25 shows that the photoproducts formed following 308 nm irradiation of (η^6-pyridine)$Cr(CO)_3$ in a methane matrix, which exhibit a broad absorption in the visible region of the spectrum When the photochemistry of (η^6-2,6-bis(trimethylsilyl)pyridine)$Cr(CO)_3$ is investigated in a N_2 matrix, the predominant photoproduct is the dicarbonyl species, even following long wavelength irradiation However the process is very inefficient Weak bands were observed which could be assigned as the ring-slip product, however these bands were so weak it proved impossible to detect any $\nu_{N\text{-}N}$ bands associated with this species Therefore it is not possible to ascertain if the ring-slip product interacts with the N_2 matrix UV/vis flash photolysis experiments of (η^6-2,6-bis(trimethylsilyl)pyridine)$Cr(CO)_3$ in acetonitrile provided no evidence for the presence of the pentacarbonyl species, unlike analogous experiments involving (η^6-pyridine)$Cr(CO)_3$ and (η^6-lutidine)$Cr(CO)_3$ Possibly indicating that, interaction of the environment with the two vacant coordination sites (produced by the ring slip process), is hindered by the two bulky substituents α-to the nitrogen on the pyridine ring

In order to investigate the effect of these substituents, when the pyridine ring is bound to the metal *via* the η^1 interaction, the X-ray data obtained (Chapter 3) for the (η^6-2,6-bis(trimethylsilyl)pyridine)$Cr(CO)_3$ compound was examined Using the "UNLOCK MODEL" facility in Schakal -92[45] the chromium tricarbonyl unit was located 2 0 Å from the nitrogen atom This is approximately where it would be following an η^6 to

η^1 haptotropic shift Analysis of the close contacts for this orientation indicated that there was sufficient freedom to permit coordination of the pyridine nitrogen atom to the chromium tricarbonyl unit, but not to higher order carbonyl units or additional solvent or matrix molecules This explains why the presence of the trimethylsilyl groups α-to the coordinating nitrogen atom prevents the formation of the metal pentacarbonyl or metal tetracarbonyl species

The photochemistry of (η^6-pyridine)$Cr(CO)_3$ was investigated in cyclohexane and monitored by TRIR The results indicated that the primary photoinduced process resulted in the production of the dicarbonyl species, only very weak bands associated with the pentacarbonyl species were subsequently observed Two plausible explanations are possible for this observation

Firstly, that the ring slip process is only observed as a result of secondary photolysis of the CO loss product If this were the case then the ring slip product would only be observed following steady state photolysis and not be observed following pulsed laser photolysis This explanation is discounted on two grounds, firstly the ring slip product is observed in the matrix experiments, following long wavelength photolysis, in the absence of any dicarbonyl species being present Secondly, photolysis of the dicarbonyl species results in regeneration of the parent species and not the ring-slip product

The second explanation for the difference between the matrix results and the TRIR results concur with the results obtained in the UV/vis flash photolysis experiments Monitoring the recovery of the depleted parent absorption at 330 nm

following pulse photolysis at 355 nm, demonstrated that the recovery followed a biphasic time profile The faster of these recoveries, measured to occur within 40 ns, was assigned to the reversal of the ring-slip process This process would then occur within the rise-time of the TRIR equipment, preventing any observation of this process As the TRIR experiments were carried out in cyclohexane which, according to the UV/vis results, does not act as an efficient "trap" for the ring slip product, only a small amount of the pentacarbonyl species would be formed This leads to the conclusion that although the ring slip process accounts for a significant proportion of the energy absorbed, it does not lead to discernible photoproducts in solution unless the η^1 species is "trapped" by a donor solvent

The k_2 values obtained from TRIR and UV/vis flash photolysis experiments for Reaction 2 8 are the same within experimental error The TRIR results were obtained by subtracting the k_{obs} in the absence of CO from that in the presence of 9 mm CO and dividing by 9 mm The UV/vis results were obtained by dividing the k_{obs} by the concentration of CO at different concentrations of CO

$$(\eta^6\text{-pyridine})Cr(CO)_2(C_6H_{12}) + CO \xrightarrow{k_2} (\eta^6\text{-pyridine})Cr(CO)_3 + C_6H_{12} \qquad \textit{Reaction 2 8}$$

Table 2 5 contains a summary of the k_2 values obtained from UV/vis flash photolysis experiments, for the reaction of the solvated complexes with CO It can be seen that the

L	k_2 ($dm^3 M^{-1} s^{-1}$) [cyclohexane (±10%)]
pyridine	1.4×10^7
2,6-lutidine	1.5×10^7
2,6-bis(trimethylsilyl)pyridine	1.6×10^8

Table 2.5

(The second order rate constants (k_2) for the reaction of $LCr(CO)_2(S)$ with CO at 298 K)

rates for the reaction when the arene ligand is pyridine or 2,6-lutidine do not differ greatly However the rate for the reaction, when the substituents are the bulky trimethylsilyl groups, is one order of magnitude faster This increase in rate with increasing substitution on the arene ring has been observed previously [46,40] Results obtained by Poliakoff *et al* [45] indicated that substitution of the cyclopentadienyl ring changes the rate of reaction of the $(\eta^5\text{-}C_5R_5)Mn(CO)_2$(*n*-heptane) intermediates with CO, where R = H, CH_3, or C_2H_5 As the electronic factors for the ligands when R is CH_3 or C_2H_5 are similar, it was suggested that the origin of the variation in rates was steric rather than electronic As the trimethylsilyl ligands do differ electronically from the H and CH_3 ligands, both steric and electronic factors may play a role in increasing the rate of the reaction of (η^6–2,6-bis(trimethylsilyl)pyridine)$Cr(CO)_2(S)$

Scheme 2 5 summarises the overall photochemistry and subsequent thermal reactions of the (η^6-pyridine)$Cr(CO)_3$ compound The photochemistry of the (η^6-2,6-lutidine)$Cr(CO)_3$ is very similar to the reactions represented in Scheme 2 5 However the photochemistry of the (η^6-2,6-bis(trimethylsilyl)pyridine)$Cr(CO)_3$ does differ from the

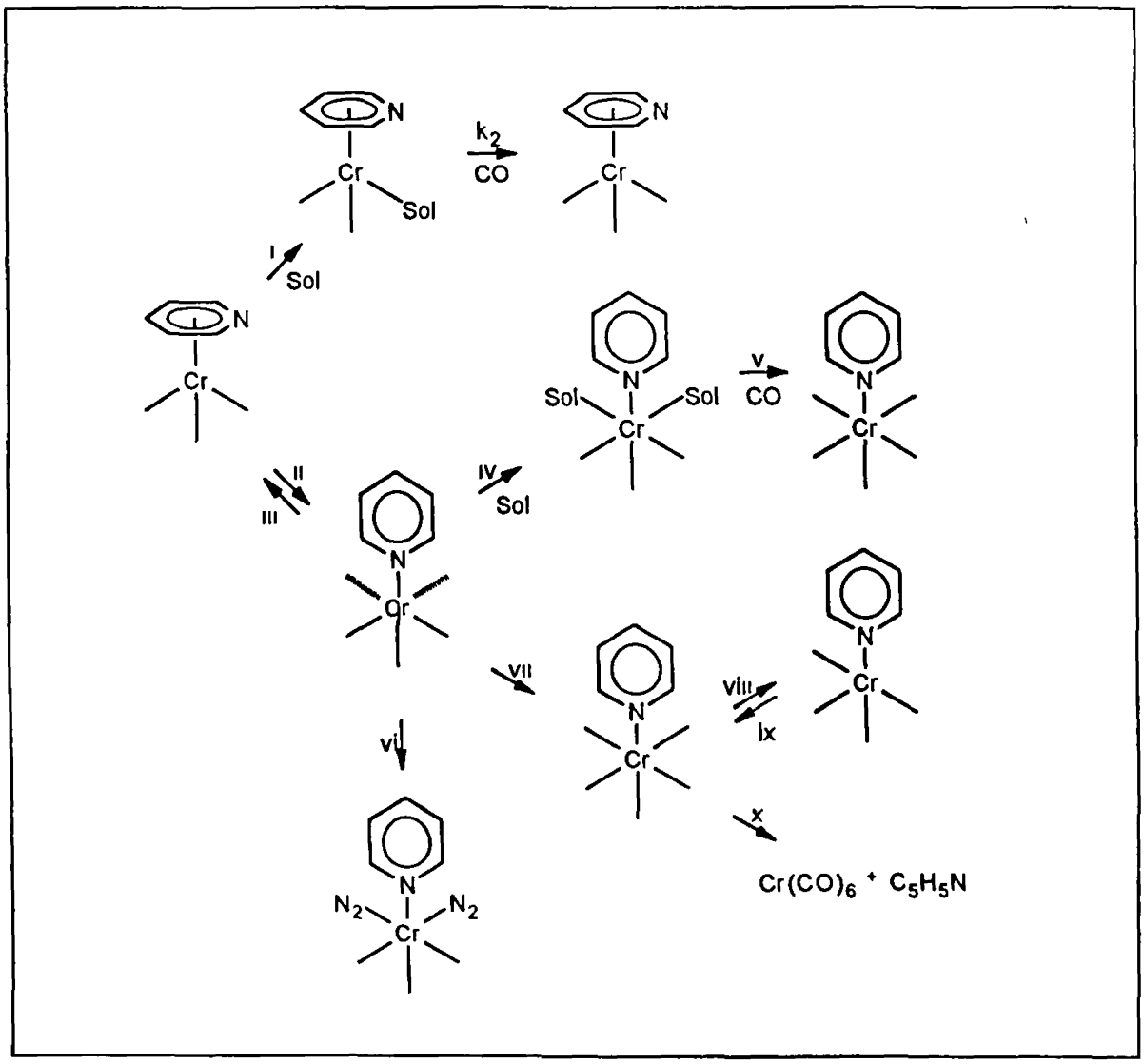

Scheme 2.5

(CO ligands are represented thus —for clarity Reaction conditions (i) λ_{exc} < 360 nm, Sol = cyclohexane, (ii) λ_{exc} > 308 nm, (iii) $\tau_{1/2}$ < 40 ns in cyclohexane, (iv) Sol = acetonitrile, benzene, cyclohexane, dimethylsulphoxide, or methanol, (v) CO saturated acetonitrile, benzene, cyclohexane, or methanol, (vi) λ_{exc} = 460 nm N_2 matrix, (vii) λ_{exc} = 460 nm 10% CO in CH_4 matrix, (viii) λ_{exc} = 250 nm 10% CO in CH_4 matrix, (ix) λ_{exc} > 530 nm 10% CO in CH_4 matrix, (x) hv 10% CO in CH_4 matrix)

above scheme The bulky substituents α-to the nitrogen on the pyridine ring play a role in hindering the ring slip process Therefore although this haptotropic rearrangement does occur, reactions (iv), (vi), or (vii) in Scheme 2 5 do not proceed for this complex The photochemistry of this complex is dominated by the extreme photoreversibility of the two photochemical pathways, resulting in a very photostable system compared to the other two complexes

2 2 7 Conclusions

Although the photochemistry of this system is relatively simple, a variety of techniques were required to elucidate the photochemical pathways of the (η^6-pyridine)$Cr(CO)_3$ compound When the data collected from the different techniques were compared, a complete picture of the photochemistry of this system was possible If however, only the TRIR technique was employed, an overly simplistic interpretation of the photochemical routes available to these compounds, would have been obtained

This study has demonstrated the importance of the ring slip process in the photochemistry of the (η^6-arene)$Cr(CO)_3$ complexes The lone pair on the nitrogen has acted as a very efficient trap for this process, even when it is sterically hindered by substituents α-to the nitrogen These results have also confirmed the importance of the solvent environment when investigating the photochemistry of organometallic compounds For instance when the photochemistry is carried out in a solvent with a strong Lewis base character, more of the products formed *via* the ring slip process can be observed However investigation in a solvent that is a weaker base, could result in this process being missed entirely, as a result of its high reversibility

REFERENCES

(Chapter 2)

[1] Strohmeier W , von Hobe D , *Z Naturforsch , Teil B,* 1963, **18**, 981

[2] (a) Strohmeier W , Hellmann H , *Z Naturforsch , Teil B,* 1963, **18**, 769

(b) Strohmeier W , Hellmann H , *Chem Ber* , 1963, **97**, 2859

(c) Strohmeier W , Hellmann H , *Chem Ber* , 1964, **97**, 1877

(d) Strohmeier W , Hellmann H , *Chem Ber* , 1965, **98**, 1598

(e) Strohmeier W , Popp G , Guttenberger J F , *Chem Ber* , 1966, **99**, 165

(f) Strohmeier W , Guttenberger J F , Muller F J , *Z Naturforsch , Teil B,* 1967, **22**, 1091

(e) Guttenberger J F , Strohmeier W , *Chem Ber* , 1967, **100**, 2807

[3] (a) Fischer E O , Kuzel P , *Z Naturforsch , Teil B,* 1961, **16**, 475

(b) Strohmeier W , von Hobe D , *Z Naturforsch , Teil B,* 1963, **18**, 770

[4] Wrighton M S , Haverty J L , *Z Naturforsch , Teil B,* 1975, **30**, 254

[5] Gilbert A , Kelly J M , Budzwait M , Koerner von Gustorf E , *Z Naturforsch , Teil B,* 1976, **31**, 1091

[6] Nasielski J , Denisoff O , *J Organomet Chem* 1975, **102**, 65

[7] (a) Trembovler V N , Baranetskaya N K , Fok N V , Zaslavskaya G B , Yavorskii B M , Setkina V N , *J Organomet Chem* , 1976, **117**, 339

(b) Trembovler V N , Yavorskii B M , Setkina V N , Baranetskaya N K , Zaslavskaya G B , Evdokimova M G , *Russ J Phys Chem* , 1974, **3**, 1231

[8] Bamford C H , Al-Lamee K G , Konstantinov C J , *J Chem Soc , Faraday Trans I,* 1977, **73**, 1406

[9] Rest A.J , Sodeau J R , Taylor D J , *J Chem Soc , Dalton Trans I,* 1978, 651

[10] Hill R S , Wrighton M S , *Organometallics,* 1987, **6**, 632

[11] Wang W , Jin P , Liu Y , She Y , Fu K-J , *J Phys Chem* , 1992, **96**, 1278

[12] Zheng Y , Wang W , Lin J , She Y , Fu K-J , *J Phys Chem* , 1992, **96**, 9821

[13] (a) Kubas G J , Ryan R R , Swanson B I ,Vergamini P J , Wasserman H J , *J Am Chem Soc* , 1984, **106**, 451

(b) Kubas G J , Ryan R R , Wrobleski D A , *J Am Chem Soc* , 1986, **108**, 1339

[14] Muetterties E L , Bleeke J R , Sievert A C , *J Organomet Chem* 1979, **178**, 197

[15] (a) Strohmeier W , Mittnacht H , *Z Phys Chem* , 1961, **29**, 339

(b) Strohmeier W , Starnico E H , *Z Phys Chem* , 1963, **38**, 315

(c) Strohmeier W , Muller M , *Z Phys Chem* , 1964, **40**, 85

[16] (a) Jackson W R , Nicholls B , Whiting M C , *J Chem Soc* 1960, 469

(b) Gracey D E F , Jackson W R , McMullen C H , Thompson N , *J Chem Soc (B),* 1969, 1197

[17] (a) Mahaffy C A L , Pauson P L , *J Chem Res (S),* 1979, 126

(b) Mahaffy C A L , Pauson P L , *J Chem Res (M),* 1979, 1752

[18] Zimmerman C L , Shaner S L , Roth S A , Willeford B R , *J Chem Res (S),* 1980, 108

[19] (a) Traylor T G , Stewart K , *Organometallics,* 1984, **3**, 325

(b) Traylor T G , Stewart K , *J Am Chem Soc* , 1984, **106**, 4445

(c) Traylor T G , Stewart K , Goldberg M J , *Organometallics*, 1986, **5**, 2062

(d) Traylor T G , Stewart K , *J Am Chem Soc* , 1986, **108**, 6977

(e) Traylor T G , Goldberg M J , *J Am Chem Soc* , 1987, **109**, 3968

(f) Traylor T G , Goldberg M J , *Organometallics*, 1987, **6**, 2413

(g) Traylor T G , Goldberg M J , *Organometallics*, 1987, **6**, 2531

[20] Albright T A , Hofmann P , Hoffmann R , Lillya C P , Dobosh P A., *J Am Chem Soc* , 1983, **105**, 3396

[21] Howell J A S , Ashford N F , Dixon D T , Kola J C , *Organometallics*, 1991, **10**, 1852

[22] "Orbital Interactions In Chemistry" Albright T A , Burdett J K , Whangbo M-H , John Wiley & Sons, New York 1985

[23] DiNardo N J , Avouris Ph , Demuth J E , *J Chem Phys* , 1984, **81**, 2169

[24] Pannell K H , Kalsotra B L , Parkanyi C , *J Heterocyclic Chem* , 1978, **15**, 1057

[25] (a) Timms P L , *Angew Chem* 1975, **87**, 295

(b) Timms P L , *Angew Chem Int Ed, Engl* , 1975, **14**, 273

[26] (a) Biedermann H G , Ofele K , Tajtelbaum J , *Z Naturforsch Teil B*, 1976, **31**, 321

(b) Biedermann H G , Ofele K , Schuhbaur N , Tajtelbaum J , *Angew Chem Int Ed. Engl* , 1975, **14**, 639

[27] (a) Simons L H , Riley P E , Davis R E , Lagowski J J , *J Am Chem Soc* , 1976, **98**, 1044

(b) Riley P E , Davis R E *Inorg Chem* , 1976, **15**, 2735

[28] Fischer E O , Ofele K , *J Organomet Chem* , 1967, **8**, 5

[29] Morris R H , Ressner J M , *J Chem Soc , Chem Commun* , 1983, 909

[30] (a) Chaudret B , Jalon F A , *J Chem Soc , Chem Commun* , 1988, 711

(b) Fish R H , Kim H -S , Fong R H , *Organometallics,* 1989, **8**, 1375

[31] Elschenbroich C , Koch J , Kroker J , Wunsch M , Massa W , Baum G , Stork G , *Chem Ber , Teil B,* 1988, **121**, 1983

[32] Davies S G , Shipton M R , *J Chem Soc , Chem Commun* , 1989, 995

[33] Davies S G , Shipton M R , *J Chem Soc , Perkin Trans 1,* 1991, 501

[34] Davies S G , Shipton M R , *J Chem Soc , Perkin Trans 1,* 1991, 757

[35] (a) Wrighton M , Hammond G S , Gray H B , *J Am Chem Soc* , 1971, **93**, 4336

(b) Wrighton M , Hammond G S , Gray H B , *Inorg Chem* , 1972, **11**, 3122

[36] Boxhoorn G , Oskam A , Gibson E P , Narayanaswamy R , Rest A J , *Inorg Chem* , 1981, **20**, 783

[37] Lees A J , *J Am Chem Soc* , 1982, **104**, 2038

[38] Chun S , Getty E E , Lees A J , *Inorg Chem* , 1984, **23**, 2155

[39] Manuta D M , Lees A J , *Inorg Chem* , 1983, **22**, 3825

[40] McGrath I M , *Ph D Thesis,* Dublin City University, 1993

[41] Creaven B S , George M W , Ginzburg A G , Hughes C , Kelly J M , Long C , McGrath I M , Pryce M T , *Organometallics,* 1993, **12**, 3127

[42] George M W , Haward M T , Hamley P A , Hughes C , Johnson F P A , Popov V K ,

Poliakoff M , *J Am Chem Soc* , 1993, **115**, 2286

[43] Perutz R N , Turner J J , *J Am Chem Soc* , 1975, **75**, 4791

[44] Makrancszy J , Megyery-Balog K , Rosz L , Patyt D ,

Hungarian J Indust Chem , 1976, **4**, 269

[45] Keller E , SCHAKAL-92, A programme for Graphical representation of Molecular Structures, Kristallographisches Institut der Universitaet, Freiburg, Germany, 1992

[46] Johnson F P A , George M W , Bagratashvili V N , Vereshchagina L N , Poliakoff M ,

J Chem Soc , Mendeleev Commun , 1991, 26

CHAPTER 3

3.1 LITERATURE SURVEY

3 1 1 X-ray single crystal diffraction

The essential feature of a crystal is its internal regularity, not its external form Occasionally objects have gleaming faces, which are generally associated with crystals, and turn out to be amorphous Some crystals appear to lack any gleaming faces and actually prove to be crystalline Therefore the internal regularity is the determining factor in identifying a crystal A crystal consists of a repetition of three dimensional blocks which are called the unit cells Each of these unit cells may contain one or more molecules, and all the unit cells are identical The shape of the unit cell is characteristic of the material involved These shapes can be grouped into families, which are known as crystal systems

Diffraction methods for determining structural information are all based on the same theory The methods differ from each other mainly in the source of the beam that strikes the atoms The beam could consist of X-rays, neutrons or electrons and the each method has different advantages and restrictions When a beam of X-rays strikes two atoms, the scattered X-ray beams in a certain direction will be out of phase with each other to an extent that depends on the wavelength of the X-rays, the distance between the atoms, and their orientation This phase difference could either result in the beams cancelling each other out, resulting in a reduction of the diffracted beam, or constructive interference resulting in a stronger beam

X-ray diffraction from single crystals is by far the most important of all the structural techniques, with about 10,000 structures being reported every year This technique allows the precise measurement of bond angles and bond lengths The X-rays are diffracted by the electrons in the atoms, this results in one of the limitations of this technique If the molecule contains "heavy" atoms, (*i e* those of high atomic number containing many electrons), these atoms will influence the scattering more than the lighter atoms, thus possibly obscuring the presence of these smaller atoms Hydrogen atoms are particularly affected by this, thus the errors in the hydrogen positions are greater than the larger atoms Therefore the positions of the hydrogen atoms are often assumed The neutron diffraction technique can be employed to locate the hydrogen atoms, as the neutrons are diffracted by the nuclei, however a source of neutrons is very expensive therefore this technique is not as widely employed as the X-ray diffraction method Even with the lack of information of the lighter atoms, this method has been employed to analyse the structure of complicated crystals, containing hundreds and thousands of atoms in the unit cell Since the location of an atom in the molecule, obtained from X-ray diffraction, is an average of all the positions it occupied during the determination, the resultant structure is often presented in terms of thermal ellipsoids These are probability indicators of where the atoms are most likely to be found

3 1 2 Crystal structures obtained of related compounds

The three compounds examined in this study all contain a pyridine ring, or a substituted pyridine ring, bound in a η^6 fashion to a chromium atom The crystal

structure of bis(η^6-2,6-dimethylpyridine)Cr has been reported [1] It was found that the crystals exhibited two different morphologies, one proved to be triclinic (Form A) and the other form was orthorhombic (Form B) In the triclinic form the chromium was found to be an inversion centre and the pyridine rings were strictly parallel The orthorhombic form contains a C_2 axis that is parallel to the nitrogen and the *para* carbon, and contains chromium The methyl groups are staggered with respect to the groups on the opposite ring

The geometrical features of the two morphologies are similar, the crystal to ring atom distances are 2 136 Å for both forms For comparison the mean Cr-C distance in bis(η^6-benzene)Cr is 2 142 Å,[2] or 2 13 Å,[3] and in (η^6-benzene)$Cr(CO)_3$ the distance has been reported as 2 243 Å[4] or 2 221 Å [5] The pyridine rings were found to be planar in the triclinic form, but slightly boat shaped in the orthorhombic form, with the nitrogen and the *para* carbon being slightly distorted towards the Cr atom The methyl groups in the triclinic form lie out of the pyridine plane and away from the Cr, however no deviation from the pyridine plane is observed for the orthorhombic crystal

Elschenbroich *et al* [6] substituted the pyridine ring at the 2 and 6 positions with the bulky trimethylsilyl groups, which prevented the nitrogen being σ bound to the metal Therefore the pyridine ring could be complexed to chromium in an η^6 fashion and then the bulky substituents could be removed to produce the bis(η^6-pyridine)Cr compound Crystals were grown of this compound, it was found that the average Cr to carbon (or nitrogen) in the ring was 2 133 Å, which was very similar to the average distance observed in the bis(η^6-2,6-dimethylpyridine)Cr complex The carbon to nitrogen

bond distance in "free" pyridine, obtained from microwave measurements, was reported to be 1.34 Å,[7] in this compound it was found to be 1.38 Å. The carbon to carbon distances were the same, 1.40 Å in both cases. The internal angles at the nitrogen and the two carbons *meta* to the nitrogen are practically the same 118°, the carbons at the 4 and 6 positions have angles of ~121°, however the angle at the carbon at the 2 position is 123°, which is close to the value for free pyridine at this position, 124°.

Table 3.1 contains a summary of the bond lengths, and Table 3.2 contains the bond angles at the respective atoms, obtained for the pyridine ring in the three different compounds. The individual atoms are numbered as depicted in Figure 3.1.

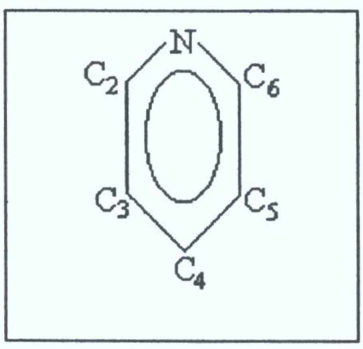

Figure 3.1

(Numbering employed for the atoms in the pyridine ring in Table 3.1 and 3.2)

Bonds	Free pyridine	bis(η^6-2,6-dimethylpyridine)Cr		bis(η^6-pyridine)Cr
		Form A	Form B	
N-C_2	1.34 (5)	1.405 (11)	1.382 (4)	1.38 (4)
C_2-C_3	1.39 (5)	1.386 (13)	1.390 (6)	1.40 (4)
C_3-C_4	1.40 (5)	1.394 (14)	1.394 (6)	1.39 (4)
C_4-C_5	1.40 (5)	1.423 (13)	1.413 (6)	1.40 (4)
C_5-C_6	1.39 (5)	1.372 (12)	1.395 (5)	1.41 (4)
C_6-N	1.34 (5)	1.373 (11)	1.378 (4)	1.38 (4)

Table 3.1

(Bond lengths (Å) in the pyridine ring obtained from references 7, 1, and 6)

Bond Angles	Free pyridine	bis(η^6-2,6-dimethylpyridine)Cr		bis(η^6-pyridine)Cr
		Form A	Form B	
N	116 7	116 8 (7)	116 9 (2)	118 0 (3)
C_2	124	121 0 (8)	122 3 (3)	123 4 (3)
C_3	118 6	122 3 (8)	120 5 (3)	117 3 (3)
C_4	118 1	115 8 (9)	117 8 (4)	121 5 (3)
C_5	118 6	121 1 (8)	119 4 (4)	118 7 (3)
C_6	124	122 9 (7)	122 8 (3)	121 3 (3)

Table 3.2

(Bond angles (^{0}) at the relevant atom in the pyridine ring from references 7, 1, and 6)

3.2 RESULTS AND DISCUSSION

The full lists of data are presented in Appendix 3, including the tables containing the crystal data, intensity measurements, and refinements for the three compounds

3 2 1 Data collection for (η^6-pyridine)Cr(CO)$_3$

The compound (η^6-pyridine)Cr(CO)$_3$ was synthesised by the method described by Davies and Shipton[8] and suitable crystals were grown from diethyl ether/*n*-hexane solution Collection of the crystallographic data was carried out with an Enraf-Nonius CAD-4 diffractometer, at Trinity College Dublin

A yellow crystal of dimensions 0 9 × 0 8 × 0 6 mm was selected for the molecular structure determination Mo Kα radiation with λ of 0 71069 Å was used in the analysis of the compound at 293 K The number of reflections measured was 1589, and the index range was h = -10 to 9, k = 0 to 7, and l = 0 to 10 The unit cell was found to be monoclinic with unit cell dimensions of a = 10 752 (5) Å, b = 7 652 (5) Å, and c = 11 110 (2) Å and β = 111 8 (5)^0 The density was calculated to be 1 684 g cm^{-3} The space group $P2_1/c$ was established with Z = 4

Data reduction was carried out using NRCVAX DATRD2[9], programs that were employed to solve the structure NRCVAX SOLVER, and to refine the structure NRCVAX LSTSQ John N Low at the University of Dundee assisted in solving the structure of this compound Molecular graphics were obtained by ORTEPH [10] The hydrogen atoms were located on a difference map and then given normalised bond lengths of 1 08 Å and allowed to ride on their parent atoms The final calculated R values were R = 0 044 and wR = 0 061

3 2 2 Molecular structure of (η^6-pyridine)Cr(CO)$_3$

Figure 3 2 contains a view of the molecule with atomic numbering scheme The atoms are depicted as displacement ellipsoids drawn at the 30 % probability level Table 3 3 contains the fractional atomic coordinates and equivalent isotropic displacement parameters Table 3 4 contains selected geometric parameters for (η^6-pyridine)Cr(CO)$_3$ Table 3 5 contains a selected bond angles for the compound

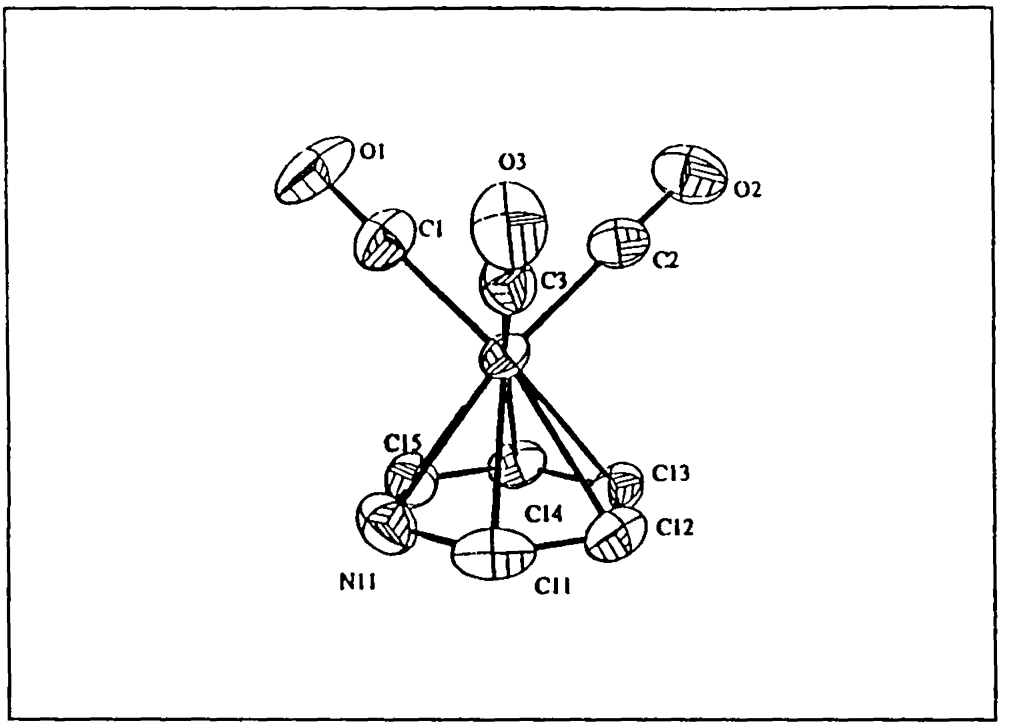

Figure 3.2

(ORTEP diagram for the molecular structure of (η^6-pyridine)Cr(CO)$_3$ Hydrogen atoms omitted for clarity)

Atom	x	y	z	U_{eq}
Cr1	0 24257 (5)	0 02605 (9)	0 18428 (5)	0 0427 (6)
C1	0 3175 (4)	-0 0975 (7)	0 3383 (5)	0 070 (3)
O1	0 3647 (3)	-0 1745 (6)	0 4330 (3)	0 111 (3)
C2	0 1775 (4)	-0 1758 (6)	0 1000 (4)	0 058 (3)
O2	0 1344 (3)	-0 3074 (5)	0 0447 (3)	0 089 (3)
C3	0 0883 (5)	0 0442 (5)	0 2178 (4)	0 052 (3)
O3	-0 0076 (4)	0 0527 (5)	0 2408 (3)	0 076 (2)
N11	0 3461 (4)	0 2752 (5)	0 2494 (4)	0 072 (3)
C11	0 2300 (5)	0 3047 (6)	0 1449 (6)	0 074 (4)
C12	0 1985 (4)	0 2192 (6)	0 0255 (4)	0 064 (3)
C13	0 2871 (4)	0 1000 (6)	0 0121 (4)	0 063 (3)
C14	0 4082 (5)	0 0677 (6)	0 1161 (4)	0 061 (3)
C15	0 4319 (4)	0 1561 (6)	0 2304 (4)	0 066 (3)

Table 3 3

(Fractional atomic coordinates and equivalent isotropic displacement parameters ($Å^2$), e s d's in brackets, $U_{eq} = (1/3)\Sigma_i\Sigma_j U_{ij}a_i^*a_j^*a_i a_j$)

Bond	Length (Å)	Bond	Length (Å)
Cr1-C1	1 857 (5)	C1-O1	1 146 (6)
Cr1-C2	1 825 (5)	C2-O2	1 164 (6)
Cr1-C3	1 835 (5)	C3-O3	1 153 (6)
Cr1-N11	2 190 (4)	N11-C11	1 371 (7)
Cr1-C11	2 171 (5)	N11-C15	1 368 (7)
Cr1-C12	2 213 (4)	C11-C12	1 404 (8)
Cr1-C13	2 211 (4)	C12-C13	1 366 (7)
Cr1-C14	2 202 (4)	C13-C14	1 405 (6)
Cr1-C15	2 149 (4)	C14-C15	1 376 (7)

Table 3.4

(Selected bond lengths for (η^6-pyridine)Cr(CO)$_3$)

Bond angle	(°)
C11-N11-C15	115 3 (7)
N11-C15-C14	124 3 (7)
C15-C14-C13	118 0 (7)
C14-C13-C12	120 5 (8)
C13-C12-C11	117 9 (8)
C12-C11-N11	124 0 (8)

Table 3.5

(Internal bond angles in the pyridine ring for (η^6-pyridine)Cr(CO)$_3$)

3 2 3 Data collection for (η^6-2,6-dimethylpyridine)Cr(CO)$_3$

The compound (η^6-2,6-dimethylpyridine)Cr(CO)$_3$ was synthesised by the method described in Chapter 4 and suitable crystals were grown from diethyl ether/*n*-hexane solution Collection of the crystallographic data was carried out with an Enraf-Nonius CAD-4 automatic diffractometer, at Trinity College Dublin

A yellow crystal of dimensions 0 5 × 0 5 × 0 25 mm was selected for the molecular structure determination Mo Kα radiation with λ of 0 71069 Å was used in the analysis of the compound at room temperature The number of reflections measured was

1790, of which 940 were independent reflections The index range was h = 0 to 13, k = -7 to 7, and l = 0 to 14 The unit cell was found to be orthorhombic, with unit cell dimensions of a = 13 0308 (13) Å, b = 6 2875 (6) Å, and c = 12 7099 (10) Å The density was calculated to be 1 551 g cm^{-3} The space group $Pna2_1$ was established with $Z = 4$

The structures were solved using the Patterson strategy of Shelxs-86[11] and refined by full matrix least squares on F^2 using Shelxs-93 [12] Manipulations of the molecular structures were made using Schakal-92 [13] The final calculated R values were R = 0 024 and wR^2 = 0 060

3 2 4 Molecular structure of (η^6-2,6-dimethylpyridine)Cr(CO)$_3$

Figure 3 3 contains an Ortep diagram of the molecular structure of (η^6-2,6-dimethylpyridine)$Cr(CO)_3$, with the atomic numbering scheme employed in the following tables Table 3 6 contains the fractional atomic coordinates and equivalent isotropic displacement parameters Table 3 7 contains selected geometric parameters for (η^6-2,6-dimethylpyridine)$Cr(CO)_3$ Table 3 8 contains a selected bond angles for the compound

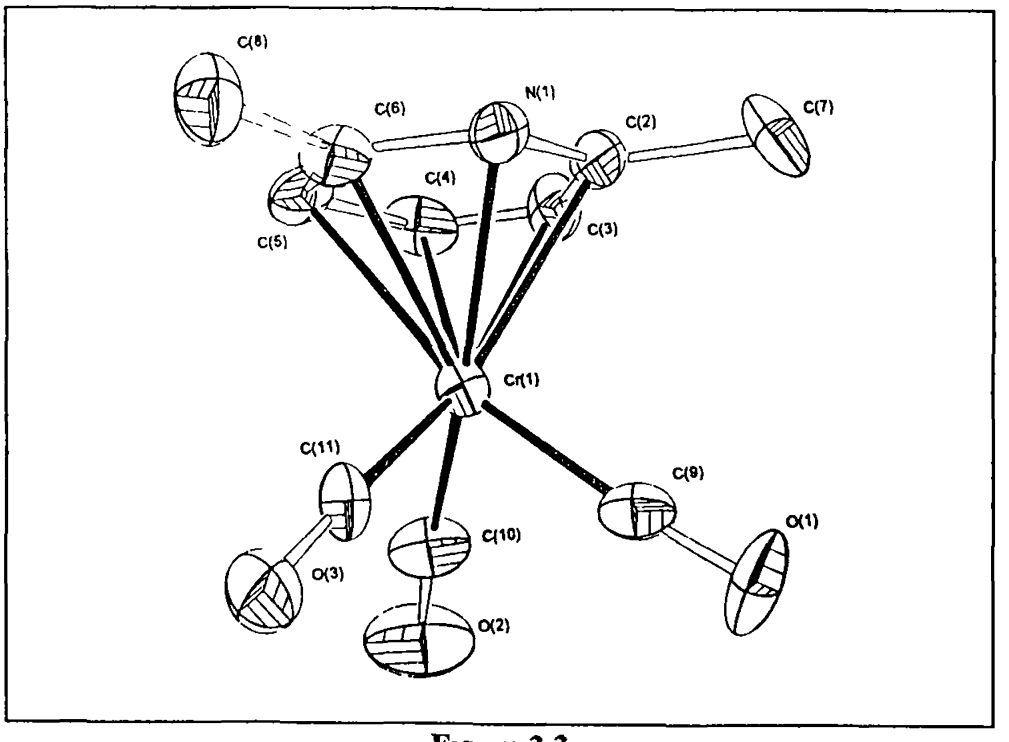

Figure 3.3

(ORTEP diagram for the molecular structure of (η^6-dimethylpyridine)Cr(CO)$_3$

Hydrogen atoms omitted for clarity)

Atom	x	y	z	U_{eq}
Cr1	0 7418 (1)	0 1403 (1)	0 2839 (5)	0 028 (1)
N1	0 8652 (3)	-0 1031 (6)	0 2811 (16)	0 036 (1)
O1	0 5959 (11)	-0 0471 (23)	0 1269 (8)	0 066 (4)
O2	0 6171 (4)	0 5429 (7)	0 2759 (22)	0 082 (2)
O3	0 5951 (9)	-0 0309 (21)	0 4419 (8)	0 054 (3)
C2	0 8723 (13)	0 0109 (28)	0 1924 (9)	0 039 (4)
C3	0 8808 (18)	0 2265 (29)	0 1923 (12)	0 040 (4)
C4	0 8844 (4)	0 3395 (9)	0 2787 (20)	0 042 (2)
C5	0 8830 (15)	0 2287 (30)	0 3769 (12)	0 040 (4)
C6	0 8699 (13)	0 0026 (20)	0 3723 (10)	0 035 (3)
C7	0 8654 (21)	-0 1261 (32)	0 0963 (16)	0 075 (6)
C8	0 8733 (18)	-0 1228 (24)	0 4689 (13)	0 051 (4)
C9	0 6492 (13)	0 0308 (27)	0 1870 (11)	0 038 (4)
C10	0 6654 (4)	0 3877 (8)	0 2830 (22)	0 047 (2)
C11	0 6551 (13)	0 0310 (28)	0 3818 (10)	0 037 (4)

Table 3 6

(Fractional atomic coordinates and equivalent isotropic displacement parameters (Å^2),

e s d's in brackets, $U_{eq} = (1/3)\Sigma_i\Sigma_j U_{ij}a_i^*a_j^*a_i a_j$)

Bond	Length (Å)	Bond	Length (Å)
Cr1-C11	1 820 (2)	N1-C2	1 340 (2)
Cr1-C10	1 847 (5)	O1-C9	1 140 (2)
Cr1-C9	1 860 (2)	O2-C10	1 165 (7)
Cr1-C6	2 191 (14)	O3-C11	1 160 (2)
Cr1-C2	2 210 (2)	C2-C3	1 360 (3)
Cr1-N1	2 220 (4)	C2-C7	1 500 (2)
Cr1-C4	2 242 (5)	C3-C4	1 310 (3)
Cr1-C5	2 260 (2)	C4-C5	1 430 (3)
Cr1-C3	2 220 (2)	C5-C6	1 430 (2)
N1-C6	1 340 (2)	C6-C8	1 460 (2)

Table 3.7

(Selected bond lengths for (η^6-2,6 dimethylpyridine)Cr(CO)$_3$)

Bond angle	(°)
C6-N1-C2	117 4 (5)
N1-C2-C3	122 7 (12)
C2-C3-C4	122 9 (12)
C3-C4-C5	117 9 (5)
C4-C5-C6	116 8 (11)
C5-C6-N1	122 2 (10)

Table 3.8

(Internal bond angles in the pyridine ring for (η^6-dimethylpyridine)Cr(CO)$_3$)

3 2 5 Data collection for (η^6-2,6-bis(trimethylsilyl)pyridine)Cr(CO)$_3$

The compound (η^6-2,6-bis(trimethylsilyl)pyridine)Cr(CO)$_3$ was synthesised by the method described by Davies and Shipton[8] and suitable crystals were grown from diethyl ether/*n*-hexane solution Collection of the crystallographic data was carried out with an Enraf-Nomus CAD-4 automatic diffractometer, at Trinity College Dublin

A yellow crystal of dimensions 0 4 × 0 4 × 0 3 mm was selected for the molecular structure determination Mo Kα radiation with λ of 0 71069 Å was used in the analysis of the compound at room temperature The number of reflections measured was 3326, of which 3096 were independent reflections The index range was h = 0 to 8, k = 0 to 23, and l = -11 to 11 The unit cell was found to be monoclinic, with unit cell dimensions of a = 7 7088 (6) Å, b = 23 0928 (9) Å, and c = 10 4365 (8) Å The density was calculated to be 1 296 g cm^{-3} The space group $P2_1/n$ was established with Z = 4

The structures were solved using the Patterson strategy of Shelxs-86[11] and refined by full matrix least squares on F^2 using Shelxs-93 [12] Manipulations of the molecular structures were made using Schakal-92 [13] The final calculated R values were R = 0 032 and wR^2 = 0 078

3 2 6 Molecular structure of (η^6-2,6-bis(trimethylsilyl)pyridine)Cr(CO)$_3$

Figure 3 4 contains an Ortep diagram of the molecular structure of (η^6-2,6-bis(trimethylsilyl)pyridine)Cr(CO)$_3$, with the atomic numbering scheme employed in the following tables Table 3 9 contains the fractional atomic coordinates and equivalent isotropic displacement parameters Table 3 10 contains selected geometric parameters for (η^6-bis(trimethylsilyl)pyridine)Cr(CO)$_3$ Table 3 11 contains a selected bond angles for the compound

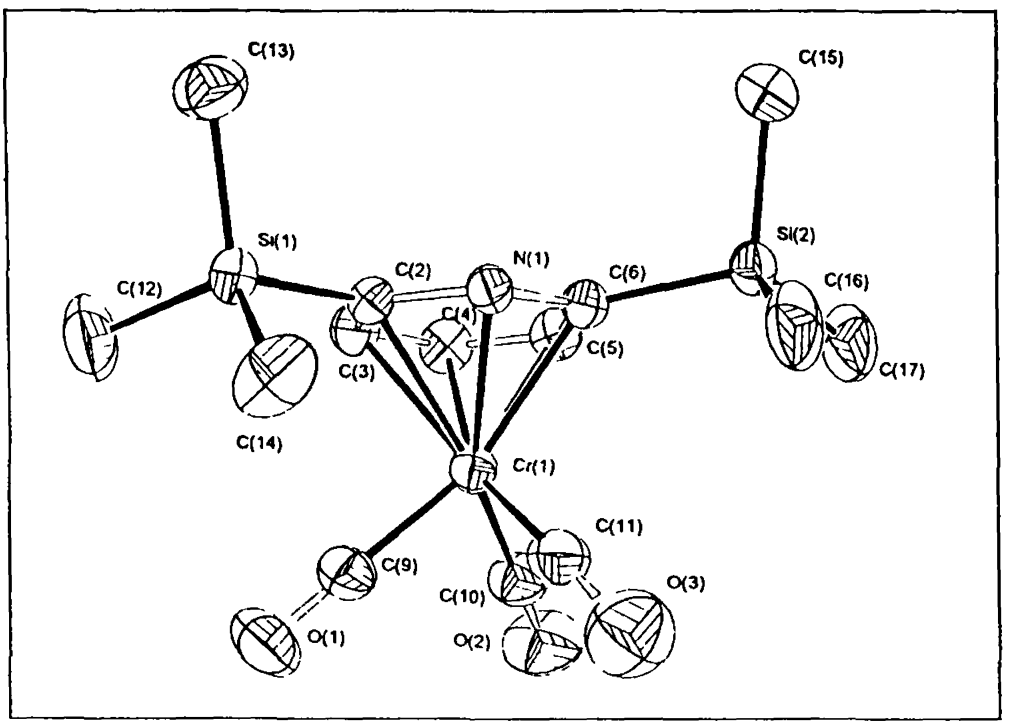

Figure 3.4

(ORTEP diagram for the molecular structure of (η^6-bis(trimethylsilyl)pyridine)Cr(CO)$_3$ Hydrogen atoms omitted for clarity)

Atom	x	y	z	U_{eq}
Cr1	0 2487 (1)	0 1253 (1)	0 0330 (1)	0 037 (1)
Si1	0 1267 (1)	0 2731 (1)	0 1137 (1)	0 040 (1)
Si2	0 1739 (1)	0 0601 (1)	0 3521 (1)	0 045 (1)
N1	0 1911 (3)	0 1633 (1)	0 2140 (2)	0 035 (1)
O1	0 1284 (4)	0 1859 (1)	-0 2156 (2)	0 080 (1)
O2	0 3895 (4)	0 0346 (1)	-0 1308 (3)	0 095 (1)
O3	-0 1025 (4)	0 0684 (1)	-0 0135 (3)	0 095 (1)
C2	0 2651 (3)	0 2051 (1)	0 1458 (2)	0 035 (1)
C3	0 4298 (4)	0 1956 (1)	0 1029 (3)	0 043 (1)
C4	0 5165 (4)	0 1435 (1)	0 1267 (3)	0 047 (1)
C5	0 4405 (4)	0 1012 (1)	0 1987 (3)	0 045 (1)
C6	0 2796 (4)	0 1113 (1)	0 2437 (2)	0 037 (1)
C9	0 1762 (4)	0 1631 (1)	-0 1190 (3)	0 051 (1)
C10	0 3363 (5)	0 0691 (2)	-0 0671 (3)	0 058 (1)
C11	0 0337 (4)	0 0889 (2)	0 0071 (3)	0 055 (1)
C12	0 2188 (6)	0 3162 (2)	-0 0122 (4)	0 083 (1)
C13	0 1375 (5)	0 3162 (2)	0 2646 (3)	0 066 (1)
C14	-0 1011 (4)	0 2496 (2)	0 0619 (4)	0 073 (1)
C15	0 2329 (6)	0 0874 (2)	0 5192 (3)	0 075 (1)
C16	-0 0671 (5)	0 0623 (2)	0 3100 (4)	0 072 (1)
C17	0 2617 (6)	-0 0139 (2)	0 3339 (4)	0 083 (1)

Table 3.9

(Fractional atomic coordinates and equivalent isotropic displacement parameters ($Å^2$), e s d's in brackets, $U_{eq} = (1/3)\Sigma_i\Sigma_j U_{ij}a_i^*a_j^*a_i a_j$)

Bond	Length (Å)	Bond	Length (Å)
Cr1-C11	1 846 (3)	N1-C2	1 367 (3)
Cr1-C10	1 846 (3)	O1-C9	1 155 (4)
Cr1-C9	1 835 (3)	O2-C10	1 146 (4)
Cr1-C6	2 205 (3)	O3-C11	1 147 (4)
Cr1-C2	2 183 (3)	C2-C3	1 416 (4)
Cr1-N1	2 180 (2)	C2-Si1	1 904 (3)
Cr1-C4	2 209 (3)	C3-C4	1 382 (4)
Cr1-C5	2 198 (3)	C4-C5	1 405 (4)
Cr1-C3	2 204 (3)	C5-C6	1 400 (4)
N1-C6	1 397 (3)	C6-Si2	1 890 (3)

Table 3 10

(Selected bond lengths for (η^6-2,6 bis(trimethylsilyl)pyridine)Cr(CO)$_3$)

Bond angle	(°)
C6-N1-C2	119 2 (2)
N1-C2-C3	120 3 (3)
C2-C3-C4	120 7 (3)
C3-C4-C5	118 4 (3)
C4-C5-C6	120 8 (3)
C5-C6-N1	119 8 (2)

Table 3.11

(Internal bond angles in the pyridine ring for (η^6-bis(trimethylsilyl)pyridine)Cr(CO)$_3$)

3 2 7 Discussion

In all three complexes the chromium atom is situated directly below the arene ring centroid, the arene ring is essentially planar, and the chromiumtricarbonyl unit is coordinated *via* the π system of the heteroarene ring The mean chromium to ring-atom distance for (η^6-pyridine)Cr(CO)$_3$ **(1)**, (η^6-2,6-dimethylpyridine)Cr(CO)$_3$ **(2)**, and (η^6-bis(trimethylsilyl)pyridine)Cr(CO)$_3$ **(3)** is 2 189, 2 224, and 2 196 Å respectively These distances are longer then the distances reported for the bis(η^6-pyridine)Cr and the bis(η^6-2,6-dimethylpyridine)Cr compounds, 2 133 and 2 136 Å, but shorter than the corresponding distances for the (η^6-benzene)Cr(CO)$_3$ complex 2 242 Å

The conformation of the tricarbonyl unit in compound **3** is staggered, which is the more common conformation observed for (η^6-arene)Cr(CO)$_3$ complexes [14] However, compounds **1** and **2** adopt an eclipsed conformation, where in compound **1** the carbonyl groups eclipse C11, C13 and C15, and in compound **2** the carbonyl groups eclipse C2, C4, and C6 This results in the carbonyl group C10-O2 being *trans* to the nitrogen in complex **2**, and the carbonyl group C2-O2 is *trans* to the nitrogen in compound **1**

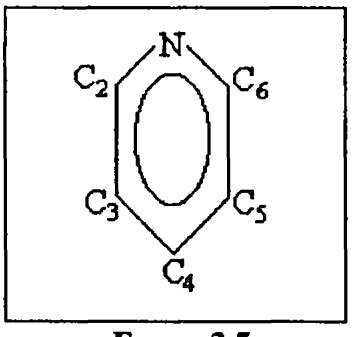

Figure 3.5

(Pyridine ring with atom numbering employed for Table 3 12)

	Angles at the respective atoms in the arene ring (°)			
	free pyridine[7]	Compound **1**	Compound **2**	Compound **3**
N	116 7	115 3 (7)	117 4 (5)	119 2(2)
C2	124	124 3 (7)	122 7 (12)	120 3 (3)
C3	118 6	118 0 (7)	122 9 (12)	120 7 (3)
C4	118 1	120 5 (8)	117 9 (5)	118 4 (3)
C5	118 6	117 9 (8)	116 8 (11)	120 8 (3)
C6	124	124 0 (8)	122 2 (10)	119 8 (2)

Table 3.12

(Bond angles in the pyridine ring for the three complexes in this study and free pyridine)

It can be seen from Table 3 12 that upon substitution at the pyridine ring the angle at the nitrogen atom becomes more obtuse and the two angles at the C2 and C6 become more acute The angles for the uncomplexed 2,6-dimethylpyridine and 2,6-bis(trimethylsilyl)pyridine are not known therefore the effect of coordination of the chromiumtricarbonyl unit cannot be obtained However examination of the differences between the free and complexed pyridine show that a slight distortion of the pyridine ring occurs Comparison of the bond angles in the bis(η^6-2,6-dimethylpyridine)Cr and

compound **2** shows that the angles are very similar with only a slight distortion observed at C4 and C5

	Bond lengths in the arene ring (Å)			
	free pyridine[7]	Compound **1**	Compound **2**	Compound **3**
N-C2	1 340 (5)	1 371 (7)	1 340 (2)	1 367 (3)
C2-C3	1 390 (5)	1 404 (8)	1 360 (3)	1 416 (4)
C3-C4	1 400 (5)	1 366 (7)	1 310 (3)	1 382 (4)
C4-C5	1 400 (5)	1 405 (6)	1 430 (3)	1 405 (4)
C5-C6	1 390 (5)	1 376 (7)	1 430 (2)	1 400 (4)
C6-N	1 340 (5)	1 368 (7)	1 340 (2)	1 397 (3)

Table 3.13

(Bond lengths in the pyridine ring for the three complexes in this study, and "free" pyridine for comparison)

The bond lengths in compounds **1** and **3** appear to be very similar, however in compound **2** the first three bond lengths in Table 3 13 are significantly shorter than the other two compounds A slight distortion of the pyridine ring can be seen as a result of complexation with the chromiumtricarbonyl unit, compared with the free pyridine Comparison of the bond lengths observed for the bis(η^6-2,6-dimethylpyridme)Cr compound (Table 3 1) to the (η^6-2,6-dimethylpyridine)$Cr(CO)_3$ complex shows a significant variation in lengths of all the bonds

3 2 8 Conclusions

The three complexes all possess planar arene rings, with the chromium atom situated directly below the arene ring The (η^6-bis(trimethylsilyl)pyridine)$Cr(CO)_3$ compound is the only one to exhibit the common staggered conformation, where the carbonyl groups eclipse the ring bond centres The conformation of the other two complexes is the more unusual eclipsed form A slight distortion of the pyridine ring can be observed upon complexation to the chromiumtricarbonyl unit

REFERENCES

(Chapter 3)

[1] (a) Simons L H , Riley P E , Davis R E , Lagowski J J , *J Am Chem Soc* , 1976, **98**, 1044

(b) Riley P E , Davis R E , *Inorg Chem* , 1976, **15**, 2736

[2] Keulen E , Jellinek F , *J Organomet Chem* , 1966, **5**, 490

[3] Ibers J A , *J Phys Chem* 1964, **40**, 3129

[4] Rees B , Coppens P , *Acta Crystallogr , Sect B,* 1973, **29**, 2516

[5] Bailey M F , Dahl L F , *Inorg Chem* , 1965, **4**, 1314

[6] Elschenbroich C , Koch J , Kroker J , Wunsch M , Massa W , Baum G , Stork G , *Chem Ber , Teil A,* 1988, **121**, 1983

[7] Bak B , Hansen L , Rastrup-Andersen J , *J Chem Phys* , 1954, **22**, 2013

[8] Davies S G , Shipton M R , *J Chem Soc , Perkin Trans 1,* 1991, 501

[9] Gabe E J , Le Page Y , Charland J,-P , Lee F L , White P S , *J Appl Cryst* , 1989, **22**, 384

[10] Johnson C K , ORTEPH Report ORNL-5138 Oak Ridge National Laboratory, Tennessee, USA

[11] Sheldrick G M SHELXS-86, Programme for Crystal Structure Determination, *Acta Cryst* , 1990, **A46**, 467

[12] Sheldrick G M SHELXS-93, Programme for Crystal Structure Refinement, University

of Göttingen, Gottingen, Germany 1993

[13] Keller E SCHAKAL-92, A programme for Graphical representation of Molecular Structures, Kristallographisches Institut der Universitaet, Freiburg, Germany 1992

[14] Meutterties E L , Bleeke J P , Wucherer E J , Albright T A , *Chem Rev* , 1982, **82**, 499

CHAPTER 4

4 EXPERIMENTAL

4 1 Materials

The following solvents were of spectroscopic grade and were used without further purification cyclohexane, decane, dodecane, heptane, methylcyclohexane (Aldrich) Argon and carbon monoxide was supplied by air products and IIG respectively Chromium hexacarbonyl, molybendum hexacarbonyl, and tungsten hexacarbonyl (Aldrich) were all used without further purification Tetrahydrofuran was dried over sodium and benzophenone, and stored under argon and sodium Diethyl ether, petroleum ether (40°-60°) and 2,6-lutidine were received from Aldrich and used without further purification Diethyl ether was dried and stored over sodium for the synthesis of (η^6-bis(trimethylsilyl)pyridine)$Cr(CO)_3$ Aluminium oxide was activated neutral, standard grade *ca* 150 mesh (Aldrich) The following materials were used without further purification 2,6-dibromopyridine, butyllithium 2 5 M solution in hexanes, trimethylsilyl chloride, milli-Q water, and tetrabutylammonium fluoride (Aldrich) 1,4-Dioxan was dried over sodium and benzophenone and filtered through activated alumina prior to use

4 2 Equipment

Infrared spectra were recorded on a Perkin Elmer 983-G, a Nicolet 205 FTIR spectrometer, or a Perkin Elmer 2000 FTIR spectrometer using a 0 1 mm sodium chloride solution cell UV/vis spectra were recorded on a Hewlett Packard 8452A

photodiode array spectrometer using a quartz cell of 1 cm pathlength NMR measurements were performed on a Bruker model AC 400 MHz spectrometer

4 3 Synthesis of (η^6-2,6-bis(trimethylsilyl)pyridine)Cr(CO)$_3$

This compound was synthesised according to the method described by Davies and Shipton [1] 2,6-dibromopyridine (12 5 g, 52 5 mmol) was added as a solid to butyllithium (50 mL, 110 mmol) in dry diethyl ether (100 mL) under nitrogen at -78 °C, the mixture was stirred at this temperature for 1 5 hours Trimethylsilyl chloride (12 mL, 110 mmol) in dry diethyl ether (10 mL) was added dropwise, the mixture was allowed to warm to room temperature, and the stirring was continued overnight The resulting light tan suspension was filtered through Celite and the solvent was evaporated to give a yellow oil Distillation of this oil (94 - 96 ^{0}C), under reduced pressure, produced a colourless oil The ^{1}H NMR data showed a peak at 0 33 ppm assigned to the 18 methyl hydrogens, and a multiplet at 7 44-7 36 ppm assigned to the three aromatic hydrogens These values are similar to the values reported in the literature

2,6-Bis(trimethylsilyl)pyridine (1 g) was placed in a two necked round bottom flask and was degassed with argon Chromium hexacarbonyl (~1 8 g) and filtered 1,4-dioxan (25 mL) was added This solution was further degassed prior to being heated to reflux The reaction was heated to its reflux temperature under argon for 24 - 30 hours, until brown/green precipitate was produced The mixture was allowed to cool and the solution was decanted from the unreacted chromium hexacarbonyl It was then

filtered through alumina and evaporated to produce a yellow oil This oil was then chromatographed on a flash silica column (eluent, petroleum ether diethyl ether, 15 1, v/v), with positive argon pressure, resulting in a yellow oil, that under prolonged pumping produced an amber crystalline solid The spectroscopic information for this compound is presented in Table 2 1

4 4 Synthesis of (η^6-pyridine)Cr(CO)$_3$

To (η^6-2,6-bis(trimethylsilyl)pyridine)Cr(CO)$_3$ (120 mg) in dry THF (20 mL) at -78 ^{0}C, was added tetrabutylammonium fluoride (240 mg) and 3 drops of milli-Q water The mixture was stirred, protected from the light, warmed to room temperature and stirred for 1 5 hours Removal of the solvent gave a dark oil that was immediately flash chromatographed (eluent, diethyl ether) with positive argon pressure, to produce a yellow solution When the solvent was evaporated a yellow crystalline product was formed, spectroscopic information can be observed in Table 2 1

4 5 Synthesis of (η^6-2,6-dimethylpyridine)Cr(CO)$_3$

This compound was synthesised in a similar way to described by Mahaffy *et al* [2] with minor alterations Chromium hexacarbonyl (0 6 g) was added as a solid to dry THF (10 mL) and 2,6-dimethylpyridine (50 mL) The reaction mixture was degassed for 0 5 hour with argon, and was then heated to reflux temperature for ~15 hours The reaction mixture was allowed to cool, the solution was decanted from the unreacted

chromium hexacarbonyl and the solvent evaporated under reduced pressure The resulting yellow solid was purified by column chromatography on an alumina column (eluent, petroleum ether diethyl ether, 7 3, v/v) Spectroscopic information for this complex is presented in Table 2 1

4 6 Attempted synthesis of molybendum and tungsten analogues

In order to investigate if photochemical haptotropic rearrangements could also be observed for the normally photochemically inert tungsten system, the synthesis of (η^6-2,6-dimethylpyridine)$W(CO)_3$ and (η^6-2,6-bis(trimethylsilyl)pyridine)$W(CO)_3$ was attempted Direct complexation of $Mo(CO)_6$ or $W(CO)_6$ with 2,6-dimethylpyridine resulted in the production of two complexes However upon separation of these complexes it transpired that, one of these products was the pentacarbonyl, as was expected, however the second band was not a tricarbonyl species, it could possibly have been the tetracarbonyl species Further heating resulted in degradation of the products The complex $(CH_3CN)_3W(CO)_3$ was formed to act as a precursor, it was refluxed in 2,6-dimethylpyridine (4 h), in a variation of the method described by King and Fronzaglia [3] However this still resulted in the 2,6-dimethylpyridine bonding to the metal in the σ-fashion It was decided that possibly 2,6-dimethylpyridine did not offer enough steric hindrance, therefore the ligand 2,6-bis(trimethylsilyl)pyridine was employed However, even with this increased steric hindrance the preferred mode of bonding was *via* a σ interaction, producing the pentacarbonyl species

4 7 Laser flash photolysis

4 7.1 Sample preparation for laser flash photolysis with UV/vis detection.

Samples were prepared in a specially designed degassing bulb that was attached to a fluorescence cell This cell was cleaned thoroughly by steeping in chromic acid for at least 24 hours prior to use All the samples were prepared such that the absorbance values were between 0 5 and 1 5 absorbance units at 355 nm (excitation wavelength) The concentration could then be calculated from previously calculated extinction coefficients All the absorbance readings were recorded on the UV/vis spectrometer, and any changes in the ground state absorption spectrum was also recorded during the experiment The samples were then degassed by three cycles of freeze-pump-thaw procedure to 10^{-3} Torr, followed by a substantial liquid pump phase in order to remove any impurities e g water Either argon, or a required pressure of carbon monoxide, was then added to the cell to check to reversibility of the processes being investigated The concentration of CO was calculated to be $9\ 0 \times 10^{-3}$ M in cyclohexane, $8\ 5 \times 10^{-3}$ M in *n*-decane, $6\ 8 \times 10^{-3}$ M in *n*-dodecane, and $1\ 2 \times 10^{-2}$ M in *n*-heptane, at one atmosphere of CO [4] The concentration in methylcyclohexane was taken as the same as cyclohexane, $9\ 0 \times 10^{-3}$ M During the preparation the samples were protected from light

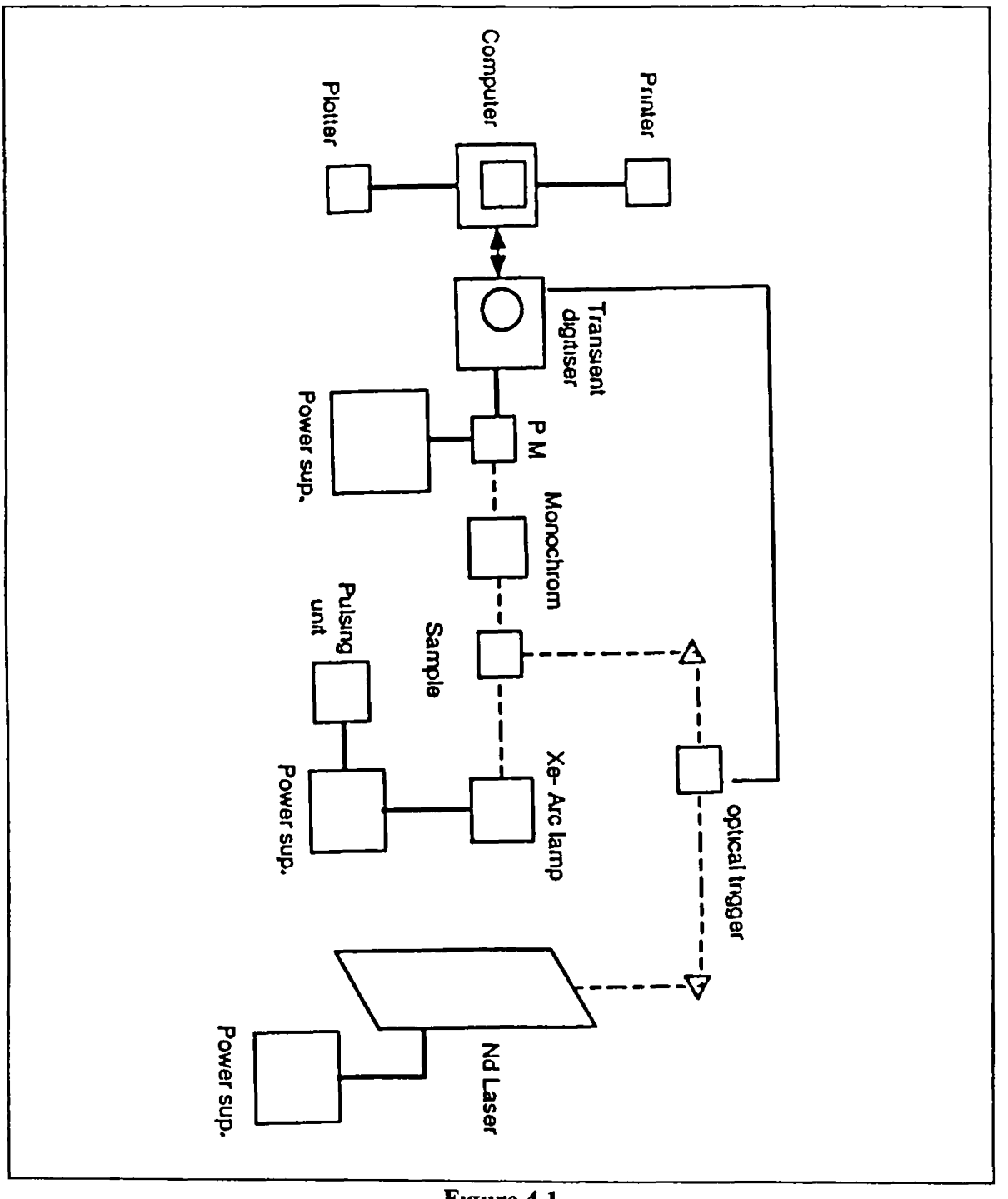

Figure 4.1

(A schematic diagram of the laser system used in the laser flash photolysis experiments with UV/vis detection)

4.7.2 Laser flash photolysis with UV/vis detector apparatus

A schematic diagram of the flash photolysis instrumentation is presented in Figure 4 1 The excitation source in a Nd-YAG (neodynium yttrium aluminium garnet) laser which operates at 1064 nm, but can be frequency doubled, tripled, or quadrupled to generate a second, third, or fourth harmonic frequency at 532, 355, or 266 nm respectively The power of the laser can be varied by applying different voltages across the amplifier flash tube The pulse time is approximately 10 ns At 355 nm, which is the excitation wavelength employed in this study, the energy is typically 45 mJ per pulse The circular laser pulse is directed *via* two Pellin-Broca prisms onto the sample cuvette When the pulse passes through the power meter situated after the first prism, but before the sample cuvette, the oscilloscope is triggered The monitoring light source is an air cooled 275 watt Xenon arc lamp arranged at right angles to the laser beam The monitoring beam passes through the sample and is directed to the entrance slit of an Applied Photophysics f/3 monochromator *via* a circular lense UV/vis filters were employed ($\lambda > 410$ nm or $\lambda > 345$ nm) between the monitoring source and the sample to prevent excessive sample photodegradation A Hamatsu five stage photomultiplier operating at 850 V was placed at the exit slit of the monochromator The aborbance changes were measured by a transient digitiser (oscilloscope) *via* a variable load resistor The digitiser, a Hewlett Packard HP 54510A oscilloscope was interfaced to an Olivetti PCS 286 microcomputer *via* an IEEE bus All signals were stored on floppy discs

A typical transient signal was obtained by the following procedure An I_o was recorded, which corresponds to the amount of light that passes through the solution

before the laser flash It was measured by obtaining the difference in mV of the amount of light transmitted by the solution, when the shutter of the monitoring beam is opened and then closed Therefore a typical trace depicts the change in voltage with time, which corresponds to the time resolved absorbance The resultant transient signals were analysed using first order kinetics If all the data is collected with the same time bases and voltage settings, a two dimensional spectra can be obtained in a "point by point" manner, which produces a spectrum over the wavelength range at a fixed time interval

4.7.3 Laser flash photolysis with TRIR detection apparatus

The instrumentation for the laser flash photolysis experiments with TRIR detection has been described elsewhere [5] The instrumentation employed in these studies consisted of a Lambda Physik EMG 200 excimer laser (λ = 308 nm with XeCl, output attenuated to 90 -100 mJ per pulse) as the excitation source A normal IR flow cell with CaF_2 windows and d = 1 mm was used A globar served as the monitoring light source, with a HgCdTe photodiode detector The system has a response time of 1-2 μs and a spectral resolution of 3-4 cm^{-1} The experiments were carried out at room temperature The routine procedure for preparing the stock solution involved three freeze-pump-thaw procedures, followed by saturation with the desired gas atmosphere in the reservoir (1 atmosphere) During the intervals between the laser shots the cell was emptied and refilled with fresh stock solution from the reservoir through a magnetic valve system TRIR difference spectra were built up by the "point by point" method

4 8 Matrix isolation instrumentation

The instrumentation employed for the matrix isolation experiments have been described elsewhere [6] The set-up consists of an Air Products Model CS 202 Displex closed-cycle helium refrigerator, which cools a NaCl spectroscopic window to 10-12 K The window temperature is monitored separately by a thermocouple embedded in a cavity close to the window centre The flow of the matrix gases (>99 99 %, L'Air Liquide), 1 5-2 mmol h^{-1}, is controlled by a calibrated micrometer needle valve and a vacuummeter assembly The pressure in the gas inlet line is continuously checked by a separate thermotron gauge Evaporation rates were controlled by first depositing onto a quartz crystal microbalance, mounted in good thermal contact to the side of the target window holder In general the guest host ratio was better then 1 1000 Infrared spectra were recorded on a Perkin-Elmer Model 1720 FTIR spectrometer

4 9 Steady state photolysis with NMR monitoring

The samples were prepared in a degassable quartz NMR tube in the deuterated solvent of choice The solution was then subjected to three freeze-pump-thaw procedures Great care was necessary as the quartz in the NMR tube was very thin and could crack very easily The samples were protected from the light with aluminium foil, however exposure to the light was necessary to verify that the solution had melted prior to further freezing The sample was liquid pumped and then saturated with 1 atm of carbon monoxide A NMR spectra was obtained of the starting compound, then the solution was

placed in front of an air cooled 275 watt xenon arc lamp, with a UV/vis filter ($\lambda > 410$ nm), and turned manually for a prescribed time period

4 10 Determination of extinction coefficients

The extinction coefficients were determined at 355 nm (excitation wavelength) for all the compounds To obtain the concentrations of the compounds, the Beer-Lambert law was employed The Beer-Lambert law is given by

$$A = \varepsilon\ c\ l$$

where A = absorbance at the excitation wavelength (A U)

ε = molar extinction coefficient ($dm^3\ mol^{-1}\ cm^{-1}$)

c = concentration (mol dm^{-3})

l = pathlength of cell (1 cm)

The extinction coefficients for the (η^6-arene)$Cr(CO)_3$ compounds are presented in Appendix 2A The extinction coefficients for the $M(CO)_6$ (where M = Cr, Mo, or W) are given in Appendix 1A.

4 11 Determination of the concentration of CO in an alkane solvent

The solubility of CO in hydrocarbon solvents was determined using the mole fraction data reported by Makranczy *et al*[4] The calculations for cyclohexane are given as an example,

- solubility of CO at 298 K (expressed as a mole fraction) = 9 94 × 10^{-4} $moles^{-1}$,
- 1 litre of cyclohexane = 779 g,
- 1 mole of cyclohexane = 84 g

$\Rightarrow$ moles/litre = 1 / 84 × 779 $\Rightarrow$ = 9 274 moles/litre

$$\Rightarrow \quad 9\,94 \times 10^{-4}\ \text{moles}^{-1} = \frac{\#[CO]}{9\,274\ \text{moles/litre}}$$

$\Rightarrow$ [CO] = 9 1 × 10^{-3} M at 1 atmosphere

4 12 Determination of the activation parameters

The activation parameters were obtained from Eyring and Arrhenius plots The activation energy can be obtained from the slope of the line in the Arrhenius plot The Arrhenius equation is given by

$$\ln k_2 = -E^{\neq}_{act}/RT + \ln A$$

where k_2 = rate of decay (l mol^{-1} s^{-1})

REFERENCES

(Chapter 4)

[1] Davies S G , Shipton M R , *J Chem Soc , Perkin Trans 1,* 1991, 501

[2] Mahaffy C A L , Pauson P L , *Inorg Synth* , 1979, **19**, 154

[3] King R B , Fronzaglia A , *Inorg Chem* , 1966, **5**, 1837

[4] Makranczy J , Megyery-Balog K , Rosz L , Patyt D , *Hungarian J Indust Chem* , 1976, **4**, 269

[5] Schnaffer K , Grevels F -W , *J Mol Struct* , 1988, **173**, 51

[6] (a) Gerhartz W , Grevels F -W , Klotzbucher W E , *Organometallics,* 1987, **6**, 1850

(b) Klotzbucker W E , *Cryogenics,* 1983, **23**, 554

(c) Grevels F -W , Klotzbucker W E , *Inorg Chem* , 1981, **20**, 3002

APPENDIX 1

SECTION A

1 A 1 Extinction coefficients of $Cr(CO)_6$ in alkane solvents

$Cr(CO)_6$ in Cyclohexane

Concentration (x 10^{-3} M)	Absorbance @ 354 nm (A U)
0	0
1 0	0 212
1 5	0 296
2 0	0 399
2 5	0 505
3 0	0 615

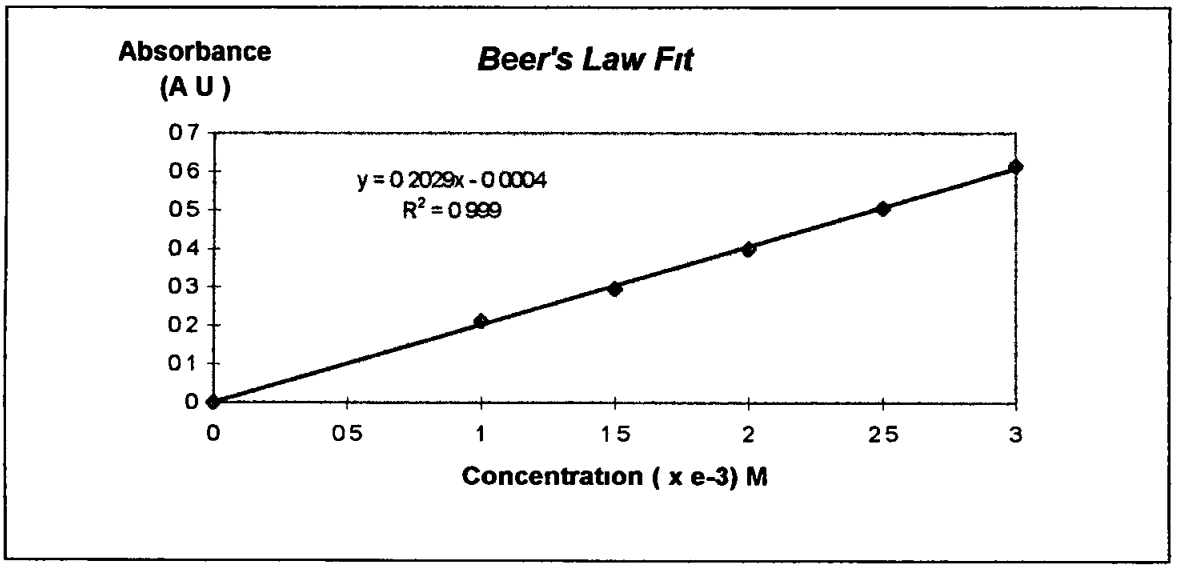

Therefore the extinction coefficient for $Cr(CO)_6$ in cyclohexane at 354 nm is 2 0 x 10^2 dm^3 mol^{-1} cm^{-1}

$Cr(CO)_6$ in Methylcyclohexane

Concentration (x 10^3 M)	Absorbance @ 354 nm (A U)
0	0
1 0	0 232
1 5	0 341
2 0	0 469
2 5	0 575
3 0	0 693

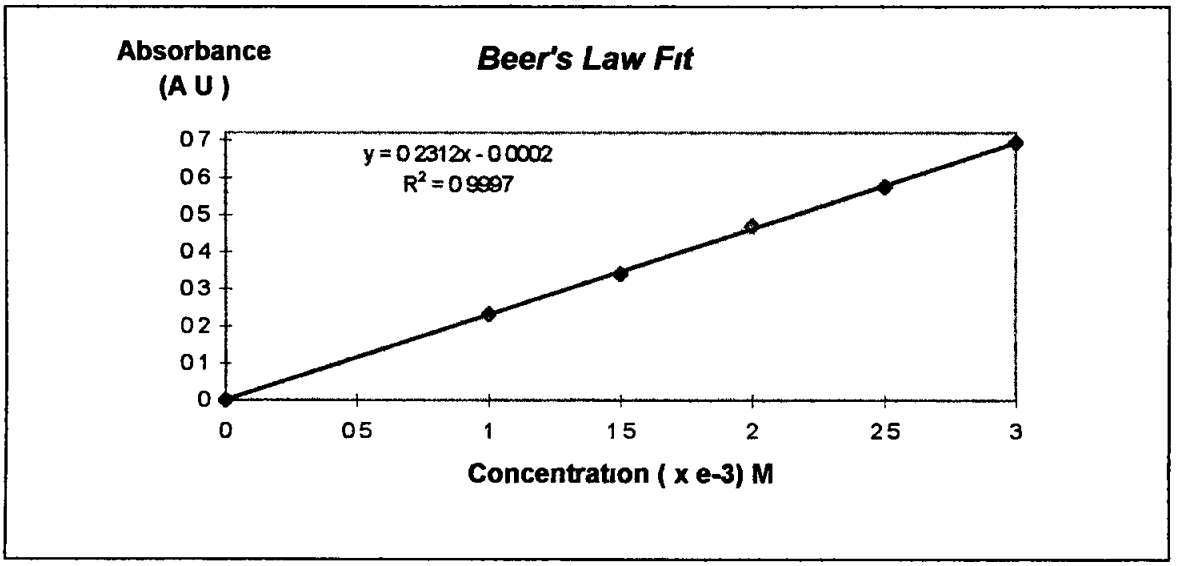

Therefore the extinction coefficient for $Cr(CO)_6$ at 354 nm in methylcyclohexane is 2 31 x 10^2 dm^3 mol^{-1} cm^{-1}

$Cr(CO)_6$ in Heptane

Concentration (x 10^{-3} M)	Absorbance @ 354 nm (A U)
0	0
1 0	0 235
1 5	0 352
2 0	0 468
2 5	0 580
3 0	0 682

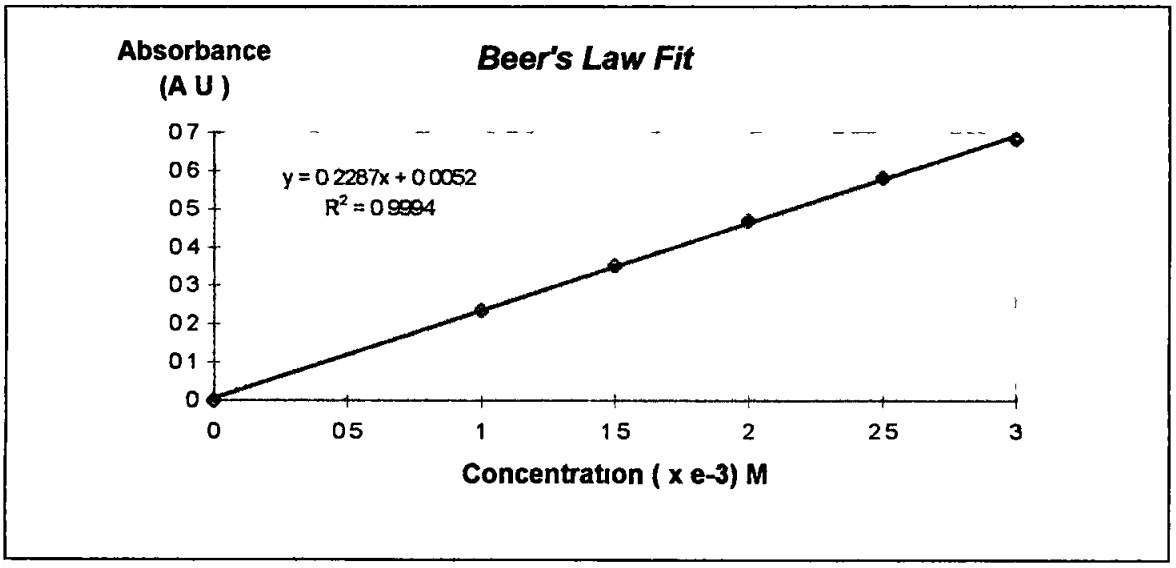

Therefore the extinction coefficient for $Cr(CO)_6$ in heptane at 354 nm is 2 29 x 10^2 dm^3 mol^{-1} cm^{-1}

1 A 2 Extinction coefficient of $Mo(CO)_6$

$Mo(CO)_6$ in Cyclohexane

Concentration (x 10^{-3} M)	Absorbance @ 354 nm (A U)
0	0
0 25	0 061
0 50	0 126
0 75	0 187
1 00	0 262
1 50	0 392

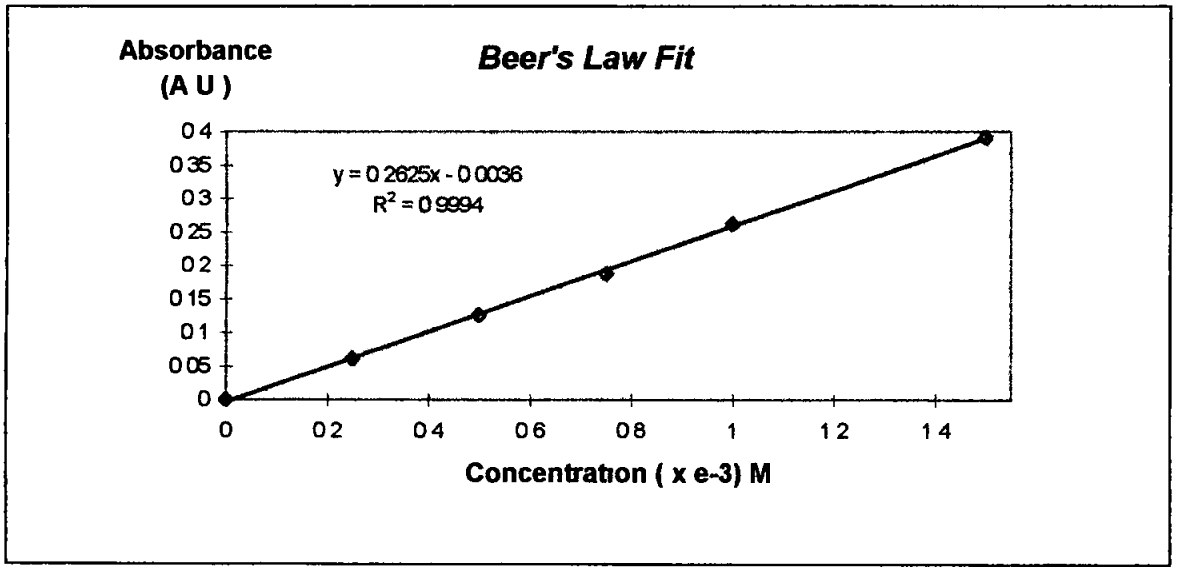

Therefore the extinction coefficient for $Mo(CO)_6$ in cyclohexane at 354 nm is 2 63 x 10^2 dm^3 mol^{-1} cm^{-1}

1 A 3 Extinction coefficient of $W(CO)_6$

$W(CO)_6$ in Cyclohexane

Concentration (x 10^{-3} M)	Absorbance @ 354 nm (A U)
0	0
0 25	0 181
0 50	0 377
0 75	0 583
1 00	0 821
1 50	1 242

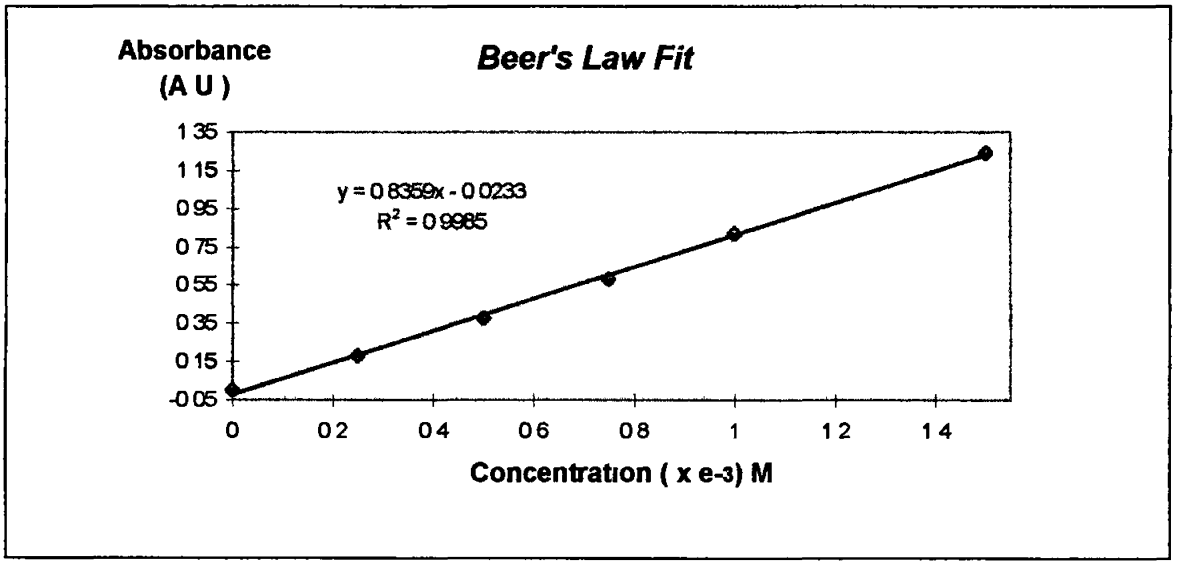

Therefore the extinction coefficient for $W(CO)_6$ in cyclohexane at 354 nm is 8 36 x 10^2 dm^3 mol^{-1} cm^{-1}

SECTION B

The following data was employed to obtain the activation parameters for Reaction A, where M = Cr, Mo, or W

$$M(CO)_5(S) + CO \rightarrow M(CO)_6 \qquad \textit{Reaction A}$$

$Cr(CO)_6$ IN CYCLOHEXANE

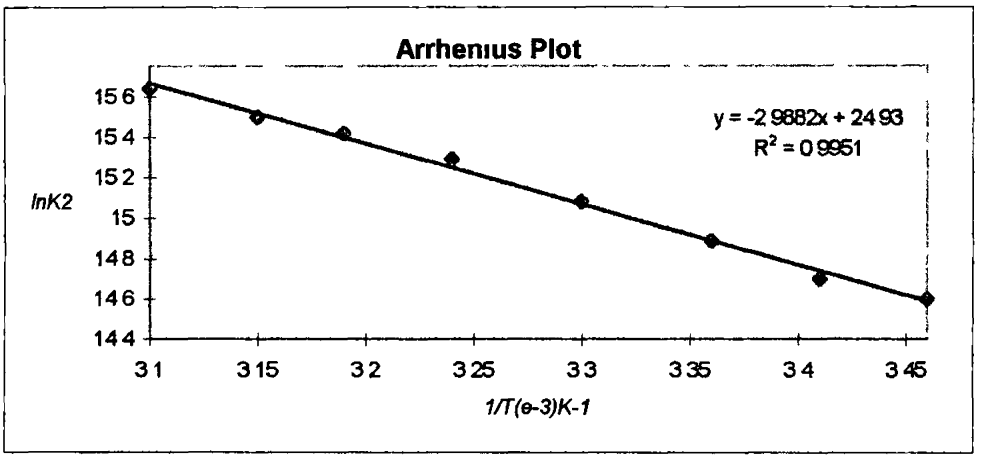

Arrhenius data

1/T (e-3)	*ln k2*
3 1	15 64
3 15	15 5
3 19	15 42
3 24	15 29
3 3	15 08
3 36	14 89
3 41	14 7
3 46	14 6

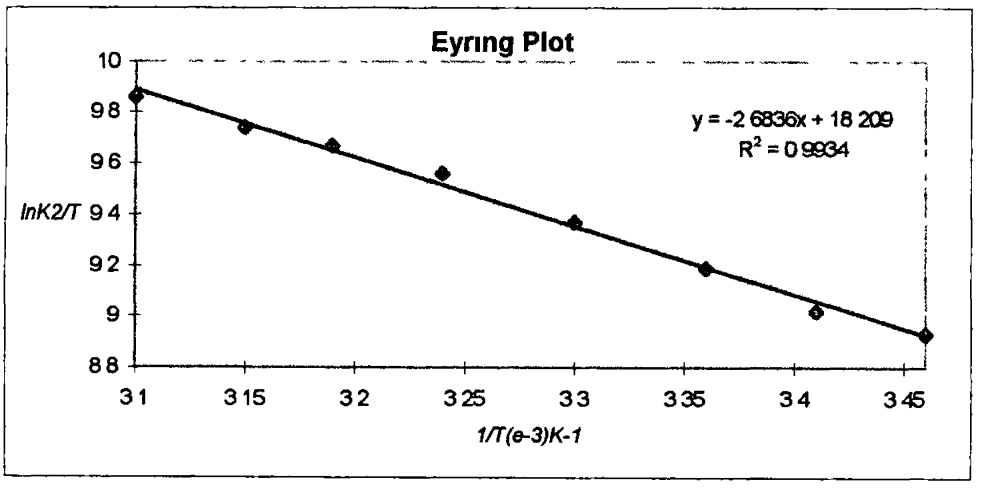

Eyring data

1/T (e-3)	*ln K2/T*
3 1	9 86
3 15	9 74
3 19	9 67
3 24	9 56
3 3	9 37
3 36	9 19
3 41	9 02
3 46	8 93

$Cr(CO)_6$ IN METHYLCYCLOHEXANE

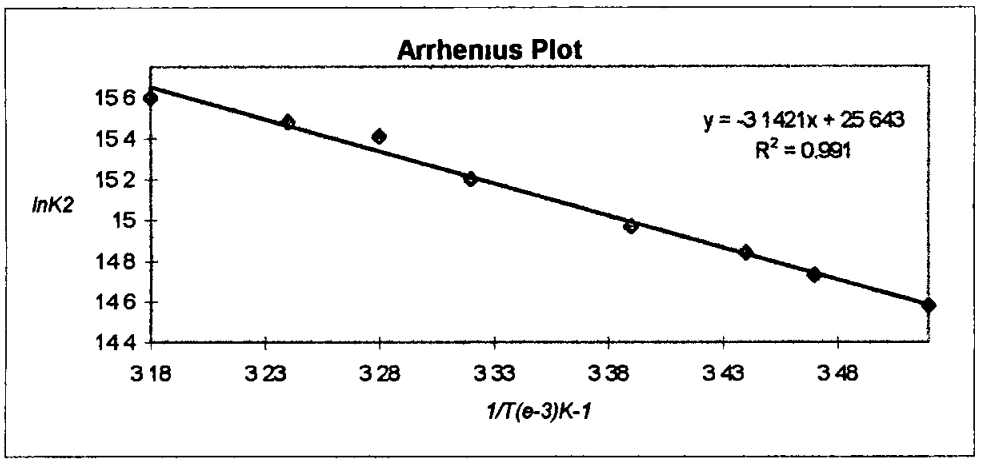

Arrhenius data

1/T (e-3)	ln k2
3 18	15 6
3 24	15 48
3 28	15 41
3 32	15 2
3 39	14 97
3 44	14 84
3 47	14 73
3 52	14 58

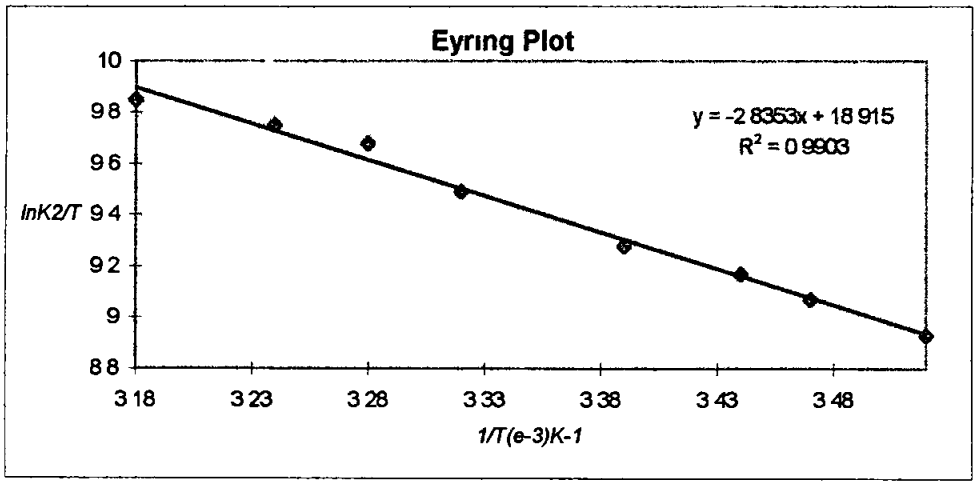

Eyring data

1/T (e-3)	ln K2/T
3 18	9 85
3 24	9 75
3 28	9 68
3 32	9 49
3 39	9 28
3 44	9 17
3 47	9 07
3 52	8 93

$Cr(CO)_6$ IN HEPTANE

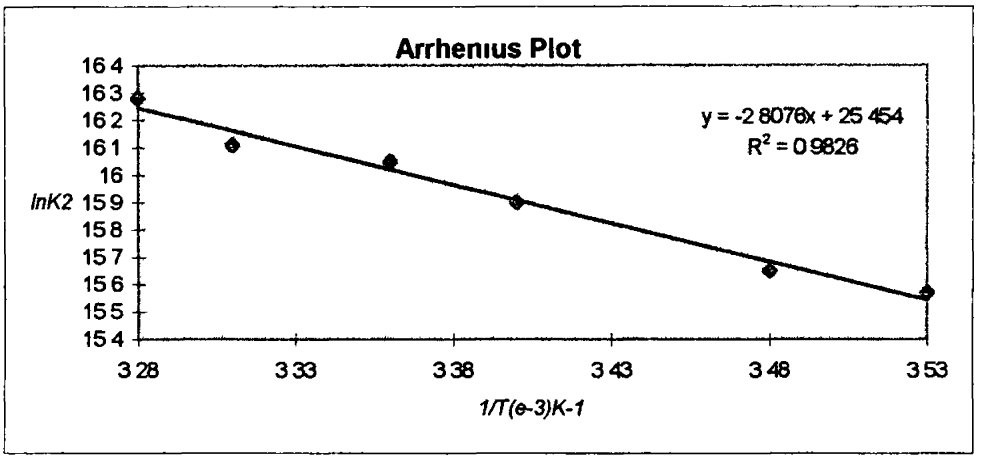

Arrhenius data

1/T (e-3)	ln k2
3 28	16 28
3 31	16 11
3 36	16 05
3 4	15 9
3 48	15 65
3 53	15 57

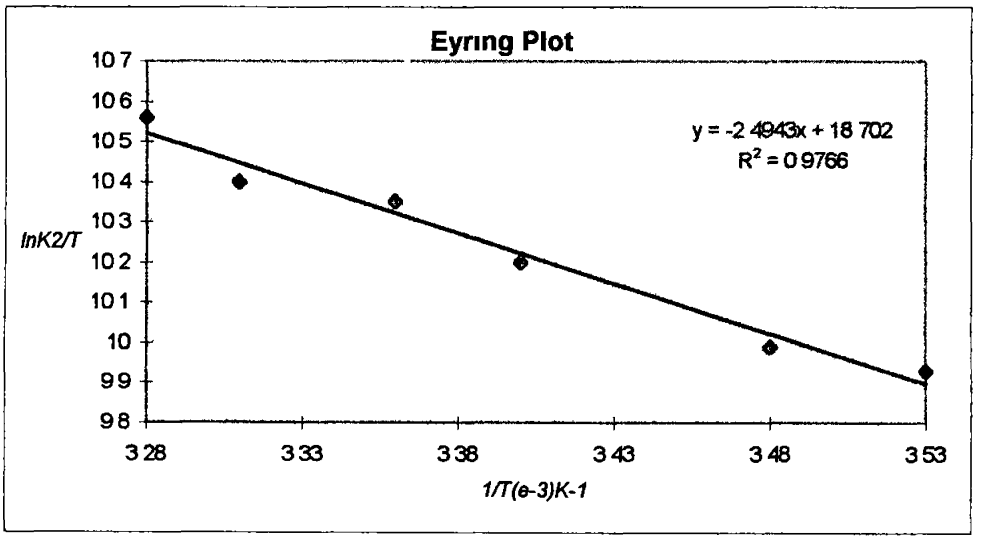

Eyring data

1/T (e-3)	ln K2/T
3 28	10 56
3 31	10 4
3 36	10 35
3 4	10 2
3 48	9 99
3 53	9 93

$Cr(CO)_6$ IN DECANE

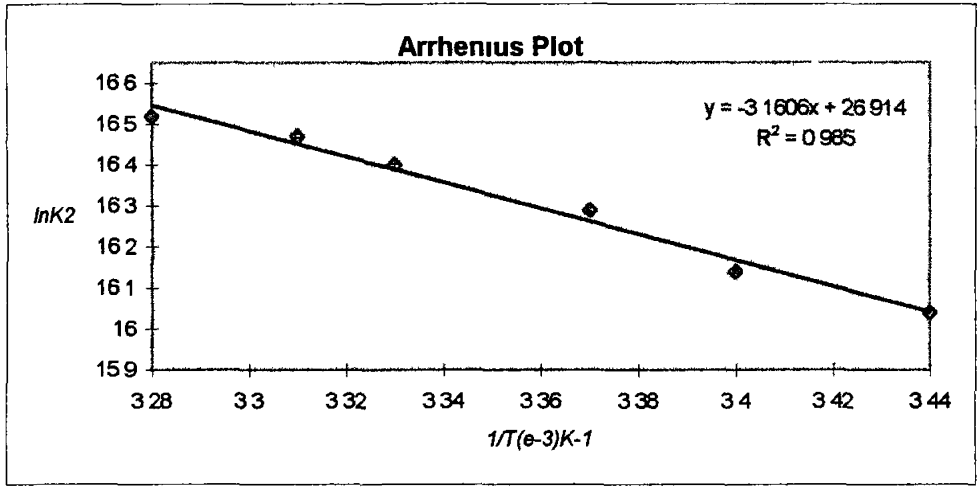

Arrhenius data

1/T (e-3)	ln k2
3 28	16 52
3 31	16 47
3 33	16 4
3 37	16 29
3 4	16 14
3 44	16 04

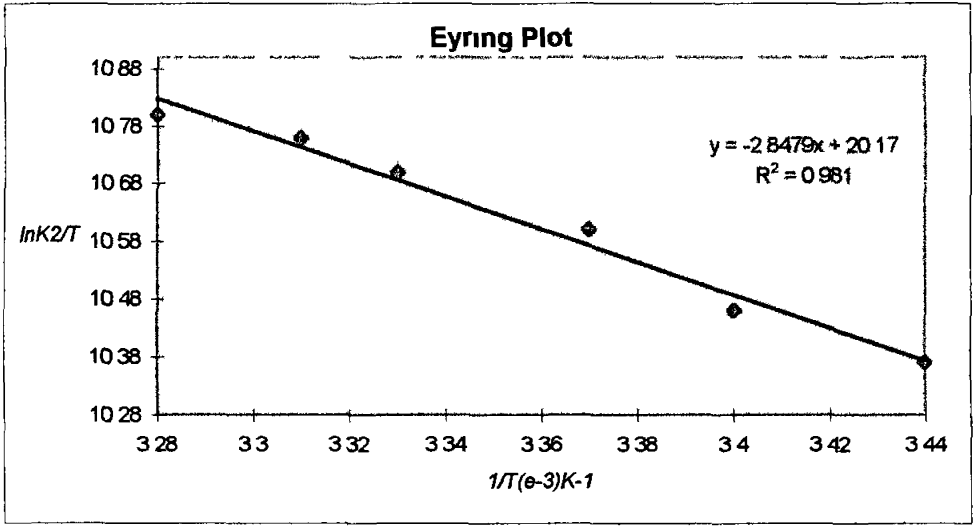

Eyring data

1/T (e-3)	ln K2/T
3 28	10 8
3 31	10 76
3 33	10 7
3 37	10 6
3 4	10 46
3 44	10 37

$Cr(CO)_6$ IN DODECANE

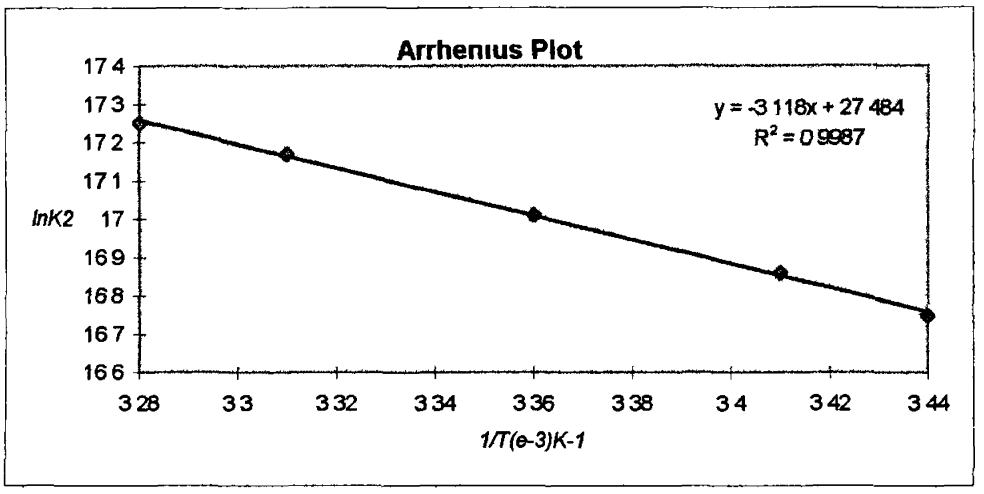

Arrhenius data

1/T (e-3)	ln k2
3 28	17 25
3 31	17 17
3 36	17 01
3 41	16 86
3 44	16 75

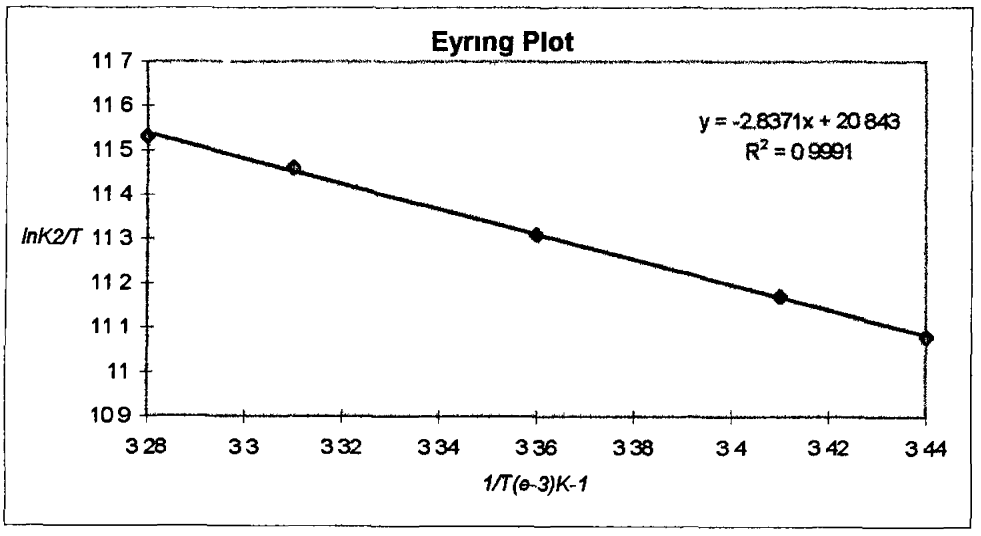

Eyring data

1/T (e-3)	ln K2/T
3 28	11 53
3 31	11 46
3 36	11 31
3 41	11 17
3 44	11 08

$Mo(CO)_6$ IN CYCLOHEXANE

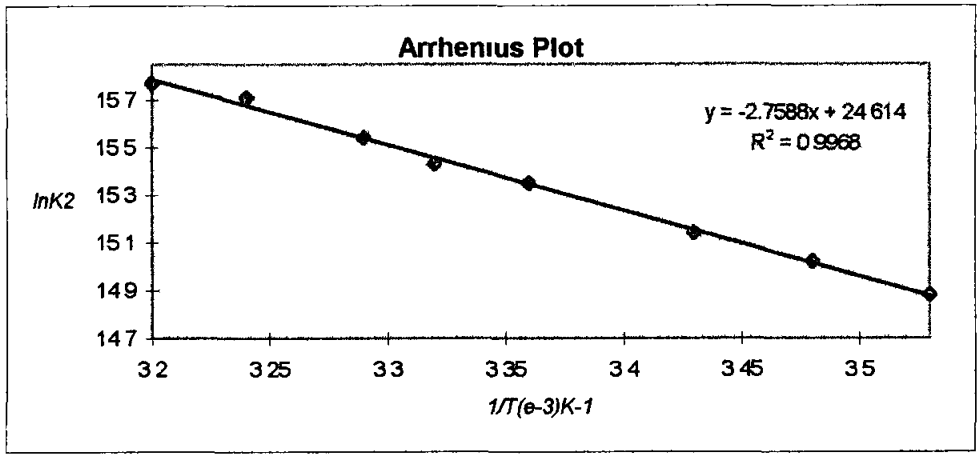

Arrhenius data

1/T (e-3)	ln k2
3.2	15.77
3.24	15.71
3.29	15.54
3.32	15.43
3.36	15.35
3.43	15.14
3.48	15.02
3.53	14.88

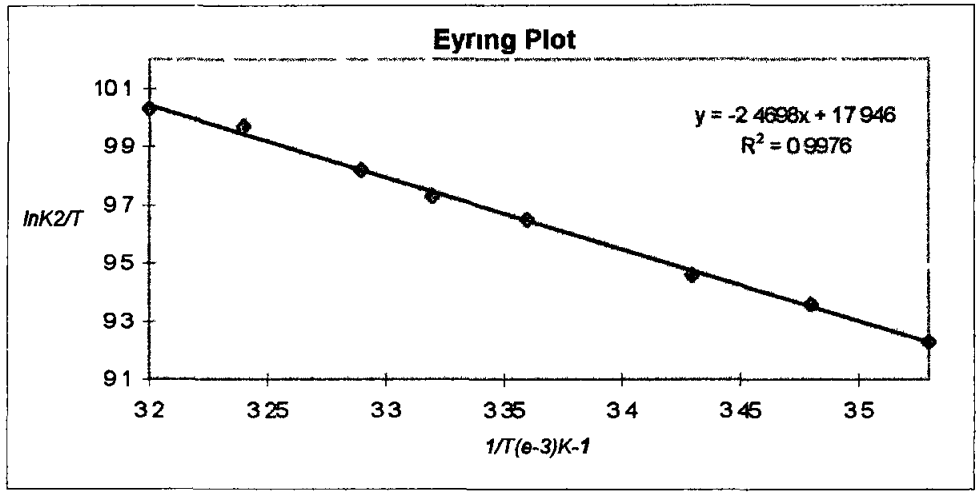

Eyring data

1/T (e-3)	ln K2/T
3.2	10.03
3.24	9.97
3.29	9.82
3.32	9.73
3.36	9.65
3.43	9.46
3.48	9.36
3.53	9.23

$Mo(CO)_6$ IN METHYLCYCLOHEXANE

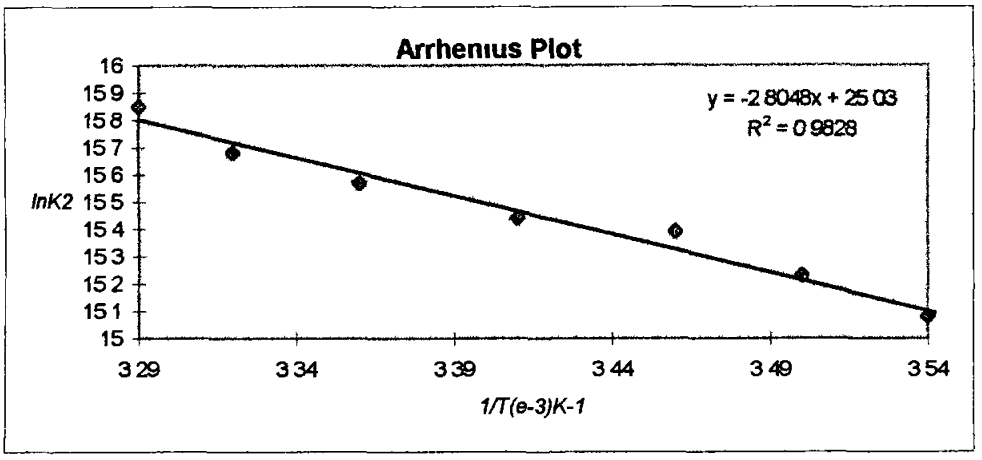

Arrhenius data

1/T (e-3)	ln k2
3 29	15 85
3 32	15 68
3 36	15 57
3 41	15 44
3 46	15 39
3 5	15 23
3 54	15 08
3 58	14 98

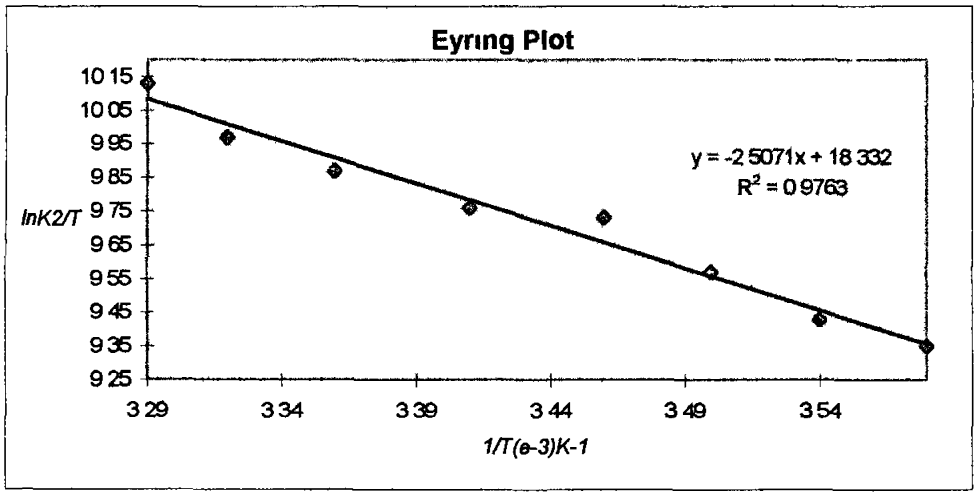

Eyring data

1/T (e-3)	ln K2/T
3 29	10 13
3 32	9 97
3 36	9 87
3 41	9 76
3 46	9 73
3 5	9 57
3 54	9 43
3 58	9 35

$Mo(CO)_6$ IN HEPTANE

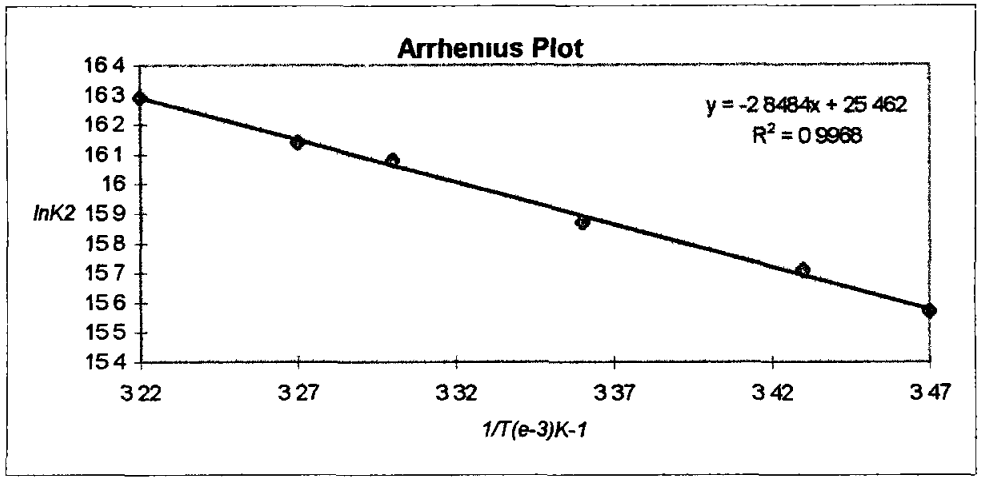

Arrhenius data

1/T (e-3)	ln k2
3 22	16 29
3 27	16 14
3 3	16 08
3 36	15 87
3 43	15 71
3 47	15 57

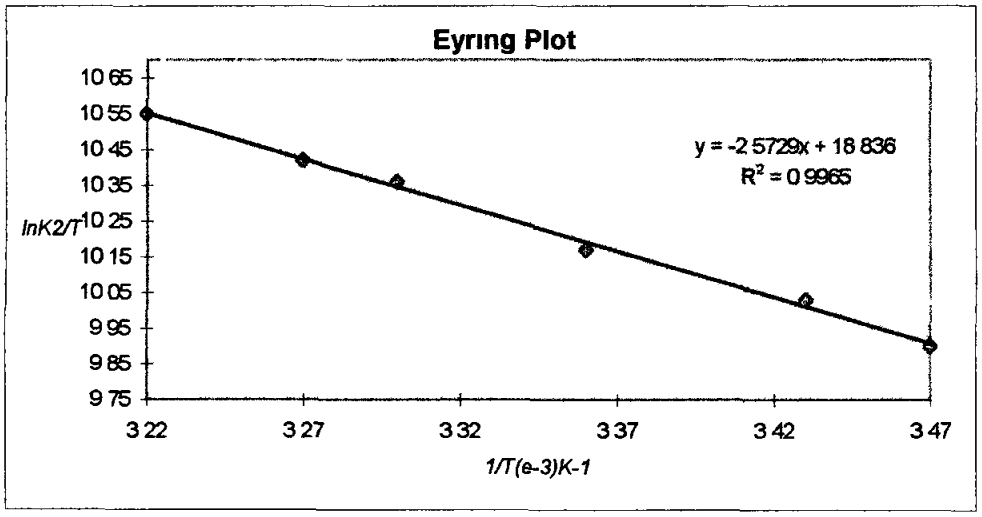

Eyring data

1/T (e-3)	ln K2/T
3 22	10 55
3 27	10 42
3 3	10 36
3 36	10 17
3 43	10 03
3 47	9 9

$Mo(CO)_6$ IN DECANE

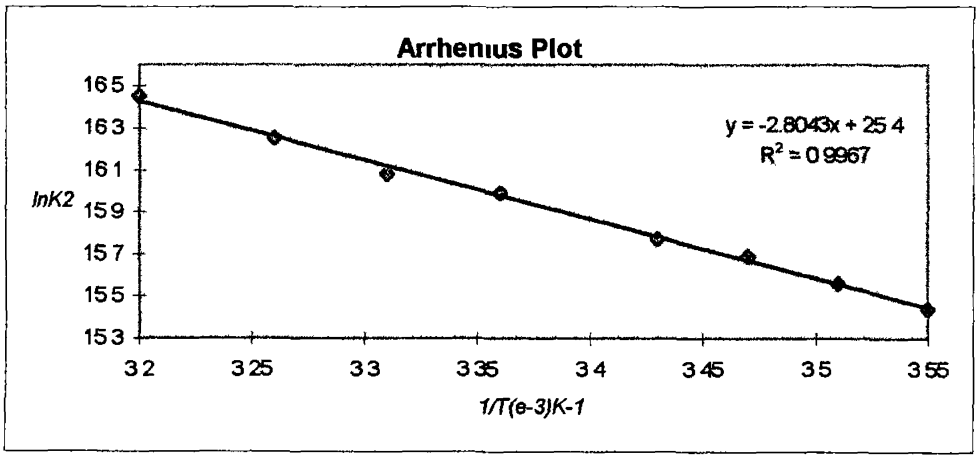

Arrhenius data

1/T (e-3)	ln k2
3.2	16.45
3.26	16.25
3.31	16.08
3.36	15.99
3.43	15.77
3.47	15.69
3.51	15.56
3.55	15.44

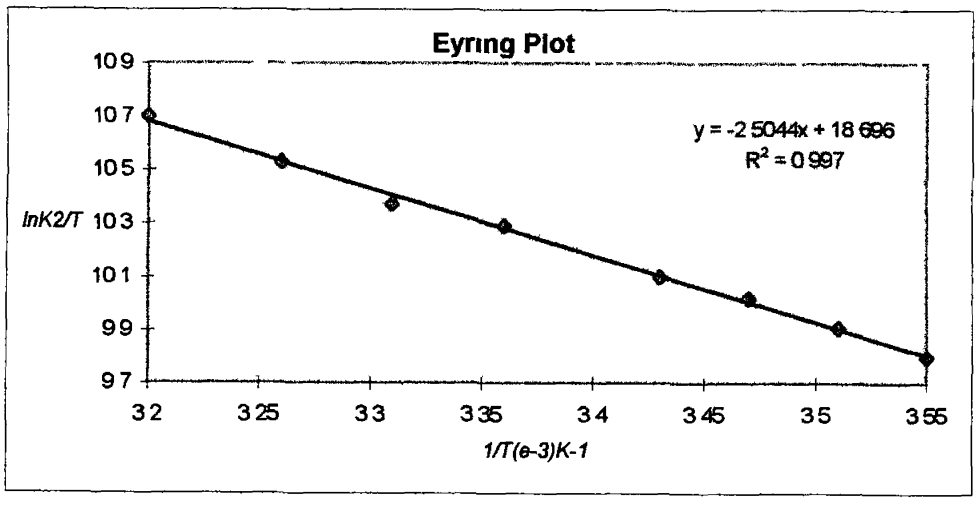

Eyring data

1/T (e-3)	ln K2/T
3.2	10.7
3.26	10.53
3.31	10.37
3.36	10.29
3.43	10.1
3.47	10.02
3.51	9.91
3.55	9.8

$Mo(CO)_6$ IN DODECANE

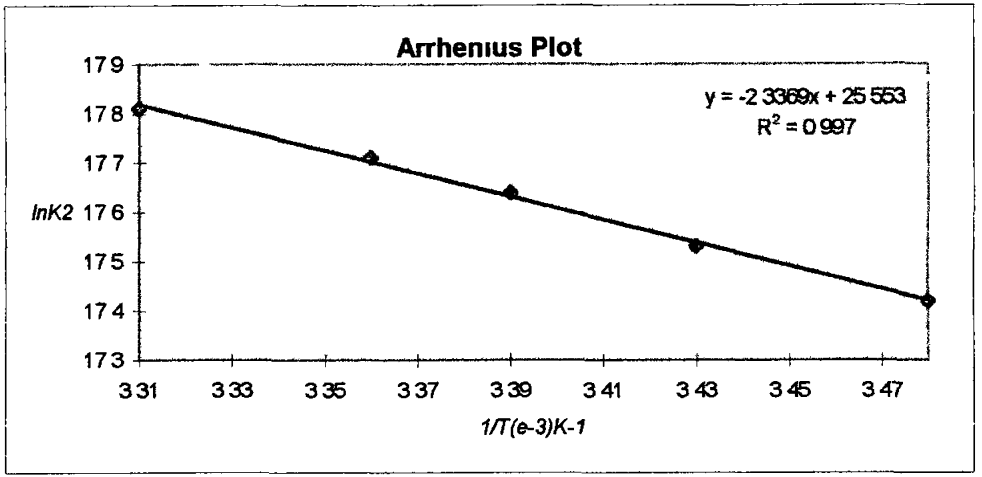

Arrhenius data

1/T (e-3)	ln k2
3 31	17 81
3 36	17 71
3 39	17 64
3 43	17 53
3 48	17 42

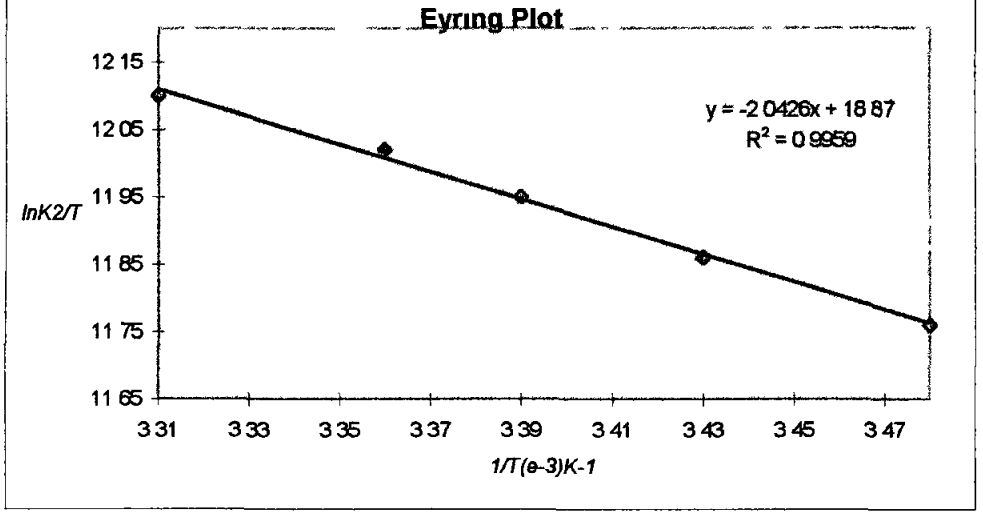

Eyring data

1/T (e-3)	ln K2/T
3 31	12 1
3 36	12 02
3 39	11 95
3 43	11 86
3 48	11 76

$W(CO)_6$ IN CYCLOHEXANE

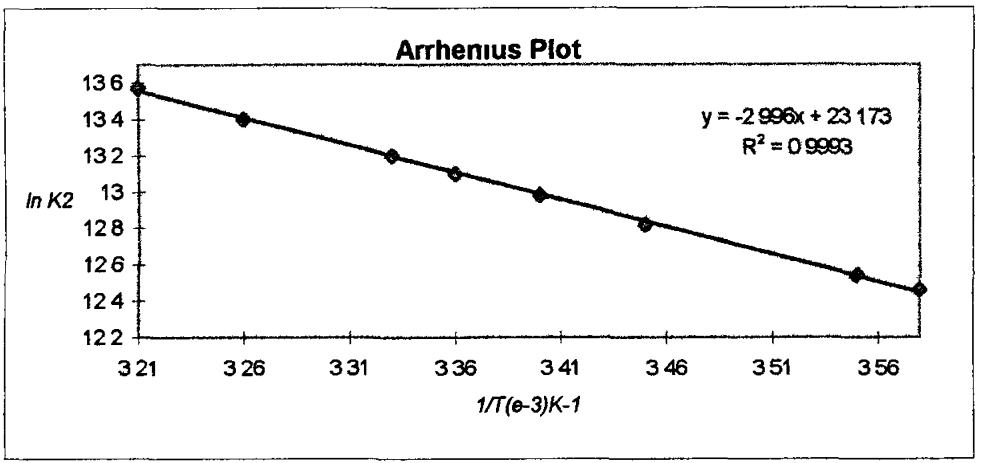

Arrhenius data

1/T (e-3)	ln k2
3 21	13 57
3 26	13 4
3 33	13 2
3 36	13 1
3 4	12 98
3 45	12 82
3 55	12 54
3 58	12 46

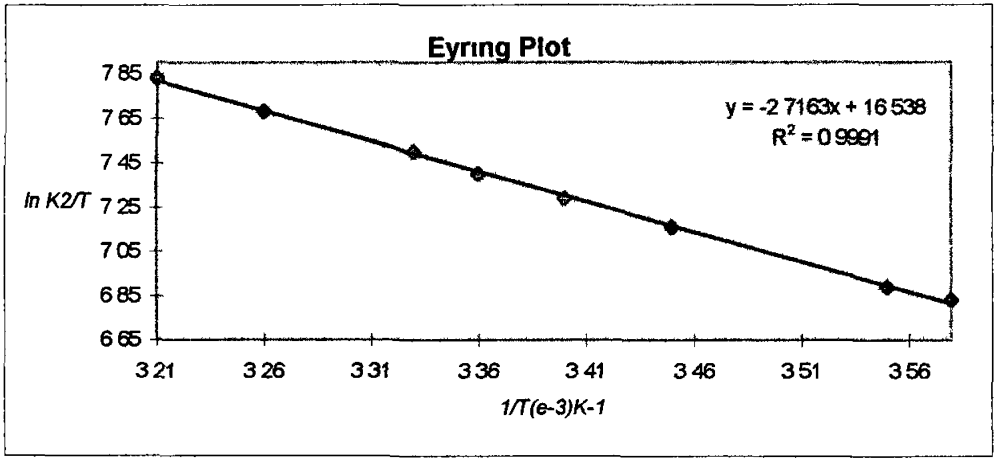

Eyring data

1/T (e-3)	ln K2/T
3 21	7 83
3 26	7 68
3 33	7 5
3 36	7 4
3 4	7 29
3 45	7 16
3 55	6 89
3 58	6 83

$W(CO)_6$ IN METHYLCYCLOHEXANE

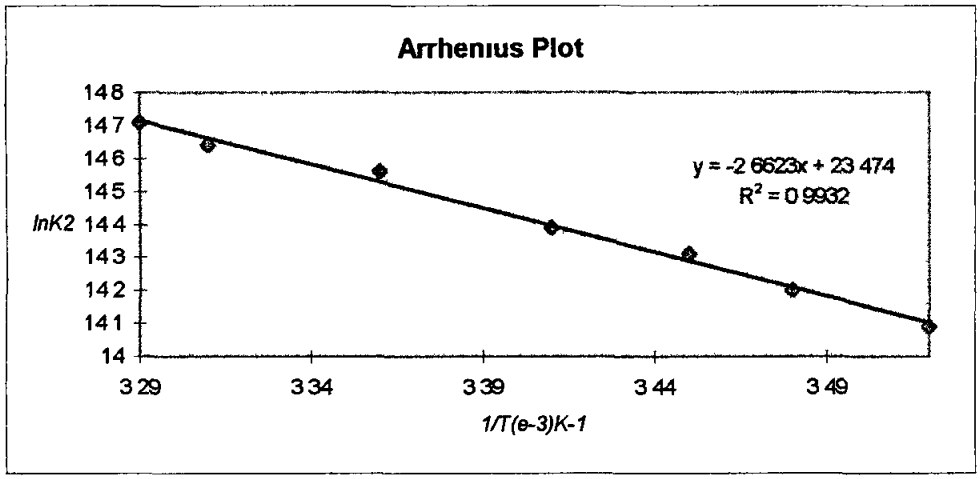

Arrhenius data

1/T (e-3)	ln k2
3 29	14 71
3 31	14 64
3 36	14 56
3 41	14 39
3 45	14 31
3 48	14 2
3 52	14 09

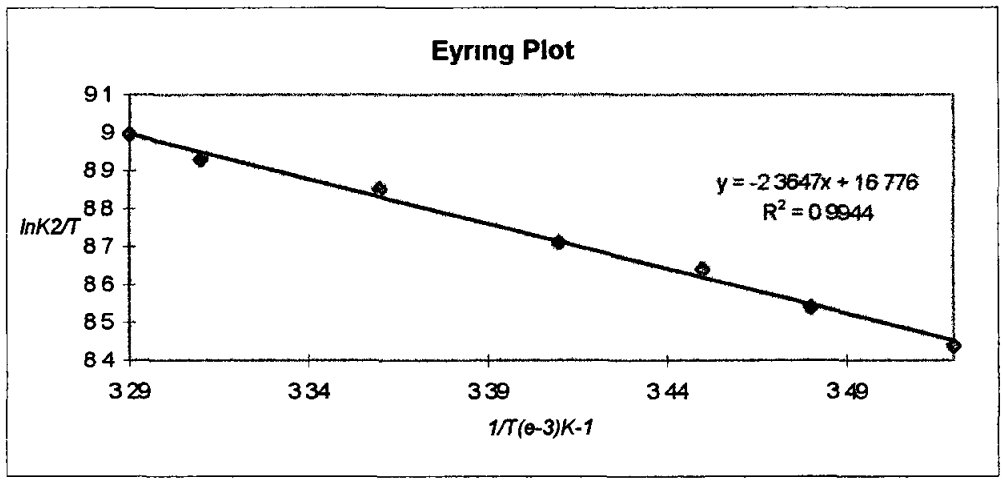

Eyring data

1/T (e-3)	ln K2/T
3 29	8 996
3 31	8 93
3 36	8 85
3 41	8 71
3 45	8 64
3 48	8 54
3 52	8 44

$W(CO)_6$ IN HEPTANE

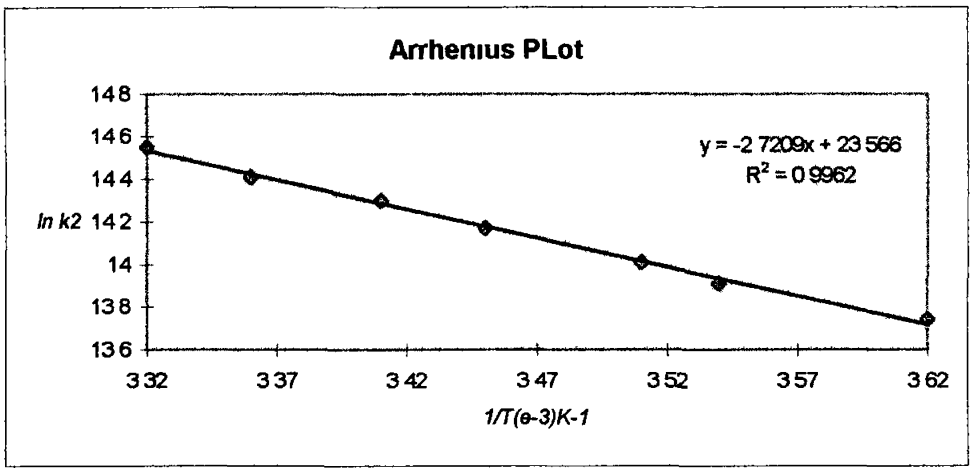

Arrhenius data

1/T (e-3)	ln k2
3 32	14 55
3 36	14 41
3 41	14 3
3 45	14 17
3 51	14 01
3 54	13 91
3 62	13 74

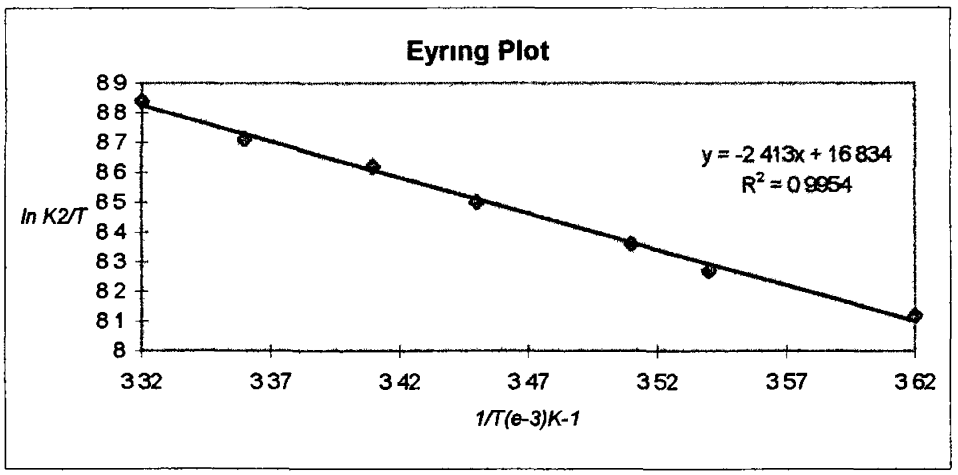

Eyring data

1/T (e-3)	ln K2/T
3 32	8 84
3 36	8 71
3 41	8 62
3 45	8 5
3 51	8 36
3 54	8 27
3 62	8 12

$W(CO)_6$ IN DECANE

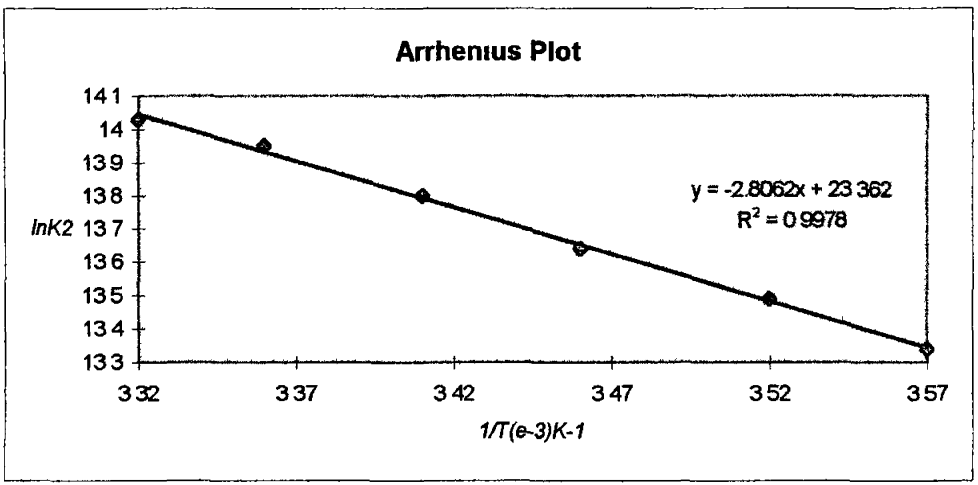

Arrhenius data

1/T (e-3)	ln k2
3.32	14.03
3.36	13.95
3.41	13.8
3.46	13.64
3.52	13.49
3.57	13.34

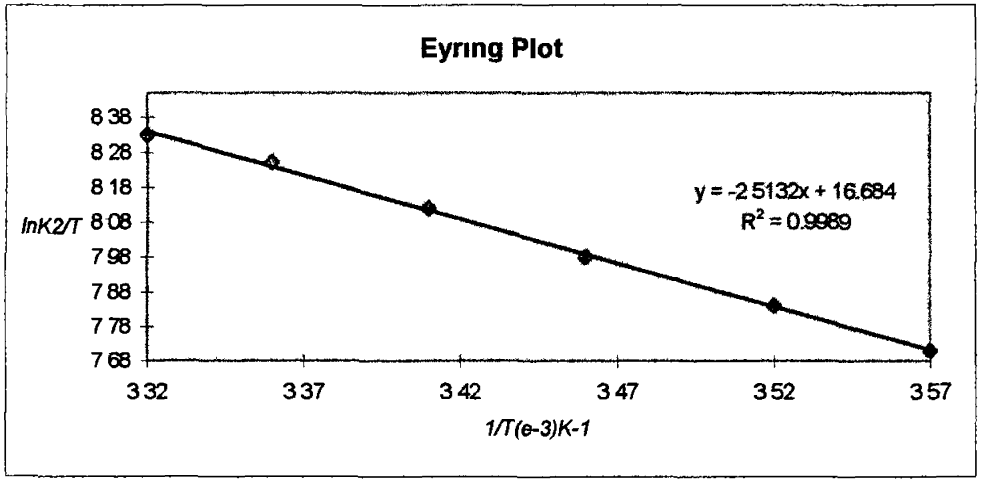

Eyring data

1/T (e-3)	ln K2/T
3 32	8 33
3 36	8 25
3 41	8 12
3 46	7 98
3 52	7 84
3 57	7 71

$W(CO)_6$ IN DODECANE

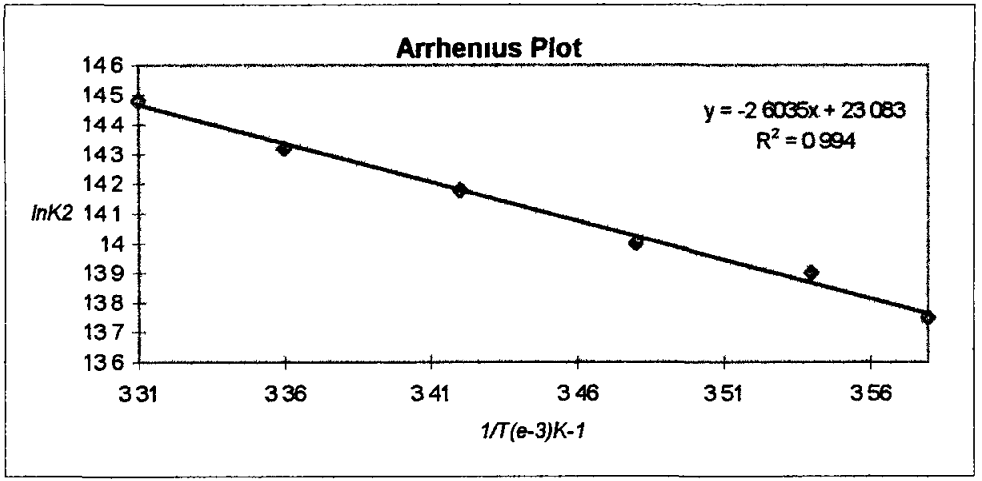

Arrhenius data

1/T (e-3)	ln k2
3 31	14 48
3 36	14 32
3 42	14 18
3 48	14
3 54	13 9
3 58	13 75

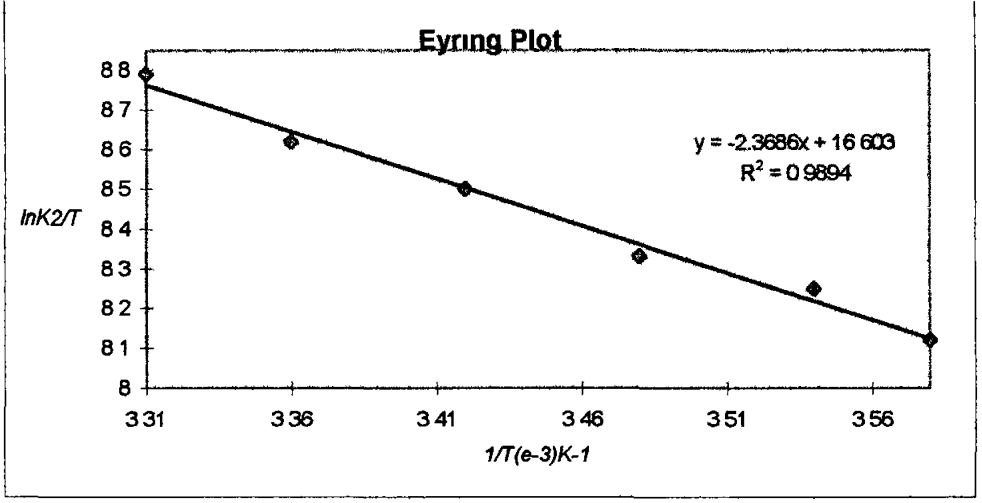

Eyring data

1/T (e-3)	ln K2/T
3.31	8.79
3.36	8.62
3.42	8.5
3.48	8.33
3.54	8.25
3.58	8.12

APPENDIX 2

SECTION A

2 A Extinction coefficients for the (η^6-arene)Cr(CO)$_3$ compounds

(1) (η^6-pyridine)Cr(CO)$_3$

Concentration (x 10^{-4} M)	Absorbance @ **354 nm** (A U)
0	0
1	0 277
2	0 492
3	0 837
4	1 220
5	1 589

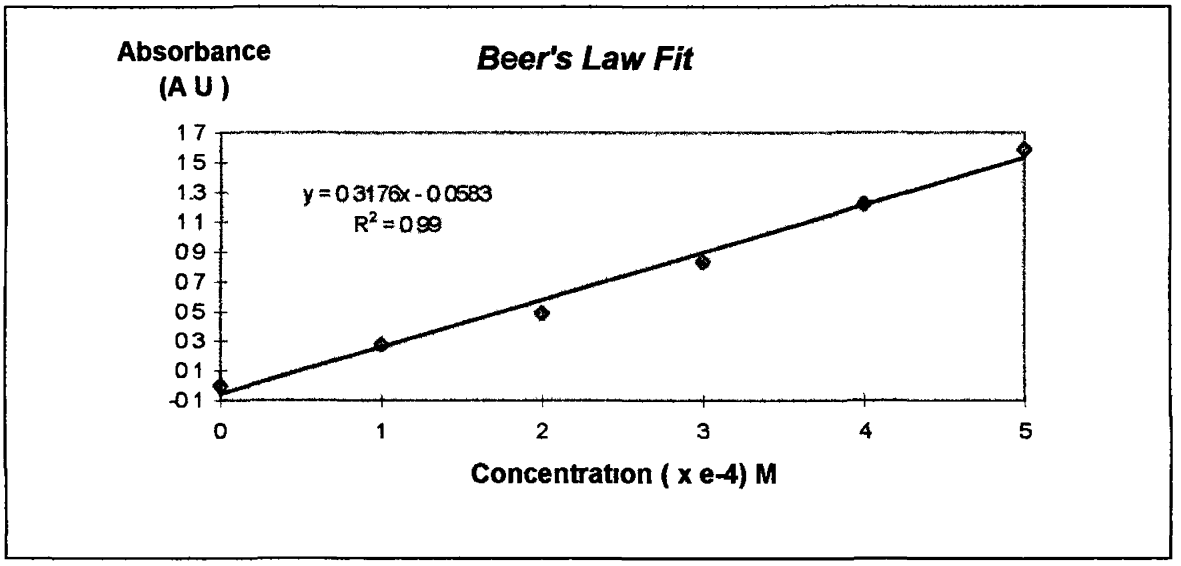

Therefore the extinction coefficient for (η^6-pyridine)Cr(CO)$_3$ in cyclohexane at 354 nm is 3 2 x 10^3 dm^3 mol^{-1} cm^{-1}

Concentration (x 10^{-4} M)	Absorbance @ **316 nm** (A U)
0	0
1	1 042
2	1 851
3	2 883
4	3 486

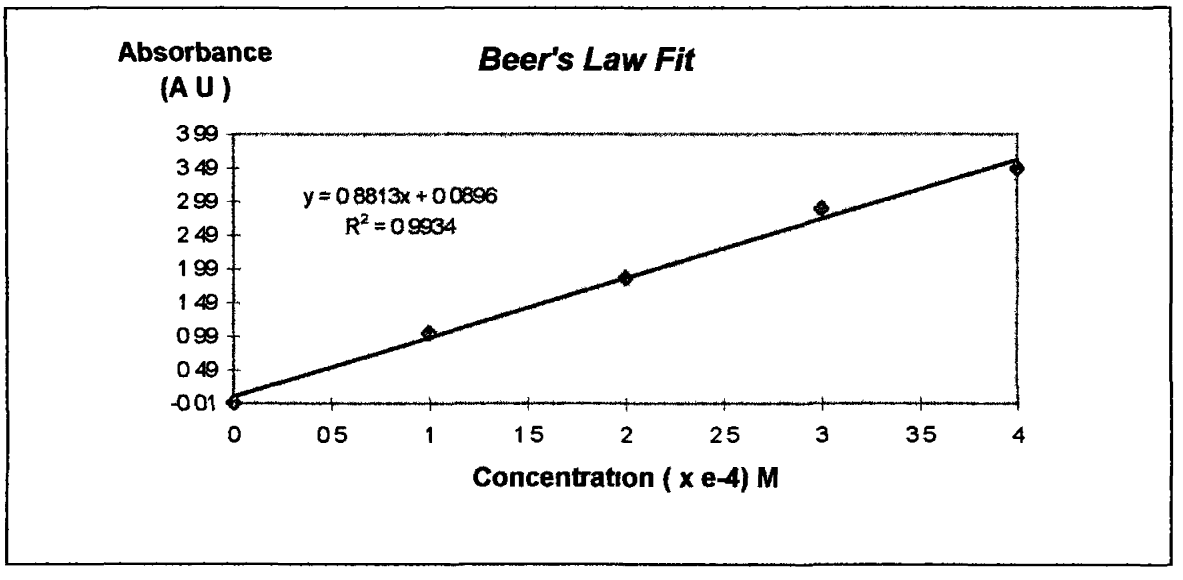

Therefore the extinction coefficient for (η^6-pyrdine)$Cr(CO)_3$ in cyclohexane at 316 nm is 8 8 x 10^3 dm^3 mol^{-1} cm^{-1}

(2) (η^6-2,6-dimethylpyridine)$Cr(CO)_3$

Concentration (x 10^{-4} M)	Absorbance @ **354 nm** (A U)
0	0
0 4	0 069
1	0 191
1 6	0 328
2	0 401
4	0 832

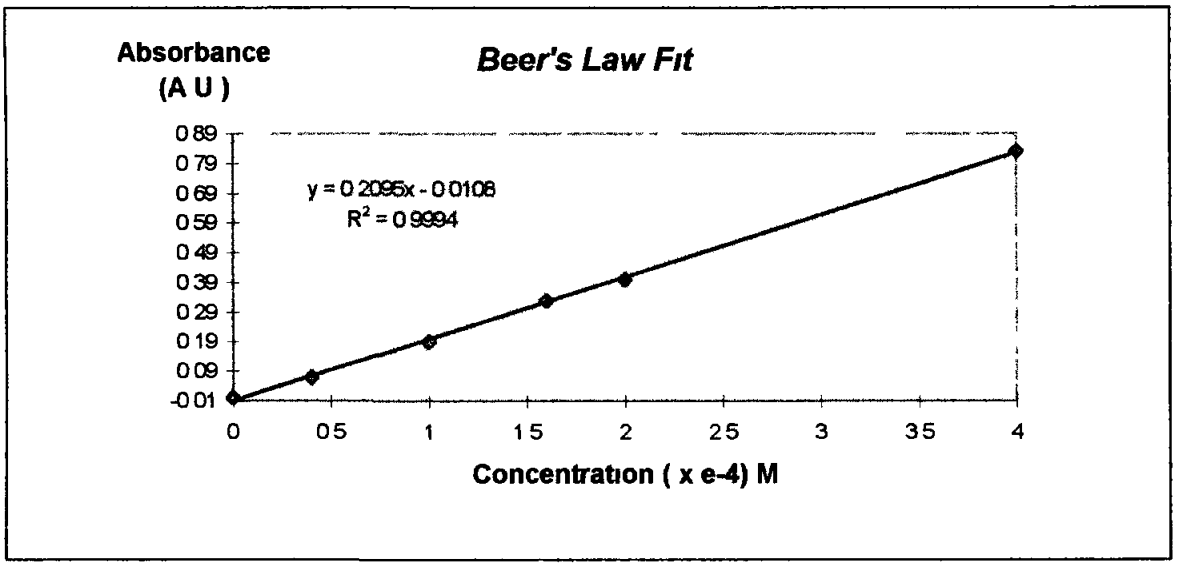

Therefore the extinction coefficient for (η^6-2,6-lutidine)$Cr(CO)_3$ in cyclohexane at 354 nm is 2 1 x 10^3 dm^3 mol^{-1} cm^{-1}

Concentration (x 10^{-4} M)	Absorbance @ **318 nm** (A U)
0	0
0 4	0 205
1	0 558
1 6	0 961
2	1 165
4	2 390

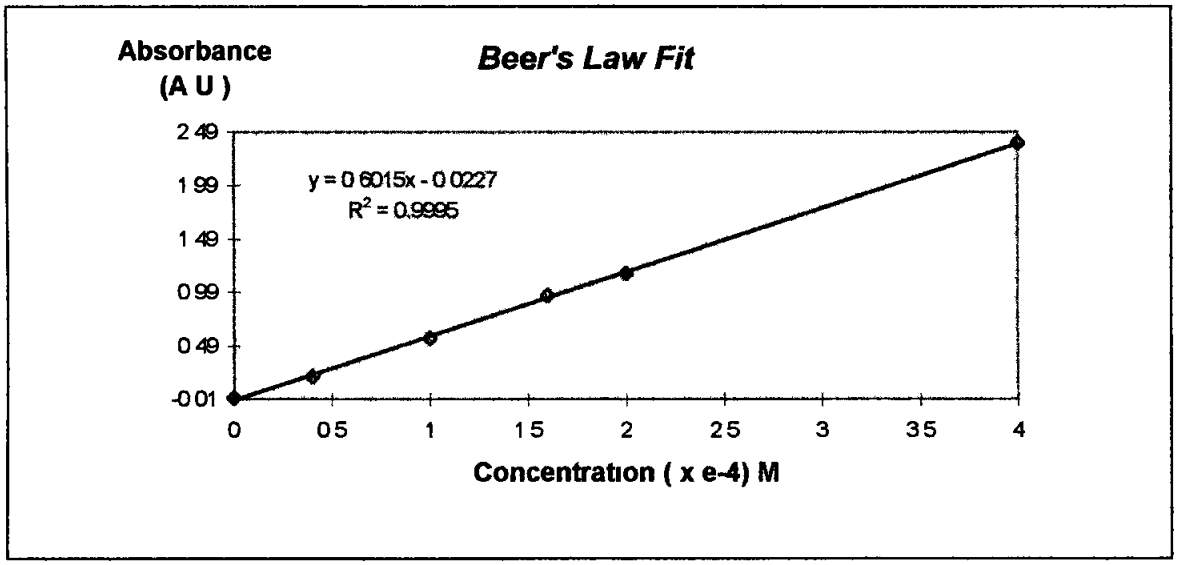

Therefore the extinction coefficient for (η^6-2,6-lutidine)$Cr(CO)_3$ in cyclohexane at 318 nm is 6 1 x 10^3 dm^3 mol^{-1} cm^{-1}

(3) (η^6-2,6-bis(trimethylsilyl)pyridine)Cr(CO)$_3$

Concentration (x 10^{-4} M)	Absorbance @ **354 nm** (A U)
0	0
0 5	0 164
1 1	0 433
1 9	0 693
2 3	0 836
4 7	1 749

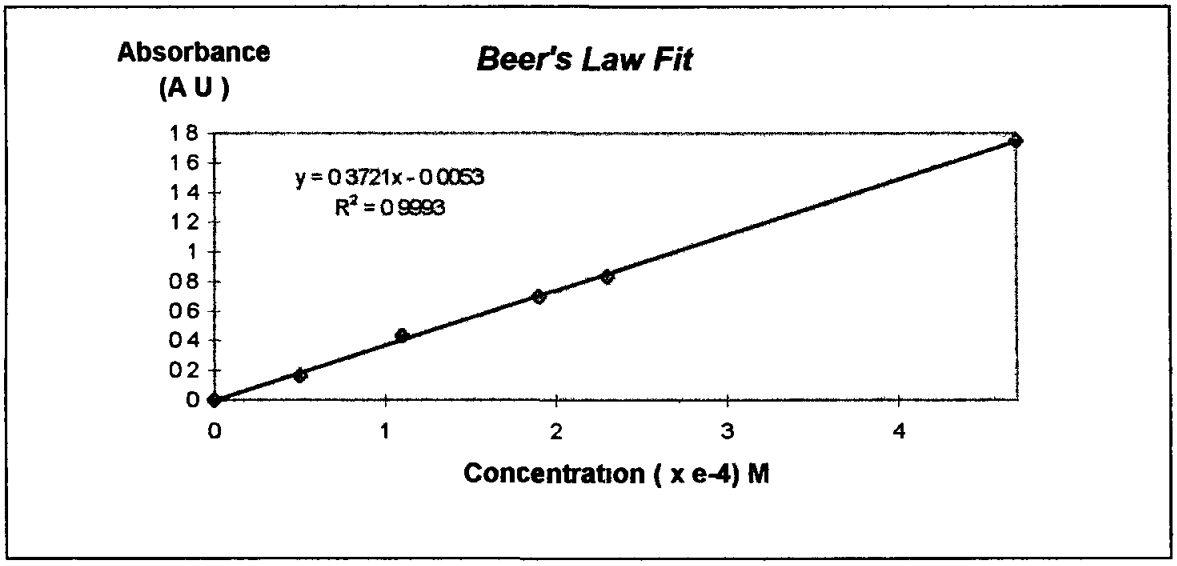

Therefore the extinction coefficient for (η^6-2,6-bis(trimethylsilyl)pyridine)Cr(CO)$_3$ in cyclohexane at 354 nm is 3 7 x 10^3 dm^3 mol^{-1} cm^{-1}

Concentration (x 10^{-4} M)	Absorbance @ **324 nm** (A U)
0	0
0 5	0 384
1 1	1 008
1 9	1 609
2 3	1 949
4 7	3 686

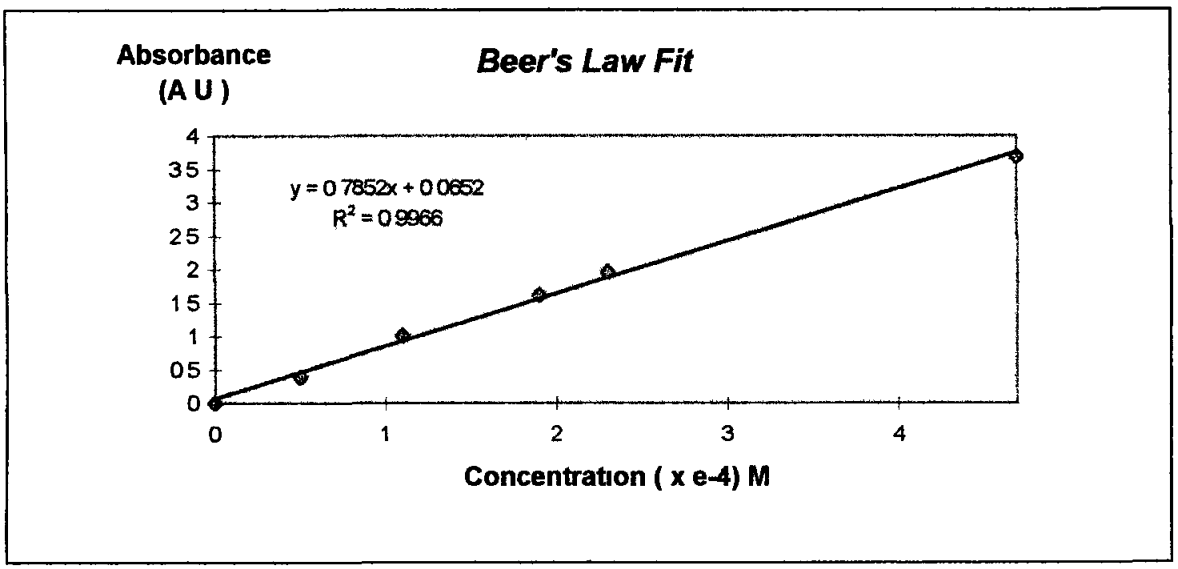

Therefore the extinction coefficient for (η^6-2,6-bis(trimethylsilyl)pyridine)Cr(CO)$_3$ in cyclohexane at 324 nm is 7 9 x 10^3 dm^3 mol^{-1} cm^{-1}

Infrared spectrum, at room temperature, of (η^6-pyridine)$Cr(CO)_3$ in cyclohexane

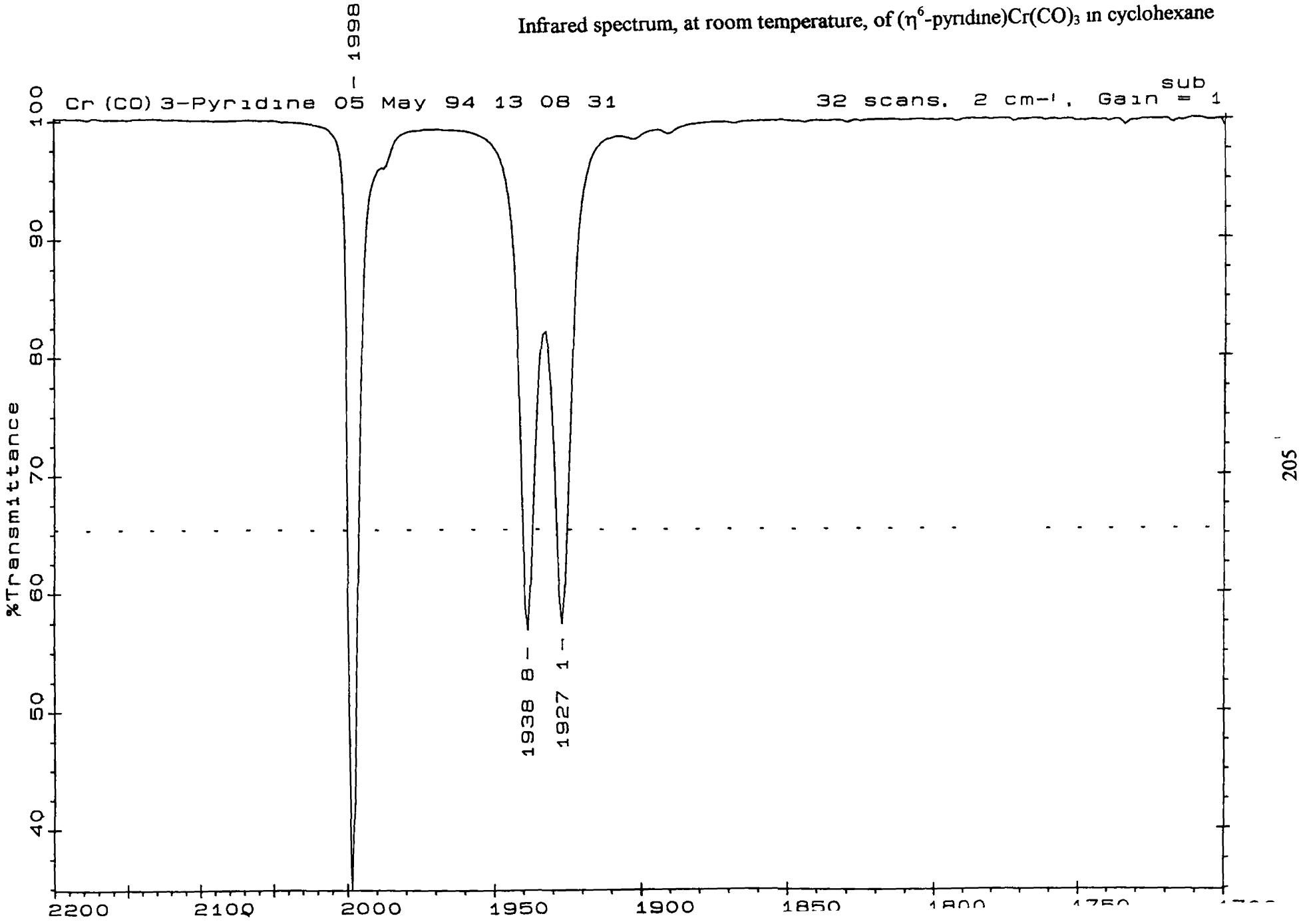

Infrared spectrum, at room temperature, of (η^6-2,6-lutidine)$Cr(CO)_3$ in cyclohexane

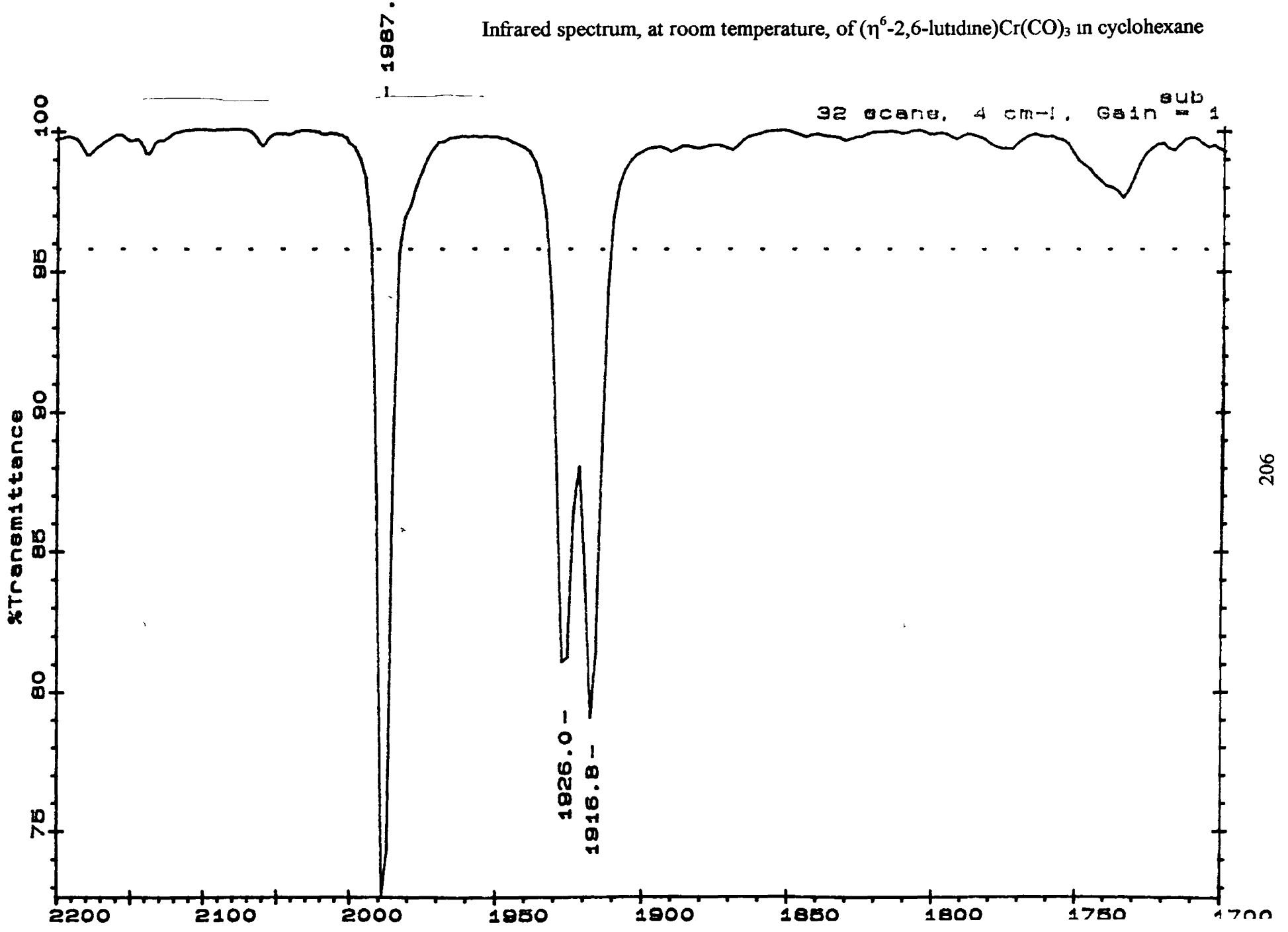

Infrared spectrum at room temperature of (η^6-2,6-(TMS)pyridine)$Cr(CO)_3$ in cyclohexane

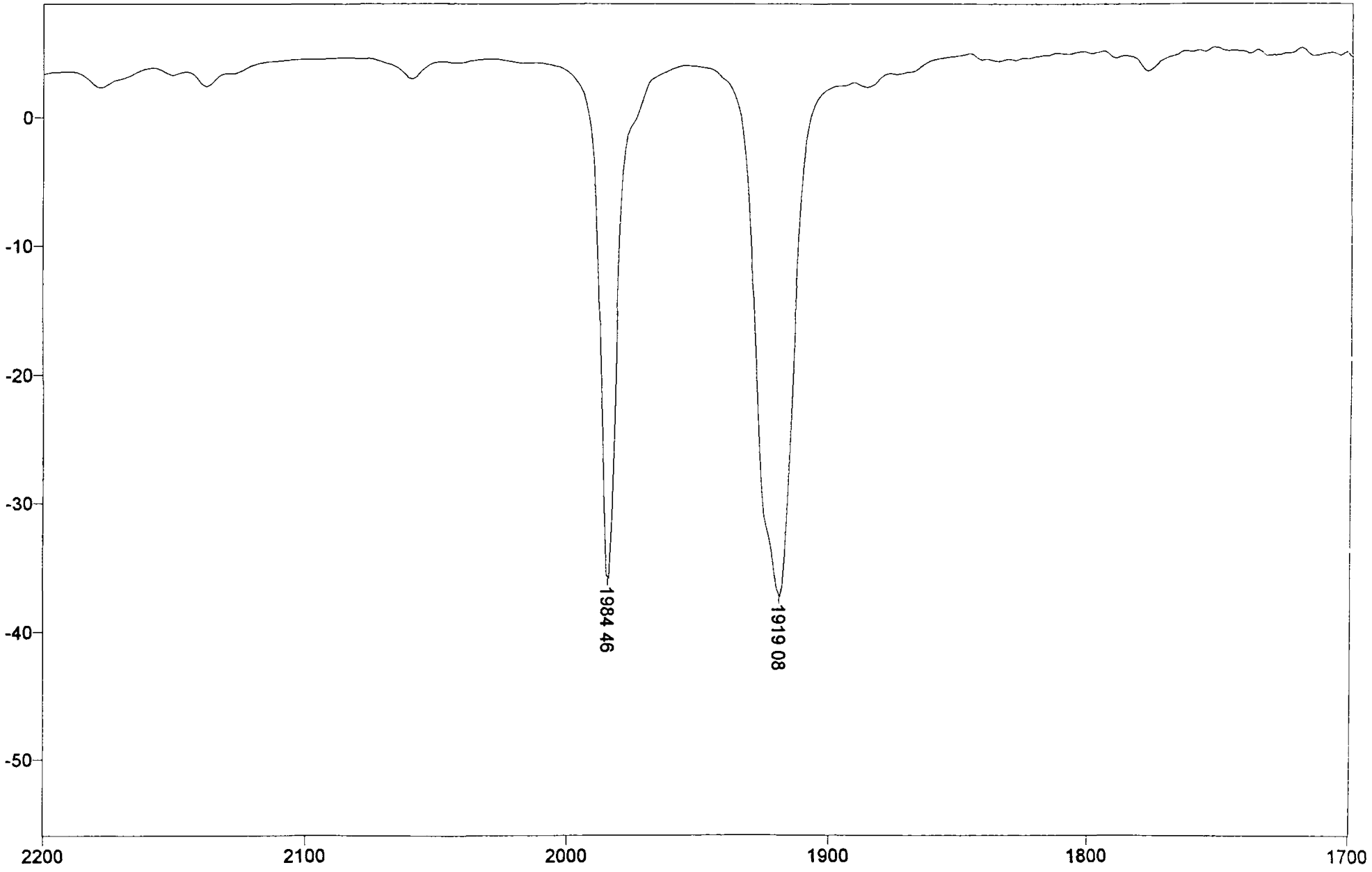

Transmittance / Wavenumber (cm-1)

Number of Scans= 4 Apodization= Strong

^{1}H NMR spectrum of (η^6-pyridme)Cr(CO)$_3$ in $CDCl_3$

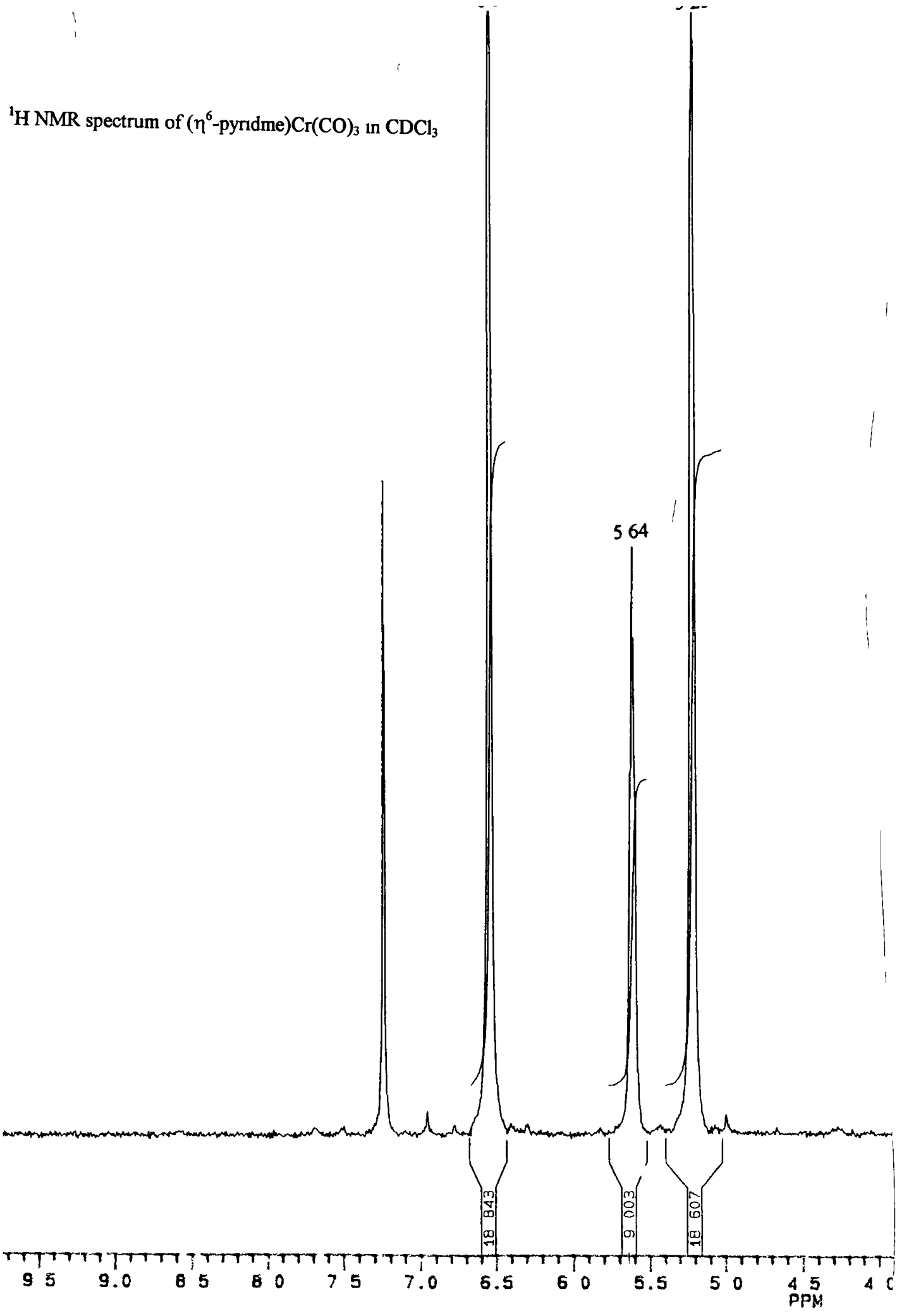

^{13}C NMR spectrum of (η^6-pyridine)$Cr(CO)_3$ in $CDCl_3$

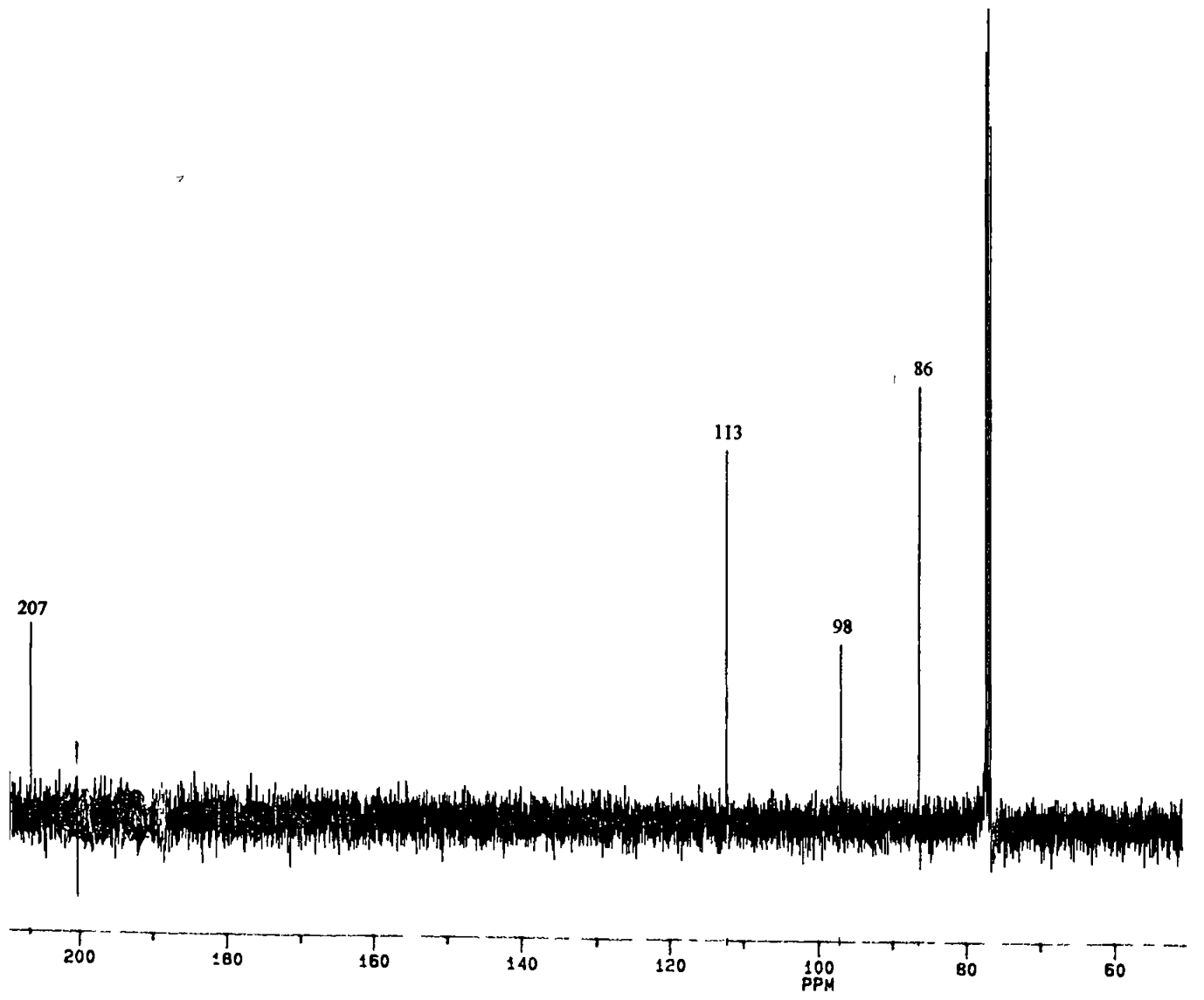

^{1}H NMR spectrum of (η^6-2,6-(TMS)pyridine)Cr(CO)$_3$ in $CDCl_3$

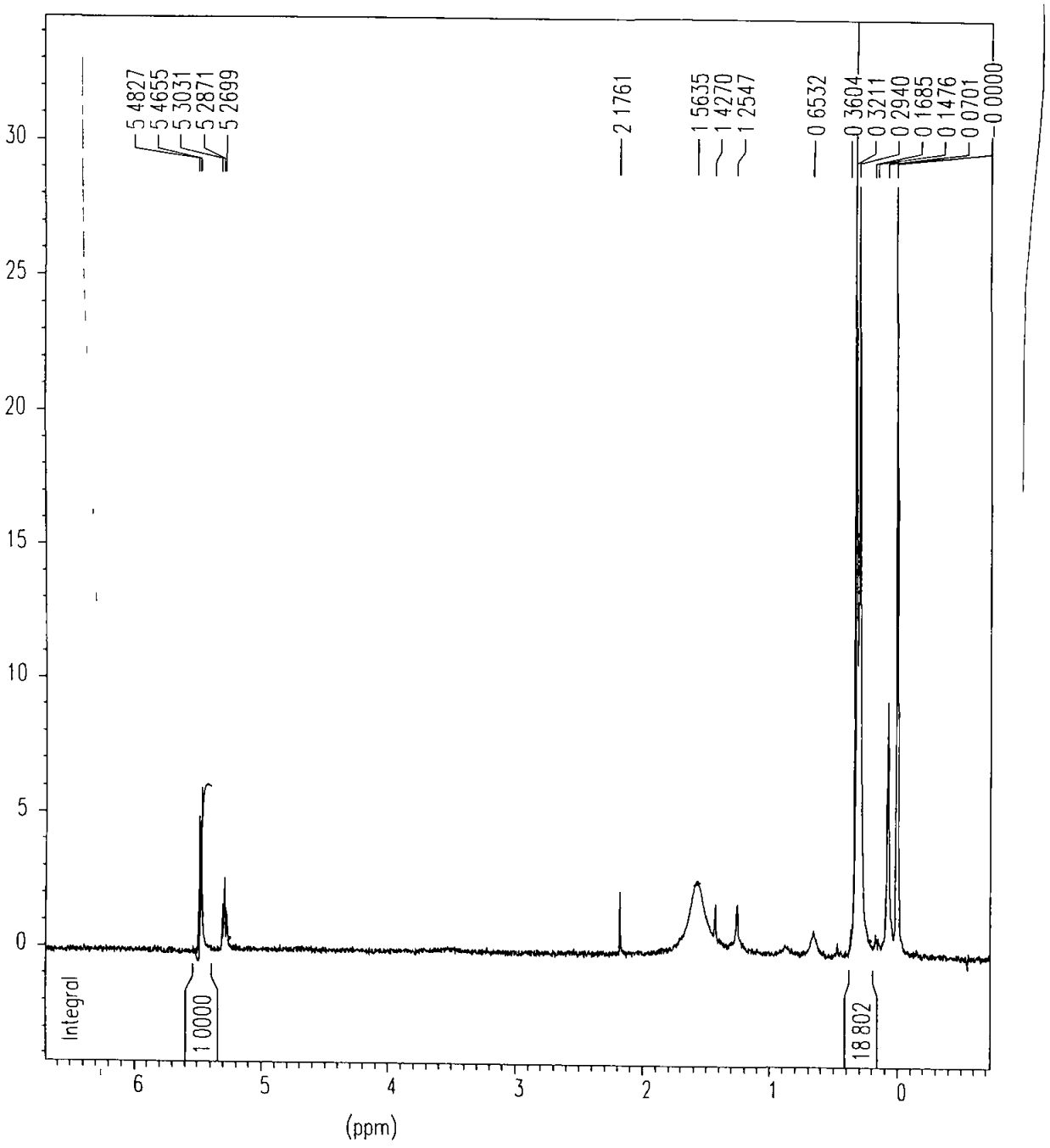

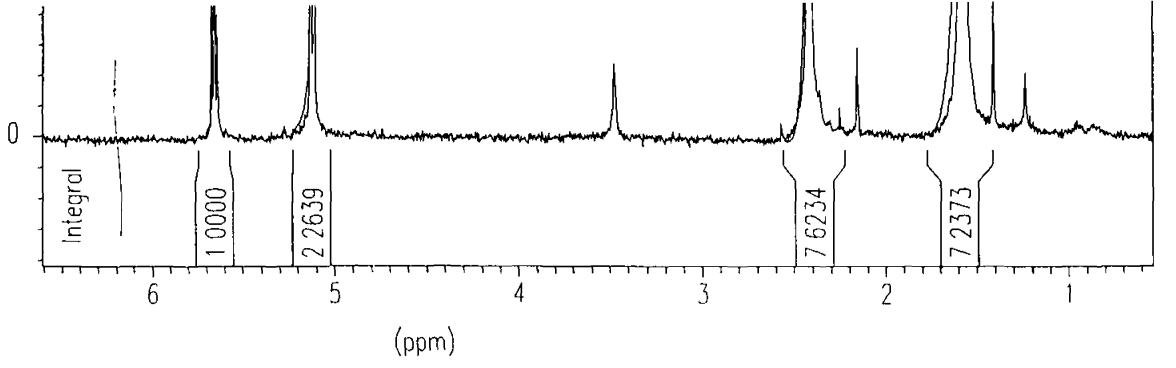
0
Integral
1 0000
2 2639
7 6234
7 2373
6
5
4
3
2
1
(ppm)

^{1}H NMR spectrum of (η^{6}-2,6-lutidine)Cr(CO)$_3$ in $CDCl_3$

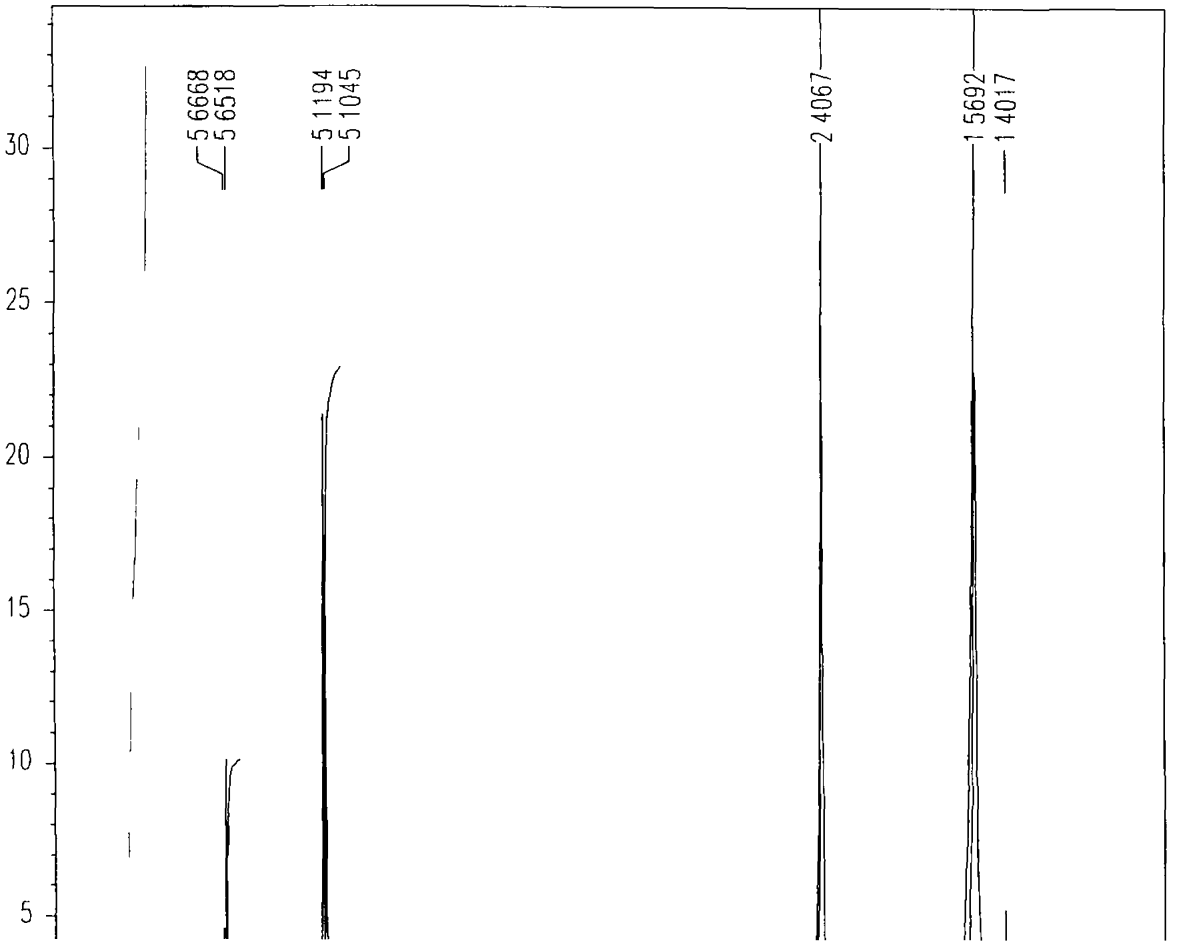

SECTION B

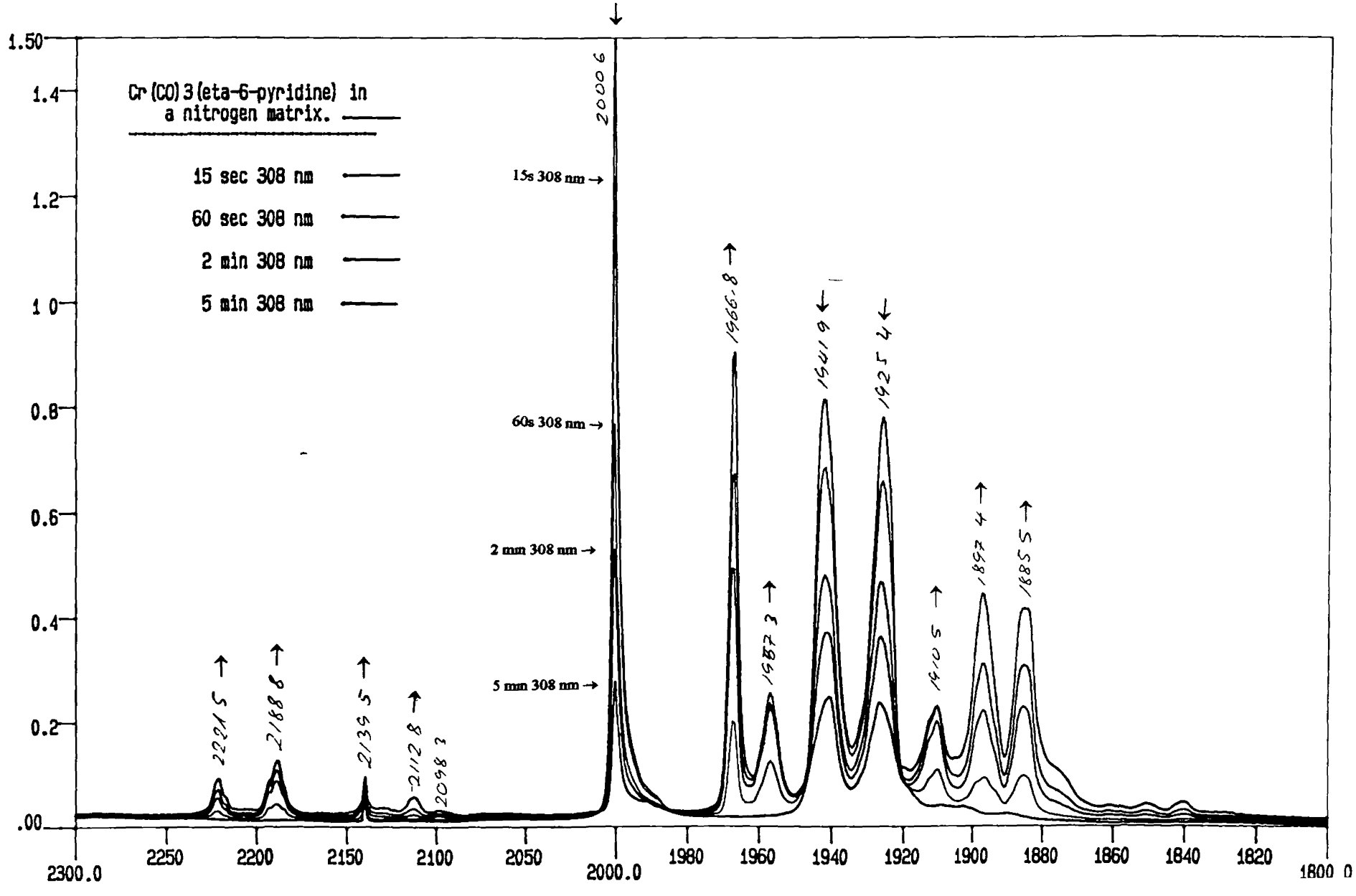
Cr(CO)3(eta-6-pyridine) in a nitrogen matrix.
15 sec 308 nm
60 sec 308 nm
2 min 308 nm
5 min 308 nm
15s 308 nm
60s 308 nm
2 mm 308 nm
5 mm 308 nm
2000.6
1966.8
1941.9
1925.4
1882.2
1910.5
1892.4
1885.5
2214.5
2168.6
2139.5
2112.8
2098.3
1.50
1.4
1.2
1.0
0.8
0.6
0.4
0.2
.00
2300.0
2250
2200
2150
2100
2050
2000.0
1980
1960
1940
1920
1900
1880
1860
1840
1820
1800.0

A

(η^6-pyridine)$Cr(CO)_3$ in a CH_4 CO matrix (10 1)

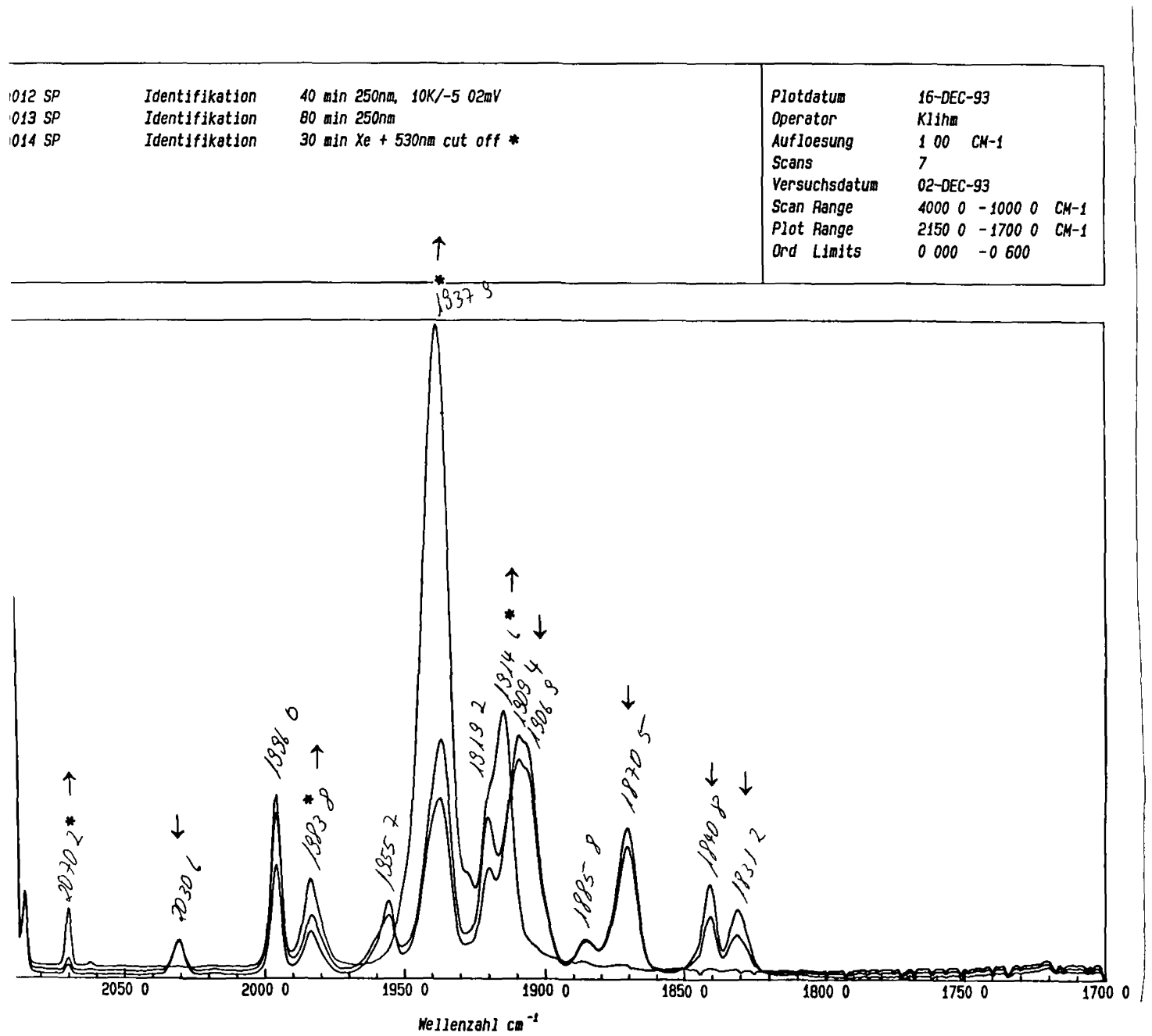

A

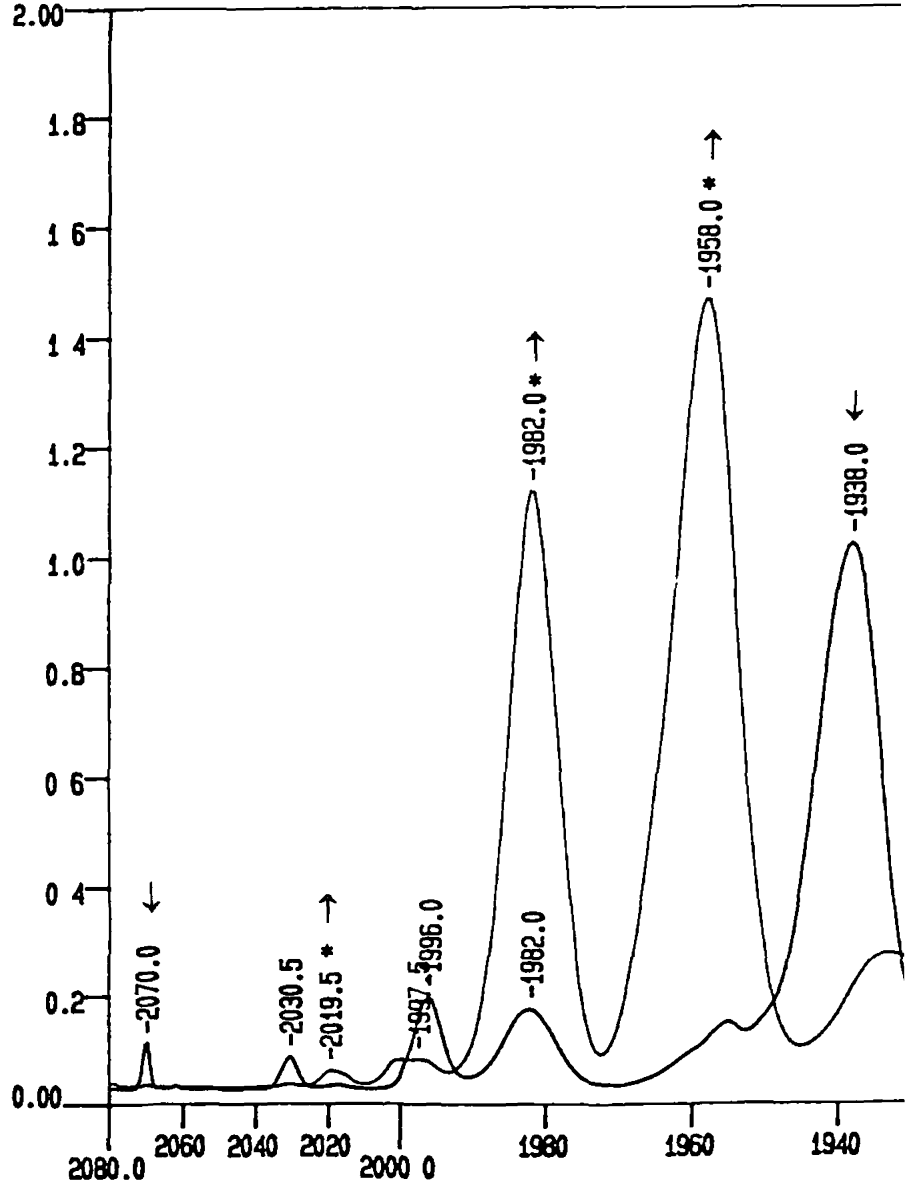
2.00
1.8
1 6
1 4
1.2
1.0
0.8
0 6
0 4
0.2
0.00
-2070.0
-2030.5
-2019.5 *
-1997.5
-1996.0
-1982.0
-1982.0 *
-1958.0 *
-1938.0
2080.0
2060
2040
2020
2000 0
1980
1960
1940

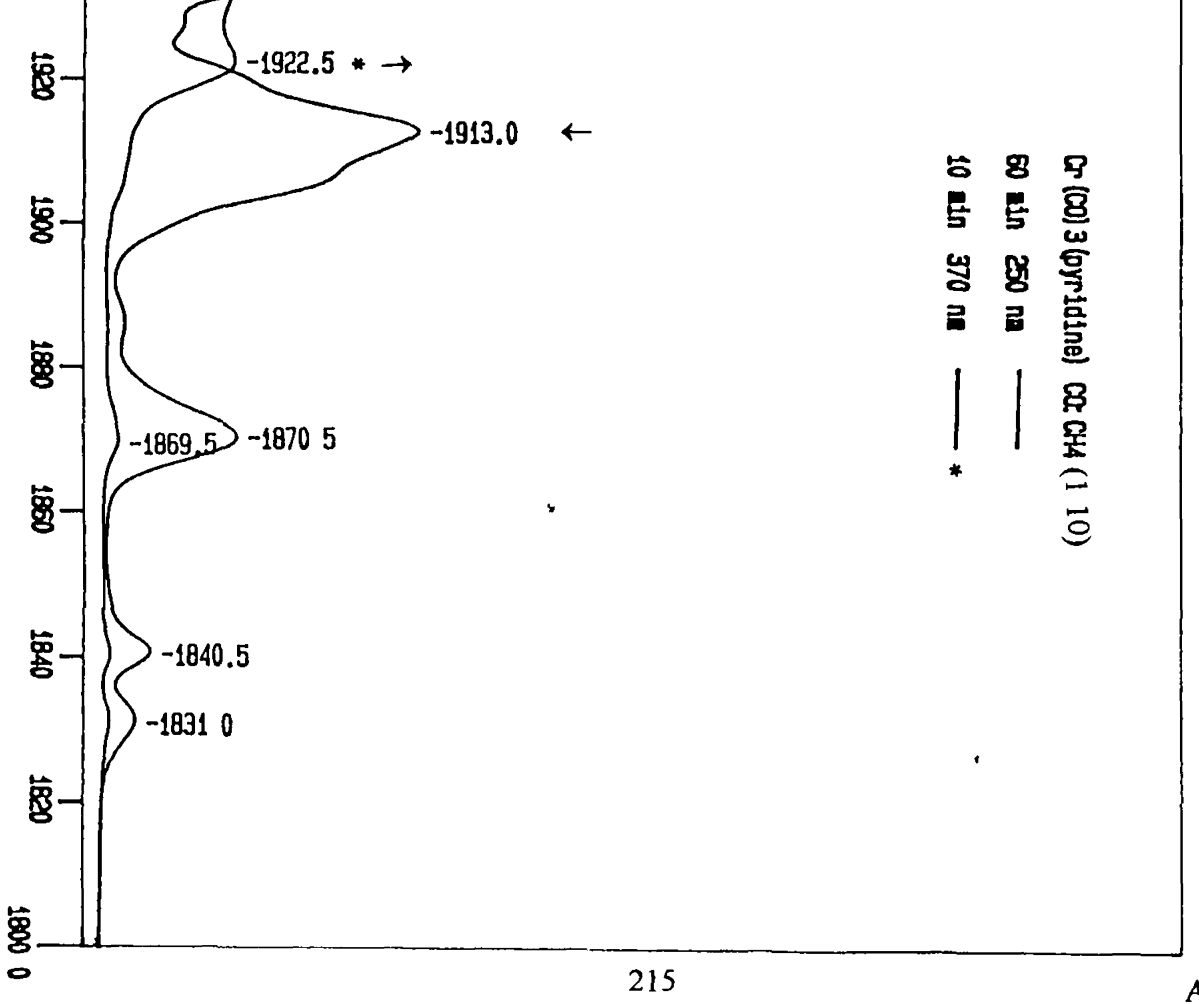

Appendix 2B(iii)

APPENDIX 3

Crystal data, intensity measurements, and refinements for the three compounds

	L = pyridine	L = 2,6-dimethylpyridine	L = 2,6-bis(TMS)pyridine
Formula	$C_8H_5NO_3Cr$	$C_{10}H_9NO_3Cr$	$C_{14}H_{21}NO_3CrSi_2$
Crystal system	monoclinic	orthorhombic	monoclinic
Space group	$P2_1/c$	$Pna2_1$	$P2_1/n$
a,Å	10 752 (5)	13 0308 (13)	7 7088 (6)
b,Å	7 652 (5)	6 2875 (6)	23 0928 (9)
c,Å	11 110 (2)	12 7099 (10)	10 4365 (8)
β,°	111 80 (5)		97 312 (4)
Volume, Å^3	848 7 (7)	1041 3 (2)	1842 (2)
Z	4	4	4
Density, g cm^{-3} *	1 684	1 551	1 296
Abs coeff , mm^{-1}	1 28	1 082	0 758
Crystal size, mm	0 90 × 0 80 × 0 60	0 50 × 0 50 × 0 25	0 40 × 0 40 × 0 30
θ range, °	1 00-22 00	3 13-25 47	1 76-24 96
Index ranges h, k, l	-10→9,0→7,0→10	0→13,-7→7,0→14	0→8,0→23,-11→11
Reflections collected	1589	1790	3326
Independent reflections	791 (R_{int} = 0 046)	940 (R_{int} = 0 031)	3096 (R_{int} = 0 0177)
Refinement method	on F	full matrix on F^2	full matrix on F^2
Data, restraints, parameters	791, 0 , 118	940 ,1, 155	3096, 0 , 203
Goodness-of-fit on F^2		0 907	1 082
Final R indices [I >2σ(I)]		R_1 = 0 024 , wR^2 = 0 060	R_1 = 0 032 , wR^2 = 0 078
R indices (all data)	R = 0 044 , wR = 0 061	R_1 = 0 055 , wR^2 = 0 076	R_1 = 0 074 , wR^2 = 0 092
Max diff peak, hole, eÅ^3	0 38 , -0 28	0 302 , -0 253	0 308 , -0 229

(Crystal data, intensity measurements, and refinements for (η^6-L)Cr(CO)$_3$ compounds
** = calculated value)*

Structural parameters for

(η^6-2,6-dimethylpyridine)$Cr(CO)_3$

Table 1a Atomic coordinates (x 10^4) and equivalent isotropic displacement parameters (A^2 x 10^3) for $C_{10}H_9CrNO_3$ U(eq) is defined as one third of the trace of the orthogonalized Uij tensor

	x	y	z	U(eq)
Cr(1)	7418(1)	1403(1)	2839(5)	28(1)
N(1)	8652(3)	-1031(6)	2811(16)	36(1)
O(1)	5959(11)	-471(23)	1269(8)	66(4)
O(2)	6171(4)	5429(7)	2759(22)	82(2)
O(3)	5951(9)	-309(21)	4419(8)	54(3)
C(2)	8723(13)	109(28)	1924(9)	39(4)
C(3)	8808(18)	2265(29)	1923(12)	40(4)
C(4)	8844(4)	3395(9)	2787(20)	42(2)
C(5)	8830(15)	2287(30)	3769(12)	40(4)
C(6)	8699(13)	26(20)	3723(10)	35(3)
C(7)	8654(21)	-1261(32)	963(16)	75(6)
C(8)	8733(18)	-1228(24)	4689(13)	51(4)
C(9)	6492(13)	308(27)	1870(11)	38(4)
C(10)	6654(4)	3877(8)	2830(22)	47(2)
C(11)	6551(13)	310(28)	3818(10)	37(4)

Table 2a Bond lengths [A] and angles [deg] for $C_{10}H_9CrNO_3$

Cr(1)-C(11)	1 82(2)
Cr(1)-C(10)	1 847(5)
Cr(1)-C(9)	1 86(2)
Cr(1)-C(6)	2 191(14)
Cr(1)-C(2)	2 21(2)
Cr(1)-N(1)	2 220(4)
Cr(1)-C(4)	2 242(5)
Cr(1)-C(5)	2 26(2)
Cr(1)-C(3)	2 22(2)
N(1)-C(6)	1 34(2)
N(1)-C(2)	1 34(2)
O(1)-C(9)	1 14(2)
O(2)-C(10)	1 165(7)
O(3)-C(11)	1 16(2)
C(2)-C(3)	1 36(3)
C(2)-C(7)	1 50(2)
C(3)-C(4)	1 31(3)
C(4)-C(5)	1 43(3)
C(5)-C(6)	1 43(2)
C(6)-C(8)	1 46(2)
C(11)-Cr(1)-C(10)	89 3(8)
C(11)-Cr(1)-C(9)	84 8(2)
C(10)-Cr(1)-C(9)	87 6(8)
C(11)-Cr(1)-C(6)	88 4(7)
C(10)-Cr(1)-C(6)	138 3(8)
C(9)-Cr(1)-C(6)	133 6(6)
C(11)-Cr(1)-C(2)	134 3(7)
C(10)-Cr(1)-C(2)	136 1(8)
C(9)-Cr(1)-C(2)	90 8(7)
C(6)-Cr(1)-C(2)	62 6(2)
C(11)-Cr(1)-N(1)	101 6(7)
C(10)-Cr(1)-N(1)	166 1(2)
C(9)-Cr(1)-N(1)	101 8(6)
C(6)-Cr(1)-N(1)	35 3(6)
C(2)-Cr(1)-N(1)	35 2(6)
C(11)-Cr(1)-C(4)	138 3(8)
C(10)-Cr(1)-C(4)	88 6(2)
C(9)-Cr(1)-C(4)	136 6(8)
C(6)-Cr(1)-C(4)	66 7(5)
C(2)-Cr(1)-C(4)	63 5(6)
N(1)-Cr(1)-C(4)	77 5(2)
C(11)-Cr(1)-C(5)	104 0(7)
C(10)-Cr(1)-C(5)	103 6(7)
C(9)-Cr(1)-C(5)	165 7(7)
C(6)-Cr(1)-C(5)	37 5(6)
C(2)-Cr(1)-C(5)	74 9(5)
N(1)-Cr(1)-C(5)	65 6(5)
C(4)-Cr(1)-C(5)	37 1(8)
C(11)-Cr(1)-C(3)	163 6(7)
C(10)-Cr(1)-C(3)	103 3(7)
C(9)-Cr(1)-C(3)	105 9(6)
C(6)-Cr(1)-C(3)	75 2(6)
C(2)-Cr(1)-C(3)	35 7(7)
N(1)-Cr(1)-C(3)	64 5(6)
C(4)-Cr(1)-C(3)	34 1(8)
C(5)-Cr(1)-C(3)	63 2(2)
C(6)-N(1)-C(2)	117 4(5)
C(6)-N(1)-Cr(1)	71 1(7)
C(2)-N(1)-Cr(1)	72 2(7)

C(3)-C(2)-N(1)	122 7(12)
C(3)-C(2)-C(7)	125 3(13)
N(1)-C(2)-C(7)	112 0(14)
C(3)-C(2)-Cr(1)	72 3(10)
N(1)-C(2)-Cr(1)	72 6(7)
C(7)-C(2)-Cr(1)	126 4(14)
C(4)-C(3)-C(2)	122 9(12)
C(4)-C(3)-Cr(1)	73 9(9)
C(2)-C(3)-Cr(1)	71 9(10)
C(3)-C(4)-C(5)	117 9(5)
C(3)-C(4)-Cr(1)	72 0(10)
C(5)-C(4)-Cr(1)	72 0(9)
C(4)-C(5)-C(6)	116 8(11)
C(4)-C(5)-Cr(1)	70 9(8)
C(6)-C(5)-Cr(1)	68 7(8)
N(1)-C(6)-C(5)	122 2(10)
N(1)-C(6)-C(8)	117 5(10)
C(5)-C(6)-C(8)	119 9(11)
N(1)-C(6)-Cr(1)	73 5(7)
C(5)-C(6)-Cr(1)	73 7(8)
C(8)-C(6)-Cr(1)	132 0(14)
O(1)-C(9)-Cr(1)	176(2)
O(2)-C(10)-Cr(1)	176(3)
O(3)-C(11)-Cr(1)	176(2)

Symmetry transformations used to generate equivalent atoms

Table 3a Anisotropic displacement parameters (A^2 x 10^3) for $C_{10}H_9CrNO_3$
The anisotropic displacement factor exponent takes the form
$-2\ pi^2\ [\ h^2\ a^{*2}\ U11 +\quad +\ 2\ h\ k\ a^*\ b^*\ U12\ ]$

	U11	U22	U33	U23	U13	U12
Cr(1)	31(1)	24(1)	28(1)	1(2)	1(2)	0(1)
N(1)	35(2)	29(2)	43(3)	-15(6)	-12(9)	5(2)
O(1)	78(9)	76(8)	44(6)	-13(6)	-27(6)	-23(7)
O(2)	62(3)	38(2)	146(7)	5(9)	-2(10)	14(2)
O(3)	49(6)	68(6)	45(6)	2(6)	5(5)	-6(5)
C(2)	26(6)	68(9)	23(7)	4(6)	4(6)	2(7)
C(3)	52(11)	42(9)	25(8)	10(7)	3(8)	1(9)
C(4)	35(3)	35(3)	56(5)	21(8)	14(8)	-4(2)
C(5)	29(8)	40(9)	50(9)	-10(8)	-14(8)	-5(8)
C(6)	41(7)	19(5)	44(8)	11(5)	-1(7)	8(6)
C(7)	66(11)	94(13)	65(11)	-48(8)	12(9)	23(9)
C(8)	68(10)	48(8)	38(7)	1(5)	0(7)	2(7)
C(9)	26(8)	38(9)	50(8)	10(7)	3(6)	0(6)
C(10)	39(3)	33(3)	69(4)	15(10)	-3(11)	0(2)
C(11)	48(10)	42(9)	20(6)	0(6)	1(7)	-2(7)

Table 4a Hydrogen coordinates (x 10^4) and isotropic displacement parameters (A^2 x 10^3) for $C_{10}H_9CrNO_3$

	x	y	z	U(eq)
H(3)	8841(47)	2851(113)	1355(62)	4(14)
H(4)	8983(81)	4678(195)	2556(147)	171(63)
H(5)	8823(99)	3147(191)	4513(106)	92(55)
H(7A)	9132(81)	-2408(150)	872(113)	82(23)
H(7B)	8702(102)	-306(196)	376(89)	82(23)
H(7C)	7970(45)	-1821(198)	1005(111)	82(23)
H(8A)	8496(102)	-2630(102)	4516(117)	82(23)
H(8B)	8325(90)	-662(222)	5252(74)	82(23)
H(8C)	9439(32)	-1295(229)	4905(95)	82(23)

Observed and calculated structural factors for

(η^6-2,6-dimethylpyridine)$Cr(CO)_3$

Appendix 3

Table 5a Observed and calculated structure factors

Page 1

h	k	l	10Fo	10Fc	10s	h	k	l	10Fo	10Fc	10s	h	k	l	10Fo	10Fc	10s
2	0	0	881	923	3	12	0	1	168	166	3	4	1	2	243	236	1
4	0	0	1421	1543	4	0	1	1	943	990	22	5	1	2	338	337	4
6	0	0	586	604	4	1	1	1	1029	1081	20	6	1	2	276	284	4
8	0	0	1073	1109	7	2	1	1	679	664	7	7	1	2	168	169	1
10	0	0	317	313	3	3	1	1	87	97	2	8	1	2	32	44	31
12	0	0	0	53	1	4	1	1	372	366	5	9	1	2	0	32	1
1	1	0	164	166	1	5	1	1	116	126	1	10	1	2	0	32	1
2	1	0	73	65	2	6	1	1	415	426	5	11	1	2	113	108	5
3	1	0	339	338	3	7	1	1	415	415	3	12	1	2	167	163	2
4	1	0	467	453	4	8	1	1	381	378	2	13	1	2	120	114	4
5	1	0	151	142	2	9	1	1	367	370	2	0	2	2	41	41	3
6	1	0	351	321	2	10	1	1	199	193	2	1	2	2	707	714	6
7	1	0	476	463	3	11	1	1	193	188	2	2	2	2	45	48	11
8	1	0	120	109	2	12	1	1	149	147	4	3	2	2	548	554	2
9	1	0	22	16	22	13	1	1	49	45	21	4	2	2	232	224	1
10	1	0	0	26	1	1	2	1	282	269	2	5	2	2	580	591	5
11	1	0	87	91	4	2	2	1	605	587	11	6	2	2	230	225	2
12	1	0	248	248	2	3	2	1	341	323	2	7	2	2	498	506	4
13	1	0	202	197	2	4	2	1	110	109	1	8	2	2	0	34	1
0	2	0	713	702	3	5	2	1	0	27	1	9	2	2	307	304	2
1	2	0	229	237	1	6	2	1	234	239	1	10	2	2	47	39	17

for C9H10CrNO3

h	k	l	10Fo	10Fc	10s	h	k	l	10Fo	10Fc	10s
10	1	3	194	189	2	3	2	4	618	623	3
11	1	3	212	207	2	4	2	4	42	46	30
12	1	3	179	178	3	5	2	4	714	719	4
13	1	3	49	54	13	6	2	4	92	98	2
1	2	3	198	190	2	7	2	4	428	432	6
2	2	3	278	265	2	8	2	4	0	29	1
3	2	3	108	99	1	9	2	4	182	177	2
4	2	3	90	87	2	10	2	4	89	87	9
5	2	3	113	112	2	11	2	4	194	190	2
6	2	3	0	34	1	12	2	4	84	90	27
7	2	3	173	169	1	13	2	4	180	179	3
8	2	3	93	94	3	1	3	4	210	215	1
9	2	3	300	301	2	2	3	4	68	67	3
10	2	3	0	26	1	3	3	4	142	146	2
11	2	3	144	148	2	4	3	4	48	53	5
12	2	3	0	44	1	5	3	4	62	64	4
13	2	3	72	71	5	6	3	4	99	93	3
0	3	3	411	418	2	7	3	4	134	135	2
1	3	3	557	555	7	8	3	4	0	54	1
2	3	3	225	229	1	9	3	4	172	178	2
3	3	3	313	312	2	10	3	4	0	9	1

Appendix 3

h	k	l	10Fo	10Fc	10s	h	k	l	10Fo	10Fc	10s	h	k	l	10Fo
2	2	0	154	152	2	7	2	1	12	17	11	11	2	2	195
3	2	0	1040	1030	3	8	2	1	0	51	1	12	2	2	66
4	2	0	677	634	8	9	2	1	252	246	2	13	2	2	152
5	2	0	783	784	4	10	2	1	45	35	17	1	3	2	242
6	2	0	101	105	2	11	2	1	266	267	3	2	3	2	166
7	2	0	321	332	2	12	2	1	84	82	4	3	3	2	137
8	2	0	45	25	17	13	2	1	101	104	4	4	3	2	120
9	2	0	279	278	2	0	3	1	61	45	13	5	3	2	126
10	2	0	5	5	5	1	3	1	312	324	6	6	3	2	40
11	2	0	256	259	2	2	3	1	390	389	2	7	3	2	127
12	2	0	7	5	7	3	3	1	604	617	6	8	3	2	0
13	2	0	173	168	2	4	3	1	558	539	3	9	3	2	265
1	3	0	145	140	1	5	3	1	558	549	3	10	3	2	27
2	3	0	325	314	4	6	3	1	31	41	31	11	3	2	126
3	3	0	0	54	1	7	3	1	339	338	2	12	3	2	82
4	3	0	276	281	1	8	3	1	0	36	1	13	3	2	25
5	3	0	94	90	2	9	3	1	220	218	2	0	4	2	408
6	3	0	111	91	2	10	3	1	201	205	2	1	4	2	85
7	3	0	122	122	5	11	3	1	148	148	2	2	4	2	449
8	3	0	122	121	6	12	3	1	194	194	4	3	4	2	277
9	3	0	253	254	2	13	3	1	133	133	3	4	4	2	435
10	3	0	140	133	6	1	4	1	44	52	8	5	4	2	175

10Fc	10s	h	k	l	10Fo	10Fc	10s	h	k	l	10Fo	10Fc	10s
195	2	4	3	3	161	167	1	11	3	4	62	70	62
64	5	5	3	3	431	441	3	12	3	4	65	64	25
152	3	6	3	3	257	252	1	13	3	4	81	87	5
234	1	7	3	3	392	387	2	0	4	4	772	775	5
164	1	8	3	3	133	124	2	1	4	4	132	137	2
142	1	9	3	3	186	187	2	2	4	4	430	423	2
115	2	10	3	3	56	61	25	3	4	4	271	272	3
125	2	11	3	3	189	190	2	4	4	4	88	82	3
35	10	12	3	3	122	121	3	5	4	4	75	70	4
124	2	13	3	3	153	141	5	6	4	4	220	215	1
21	1	1	4	3	121	122	2	7	4	4	0	35	1
272	1	2	4	3	99	96	2	8	4	4	343	342	2
38	27	3	4	3	0	28	1	9	4	4	144	145	5
130	4	4	4	3	77	87	5	10	4	4	242	241	2
75	4	5	4	3	156	157	3	11	4	4	140	142	8
48	25	6	4	3	134	145	2	12	4	4	104	103	4
418	2	7	4	3	40	37	12	1	5	4	98	92	5
88	2	8	4	3	93	91	3	2	5	4	0	13	1
442	3	9	4	3	30	10	30	3	5	4	105	108	5
282	1	10	4	3	0	39	1	4	5	4	138	143	3
422	6	11	4	3	35	47	22	5	5	4	80	79	4
178	2	12	4	3	106	103	4	6	5	4	113	115	3

Appendix 3

h	k	l	10Fo	10Fc	10s	h	k	l	10Fo	10Fc	10s	h	k	l	10Fo
11	3	0	163	165	2	2	4	1	0	37	1	6	4	2	292
12	3	0	132	133	3	3	4	1	79	84	23	7	4	2	6
13	3	0	0	8	1	4	4	1	121	123	2	8	4	2	183
0	4	0	223	244	1	5	4	1	63	55	19	9	4	2	83
1	4	0	160	165	1	6	4	1	125	125	2	10	4	2	210
2	4	0	497	501	3	7	4	1	156	152	3	11	4	2	112
3	4	0	124	116	2	8	4	1	104	105	3	12	4	2	190
4	4	0	551	548	4	9	4	1	38	50	37	1	5	2	13
5	4	0	217	221	1	10	4	1	124	123	3	2	5	2	29
6	4	0	233	227	1	11	4	1	37	20	19	3	5	2	0
7	4	0	167	163	3	12	4	1	73	81	15	4	5	2	72
8	4	0	188	189	2	0	5	1	380	379	2	5	5	2	15
9	4	0	0	24	1	1	5	1	0	24	1	6	5	2	82
10	4	0	243	241	2	2	5	1	309	308	2	7	5	2	41
11	4	0	45	47	9	3	5	1	139	139	3	8	5	2	90
12	4	0	169	168	2	4	5	1	306	304	2	9	5	2	90
1	5	0	0	54	1	5	5	1	169	165	2	10	5	2	94
2	5	0	215	216	5	6	5	1	340	341	2	11	5	2	0
3	5	0	76	67	4	7	5	1	104	102	3	0	6	2	153
4	5	0	15	16	14	8	5	1	202	206	2	1	6	2	121
5	5	0	0	9	1	9	5	1	0	38	1	2	6	2	136
6	5	0	0	23	1	10	5	1	112	106	4	3	6	2	303

10Fc	10s	h	k	l	10Fo	10Fc	10s	h	k	l	10Fo	10Fc	10s
292	2	0	5	3	447	444	3	7	5	4	127	122	3
30	6	1	5	3	148	147	3	8	5	4	0	2	1
189	3	2	5	3	363	359	2	9	5	4	0	26	1
90	19	3	5	3	33	46	33	10	5	4	0	49	1
204	2	4	5	3	197	199	2	0	6	4	84	85	21
109	3	5	5	3	83	87	10	1	6	4	192	191	2
188	3	6	5	3	201	199	2	2	6	4	115	113	3
14	12	7	5	3	136	134	7	3	6	4	233	234	2
33	28	8	5	3	284	281	2	4	6	4	167	166	2
32	1	9	5	3	77	68	25	5	6	4	186	183	4
72	4	10	5	3	186	186	2	6	6	4	164	168	2
40	15	1	6	3	68	74	17	7	6	4	147	146	3
85	4	2	6	3	23	27	23	8	6	4	85	82	62
68	41	3	6	3	0	21	1	1	7	4	22	34	22
93	5	4	6	3	27	33	26	2	7	4	118	116	3
90	4	5	6	3	107	114	3	3	7	4	61	50	24
98	4	6	6	3	47	45	34	2	0	5	69	90	3
30	1	7	6	3	61	59	7	4	0	5	0	18	1
155	2	8	6	3	0	37	1	6	0	5	78	86	4
121	3	0	7	3	25	34	24	8	0	5	313	318	3
136	2	1	7	3	183	180	2	10	0	5	200	203	3
300	4	2	7	3	43	43	42	12	0	5	38	26	17

Appendix 3

h	k	l	10Fo	10Fc	10s	h	k	l	10Fo	10Fc	10s	h	k
7	5	0	56	63	13	11	5	1	36	25	13	4	6
8	5	0	178	182	2	1	6	1	37	34	9	5	6
9	5	0	109	112	3	2	6	1	0	2	1	6	6
10	5	0	145	148	3	3	6	1	19	16	19	7	6
11	5	0	22	37	22	4	6	1	0	19	1	8	6
0	6	0	188	190	2	5	6	1	23	24	23	1	7
1	6	0	63	58	5	6	6	1	62	55	5	2	7
2	6	0	138	144	2	7	6	1	89	83	10	3	7
3	6	0	329	325	2	8	6	1	53	49	11	4	7
4	6	0	111	114	3	0	7	1	0	14	1	2	0
5	6	0	393	387	3	1	7	1	221	222	2	4	0
6	6	0	128	128	4	2	7	1	0	14	1	6	0
7	6	0	140	140	4	3	7	1	211	209	2	8	0
8	6	0	105	108	3	4	7	1	22	43	21	10	0
9	6	0	0	24	1	5	7	1	165	163	2	12	0
1	7	0	0	18	1	0	0	2	1735	1657	13	0	1
2	7	0	80	93	8	2	0	2	966	987	4	1	1
3	7	0	23	26	22	4	0	2	199	185	2	2	1
4	7	0	24	24	24	6	0	2	379	386	3	3	1
5	7	0	0	32	1	8	0	2	665	655	5	4	1
2	0	1	246	253	2	10	0	2	359	366	3	5	1
4	0	1	242	238	2	12	0	2	135	137	3	6	1
6	0	1	560	545	4	1	1	2	308	297	3	7	1

l	10Fo	10Fc	10s	h	k	l	10Fo	10Fc	10s	h	k	l	10Fo	10Fc	10s
2	128	130	3	3	7	3	218	215	2	0	1	5	0	68	1
2	282	277	1	4	7	3	25	23	25	1	1	5	79	107	2
2	142	141	3	0	0	4	489	491	3	2	1	5	480	491	3
2	138	135	3	2	0	4	808	824	5	3	1	5	521	514	3
2	113	113	4	4	0	4	768	801	5	4	1	5	757	751	4
2	53	38	10	6	0	4	374	381	3	5	1	5	581	573	4
2	42	56	42	8	0	4	359	353	3	6	1	5	355	350	2
2	57	54	17	10	0	4	306	302	3	7	1	5	259	266	3
2	0	19	1	12	0	4	193	193	3	8	1	5	91	88	3
3	34	49	8	1	1	4	428	425	3	9	1	5	98	94	3
3	468	454	4	2	1	4	324	312	2	10	1	5	180	181	2
3	206	185	2	3	1	4	286	283	2	11	1	5	109	112	7
3	0	10	1	4	1	4	117	117	1	12	1	5	238	233	2
3	211	208	2	5	1	4	232	235	1	13	1	5	114	113	4
3	184	182	3	6	1	4	0	26	1	1	2	5	311	288	2
3	957	965	10	7	1	4	159	164	2	2	2	5	29	24	11
3	232	220	3	8	1	4	117	114	2	3	2	5	252	241	2
3	580	586	6	9	1	4	167	167	2	4	2	5	115	115	3
3	1125	1118	24	10	1	4	143	139	2	5	2	5	138	134	2
3	351	351	2	11	1	4	137	134	3	6	2	5	48	52	10
3	581	562	3	12	1	4	113	111	3	7	2	5	0	33	1
3	412	421	2	13	1	4	0	27	1	8	2	5	63	67	36
3	13	32	13	0	2	4	272	275	3	9	2	5	301	302	2

Appendix 3

h	k	l	10Fo	10Fc	10s	h	k	l	10Fo	10Fc	10s	h	k
8	0	1	156	157	2	2	1	2	197	208	2	8	1
10	0	1	137	137	3	3	1	2	144	150	1	9	1

l	10Fo	10Fc	10s	h	k	l	10Fo	10Fc	10s	h	k	l	10Fo	10Fc	10s
3	298	303	3	1	2	4	364	381	2	10	2	5	0	8	1
3	257	263	1	2	2	4	106	98	1	11	2	5	211	218	3

Table 5a Observed and calculated structure factors for C9H10CrNO3
Page 2

h	k	l	10Fo	10Fc	10s	h	k	l	10Fo	10Fc	10s	h	k	l	10Fo	10Fc	10s	h	k	l	10Fo	10Fc	10s	h	k	l	10Fo	10Fc	10s
12	2	5	64	66	15	10	3	6	47	30	11	4	5	7	105	107	3	7	1	9	81	86	4	8	4	10	102	109	7
13	2	5	0	33	1	11	3	6	80	82	5	5	5	7	0	13	1	8	1	9	240	238	2	1	5	10	0	17	1
0	3	5	72	80	3	12	3	6	89	91	5	6	5	7	232	229	2	9	1	9	246	249	2	2	5	10	0	19	1
1	3	5	616	612	4	0	4	6	680	675	4	7	5	7	120	127	3	10	1	9	120	120	3	3	5	10	3	36	3
2	3	5	217	214	1	1	4	6	187	186	2	8	5	7	217	219	2	11	1	9	147	149	3	4	5	10	57	48	8
3	3	5	317	325	2	2	4	6	407	406	2	1	6	7	28	30	27	12	1	9	88	85	28	5	5	10	39	26	16
4	3	5	345	341	2	3	4	6	112	109	3	2	6	7	18	14	18	1	2	9	79	87	30	2	0	11	178	179	3
5	3	5	153	158	3	4	4	6	30	21	30	3	6	7	0	35	1	2	2	9	14	32	13	4	0	11	133	138	3
6	3	5	215	213	1	5	4	6	82	84	5	4	6	7	32	25	25	3	2	9	100	91	3	6	0	11	257	260	2
7	3	5	273	265	2	6	4	6	130	129	8	5	6	7	0	32	1	4	2	9	63	65	63	8	0	11	33	19	33
8	3	5	0	54	1	7	4	6	60	61	5	0	0	8	566	567	5	5	2	9	43	26	11	10	0	11	41	64	41
9	3	5	361	361	2	8	4	6	393	389	5	2	0	8	490	484	5	6	2	9	0	14	1	0	1	11	297	301	5
10	3	5	23	47	22	9	4	6	78	75	4	4	0	8	360	362	3	7	2	9	79	77	6	1	1	11	350	346	2
11	3	5	201	208	2	10	4	6	240	240	3	6	0	8	301	295	3	8	2	9	78	91	4	2	1	11	221	218	3
12	3	5	107	105	28	11	4	6	108	108	4	8	0	8	266	261	2	9	2	9	132	139	3	3	1	11	83	87	3
1	4	5	78	73	3	1	5	6	144	147	2	10	0	8	236	240	3	10	2	9	0	16	1	4	1	11	164	158	2
2	4	5	238	246	1	2	5	6	110	114	3	12	0	8	170	171	4	11	2	9	109	109	4	5	1	11	21	18	21
3	4	5	98	103	3	3	5	6	112	116	3	1	1	8	0	21	1	0	3	9	210	209	2	6	1	11	198	202	5
4	4	5	156	155	2	4	5	6	79	85	4	2	1	8	29	28	13	1	3	9	243	239	3	7	1	11	186	181	3
5	4	5	11	30	10	5	5	6	137	136	2	3	1	8	16	28	15	2	3	9	154	153	2	8	1	11	172	164	4
6	4	5	336	337	2	6	5	6	45	53	8	4	1	8	108	103	2	3	3	9	244	242	1	9	1	11	238	237	3
7	4	5	0	16	1	7	5	6	98	98	3	5	1	8	0	43	1	4	3	9	121	122	2	10	1	11	82	81	5
8	4	5	0	28	1	8	5	6	0	34	1	6	1	8	131	130	2	5	3	9	328	328	2	1	2	11	89	98	3

Appendix 3

h	k	l	10Fo	10Fc	10s	h	k	l	10Fo	10Fc	10s	h	k	l	10Fo	10Fc	10s
9	4	5	0	24	1	9	5	6	0	44	1	7	1	8	76	85	4
10	4	5	86	93	18	0	6	6	91	89	4	8	1	8	19	59	19
1_	4	5	0	30	1	1	6	6	198	201	2	9	1	8	9_	92	3
0	5	5	509	511	3	2	6	6	94	95	3	10	1	8	0	53	1
_	5	5	262	261	1	3	6	6	163	156	2	11	1	8	85	83	4
2	5	5	304	300	2	4	6	6	142	145	2	12	1	8	82	91	19
3	5	5	60	66	5	5	6	6	182	179	2	0	2	8	0	33	1
4	5	5	103	102	3	6	6	6	160	157	2	1	2	8	38_	387	2
5	5	5	74	77	6	2	0	7	378	387	3	2	2	8	76	68	3
6	5	5	225	225	3	4	0	7	44	46	7	3	2	8	383	384	2
7	5	5	182	178	4	6	0	7	2_	28	21	4	2	8	93	87	3
8	5	5	276	277	2	8	0	7	248	252	2	5	2	8	355	347	2
9	5	5	161	173	3	10	0	7	126	130	4	6	2	8	84	83	18
10	5	5	130	134	3	12	0	7	43	56	16	7	2	8	292	299	2
1	6	5	0	21	1	0	1	7	310	312	4	8	2	8	68	68	4
2	6	5	12	35	11	1	1	7	187	203	1	9	2	8	224	227	2
3	6	5	0	63	1	2	1	7	41_	416	10	10	2	8	20	17	19
4	6	5	0	12	1	3	1	7	29_	294	7	11	2	8	142	142	5
5	6	5	45	59	17	4	1	7	44_	436	3	12	2	8	0	24	1
6	6	5	9	35	9	5	1	7	464	460	3	1	3	8	37	66	36
7	6	5	0	12	1	6	1	7	245	245	1	2	3	8	33	17	10
0	7	5	0	40	1	7	1	7	246	247	1	3	3	8	64	64	5
_	7	5	176	171	2	8	1	7	173	167	4	4	3	8	92	91	3
2	7	5	0	40	1	9	1	7	0	44	1	5	3	8	17	32	17

h	k	l	10Fo	10Fc	10s	h	k	l	10Fo	10Fc	10s
6	3	9	120	123	3	2	2	11	59	65	15
7	3	9	239	240	3	3	2	11	116	115	2
8	3	9	76	74	44	4	2	11	35	29	9
9	3	9	93	91	4	5	2	11	0	18	1
10	3	9	59	60	25	6	2	11	58	50	23
1	4	9	83	80	3	7	2	11	0	24	1
2	4	9	35	51	25	8	2	11	0	39	1
3	4	9	59	62	23	9	2	11	102	104	4
4	4	9	0	19	1	0	3	11	77	81	4
5	4	9	85	84	4	1	3	11	170	169	2
6	4	9	38	61	16	2	3	11	138	131	4
7	4	9	70	73	5	3	3	11	235	227	2
8	4	9	107	105	3	4	3	11	164	173	2
9	4	9	0	13	1	5	3	11	249	250	2
0	5	9	186	186	3	6	3	11	0	65	1
1	5	9	0	36	1	7	3	11	156	163	3
2	5	9	208	209	2	8	3	11	32	16	32
3	5	9	75	69	8	1	4	11	0	42	1
4	5	9	213	215	2	2	4	11	0	11	1
5	5	9	102	107	4	3	4	11	35	31	18
6	5	9	175	175	2	4	4	11	32	23	14
1	6	9	0	20	1	5	4	11	23	43	23
0	0	-0	697	705	5	6	4	11	67	58	10
2	0	-0	449	449	4	0	5	11	101	95	3

Appendix 3

h	k	l	10Fo	10Fc	10s	h	k	l	10Fo	10Fc	10s	h	k	l	10Fo	10Fc	10s
0	0	6	957	940	5	10	1	7	187	188	2	6	3	8	4_	58	41
2	0	6	463	479	4	11	1	7	137	132	5	7	3	8	87	87	4
4	0	6	342	358	3	12	1	7	151	153	3	8	3	8	0	12	1
6	0	6	612	614	5	13	1	7	126	121	3	9	3	8	145	148	2
8	0	6	319	317	3	1	2	7	0	23	1	10	3	8	0	26	1
10	0	6	126	133	4	2	2	7	154	163	1	11	3	8	84	77	5
12	0	6	231	228	3	3	2	7	77	70	3	0	4	8	345	334	2
_	1	6	144	129	1	4	2	7	122	119	2	1	4	8	112	114	3
2	1	6	264	243	3	5	2	7	30	40	30	2	4	8	284	283	1
3	1	6	74	79	2	6	2	7	91	93	24	3	4	8	128	131	2
4	1	6	153	154	3	7	2	7	74	72	4	4	4	8	214	214	3
5	1	6	171	161	4	8	2	7	50	58	10	5	4	8	92	96	3
6	1	6	30	20	9	9	2	7	196	197	4	6	4	8	21_	212	2
7	1	6	253	250	2	10	2	7	0	23	1	7	4	8	0	41	1
8	1	6	48	57	7	11	2	7	156	164	2	8	4	8	187	189	2
9	1	6	259	256	2	12	2	7	0	46	1	9	4	8	14	68	14
10	1	6	169	169	2	0	3	7	124	125	2	10	4	8	127	128	3
1_	1	6	14	21	14	1	3	7	362	360	2	1	5	8	0	21	1
12	1	6	108	111	3	2	3	7	224	220	2	2	5	8	0	20	1
13	1	6	0	9	1	3	3	7	380	378	2	3	5	8	29	38	29
0	2	6	35	36	5	4	3	7	224	224	4	4	5	8	52	49	22
1	2	6	115	139	4	5	3	7	2_5	209	3	5	5	8	19	4	19
2	2	6	243	236	1	6	3	7	102	100	3	6	5	8	106	102	7
3	2	6	780	761	5	7	3	7	2_8	215	2	7	5	8	45	55	35
4	2	6	141	136	2	8	3	7	96	103	3	8	5	8	60	57	7
5	2	6	674	658	6	9	3	7	277	278	2	0	6	8	92	100	4

h	k	l	10Fo	10Fc	10s	h	k	l	10Fo	10Fc	10s
4	0	-0	43	52	12	1	5	11	0	12	1
6	0	-0	81	87	6	2	5	11	158	161	4
8	0	-0	419	417	4	3	5	11	84	80	5
10	0	-0	288	283	3	0	0	12	601	602	6
1	1	-0	156	163	4	2	0	12	264	261	2
2	1	-0	0	43	1	4	0	12	0	45	1
3	1	-0	20	52	19	6	0	12	219	214	3
4	1	-0	82	88	25	8	0	12	307	313	3
5	1	-0	207	213	2	1	1	12	0	26	1
6	1	-0	83	91	28	2	1	12	27	25	27
7	1	-0	0	68	1	3	1	12	18	23	17
8	1	-0	0	22	1	4	1	12	74	82	4
9	1	-0	28	33	27	5	1	12	0	27	1
10	1	-0	14	26	14	6	1	12	89	93	12
11	1	-0	48	49	17	7	1	12	90	98	9
0	2	-0	44	49	44	8	1	12	32	4	31
1	2	-0	294	288	2	9	1	12	55	42	24
2	2	-0	30	17	30	0	2	12	34	43	34
3	2	-0	291	287	2	1	2	12	193	189	2
4	2	-0	91	91	3	2	2	12	33	41	18
5	2	-0	313	317	3	3	2	12	270	268	2
6	2	-0	191	191	2	4	2	12	97	106	3
7	2	-0	235	240	2	5	2	12	240	239	4
8	2	-0	19	10	18	6	2	12	43	51	42
9	2	-0	128	131	3	7	2	12	147	143	3
10	2	-0	64	80	6	8	2	12	30	33	18

Appendix 3

h	k	l	10Fo	10Fc	10s	h	k	l	10Fo	10Fc	10s	h	k	l	10Fo	10Fc	10s
6	2	6	167	163	2	10	3	7	93	93	4	1	6	8	13_	127	3
7	2	6	216	217	1	11	3	7	146	147	3	2	6	8	98	94	8
8	2	6	60	66	5	12	3	7	67	68	11	3	6	8	17_	173	4
9	2	6	162	165	2	1	4	7	105	94	3	4	6	8	114	103	3
10	2	6	199	200	2	2	4	7	115	118	2	2	0	9	113	113	3
1_	2	6	216	220	2	3	4	7	64	69	20	4	0	9	224	226	2
12	2	6	7	17	6	4	4	7	134	138	3	6	0	9	23_	223	2
13	2	6	152	149	5	5	4	7	37	34	36	8	0	9	33	30	18
_	3	6	93	83	2	6	4	7	196	200	2	10	0	9	0	33	1
2	3	6	122	122	2	7	4	7	42	40	41	12	0	9	157	150	4
3	3	6	0	8	1	8	4	7	0	14	1	0	1	9	467	466	3
4	3	6	115	118	4	9	4	7	52	52	11	1	1	9	246	245	2
5	3	6	166	159	2	10	4	7	0	8	1	2	1	9	305	305	2
6	3	6	130	129	2	0	5	7	430	434	3	3	1	9	330	331	2
7	3	6	107	104	3	1	5	7	136	135	3	4	1	9	160	156	4
8	3	6	0	24	1	2	5	7	238	239	2	5	1	9	117	114	3
9	3	6	86	82	4	3	5	7	23	21	22	6	1	9	234	236	1

h	k	l	10Fo	10Fc	10s	h	k	l	10Fo	10Fc	10s
1	3	-0	30	38	29	1	3	12	0	19	1
2	3	-0	216	222	1	2	3	12	50	66	10
3	3	-0	29	30	13	3	3	12	0	21	1
4	3	-0	53	45	6	4	3	12	40	50	10
5	3	-0	0	25	1	5	3	12	19	45	19
6	3	-0	84	86	32	6	3	12	0	9	1
7	3	-0	135	134	3	7	3	12	48	43	47
8	3	-0	0	15	1	0	4	12	118	117	8
9	3	-0	134	139	7	1	4	12	73	70	5
0	4	-0	224	219	2	2	4	12	186	186	2
1	4	-0	62	54	5	3	4	12	63	59	6
2	4	-0	213	209	2	4	4	12	211	212	2
3	4	-0	125	124	3	5	4	12	77	74	5
4	4	-0	230	226	2	2	0	13	0	59	1
5	4	-0	78	83	5	4	0	13	13	16	12
6	4	10	203	198	4	6	0	13	86	93	6
7	4	-0	43	58	43	8	0	13	81	89	7

Table 5a. Observed and calculated structure factors for C9H10CrNO3
Page 3

h	k	l	10Fo	10Fc	10s	h	k	l	10Fo	10Fc	10s	h	k	l	10Fo	10Fc	10s	h	k	l	10Fo	10Fc	10s	h	k	l	10Fo	10Fc	10s
0	1	13	215	215	3	1	2	13	0	13	_	1	3	13	117	114	5	4	0	14	211	209	3	0	2	14	42	50	13
1	1	13	170	169	2	2	2	13	0	36	_	2	3	13	107	106	5	6	0	14	195	197	3	1	2	14	147	142	2
2	1	13	176	172	2	3	2	13	0	21	_	3	3	13	222	222	2	1	1	14	0	25	1	2	2	14	43	48	43
3	1	13	79	77	17	4	2	13	57	59	56	4	3	13	107	111	5	2	1	14	0	22	1	3	2	14	200	196	7
4	1	13	127	126	3	5	2	13	59	57	9	5	3	13	164	162	2	3	1	14	0	29	1	4	2	14	0	27	1
5	1	13	135	136	3	6	2	13	0	17	_	1	4	13	2	35	2	4	1	14	43	45	13	5	2	14	177	179	2
6	1	13	139	136	3	7	2	13	52	50	1_	0	0	14	176	183	3	5	1	14	0	17	1	1	3	14	0	45	1
7	1	13	150	149	3	0	3	13	64	61	3_	2	0	14	179	172	3	6	1	14	48	48	47	2	3	14	0	12	1

Structural parameters for

(η^6-2,6-bis(trimethylsilyl)pyridine)$Cr(CO)_3$

Table 1b Atomic coordinates (x 10^4) and equivalent isotropic displacement parameters (A^2 x 10^3) for $C_{14}H_{21}CrNO_3Si_2$ U(eq) is defined as one third of the trace of the orthogonalized U_{ij} tensor

	x	y	z	U(eq)
Cr(1)	2487(1)	1253(1)	330(1)	37(1)
Si(1)	1267(1)	2731(1)	1137(1)	40(1)
Si(2)	1739(1)	601(1)	3521(1)	45(1)
N(1)	1911(3)	1633(1)	2140(2)	35(1)
O(1)	1284(4)	1859(1)	-2156(2)	80(1)
O(2)	3895(4)	346(1)	-1308(3)	95(1)
O(3)	-1025(4)	684(1)	-135(3)	95(1)
C(2)	2651(3)	2051(1)	1458(2)	35(1)
C(3)	4298(4)	1956(1)	1029(3)	43(1)
C(4)	5165(4)	1435(1)	1267(3)	47(1)
C(5)	4405(4)	1012(1)	1987(3)	45(1)
C(6)	2796(4)	1113(1)	2437(2)	37(1)
C(9)	1762(4)	1631(1)	-1190(3)	51(1)
C(10)	3363(5)	691(2)	-671(3)	58(1)
C(11)	337(4)	889(2)	71(3)	55(1)
C(12)	2188(6)	3162(2)	-122(4)	83(1)
C(13)	1375(5)	3162(2)	2646(3)	66(1)
C(14)	-1011(4)	2496(2)	619(4)	73(1)
C(15)	2329(6)	874(2)	5192(3)	75(1)
C(16)	-671(5)	623(2)	3100(4)	72(1)
C(17)	2617(6)	-139(2)	3339(4)	83(1)

Table 2b Bond lengths [Å] and angles [°] for $C_{14}H_{21}CrNO_3Si_2$

Cr(1)-C(9)	1 835(3)
Cr(1)-C(10)	1 846(3)
Cr(1)-C(11)	1 846(3)
Cr(1)-N(1)	2 180(2)
Cr(1)-C(2)	2 183(3)
Cr(1)-C(5)	2 198(3)
Cr(1)-C(6)	2 205(3)
Cr(1)-C(3)	2 204(3)
Cr(1)-C(4)	2 209(3)
Si(1)-C(14)	1 851(3)
Si(1)-C(13)	1 856(3)
Si(1)-C(12)	1 859(4)
Si(1)-C(2)	1 904(3)
Si(2)-C(16)	1 854(4)
Si(2)-C(17)	1 857(3)
Si(2)-C(15)	1 856(3)
Si(2)-C(6)	1 890(3)
N(1)-C(2)	1 367(3)
N(1)-C(6)	1 397(3)
O(1)-C(9)	1 155(4)
O(2)-C(10)	1 146(4)
O(3)-C(11)	1 147(4)
C(2)-C(3)	1 416(4)
C(3)-C(4)	1 382(4)
C(4)-C(5)	1 405(4)
C(5)-C(6)	1 400(4)
C(9)-Cr(1)-C(10)	86 44(14)
C(9)-Cr(1)-C(11)	85 44(14)
C(10)-Cr(1)-C(11)	89 1(2)
C(9)-Cr(1)-N(1)	118 98(11)
C(10)-Cr(1)-N(1)	154 56(12)
C(11)-Cr(1)-N(1)	91 83(12)
C(9)-Cr(1)-C(2)	93 14(12)
C(10)-Cr(1)-C(2)	153 91(13)
C(11)-Cr(1)-C(2)	116 90(13)
N(1)-Cr(1)-C(2)	36 53(8)
C(9)-Cr(1)-C(5)	154 24(13)
C(10)-Cr(1)-C(5)	90 57(13)
C(11)-Cr(1)-C(5)	120 12(13)
N(1)-Cr(1)-C(5)	67 11(10)
C(2)-Cr(1)-C(5)	78 58(11)
C(9)-Cr(1)-C(6)	156 13(12)
C(10)-Cr(1)-C(6)	117 41(13)
C(11)-Cr(1)-C(6)	93 47(12)
N(1)-Cr(1)-C(6)	37 16(9)
C(2)-Cr(1)-C(6)	66 09(10)
C(5)-Cr(1)-C(6)	37 09(10)
C(9)-Cr(1)-C(3)	92 64(13)
C(10)-Cr(1)-C(3)	116 26(14)
C(11)-Cr(1)-C(3)	154 44(13)
N(1)-Cr(1)-C(3)	66 85(10)
C(2)-Cr(1)-C(3)	37 66(10)
C(5)-Cr(1)-C(3)	65 88(12)
C(6)-Cr(1)-C(3)	78 15(11)
C(9)-Cr(1)-C(4)	117 15(13)
C(10)-Cr(1)-C(4)	89 75(14)
C(11)-Cr(1)-C(4)	157 25(13)
N(1)-Cr(1)-C(4)	79 74(10)

C(2)-Cr(1)-C(4)	67 26(11)
C(5)-Cr(1)-C(4)	37 17(11)
C(6)-Cr(1)-C(4)	67 09(11)
C(3)-Cr(1)-C(4)	36 51(11)
C(14)-Si(1)-C(13)	110 1(2)
C(14)-Si(1)-C(12)	112 6(2)
C(13)-Si(1)-C(12)	109 4(2)
C(14)-Si(1)-C(2)	107 43(14)
C(13)-Si(1)-C(2)	109 21(14)
C(12)-Si(1)-C(2)	108 1(2)
C(16)-Si(2)-C(17)	111 6(2)
C(16)-Si(2)-C(15)	109.4(2)
C(17)-Si(2)-C(15)	111 1(2)
C(16)-Si(2)-C(6)	109 68(14)
C(17)-Si(2)-C(6)	108 9(2)
C(15)-Si(2)-C(6)	106 1(2)
C(2)-N(1)-C(6)	119 9(2)
C(2)-N(1)-Cr(1)	71 88(14)
C(6)-N(1)-Cr(1)	72 41(14)
N(1)-C(2)-C(3)	120 3(3)
N(1)-C(2)-Si(1)	114 4(2)
C(3)-C(2)-Si(1)	125 3(2)
N(1)-C(2)-Cr(1)	71 59(14)
C(3)-C(2)-Cr(1)	72 0(2)
Si(1)-C(2)-Cr(1)	127 50(13)
C(4)-C(3)-C(2)	120 7(3)
C(4)-C(3)-Cr(1)	71 9(2)
C(2)-C(3)-Cr(1)	70 4(2)
C(3)-C(4)-C(5)	118 4(3)
C(3)-C(4)-Cr(1)	71 5(2)
C(5)-C(4)-Cr(1)	71 0(2)
C(6)-C(5)-C(4)	120.8(3)
C(6)-C(5)-Cr(1)	71 7(2)
C(4)-C(5)-Cr(1)	71.8(2)
N(1)-C(6)-C(5)	119 8(2)
N(1)-C(6)-Si(2)	115 8(2)
C(5)-C(6)-Si(2)	124 4(2)
N(1)-C(6)-Cr(1)	70 43(14)
C(5)-C(6)-Cr(1)	71 2(2)
Si(2)-C(6)-Cr(1)	133 49(14)
O(1)-C(9)-Cr(1)	178 6(3)
O(2)-C(10)-Cr(1)	179 0(3)
O(3)-C(11)-Cr(1)	176 6(3)

Table 3b Anisotropic displacement parameters (A^2 x 10^3) for $C_{14}H_{21}CrNO_3Si_2$
The anisotropic displacement factor exponent takes the form
$-2\pi^2$ [$h^2 a^{*2}$ U11 + + 2 h k a* b* U12]

	U11	U22	U33	U23	U13	U12
Cr(1)	38(1)	36(1)	37(1)	-2(1)	9(1)	1(1)
Si(1)	47(1)	32(1)	42(1)	2(1)	4(1)	2(1)
Si(2)	63(1)	33(1)	40(1)	4(1)	11(1)	0(1)
N(1)	39(1)	33(1)	33(1)	1(1)	7(1)	1(1)
O(1)	100(2)	91(2)	48(1)	14(1)	3(1)	11(2)
O(2)	113(2)	85(2)	90(2)	-36(2)	22(2)	32(2)
O(3)	71(2)	129(3)	81(2)	-3(2)	-4(2)	-47(2)
C(2)	36(2)	33(2)	36(1)	-2(1)	3(1)	-4(1)
C(3)	39(2)	45(2)	47(2)	2(1)	10(1)	-9(1)
C(4)	31(2)	54(2)	58(2)	-2(2)	10(1)	2(1)
C(5)	39(2)	44(2)	51(2)	1(1)	-1(1)	11(2)
C(6)	41(2)	33(2)	37(2)	1(1)	4(1)	2(1)
C(9)	58(2)	55(2)	40(2)	-1(2)	10(2)	-2(2)
C(10)	65(2)	55(2)	55(2)	-10(2)	9(2)	9(2)
C(11)	56(2)	65(2)	44(2)	-3(2)	4(2)	-14(2)
C(12)	116(3)	62(2)	77(3)	30(2)	32(2)	11(2)
C(13)	76(3)	57(2)	63(2)	-14(2)	1(2)	14(2)
C(14)	49(2)	58(2)	106(3)	-15(2)	-13(2)	8(2)
C(15)	110(3)	72(3)	45(2)	0(2)	11(2)	-21(2)
C(16)	68(2)	82(3)	70(2)	10(2)	21(2)	-16(2)
C(17)	126(4)	43(2)	88(3)	11(2)	37(3)	15(2)

Table 4b Hydrogen coordinates (x 10^4) and isotropic displacement parameters (A^2 x 10^3) for $C_{14}H_{21}CrNO_3Si_2$

	x	y	z	U(eq)
H(3)	4702(37)	2218(12)	557(26)	41(8)
H(4)	6228(41)	1367(13)	875(28)	51(8)
H(5)	4919(35)	688(12)	2157(24)	33(7)
H(12A)	3366(6)	3273(2)	190(4)	117(4)
H(12B)	1489(6)	3502(2)	-317(4)	117(4)
H(12C)	2184(6)	2933(2)	-890(4)	117(4)
H(13A)	2560(5)	3282(2)	2907(3)	117(4)
H(13B)	980(5)	2930(2)	3315(3)	117(4)
H(13C)	641(5)	3498(2)	2497(3)	117(4)
H(14A)	-1053(4)	2274(2)	-162(4)	117(4)
H(14B)	-1749(4)	2831(2)	466(4)	117(4)
H(14C)	-1411(4)	2263(2)	1283(4)	117(4)
H(15A)	3577(6)	864(2)	5411(3)	117(4)
H(15B)	1792(6)	635(2)	5783(3)	117(4)
H(15C)	1924(6)	1266(2)	5247(3)	117(4)
H(16A)	-1082(5)	1010(2)	3205(4)	117(4)
H(16B)	-1204(5)	366(2)	3660(4)	117(4)
H(16C)	-974(5)	503(2)	2220(4)	117(4)
H(17A)	3864(6)	-135(2)	3563(4)	117(4)
H(17B)	2335(6)	-264(2)	2460(4)	117(4)
H(17C)	2106(6)	-401(2)	3900(4)	117(4)

Observed and calculated structural factors for

(η^6-2,6-bis(trimethylsilyl)pyridine)$Cr(CO)_3$

Table 5b Observed and calculated structure

Page 1

h	k	l	10Fo	10Fc	10s	h	k	l	10Fo	10Fc	10s	h	k	l	10Fo	10Fc	10s
2	0	0	1612	1445	16	2	11	0	216	206	2	-3	0	1	727	683	5
4	0	0	0	66	1	3	11	0	40	27	39	-1	0	1	1370	1294	12
6	0	0	283	287	3	4	11	0	253	256	2	1	0	1	936	961	3
8	0	0	208	-94	4	5	11	0	112	117	5	3	0	1	318	316	3
1	1	0	117	-18	1	6	11	0	189	185	4	5	0	1	303	296	2
2	1	0	581	570	4	7	11	0	139	143	6	7	0	1	84	84	8
3	1	0	272	282	2	8	11	0	0	27	1	-8	1	1	205	201	4
4	1	0	465	453	4	0	12	0	360	359	3	-7	1	1	296	296	3
5	1	0	104	-01	4	1	12	0	0	10	1	-6	1	1	271	280	2
6	1	0	130	-35	4	2	12	0	409	416	4	-5	1	1	378	383	3
7	1	0	28	10	28	3	12	0	521	508	5	-4	1	1	54	27	7
8	1	0	116	-15	7	4	12	0	379	385	4	-3	1	1	37	48	9
0	2	0	238	238	1	5	12	0	119	129	5	-2	1	1	26	48	25
1	2	0	1882	1850	12	6	12	0	290	290	3	-1	1	1	1141	1054	8
2	2	0	8	10	8	7	12	0	135	134	6	0	1	1	1061	922	7
3	2	0	935	945	5	8	12	0	171	173	5	1	1	1	1413	1230	13
4	2	0	220	223	2	1	13	0	0	54	1	2	1	1	112	99	2
5	2	0	442	436	4	2	13	0	110	110	4	3	1	1	759	755	5
6	2	0	49	66	14	3	13	0	0	17	1	4	1	1	513	518	4
7	2	0	49	79	48	4	13	0	0	58	1	5	1	1	163	158	3
8	2	0	132	-32	6	5	13	0	112	101	6	6	1	1	240	239	3
1	3	0	441	454	3	6	13	0	68	62	11	7	1	1	0	78	1
2	3	0	577	565	4	7	13	0	138	156	6	8	1	1	82	73	9
3	3	0	213	203	1	0	14	0	112	112	3	-8	2	1	103	88	7
4	3	0	216	216	2	1	14	0	721	747	6	-7	2	1	51	5	14
5	3	0	25	41	24	2	14	0	0	26	1	-6	2	1	140	142	4
6	3	0	244	241	3	3	14	0	315	317	3	-5	2	1	0	44	1
7	3	0	0	1	1	4	14	0	0	14	1	-4	2	1	354	345	3
8	3	0	0	33	1	5	14	0	123	106	5	-3	2	1	350	335	3
0	4	0	834	865	3	6	14	0	84	84	9	-2	2	1	298	304	2
1	4	0	512	509	4	7	14	0	239	229	4	-1	2	1	530	539	3
2	4	0	691	680	4	1	15	0	0	196	1	0	2	1	760	767	4
3	4	0	76	65	4	2	15	0	56	47	9	1	2	1	384	382	2
4	4	0	896	928	6	3	15	0	177	176	3	2	2	1	550	552	4
5	4	0	236	240	2	4	15	0	176	176	3	3	2	1	882	877	5
6	4	0	206	200	3	5	15	0	162	167	4	4	2	1	517	509	4
7	4	0	81	92	9	6	15	0	36	32	35	5	2	1	0	51	1
8	4	0	18	67	18	7	15	0	0	42	1	6	2	1	0	15	1
1	5	0	547	527	4	0	16	0	516	512	5	7	2	1	186	193	4
2	5	0	610	572	5	1	16	0	0	15	1	8	2	1	23	23	23
3	5	0	202	-94	2	2	16	0	455	444	4	-8	3	1	0	81	1
4	5	0	198	-95	2	3	16	0	94	87	6	-7	3	1	0	73	1
5	5	0	120	-18	4	4	16	0	235	229	3	-6	3	1	75	56	8
6	5	0	26	70	26	5	16	0	58	42	12	-5	3	1	311	316	3
7	5	0	0	33	1	6	16	0	167	162	5	-4	3	1	565	585	4
8	5	0	63	50	13	7	16	0	102	89	8	-3	3	1	149	161	2
0	6	0	470	470	4	1	17	0	97	105	5	-2	3	1	1126	1173	4
1	6	0	832	850	4	2	17	0	183	187	3	-1	3	1	56	33	3
2	6	0	323	321	3	3	17	0	63	59	9	0	3	1	1098	938	6

factors for $C_{14}H_{21}CrNO_3Si_2$

h	k	l	10Fo	10Fc	10s	h	k	l	10Fo	10Fc	10s
8	5	1	129	137	6	-4	11	1	508	503	4
-8	6	1	128	128	6	-3	11	1	440	450	4
-7	6	1	82	69	8	-2	11	1	259	271	2
-6	6	1	0	51	1	-1	11	1	913	935	5
-5	6	1	382	385	3	0	11	1	180	195	1
-4	6	1	0	8	1	1	11	1	437	439	4
-3	6	1	404	397	4	2	11	1	624	629	4
-2	6	1	777	775	5	3	11	1	0	47	1
-1	6	1	402	412	3	4	11	1	518	514	5
0	6	1	668	659	3	5	11	1	115	130	5
1	6	1	316	313	3	6	11	1	298	301	3
2	6	1	595	574	5	7	11	1	65	79	13
3	6	1	36	61	35	8	11	1	65	67	14
4	6	1	126	124	3	-8	12	1	0	2	1
5	6	1	154	154	4	-7	12	1	0	55	1
6	6	1	92	103	7	-6	12	1	0	11	1
7	6	1	34	33	34	-5	12	1	82	86	7
8	6	1	109	109	7	-4	12	1	122	128	4
-8	7	1	95	114	9	-3	12	1	79	80	6
-7	7	1	184	184	4	-2	12	1	211	228	2
-6	7	1	118	113	5	-1	12	1	101	95	3
-5	7	1	346	346	3	0	12	1	232	239	2
-4	7	1	468	483	4	1	12	1	420	419	3
-3	7	1	404	392	3	2	12	1	395	404	4
-2	7	1	417	438	4	3	12	1	151	157	3
-1	7	1	201	206	2	4	12	1	124	122	4
0	7	1	674	665	3	5	12	1	0	55	1
1	7	1	134	112	2	6	12	1	255	266	3
2	7	1	834	856	5	7	12	1	72	93	11
3	7	1	190	199	2	8	12	1	53	44	52
4	7	1	0	19	1	-8	13	1	126	126	7
5	7	1	14	39	14	-7	13	1	218	220	4
6	7	1	0	8	1	-6	13	1	361	364	4
7	7	1	0	37	1	-5	13	1	209	216	3
8	7	1	160	168	5	-4	13	1	167	163	3
-8	8	1	32	41	31	-3	13	1	125	124	4
-7	8	1	129	132	6	-2	13	1	352	347	3
-6	8	1	226	219	3	-1	13	1	66	68	6
-5	8	1	164	158	3	0	13	1	518	514	5
-4	8	1	55	49	9	1	13	1	363	365	4
-3	8	1	296	294	2	2	13	1	261	281	2
-2	8	1	236	242	2	3	13	1	405	406	4
-1	8	1	347	342	3	4	13	1	0	32	1
0	8	1	222	201	1	5	13	1	203	197	3
1	8	1	81	78	3	6	13	1	68	75	11
2	8	1	408	383	4	7	13	1	218	215	4
3	8	1	220	225	2	-7	14	1	53	42	17
4	8	1	222	235	2	-6	14	1	122	121	6
5	8	1	133	148	4	-5	14	1	247	248	3

h	k	l	10Fo	10Fc	10s	h	k	l	10Fo	10Fc	10s	h	k	l	10Fo
3	6	0	510	538	4	4	17	0	45	46	45	1	3	1	79
4	6	0	244	246	2	5	17	0	67	66	11	2	3	1	223
5	6	0	407	421	4	6	17	0	73	88	11	3	3	1	460
6	6	0	0	58	1	7	17	0	65	42	14	4	3	1	464
7	6	0	330	331	3	0	18	0	258	259	2	5	3	1	506
8	6	0	42	32	26	1	18	0	143	132	4	6	3	1	274
1	7	0	182	186	1	2	18	0	180	189	3	7	3	1	119
2	7	0	332	319	3	3	18	0	324	322	3	8	3	1	0
3	7	0	183	181	2	4	18	0	134	123	5	-8	4	1	26
4	7	0	325	320	3	5	18	0	128	122	6	-7	4	1	80
5	7	0	98	109	6	6	18	0	105	109	8	-6	4	1	97
6	7	0	43	81	43	1	19	0	99	121	6	-5	4	1	306
7	7	0	0	1	1	2	19	0	303	315	3	-4	4	1	603
8	7	0	0	6	1	3	19	0	186	192	4	-3	4	1	0
0	8	0	419	390	3	4	19	0	97	97	7	-2	4	1	469
1	8	0	0	60	1	5	19	0	0	35	1	-1	4	1	164
2	8	0	344	367	3	6	19	0	33	68	33	0	4	1	689
3	8	0	292	275	3	0	20	0	318	323	3	1	4	1	368
4	8	0	619	622	5	1	20	0	254	253	3	2	4	1	299
5	8	0	435	439	4	2	20	0	286	312	3	3	4	1	216
6	8	0	367	359	4	3	20	0	10_	104	6	4	4	1	82
7	8	0	88	57	8	4	20	0	0	37	1	5	4	1	0
8	8	0	273	268	4	5	20	0	130	129	6	6	4	1	113
1	9	0	699	666	5	6	20	0	114	94	7	7	4	1	43
2	9	0	90	79	4	1	21	0	97	98	6	8	4	1	27
3	9	0	609	591	4	2	21	0	0	118	1	-8	5	1	216
4	9	0	70	81	7	3	21	0	0	20	1	-7	5	1	39
5	9	0	0	13	1	4	21	0	133	138	6	-6	5	1	32_
6	9	0	45	51	_8	5	21	0	0	1	1	-5	5	1	215
7	9	0	50	25	_6	0	22	0	0	10	1	-4	5	1	149
8	9	0	24	14	23	1	22	0	172	171	4	-3	5	1	884
0	10	0	127	129	2	2	22	0	0	131	1	-2	5	1	96
1	10	0	100	108	3	3	22	0	224	219	3	-1	5	1	1693
2	10	0	100	79	3	4	22	0	92	88	8	0	5	1	729
3	10	0	545	552	4	5	22	0	183	180	5	1	5	1	65
4	10	0	212	224	2	1	23	0	0	5	1	2	5	1	749
5	10	0	553	549	6	2	23	0	219	235	4	3	5	1	219
6	10	0	195	191	4	3	23	0	62	93	14	4	5	1	31_
7	10	0	268	271	3	4	23	0	56	59	15	5	5	1	29_
8	10	0	0	30	1	-7	0	1	0	22	1	6	5	1	22
1	11	0	273	257	2	-5	0	1	145	148	3	7	5	1	183

10Fc	10s	h	k	l	10Fo	10Fc	10s	h	k	l	10Fo	10Fc	10s
65	3	6	8	1	47	49	16	-4	14	1	39	30	39
215	2	7	8	1	97	107	8	-3	14	1	58	65	9
481	4	8	8	1	46	39	22	-2	14	1	224	229	2
465	4	-8	9	1	20	54	20	-1	14	1	84	97	5
514	4	-7	9	1	124	129	6	0	14	1	478	482	5
265	2	-6	9	1	223	209	3	1	14	1	135	135	3
123	6	-5	9	1	204	206	3	2	14	1	239	238	2
65	1	-4	9	1	742	757	7	3	14	1	34	20	34
29	25	-3	9	1	362	369	3	4	14	1	0	44	1
75	9	-2	9	1	888	892	5	5	14	1	0	10	1
103	6	-1	9	1	28_	300	2	6	14	1	167	169	5
303	2	0	9	1	196	207	3	7	14	1	60	51	15
604	4	1	9	1	629	658	5	-7	15	1	0	110	1
42	1	2	9	1	42	27	9	-6	15	1	259	259	3
465	3	3	9	1	518	510	4	-5	15	1	207	209	3
156	1	4	9	1	266	272	2	-4	15	1	15	52	15
684	5	5	9	1	0	33	1	-3	15	1	356	356	3
353	3	6	9	1	114	106	6	-2	15	1	68	64	7
291	3	7	9	1	233	235	3	-1	15	1	146	134	3
212	2	8	9	1	0	33	1	0	15	1	382	383	3
104	5	-8	10	1	0	56	1	1	15	1	148	157	3
44	1	-7	10	1	39	17	39	2	15	1	39_	391	3
118	5	-6	10	1	183	181	4	3	15	1	294	292	2
62	20	-5	10	1	394	408	3	4	15	1	196	198	3
36	27	-4	10	1	320	312	3	5	15	1	280	277	3
214	4	-3	10	1	108	108	4	6	15	1	172	164	4
54	24	-2	10	1	58	57	6	7	15	1	8_	74	10
327	3	-1	10	1	145	132	2	-7	16	1	50	33	19
204	3	0	10	1	15_	138	1	-6	16	1	0	26	1
168	3	1	10	1	83	64	4	-5	16	1	0	52	1
882	5	2	10	1	189	201	2	-4	16	1	145	144	4
82	3	3	10	1	130	136	3	-3	16	1	0	12	1
1605	16	4	10	1	129	121	4	-2	16	1	32	48	31
731	9	5	10	1	93	87	6	-1	16	1	0	6	1
63	4	6	10	1	0	23	1	0	16	1	20	21	20
746	5	7	10	1	134	138	6	1	16	1	224	226	2
224	2	8	10	1	0	27	1	2	16	1	175	186	3
324	3	-8	11	1	110	108	7	3	16	1	298	294	2
294	2	-7	11	1	280	286	3	4	16	1	47	39	47
10	21	-6	11	1	137	142	5	5	16	1	32	52	32
184	4	-5	11	1	375	378	3	6	16	1	26	52	26

Table 5b Observed and calculated structure

Page 2

h	k	l	10Fo	10Fc	10s	h	k	l	10Fo	10Fc	10s	h	k	l	10Fo	10Fc
-7	16	1	80	86	11	2	0	2	500	518	3	-7	6	2	227	227
-7	17	1	34	27	34	4	0	2	227	234	2	-6	6	2	85	92
-6	17	1	104	93	7	6	0	2	114	119	5	-5	6	2	281	290
-5	17	1	206	201	4	8	0	2	184	178	4	-4	6	2	98	105
-4	17	1	131	-22	5	-8	1	2	190	188	4	-3	6	2	138	156
-3	17	1	380	380	3	-7	1	2	197	203	4	-2	6	2	33	47
-2	17	1	255	254	2	-6	1	2	343	347	3	-1	6	2	477	479
-1	17	1	206	212	3	-5	1	2	368	361	3	0	6	2	763	730
0	17	1	101	97	3	-4	1	2	89	89	4	1	6	2	855	867
1	17	1	32	75	31	-3	1	2	77	56	4	2	6	2	214	209
2	17	1	185	-68	3	-2	1	2	452	444	3	3	6	2	777	785
3	17	1	276	274	3	-1	1	2	209	197	2	4	6	2	216	216
4	17	1	319	312	3	0	1	2	921	920	2	5	6	2	206	201
5	17	1	255	248	3	1	1	2	574	568	4	6	6	2	149	148
6	17	1	199	200	4	2	1	2	427	410	3	7	6	2	200	198
-6	18	1	0	31	1	3	1	2	319	319	3	8	6	2	0	42
-5	18	1	160	-62	5	4	1	2	139	139	3	-8	7	2	75	73
-4	18	1	0	13	1	5	1	2	390	387	3	-7	7	2	42	20
-3	18	1	0	20	1	6	1	2	77	83	8	-6	7	2	93	100
-2	18	1	108	-16	5	7	1	2	103	87	7	-5	7	2	260	260
-1	18	1	358	363	3	8	1	2	130	139	6	-4	7	2	127	123
0	18	1	107	-09	3	-8	2	2	49	61	18	-3	7	2	165	170
1	18	1	219	223	3	-7	2	2	192	194	4	-2	7	2	586	577
2	18	1	170	-76	4	-6	2	2	142	154	4	-1	7	2	252	294
3	18	1	45	32	44	-5	2	2	480	482	4	0	7	2	964	957
4	18	1	111	-16	6	-4	2	2	159	147	2	1	7	2	367	386
5	18	1	38	46	33	-3	2	2	601	617	5	2	7	2	263	238
6	18	1	47	42	46	-2	2	2	137	134	2	3	7	2	60	49
-6	19	1	47	9	47	-1	2	2	997	1048	3	4	7	2	264	270
-5	19	1	0	37	1	0	2	2	33	20	5	5	7	2	297	297
-4	19	1	194	-92	4	1	2	2	275	269	2	6	7	2	60	68
-3	19	1	0	14	1	2	2	2	142	129	2	7	7	2	58	54
-2	19	1	272	270	3	3	2	2	400	419	4	8	7	2	79	65
-1	19	1	43	78	42	4	2	2	267	256	2	-8	8	2	203	196
0	19	1	181	-84	2	5	2	2	310	329	3	-7	8	2	81	66
1	19	1	452	452	4	6	2	2	67	66	9	-6	8	2	182	174
2	19	1	30	34	29	7	2	2	187	192	4	-5	8	2	220	232
3	19	1	285	288	3	8	2	2	83	79	9	-4	8	2	0	37
4	19	1	0	35	1	-8	3	2	58	53	14	-3	8	2	248	243
5	19	1	82	78	9	-7	3	2	43	54	43	-2	8	2	38	63
6	19	1	116	-12	7	-6	3	2	275	278	2	-1	8	2	350	345
-6	20	1	40	51	39	-5	3	2	249	246	2	0	8	2	657	677
-5	20	1	45	54	45	-4	3	2	399	423	4	1	8	2	232	225
-4	20	1	31	90	30	-3	3	2	249	245	2	2	8	2	782	777
-3	20	1	87	74	7	-2	3	2	188	190	1	3	8	2	159	153
-2	20	1	84	95	7	-1	3	2	619	619	4	4	8	2	390	392
-1	20	1	170	-72	4	0	3	2	931	936	2	5	8	2	187	190
0	20	1	280	278	3	1	3	2	723	719	4	6	8	2	173	171

e factors for $C_{14}H_{21}CrNO_3Si_2$

10s	h	k	l	10Fo	10Fc	10s	h	k	l	10Fo	10Fc	10s
3	-2	11	2	664	652	6	-4	17	2	268	270	3
7	-1	11	2	379	378	3	-3	17	2	46	40	15
2	0	11	2	613	595	4	-2	17	2	95	86	6
4	1	11	2	87	92	4	-1	17	2	301	304	2
2	2	11	2	98	113	4	0	17	2	37	24	13
33	3	11	2	359	352	3	1	17	2	123	130	4
3	4	11	2	46	29	14	2	17	2	203	192	3
5	5	11	2	213	200	3	3	17	2	87	92	7
4	6	11	2	0	28	1	4	17	2	149	139	5
2	7	11	2	0	20	1	5	17	2	172	167	4
6	-8	12	2	93	102	9	6	17	2	49	42	19
2	-7	12	2	133	138	6	-6	18	2	62	73	14
3	-6	12	2	262	256	3	-5	18	2	164	151	4
4	-5	12	2	118	114	5	-4	18	2	51	50	14
4	-4	12	2	370	372	3	-3	18	2	362	362	3
1	-3	12	2	351	360	3	-2	18	2	146	145	4
11	-2	12	2	370	359	3	-1	18	2	389	384	4
41	-1	12	2	345	335	3	0	18	2	229	229	2
7	0	12	2	298	293	3	1	18	2	206	200	3
2	1	12	2	308	303	2	2	18	2	16	14	15
3	2	12	2	463	459	5	3	18	2	106	122	6
2	3	12	2	218	222	2	4	18	2	171	163	4
5	4	12	2	212	206	3	5	18	2	215	217	4
2	5	12	2	90	76	7	6	18	2	0	81	1
4	6	12	2	0	88	1	-6	19	2	63	54	13
4	7	12	2	132	117	6	-5	19	2	45	32	19
2	-8	13	2	153	155	6	-4	19	2	49	75	48
7	-7	13	2	52	83	52	-3	19	2	164	155	4
2	-6	13	2	61	50	12	-2	19	2	0	33	1
3	-5	13	2	88	74	7	-1	19	2	0	57	1
12	-4	13	2	136	134	4	0	19	2	0	13	1
14	-3	13	2	118	125	4	1	19	2	69	69	8
10	-2	13	2	0	21	1	2	19	2	93	107	7
4	-1	13	2	443	442	4	3	19	2	73	79	9
9	0	13	2	38	41	37	4	19	2	0	2	1
3	1	13	2	403	416	4	5	19	2	0	3	1
3	2	13	2	17	8	17	6	19	2	79	88	11
1	3	13	2	96	90	5	-6	20	2	211	203	4
2	4	13	2	102	100	6	-5	20	2	0	27	1
10	5	13	2	58	66	13	-4	20	2	158	157	5
3	6	13	2	170	157	4	-3	20	2	96	92	6
3	7	13	2	0	28	1	-2	20	2	0	20	1
2	-7	14	2	224	227	4	-1	20	2	70	57	8
5	-6	14	2	35	45	34	0	20	2	309	311	2
3	-5	14	2	322	321	3	1	20	2	151	146	4
3	-4	14	2	42	47	42	2	20	2	515	496	5
3	-3	14	2	254	257	2	3	20	2	161	160	4
4	-2	14	2	71	59	7	4	20	2	186	182	4

h	k	l	10Fo	10Fc	10s	h	k	l	10Fo	10Fc	10s	h	k	l	10Fo
1	20	1	0	60	1	2	3	2	15_	138	2	7	8	2	66
2	20	1	145	145	5	3	3	2	442	434	4	8	8	2	94
3	20	1	71	83	10	4	3	2	717	727	6	-8	9	2	77
4	20	1	31	28	30	5	3	2	200	187	3	-7	9	2	10
5	20	1	0	14	1	6	3	2	0	5	1	-6	9	2	170
6	20	1	0	3	1	7	3	2	0	54	1	-5	9	2	315
-5	21	1	33	86	32	8	3	2	0	21	1	-4	9	2	127
-4	21	1	85	81	8	-8	4	2	177	183	5	-3	9	2	500
-3	21	1	0	54	1	-7	4	2	0	10	1	-2	9	2	349
-2	21	1	170	170	4	-6	4	2	103	95	6	-1	9	2	518
-1	21	1	255	250	3	-5	4	2	208	216	3	0	9	2	414
0	21	1	201	195	4	-4	4	2	546	554	4	1	9	2	172
1	21	1	339	340	3	-3	4	2	236	230	2	2	9	2	0
2	21	1	328	331	3	-2	4	2	966	1004	4	3	9	2	127
3	21	1	0	9	1	-1	4	2	167	140	1	4	9	2	40
4	21	1	86	91	8	0	4	2	533	537	3	5	9	2	63
5	21	1	74	56	10	1	4	2	655	640	4	6	9	2	63
-5	22	1	103	89	7	2	4	2	392	385	4	7	9	2	154
-4	22	1	113	110	6	3	4	2	178	177	2	8	9	2	102
-3	22	1	49	44	16	4	4	2	45_	468	4	-8	10	2	0
-2	22	1	130	139	5	5	4	2	118	113	4	-7	10	2	105
-1	22	1	0	42	1	6	4	2	345	348	3	-6	10	2	28
0	22	1	102	114	16	7	4	2	74	66	10	-5	10	2	173
1	22	1	126	140	6	8	4	2	177	179	5	-4	10	2	189
2	22	1	0	16	1	-8	5	2	0	33	1	-3	10	2	444
3	22	1	218	226	4	-7	5	2	222	220	3	-2	10	2	8_
4	22	1	33	13	33	-6	5	2	80	72	7	-1	10	2	638
5	22	1	0	60	1	-5	5	2	6_	61	9	0	10	2	64
-4	23	1	200	192	4	-4	5	2	289	294	2	1	10	2	540
-3	23	1	315	313	3	-3	5	2	58	29	6	2	10	2	39
-2	23	1	180	180	4	-2	5	2	133	143	2	3	10	2	399
-1	23	1	170	170	4	-1	5	2	804	821	4	4	10	2	310
0	23	1	134	135	5	0	5	2	526	514	3	5	10	2	30_
1	23	1	82	78	8	1	5	2	95	81	3	6	10	2	135
2	23	1	47	102	47	2	5	2	0	46	1	7	10	2	228
3	23	1	81	74	9	3	5	2	135	119	3	8	10	2	0
4	23	1	68	46	11	4	5	2	227	228	2	-8	11	2	26
-8	0	2	249	245	3	5	5	2	57	61	10	-7	11	2	78
-6	0	2	564	562	5	6	5	2	3_	33	31	-6	11	2	109
-4	0	2	646	670	6	7	5	2	48	42	18	-5	11	2	203
-2	0	2	418	432	3	8	5	2	89	83	9	-4	11	2	283
0	0	2	640	629	2	-8	6	2	0	28	1	-3	11	2	425

10Fc	10s	h	k	l	10Fo	10Fc	10s	h	k	l	10Fo	10Fc	10s
60	11	-1	14	2	29_	293	3	5	20	2	75	83	11
110	9	0	14	2	227	217	2	-5	21	2	0	47	1
79	11	1	14	2	290	305	3	-4	21	2	7_	73	10
5	9	2	14	2	140	131	4	-3	21	2	58	65	13
167	4	3	14	2	226	223	3	-2	21	2	170	166	4
318	2	4	14	2	165	163	4	-1	21	2	0	5	1
129	4	5	14	2	64	39	11	0	21	2	249	245	2
485	4	6	14	2	47	36	47	1	21	2	0	72	1
347	3	7	14	2	0	62	1	2	21	2	63	64	12
523	4	-7	15	2	187	179	4	3	21	2	60	71	13
396	3	-6	15	2	168	170	5	4	21	2	11_	118	7
166	2	-5	15	2	49	63	48	5	21	2	39	63	38
23	1	-4	15	2	173	175	3	-5	22	2	82	95	10
132	3	-3	15	2	0	59	1	-4	22	2	69	68	11
55	16	-2	15	2	84	95	6	-3	22	2	103	101	7
69	10	-1	15	2	108	107	4	-2	22	2	84	93	8
70	11	0	15	2	266	267	2	-1	22	2	96	95	7
162	5	1	15	2	232	237	2	0	22	2	106	103	4
93	8	2	15	2	96	102	5	1	22	2	352	358	3
4	1	3	15	2	73	75	8	2	22	2	268	262	3
101	7	4	15	2	0	52	1	3	22	2	219	216	4
55	27	5	15	2	97	100	7	4	22	2	122	121	6
174	3	6	15	2	0	44	1	5	22	2	167	166	5
188	3	7	15	2	172	173	5	-4	23	2	140	144	6
462	4	-7	16	2	0	51	1	-3	23	2	124	132	6
79	4	-6	16	2	145	144	5	-2	23	2	120	110	6
638	5	-5	16	2	115	117	6	-1	23	2	154	147	4
60	16	-4	16	2	364	362	3	0	23	2	35	17	34
538	4	-3	16	2	130	121	4	1	23	2	70	83	10
40	12	-2	16	2	674	679	5	2	23	2	139	152	5
403	3	-1	16	2	142	149	3	3	23	2	86	88	9
316	3	0	16	2	298	278	2	4	23	2	0	93	1
303	2	1	16	2	267	264	2	-7	0	3	342	345	3
135	5	2	16	2	15	18	14	-5	0	3	238	228	2
237	4	3	16	2	190	194	3	-3	0	3	95	82	3
51	1	4	16	2	152	151	4	-1	0	3	858	880	4
14	25	5	16	2	36	4	35	1	0	3	722	678	4
67	9	6	16	2	264	263	4	3	0	3	157	153	2
107	6	7	16	2	68	75	14	5	0	3	65	66	9
205	3	-7	17	2	50	46	20	7	0	3	117	107	6
295	3	-6	17	2	140	140	6	-8	1	3	78	82	10
417	4	-5	17	2	155	155	5	-7	1	3	110	107	6

Table 5b Observed and calculated

Page 3

h	k	l	10Fo	10Fc	10s	h	k	l	10Fo	10Fc	10s	h	k	l	1
-6	1	3	0	80	1	-1	6	3	629	627	5	6	11	3	
-5	1	3	455	450	4	0	6	3	261	295	2	7	11	3	
-4	1	3	171	-72	2	1	6	3	209	211	2	-8	12	3	
-3	1	3	336	342	3	2	6	3	329	339	3	-7	12	3	
-2	1	3	72	64	4	3	6	3	165	167	3	-6	12	3	
-1	1	3	185	-82	1	4	6	3	280	272	3	-5	12	3	
0	1	3	665	656	3	5	6	3	188	189	3	-4	12	3	
1	1	3	41	47	8	6	6	3	0	63	1	-3	12	3	
2	1	3	743	736	5	7	6	3	0	93	1	-2	12	3	
3	1	3	702	692	6	8	6	3	115	124	8	-1	12	3	
4	1	3	133	-27	3	-8	7	3	95	104	8	0	12	3	
5	1	3	35	29	24	-7	7	3	65	65	12	1	12	3	
6	1	3	112	-04	6	-6	7	3	464	461	4	2	12	3	
7	1	3	0	59	1	-5	7	3	267	271	2	3	12	3	
8	1	3	0	52	1	-4	7	3	703	705	7	4	12	3	
-8	2	3	124	-24	6	-3	7	3	36	75	35	5	12	3	
-7	2	3	163	-72	4	-2	7	3	560	560	4	6	12	3	
-6	2	3	206	210	3	-1	7	3	49	29	6	7	12	3	
-5	2	3	0	33	1	0	7	3	190	176	2	-7	13	3	
-4	2	3	276	285	2	1	7	3	569	567	4	-6	13	3	
-3	2	3	525	529	4	2	7	3	455	442	4	-5	13	3	
-2	2	3	17	45	16	3	7	3	353	360	3	-4	13	3	
-1	2	3	433	413	3	4	7	3	307	307	3	-3	13	3	
0	2	3	173	-78	1	5	7	3	227	229	3	-2	13	3	
1	2	3	739	730	4	6	7	3	213	215	3	-1	13	3	
2	2	3	159	-70	2	7	7	3	146	144	5	0	13	3	
3	2	3	138	-26	3	8	7	3	113	110	8	1	13	3	
4	2	3	264	265	2	-8	8	3	118	114	7	2	13	3	
5	2	3	93	-04	6	-7	8	3	118	103	6	3	13	3	
6	2	3	84	87	8	-6	8	3	75	71	9	4	13	3	
7	2	3	0	15	1	-5	8	3	0	50	1	5	13	3	
8	2	3	120	-26	7	-4	8	3	83	78	6	6	13	3	
-8	3	3	163	-70	5	-3	8	3	130	143	3	7	13	3	
-7	3	3	40	52	40	-2	8	3	248	240	2	-7	14	3	
-6	3	3	236	231	3	-1	8	3	71	53	4	-6	14	3	
-5	3	3	212	211	2	0	8	3	200	205	2	-5	14	3	
-4	3	3	193	201	2	1	8	3	527	510	4	-4	14	3	
-3	3	3	425	427	4	2	8	3	129	118	3	-3	14	3	
-2	3	3	174	-77	2	3	8	3	561	574	5	-2	14	3	
-1	3	3	601	602	4	4	8	3	143	137	4	-1	14	3	
0	3	3	713	688	9	5	8	3	0	49	1	0	14	3	
1	3	3	425	422	3	6	8	3	0	65	1	1	14	3	
2	3	3	166	-53	2	7	8	3	103	112	8	2	14	3	
3	3	3	333	325	3	8	8	3	48	61	48	3	14	3	
4	3	3	0	78	1	-8	9	3	136	130	6	4	14	3	
5	3	3	218	221	3	-7	9	3	114	114	6	5	14	3	
6	3	3	180	-73	4	-6	9	3	55	48	13	6	14	3	
7	3	3	156	-52	5	-5	9	3	444	441	4	7	14	3	

structure factors for $C_{14}H_{21}CrNO_3Si_2$.

10Fo	10Fc	10s	h	k	l	10Fo	10Fc	10s	h	k	l	10Fo	10Fc	10s
267	262	3	-6	18	3	93	76	8	6	1	4	0	21	1
140	149	6	-5	18	3	0	52	1	7	1	4	105	107	7
44	66	44	-4	18	3	257	257	3	8	1	4	77	73	11
134	132	6	-3	18	3	112	113	5	-8	2	4	0	105	1
117	124	6	-2	18	3	206	204	3	-7	2	4	141	145	5
235	231	3	-1	18	3	0	3	1	-6	2	4	34	44	34
519	530	4	0	18	3	165	170	2	-5	2	4	354	347	3
383	372	3	1	18	3	116	123	5	-4	2	4	115	117	4
174	188	3	2	18	3	161	155	4	-3	2	4	366	365	4
520	519	4	3	18	3	141	141	5	-2	2	4	332	327	3
263	268	1	4	18	3	39	30	39	-1	2	4	74	81	4
419	431	4	5	18	3	130	132	6	0	2	4	113	94	2
154	160	3	6	18	3	20	74	19	1	2	4	523	513	4
0	49	1	-6	19	3	157	149	5	2	2	4	69	76	5
0	4	1	-5	19	3	0	73	1	3	2	4	403	412	3
0	8	1	-4	19	3	103	100	7	4	2	4	0	27	1
79	85	10	-3	19	3	89	85	7	5	2	4	353	355	3
36	34	35	-2	19	3	96	102	6	6	2	4	160	162	4
60	47	13	-1	19	3	0	75	1	7	2	4	139	137	6
142	147	5	0	19	3	122	128	4	8	2	4	99	78	8
22	61	22	1	19	3	311	310	2	-8	3	4	56	47	14
239	239	3	2	19	3	112	121	6	-7	3	4	107	108	6
85	90	6	3	19	3	275	276	3	-6	3	4	22	47	21
63	51	7	4	19	3	176	170	4	-5	3	4	268	274	2
546	569	5	5	19	3	86	84	9	-4	3	4	228	226	2
168	163	2	-6	20	3	59	35	15	-3	3	4	84	95	4
430	433	4	-5	20	3	73	80	11	-2	3	4	423	423	4
487	482	4	-4	20	3	94	89	7	-1	3	4	242	256	2
437	438	4	-3	20	3	0	10	1	0	3	4	152	159	1
410	408	3	-2	20	3	0	25	1	1	3	4	74	62	4
110	110	6	-1	20	3	0	54	1	2	3	4	520	508	4
40	13	40	0	20	3	99	109	10	3	3	4	96	108	4
39	53	38	1	20	3	323	325	3	4	3	4	453	462	4
0	45	1	2	20	3	41	58	21	5	3	4	144	137	4
189	184	4	3	20	3	77	69	9	6	3	4	191	193	4
46	57	16	4	20	3	138	137	5	7	3	4	119	134	7
216	220	3	5	20	3	43	38	43	8	3	4	73	74	12
0	26	1	-5	21	3	333	331	3	-8	4	4	163	155	5
352	347	3	-4	21	3	97	88	7	-7	4	4	0	4	1
252	256	2	-3	21	3	158	146	4	-6	4	4	236	235	3
710	707	10	-2	21	3	75	79	9	-5	4	4	213	216	3
201	201	3	-1	21	3	17	15	17	-4	4	4	251	251	2
303	298	2	0	21	3	181	180	4	-3	4	4	157	141	2
78	76	7	1	21	3	110	119	6	-2	4	4	626	597	5
231	227	3	2	21	3	78	80	9	-1	4	4	475	487	4
17	73	17	3	21	3	181	177	4	0	4	4	1183	1176	3
0	6	1	4	21	3	38	60	37	1	4	4	157	156	2
81	50	10	5	21	3	144	150	6	2	4	4	632	632	4

h	k	l	10Fo	10Fc	10s	h	k	l	10Fo	10Fc	10s	h	k	l	10Fo
8	3	3	119	120	7	-4	9	3	148	145	3	-7	15	3	43
-8	4	3	90	91	9	-3	9	3	198	205	2	-6	15	3	142
-7	4	3	102	104	7	-2	9	3	63_	653	4	-5	15	3	64
-6	4	3	43	23	_6	-1	9	3	172	176	2	-4	15	3	47
-5	4	3	227	233	2	0	9	3	28_	297	4	-3	15	3	362
-4	4	3	291	287	2	1	9	3	347	347	3	-2	15	3	98
-3	4	3	150	168	2	2	9	3	0	47	1	-1	15	3	49_
-2	4	3	500	488	3	3	9	3	300	304	2	0	15	3	445
-1	4	3	175	196	1	4	9	3	206	207	3	1	15	3	478
0	4	3	659	620	3	5	9	3	119	109	5	2	15	3	522
1	4	3	296	265	3	6	9	3	29_	286	3	3	15	3	297
2	4	3	105	104	3	7	9	3	162	170	5	4	15	3	233
3	4	3	397	406	4	-8	10	3	87	76	9	5	15	3	52
4	4	3	257	254	2	-7	10	3	43	42	43	6	15	3	0
5	4	3	244	245	3	-6	10	3	0	26	1	-7	16	3	0
6	4	3	214	210	3	-5	10	3	0	8	1	-6	16	3	104
7	4	3	174	172	4	-4	10	3	462	467	4	-5	16	3	25_
8	4	3	90	73	9	-3	10	3	223	222	2	-4	16	3	0
-8	5	3	41	49	41	-2	10	3	643	635	4	-3	16	3	473
-7	5	3	228	226	3	-1	10	3	78	75	4	-2	16	3	100
-6	5	3	85	67	7	0	10	3	16	29	16	-1	16	3	369
-5	5	3	417	419	4	1	10	3	16_	153	2	0	16	3	292
-4	5	3	205	206	2	2	10	3	0	26	1	1	16	3	99
-3	5	3	447	443	4	3	10	3	40	17	39	2	16	3	123
-2	5	3	109	121	3	4	10	3	398	394	4	3	16	3	45
-1	5	3	1009	1018	4	5	10	3	0	1	1	4	16	3	37
0	5	3	858	852	4	6	10	3	188	188	4	5	16	3	132
1	5	3	117	103	2	7	10	3	0	49	1	6	16	3	0
2	5	3	665	660	5	-8	11	3	0	56	1	-7	17	3	0
3	5	3	362	341	3	-7	11	3	125	125	6	-6	17	3	0
4	5	3	199	191	3	-6	11	3	0	43	1	-5	17	3	0
5	5	3	300	307	3	-5	11	3	104	107	6	-4	17	3	17
6	5	3	181	169	4	-4	11	3	58	74	10	-3	17	3	0
7	5	3	340	348	3	-3	11	3	94	102	5	-2	17	3	282
8	5	3	0	89	1	-2	11	3	717	738	6	-1	17	3	385
-8	6	3	206	214	4	-1	11	3	0	11	1	0	17	3	519
-7	6	3	25	23	25	0	11	3	682	691	4	1	17	3	213
-6	6	3	172	169	4	1	11	3	68	58	6	2	17	3	270
-5	6	3	112	104	5	2	11	3	229	223	2	3	17	3	143
-4	6	3	109	119	4	3	11	3	135	131	4	4	17	3	132
-3	6	3	139	140	3	4	11	3	39	32	38	5	17	3	14_
-2	6	3	131	123	2	5	11	3	218	219	3	6	17	3	127

10Fc	10s	h	k	l	10Fo	10Fc	10s	h	k	l	10Fo	10Fc	10s
56	43	-5	22	3	0	22	1	3	4	4	422	415	3
129	5	-4	22	3	4_	50	26	4	4	4	0	12	1
69	11	-3	22	3	138	134	5	5	4	4	328	335	3
61	14	-2	22	3	16	16	16	6	4	4	239	241	3
364	3	-1	22	3	75	75	9	7	4	4	18	27	18
91	5	0	22	3	22	12	22	8	4	4	149	150	6
508	4	1	22	3	182	179	4	-8	5	4	134	136	6
443	3	2	22	3	163	164	4	-7	5	4	113	106	6
476	4	3	22	3	0	43	1	-6	5	4	86	88	7
523	4	4	22	3	185	180	4	-5	5	4	174	176	3
298	3	-4	23	3	168	170	5	-4	5	4	47_	485	4
240	3	-3	23	3	103	111	7	-3	5	4	173	170	2
106	52	-2	23	3	87	82	8	-2	5	4	688	696	5
15	1	-1	23	3	87	72	8	-1	5	4	79	83	4
20	1	0	23	3	64	47	7	0	5	4	63	41	3
100	7	1	23	3	0	40	1	1	5	4	464	445	4
251	3	2	23	3	35	31	34	2	5	4	192	189	2
32	1	3	23	3	46	88	46	3	5	4	570	567	5
466	5	4	23	3	0	41	1	4	5	4	105	111	5
99	5	-8	0	4	133	122	6	5	5	4	49	26	14
369	3	-6	0	4	394	402	3	6	5	4	25_	245	3
283	2	-4	0	4	416	436	4	7	5	4	136	134	6
100	5	-2	0	4	152	159	2	8	5	4	98	80	9
124	5	0	0	4	209	188	1	-8	6	4	38	15	37
45	17	2	0	4	650	638	6	-7	6	4	62	53	12
26	36	4	0	4	574	584	5	-6	6	4	0	11	1
124	6	6	0	4	231	226	3	-5	6	4	488	502	4
30	1	8	0	4	20	7	19	-4	6	4	82	75	6
41	1	-8	1	4	185	183	4	-3	6	4	59_	583	4
15	1	-7	1	4	123	129	5	-2	6	4	440	421	4
30	1	-6	1	4	336	326	3	-1	6	4	802	783	5
10	17	-5	1	4	42	37	15	0	6	4	44	33	25
82	1	-4	1	4	6_	50	7	1	6	4	763	750	5
283	3	-3	1	4	199	204	2	2	6	4	0	39	1
385	4	-2	1	4	15	9	14	3	6	4	243	237	2
521	3	-1	1	4	808	809	5	4	6	4	376	383	3
207	3	0	1	4	629	636	15	5	6	4	242	241	3
268	3	1	1	4	128	137	2	6	6	4	145	149	5
141	4	2	1	4	30_	314	2	7	6	4	76	66	10
128	5	3	1	4	502	507	5	-8	7	4	74	65	11
140	5	4	1	4	54	39	10	-7	7	4	166	167	4
129	6	5	1	4	243	239	3	-6	7	4	237	238	3

Table 5b Observed and calculated

Page 4

h	k	l	10Fo	10Fc	10s	h	k	l	10Fo	10Fc	10s	h	k	l
-5	7	4	500	493	4	6	12	4	104	108	8	0	19	4
-4	7	4	314	316	3	7	12	4	68	57	13	1	19	4
-3	7	4	180	-85	2	-7	13	4	159	153	5	2	19	4
-2	7	4	64	86	6	-6	13	4	98	93	7	3	19	4
-1	7	4	49	54	7	-5	13	4	69	73	9	4	19	4
0	7	4	259	258	1	-4	13	4	0	49	1	5	19	4
1	7	4	381	386	3	-3	13	4	0	8	1	-5	20	4
2	7	4	697	685	6	-2	13	4	54	62	10	-4	20	4
3	7	4	239	229	2	-1	13	4	192	188	3	-3	20	4
4	7	4	187	-85	3	0	13	4	390	394	2	-2	20	4
5	7	4	0	30	1	1	13	4	427	427	4	-1	20	4
6	7	4	0	42	1	2	13	4	497	495	4	0	20	4
7	7	4	128	-31	6	3	13	4	182	177	3	1	20	4
-8	8	4	0	26	1	4	13	4	212	205	3	2	20	4
-7	8	4	0	28	1	5	13	4	0	9	1	3	20	4
-6	8	4	71	78	10	6	13	4	51	31	18	4	20	4
-5	8	4	203	208	3	7	13	4	0	7	1	5	20	4
-4	8	4	539	538	5	-7	14	4	132	118	6	-5	21	4
-3	8	4	227	218	2	-6	14	4	105	104	7	-4	21	4
-2	8	4	695	699	6	-5	14	4	97	87	6	-3	21	4
-1	8	4	286	295	2	-4	14	4	119	117	5	-2	21	4
0	8	4	260	259	2	-3	14	4	138	129	4	-1	21	4
1	8	4	372	363	3	-2	14	4	233	239	2	0	21	4
2	8	4	279	273	2	-1	14	4	201	206	3	1	21	4
3	8	4	152	-54	3	0	14	4	373	367	2	2	21	4
4	8	4	193	200	3	1	14	4	37	35	36	3	21	4
5	8	4	16	28	15	2	14	4	43	58	16	4	21	4
6	8	4	155	-61	5	3	14	4	470	475	4	-4	22	4
-7	8	4	70	74	11	4	14	4	73	67	9	-3	22	4
-8	9	4	129	-18	6	5	14	4	230	226	3	-2	22	4
-7	9	4	0	38	1	6	14	4	0	17	1	-1	22	4
-6	9	4	87	83	7	-7	15	4	127	130	6	0	22	4
-5	9	4	244	249	3	-6	15	4	52	14	15	1	22	4
-4	9	4	230	234	2	-5	15	4	89	104	8	2	22	4
-3	9	4	686	705	5	-4	15	4	0	24	1	3	22	4
-2	9	4	121	-28	3	-3	15	4	88	84	6	4	22	4
-1	9	4	399	404	4	-2	15	4	330	328	3	-4	23	4
0	9	4	210	214	1	-1	15	4	202	213	3	-3	23	4
1	9	4	0	7	1	0	15	4	382	386	2	-2	23	4
2	9	4	315	307	3	1	15	4	443	429	4	-1	23	4
3	9	4	47	19	12	2	15	4	99	108	6	0	23	4
4	9	4	90	89	6	3	15	4	262	272	3	1	23	4
5	9	4	151	-46	5	4	15	4	116	112	6	2	23	4
6	9	4	171	-69	4	5	15	4	0	54	1	3	23	4
7	9	4	162	-59	5	6	15	4	163	167	5	-7	0	5
-8	10	4	53	22	17	-7	16	4	28	58	27	-5	0	5
-7	10	4	104	95	7	-6	16	4	170	166	5	-3	0	5
-6	10	4	177	-79	4	-5	16	4	0	29	1	-1	0	5

structure factors for $C_{14}H_{21}CrNO_3Si_2$.

10Fo	10Fc	10s	h	k	l	10Fo	10Fc	10s	h	k	l	10Fo	10Fc	10s
121	123	3	-2	3	5	129	126	3	-8	9	5	136	129	6
36	40	35	-1	3	5	405	418	3	-7	9	5	66	74	12
370	369	3	0	3	5	418	402	2	-6	9	5	143	148	5
41	38	23	1	3	5	137	136	3	-5	9	5	22	98	21
130	122	6	2	3	5	343	346	3	-4	9	5	15	66	14
148	143	5	3	3	5	234	241	2	-3	9	5	270	267	2
22	43	22	4	3	5	90	95	6	-2	9	5	206	207	2
254	251	3	5	3	5	31	62	31	-1	9	5	114	116	4
0	29	1	6	3	5	80	71	9	0	9	5	375	375	2
120	128	6	7	3	5	0	27	1	1	9	5	179	180	3
150	152	4	-8	4	5	47	44	20	2	9	5	275	281	2
130	126	3	-7	4	5	118	105	6	3	9	5	165	170	3
0	32	1	-6	4	5	276	276	3	4	9	5	74	70	8
213	211	4	-5	4	5	297	297	2	5	9	5	124	120	5
69	62	11	-4	4	5	174	164	3	6	9	5	0	5	1
192	197	4	-3	4	5	557	548	4	7	9	5	62	56	14
53	40	18	-2	4	5	496	495	4	-8	10	5	168	167	5
27	61	27	-1	4	5	937	942	5	-7	10	5	26	53	25
205	201	4	0	4	5	264	260	1	-6	10	5	0	14	1
120	117	6	1	4	5	565	563	4	-5	10	5	204	200	3
163	162	4	2	4	5	115	118	4	-4	10	5	121	120	4
14	12	14	3	4	5	251	251	2	-3	10	5	26	25	25
147	150	4	4	4	5	88	90	6	-2	10	5	601	629	5
103	95	6	5	4	5	254	259	3	-1	10	5	75	80	6
116	102	6	6	4	5	39	39	38	0	10	5	800	809	4
34	33	33	7	4	5	238	234	4	1	10	5	0	12	1
38	43	38	-8	5	5	22	12	22	2	10	5	303	303	3
121	108	6	-7	5	5	177	182	4	3	10	5	0	47	1
195	181	4	-6	5	5	245	251	3	4	10	5	58	57	12
21	17	20	-5	5	5	74	88	8	5	10	5	65	64	11
253	249	3	-4	5	5	484	489	4	6	10	5	240	235	4
0	3	1	-3	5	5	187	184	2	7	10	5	0	9	1
128	129	5	-2	5	5	74	88	5	-7	11	5	0	67	1
100	98	7	-1	5	5	178	179	2	-6	11	5	195	196	4
26	40	25	0	5	5	187	189	1	-5	11	5	0	45	1
0	43	1	1	5	5	772	769	6	-4	11	5	0	63	1
141	139	6	2	5	5	0	43	1	-3	11	5	138	148	4
145	149	5	3	5	5	248	248	2	-2	11	5	348	329	3
182	178	4	4	5	5	146	146	4	-1	11	5	122	136	4
127	126	6	5	5	5	32	90	31	0	11	5	226	228	1
0	11	1	6	5	5	75	67	10	1	11	5	114	103	4
15	22	15	7	5	5	73	52	11	2	11	5	269	273	3
119	110	6	-8	6	5	104	97	8	3	11	5	173	167	3
33	8	33	-7	6	5	41	48	25	4	11	5	60	46	11
254	248	3	-6	6	5	251	251	3	5	11	5	70	71	11
600	596	5	-5	6	5	242	248	3	6	11	5	0	10	1
257	253	2	-4	6	5	463	451	4	-7	12	5	202	205	4
222	234	2	-3	6	5	37	66	36	-6	12	5	61	52	12

h	k	l	10Fo	10Fc	10s	h	k	l	10Fo	10Fc	10s	h	k	l	10Fo
-5	10	4	0	22	1	-4	16	4	149	146	4	1	0	5	52
-4	10	4	0	62	1	-3	16	4	0	10	1	3	0	5	327
-3	10	4	275	288	2	-2	16	4	104	105	5	5	0	5	232
-2	10	4	0	34	1	-1	16	4	123	120	4	7	0	5	55
-1	10	4	845	876	6	0	16	4	269	278	2	-8	1	5	15
0	10	4	409	390	3	1	16	4	9_	94	6	-7	1	5	57
1	10	4	531	542	4	2	16	4	215	207	3	-6	1	5	106
2	10	4	119	126	4	3	16	4	120	109	5	-5	1	5	214
3	10	4	0	44	1	4	16	4	172	181	4	-4	1	5	217
4	10	4	135	125	4	5	16	4	3_	40	31	-3	1	5	447
5	10	4	41	35	21	6	16	4	145	146	6	-2	1	5	259
6	10	4	99	106	8	-6	17	4	7_	64	11	-1	1	5	148
7	10	4	168	162	5	-5	17	4	64	73	12	0	1	5	255
-8	11	4	47	50	23	-4	17	4	11_	108	6	1	1	5	73
-7	11	4	0	31	1	-3	17	4	86	103	7	2	1	5	94
-6	11	4	45	44	_8	-2	17	4	262	259	3	3	1	5	163
-5	11	4	0	8	1	-1	17	4	90	87	6	4	1	5	43
-4	11	4	182	177	3	0	17	4	208	211	3	5	1	5	262
-3	11	4	282	287	3	1	17	4	278	278	2	6	1	5	0
-2	11	4	472	479	4	2	17	4	62	63	11	7	1	5	0
-1	11	4	346	354	3	3	17	4	21_	209	3	-8	2	5	157
0	11	4	100	97	3	4	17	4	102	95	7	-7	2	5	0
1	11	4	56	59	8	5	17	4	21_	207	4	-6	2	5	310
2	11	4	0	73	1	6	17	4	148	133	6	-5	2	5	0
3	11	4	131	135	4	-6	18	4	8_	86	10	-4	2	5	426
4	11	4	0	64	1	-5	18	4	106	94	6	-3	2	5	35
5	11	4	234	232	3	-4	18	4	137	146	5	-2	2	5	648
6	11	4	56	54	_5	-3	18	4	49	48	14	-1	2	5	10_
7	11	4	80	90	_0	-2	18	4	164	167	4	0	2	5	182
-7	12	4	94	110	8	-1	18	4	154	159	4	1	2	5	198
-6	12	4	0	84	1	0	18	4	19_	185	3	2	2	5	235
-5	12	4	0	87	1	1	18	4	196	192	3	3	2	5	333
-4	12	4	153	146	4	2	18	4	29	0	28	4	2	5	310
-3	12	4	224	219	2	3	18	4	167	184	4	5	2	5	168
-2	12	4	197	203	3	4	18	4	140	142	5	6	2	5	259
-1	12	4	0	4	1	5	18	4	142	140	6	7	2	5	21_
0	12	4	75	71	4	-6	19	4	116	103	7	-8	3	5	88
1	12	4	0	55	1	-5	19	4	168	173	4	-7	3	5	140
2	12	4	296	300	2	-4	19	4	0	27	1	-6	3	5	0
3	12	4	114	116	5	-3	19	4	234	234	3	-5	3	5	255
4	12	4	279	269	3	-2	19	4	166	170	4	-4	3	5	157
5	12	4	46	23	_7	-1	19	4	253	251	3	-3	3	5	14_

10Fc	10s	h	k	l	10Fo	10Fc	10s	h	k	l	10Fo	10Fc	10s
39	7	-2	6	5	295	298	2	-5	12	5	192	196	4
329	3	-1	6	5	539	529	4	-4	12	5	44	21	43
229	3	0	6	5	692	696	4	-3	12	5	193	194	3
65	16	1	6	5	63	65	6	-2	12	5	0	30	1
28	14	2	6	5	988	991	6	-1	12	5	262	268	2
47	13	3	6	5	148	137	4	0	12	5	240	228	3
103	6	4	6	5	239	239	3	1	12	5	277	282	2
208	3	5	6	5	10_	91	7	2	12	5	237	230	3
216	2	6	6	5	84	88	9	3	12	5	226	218	3
456	5	7	6	5	86	63	9	4	12	5	116	120	6
241	2	-8	7	5	0	21	1	5	12	5	215	216	4
159	2	-7	7	5	0	39	1	6	12	5	102	96	8
254	1	-6	7	5	10_	104	6	-7	13	5	0	18	1
63	5	-5	7	5	276	272	2	-6	13	5	44	28	43
76	4	-4	7	5	12_	129	4	-5	13	5	73	75	9
160	3	-3	7	5	42	6	41	-4	13	5	258	246	3
62	42	-2	7	5	256	259	2	-3	13	5	357	353	3
253	3	-1	7	5	7_	74	5	-2	13	5	357	343	3
56	1	0	7	5	138	134	2	-1	13	5	157	158	3
4	1	1	7	5	10_	110	4	0	13	5	59	54	9
149	5	2	7	5	258	268	2	1	13	5	114	116	5
30	1	3	7	5	0	19	1	2	13	5	69	59	8
301	3	4	7	5	416	409	4	3	13	5	0	6	1
34	1	5	7	5	146	152	5	4	13	5	169	167	4
432	4	6	7	5	138	138	6	5	13	5	50	47	17
6	13	7	7	5	0	5	1	6	13	5	38	80	38
642	6	-8	8	5	25	9	24	-7	14	5	0	18	1
100	3	-7	8	5	47	49	47	-6	14	5	318	322	3
186	2	-6	8	5	147	145	4	-5	14	5	125	122	5
190	2	-5	8	5	273	274	2	-4	14	5	266	265	3
234	2	-4	8	5	64	52	8	-3	14	5	130	139	4
343	3	-3	8	5	376	381	3	-2	14	5	0	48	1
312	2	-2	8	5	0	8	1	-1	14	5	26_	268	2
183	4	-1	8	5	424	439	4	0	14	5	45	49	17
255	3	0	8	5	47	56	6	1	14	5	240	249	3
215	4	1	8	5	858	841	6	2	14	5	223	215	3
76	9	2	8	5	275	276	2	3	14	5	0	38	1
137	5	3	8	5	609	619	5	4	14	5	293	285	3
76	1	4	8	5	0	22	1	5	14	5	0	27	1
252	2	5	8	5	46	90	46	6	14	5	27	117	27
165	3	6	8	5	40	49	28	-7	15	5	129	121	7
147	3	7	8	5	49	61	19	-6	15	5	0	35	1

Table 5b Observed and calculated

Page 5

h	k	l	10Fo	10Fc	10s	h	k	l	10Fo	10Fc	10s	h	k	l
-5	15	5	107	-05	6	1	23	5	149	150	5	-8	6	6
-4	15	5	230	224	3	2	23	5	60	70	14	-7	6	6
-3	15	5	123	-18	5	-8	0	6	0	2	1	-6	6	6
-2	15	5	284	278	2	-6	0	6	157	154	4	-5	6	6
-1	15	5	294	290	3	-4	0	6	0	36	1	-4	6	6
0	15	5	109	-01	6	-2	0	6	363	363	3	-3	6	6
1	15	5	193	-97	3	0	0	6	335	353	2	-2	6	6
2	15	5	71	60	9	2	0	6	68	64	7	-1	6	6
3	15	5	0	25	1	4	0	6	419	429	4	0	6	6
4	15	5	35	50	34	6	0	6	211	214	4	1	6	6
5	15	5	119	-08	6	-8	1	6	12	21	11	2	6	6
6	15	5	63	57	15	-7	1	6	0	64	1	3	6	6
-6	16	5	71	46	11	-6	1	6	237	230	3	4	6	6
-5	16	5	209	201	4	-5	1	6	266	257	2	5	6	6
-4	16	5	52	54	13	-4	1	6	444	446	4	6	6	6
-3	16	5	311	315	2	-3	1	6	371	376	3	7	6	6
-2	16	5	93	90	7	-2	1	6	363	360	3	-8	7	6
-1	16	5	156	-54	4	-1	1	6	977	997	6	-7	7	6
0	16	5	140	-40	3	0	1	6	80	91	3	-6	7	6
1	16	5	0	16	1	1	1	6	397	405	3	-5	7	6
2	16	5	0	31	1	2	1	6	422	426	4	-4	7	6
3	16	5	74	68	9	3	1	6	42	11	15	-3	7	6
4	16	5	25	8	25	4	1	6	317	320	2	-2	7	6
5	16	5	232	238	4	5	1	6	95	96	7	-1	7	6
-6	17	5	91	95	9	6	1	6	27	7	27	0	7	6
-5	17	5	66	49	11	7	1	6	52	37	19	1	7	6
-4	17	5	120	-18	6	-8	2	6	0	22	1	2	7	6
-3	17	5	23	60	23	-7	2	6	70	64	10	3	7	6
-2	17	5	196	202	3	-6	2	6	104	109	6	4	7	6
-1	17	5	109	-01	5	-5	2	6	164	167	4	5	7	6
0	17	5	238	236	2	-4	2	6	231	237	2	6	7	6
1	17	5	228	227	3	-3	2	6	106	102	4	7	7	6
2	17	5	23	19	23	-2	2	6	352	358	3	-8	8	6
3	17	5	57	70	14	-1	2	6	37	54	36	-7	8	6
4	17	5	126	-12	6	0	2	6	474	471	3	-6	8	6
5	17	5	68	60	12	1	2	6	251	253	2	-5	8	6
-6	18	5	171	-58	5	2	2	6	255	263	2	-4	8	6
-5	18	5	184	-77	4	3	2	6	281	292	2	-3	8	6
-4	18	5	268	269	3	4	2	6	126	127	5	-2	8	6
-3	18	5	31	44	31	5	2	6	185	194	4	-1	8	6
-2	18	5	336	335	3	6	2	6	140	135	6	0	8	6
-1	18	5	245	241	3	7	2	6	0	16	1	1	8	6
0	18	5	139	-42	3	-8	3	6	85	87	9	2	8	6
1	18	5	124	-24	5	-7	3	6	85	74	9	3	8	6
2	18	5	0	75	1	-6	3	6	183	187	4	4	8	6
3	18	5	18	93	17	-5	3	6	83	79	7	5	8	6
4	18	5	237	223	4	-4	3	6	365	373	3	6	8	6
5	18	5	28	32	28	-3	3	6	293	302	2	-7	9	6

structure factors for $C_{14}H_{21}CrNO_3Si_2$.

10Fo	10Fc	10s	h	k	l	10Fo	10Fc	10s	h	k	l	10Fo	10Fc	10s
46	33	22	-6	12	6	34	13	33	-1	19	6	125	125	5
47	45	18	-5	12	6	68	63	10	0	19	6	133	130	3
61	58	11	-4	12	6	87	100	7	1	19	6	79	77	9
193	195	3	-3	12	6	181	174	3	2	19	6	187	182	4
67	56	8	-2	12	6	227	232	3	3	19	6	114	124	7
224	224	2	-1	12	6	0	15	1	4	19	6	94	96	9
82	87	5	0	12	6	103	102	5	-4	20	6	126	117	6
0	15	1	1	12	6	426	427	4	-3	20	6	126	135	6
186	186	2	2	12	6	39	43	20	-2	20	6	131	129	5
113	105	4	3	12	6	243	244	3	-1	20	6	0	43	1
102	108	5	4	12	6	47	43	19	0	20	6	48	39	18
163	162	4	5	12	6	0	40	1	1	20	6	0	7	1
34	7	33	6	12	6	19	24	19	2	20	6	37	54	37
173	166	4	-7	13	6	160	147	5	3	20	6	117	120	7
0	19	1	-6	13	6	63	59	12	-4	21	6	136	128	6
42	36	29	-5	13	6	248	254	3	-3	21	6	143	136	5
112	114	8	-4	13	6	271	274	3	-2	21	6	60	55	12
102	114	7	-3	13	6	210	212	3	-1	21	6	136	135	5
292	299	3	-2	13	6	321	319	3	0	21	6	0	41	1
290	284	3	-1	13	6	91	100	6	1	21	6	137	133	5
335	332	3	0	13	6	0	25	1	2	21	6	196	188	4
222	214	2	1	13	6	70	59	8	3	21	6	0	79	1
160	167	3	2	13	6	157	155	4	-3	22	6	74	80	11
114	131	4	3	13	6	281	277	3	-2	22	6	170	178	5
260	264	1	4	13	6	0	21	1	-1	22	6	0	36	1
423	409	4	5	13	6	145	130	5	0	22	6	0	8	1
135	129	4	6	13	6	26	45	26	1	22	6	42	7	42
494	501	5	-7	14	6	0	30	1	2	22	6	155	155	5
258	251	3	-6	14	6	0	11	1	-2	23	6	104	99	7
221	218	4	-5	14	6	0	47	1	-1	23	6	0	43	1
175	166	5	-4	14	6	0	10	1	0	23	6	209	213	3
0	16	1	-3	14	6	248	254	3	1	23	6	130	112	6
0	22	1	-2	14	6	35	42	34	-7	0	7	98	98	7
48	56	18	-1	14	6	231	233	3	-5	0	7	182	176	3
111	126	7	0	14	6	150	146	2	-3	0	7	247	245	2
219	222	3	1	14	6	67	75	9	-1	0	7	240	238	2
176	170	3	2	14	6	171	169	4	1	0	7	227	219	2
52	67	11	3	14	6	117	109	6	3	0	7	522	524	5
265	265	2	4	14	6	46	11	19	5	0	7	328	332	3
0	54	1	5	14	6	0	28	1	-8	1	7	39	64	39
154	147	2	-6	15	6	114	103	6	-7	1	7	0	15	1
135	134	4	-5	15	6	161	160	4	-6	1	7	135	132	5
225	226	3	-4	15	6	200	198	4	-5	1	7	39	61	38
46	54	15	-3	15	6	331	327	3	-4	1	7	45	41	13
65	60	10	-2	15	6	241	236	3	-3	1	7	196	191	3
81	94	9	-1	15	6	104	101	5	-2	1	7	355	350	3
0	9	1	0	15	6	265	257	5	-1	1	7	0	29	1
241	232	4	1	15	6	16	41	15	0	1	7	225	226	1

h	k	l	10Fo	10Fc	10s	h	k	l	10Fo	10Fc	10s	h	k	l	10Fo
-5	19	5	149	154	5	-2	3	6	637	652	4	-6	9	6	176
-4	19	5	0	39	1	-1	3	6	393	412	3	-5	9	6	120
-3	19	5	246	243	3	0	3	6	85_	839	7	-4	9	6	112
-2	19	5	0	10	1	1	3	6	358	357	3	-3	9	6	43
-1	19	5	155	155	4	2	3	6	25_	255	2	-2	9	6	286
0	19	5	69	72	11	3	3	6	308	306	3	-1	9	6	122
1	19	5	0	76	1	4	3	6	123	126	5	0	9	6	380
2	19	5	84	99	9	5	3	6	155	153	4	1	9	6	204
3	19	5	97	91	7	6	3	6	0	64	1	2	9	6	30_
4	19	5	0	26	1	7	3	6	59	53	16	3	9	6	8_
-5	20	5	181	186	5	-8	4	6	27	48	27	4	9	6	93
-4	20	5	103	123	7	-7	4	6	5_	66	17	5	9	6	126
-3	20	5	174	180	4	-6	4	6	193	195	4	6	9	6	188
-2	20	5	65	75	11	-5	4	6	74	87	8	-7	10	6	160
-1	20	5	163	159	4	-4	4	6	97	101	5	-6	10	6	0
0	20	5	74	74	6	-3	4	6	16	25	16	-5	10	6	204
1	20	5	269	262	3	-2	4	6	322	317	2	-4	10	6	25_
2	20	5	0	19	1	-1	4	6	315	305	3	-3	10	6	0
3	20	5	208	207	4	0	4	6	187	189	1	-2	10	6	130
4	20	5	33	9	33	1	4	6	13_	127	3	-1	10	6	92
-5	21	5	48	17	48	2	4	6	215	224	2	0	10	6	47
-4	21	5	85	85	9	3	4	6	14	50	14	1	10	6	193
-3	21	5	79	72	9	4	4	6	8_	85	8	2	10	6	147
-2	21	5	31	33	31	5	4	6	0	64	1	3	10	6	4_
-1	21	5	46	29	17	6	4	6	6_	42	13	4	10	6	46
0	21	5	48	55	17	7	4	6	11_	113	8	5	10	6	108
1	21	5	63	32	11	-8	5	6	162	158	5	6	10	6	19
2	21	5	107	108	7	-7	5	6	146	154	5	-7	11	6	132
3	21	5	147	155	5	-6	5	6	170	161	4	-6	11	6	209
4	21	5	28	83	27	-5	5	6	52_	536	5	-5	11	6	72
-4	22	5	93	81	8	-4	5	6	0	34	1	-4	11	6	97
-3	22	5	113	105	6	-3	5	6	386	392	4	-3	11	6	150
-2	22	5	156	161	5	-2	5	6	299	289	3	-2	11	6	38
-1	22	5	49	44	16	-1	5	6	402	399	3	-1	11	6	410
0	22	5	263	264	2	0	5	6	318	317	2	0	11	6	4_
1	22	5	88	78	8	1	5	6	274	256	3	1	11	6	328
2	22	5	137	136	6	2	5	6	41_	409	4	2	11	6	73
3	22	5	107	112	8	3	5	6	160	154	4	3	11	6	95
-3	23	5	93	109	9	4	5	6	219	226	3	4	11	6	232
-2	23	5	33	23	32	5	5	6	170	166	4	5	11	6	0
-1	23	5	46	24	45	6	5	6	160	154	5	6	11	6	126
0	23	5	77	95	19	7	5	6	0	39	1	-7	12	6	106

10Fc	10s	h	k	l	10Fo	10Fc	10s	h	k	l	10Fo	10Fc	10s
177	4	2	15	6	0	80	1	1	1	7	104	90	5
116	5	3	15	6	150	152	5	2	1	7	112	108	5
94	5	4	15	6	0	8	1	3	1	7	51	66	13
21	42	5	15	6	104	106	8	4	1	7	139	143	5
281	2	-6	16	6	0	34	1	5	1	7	140	143	5
137	4	-5	16	6	0	66	1	6	1	7	46	70	22
385	2	-4	16	6	35	47	35	-8	2	7	93	99	9
205	3	-3	16	6	277	277	3	-7	2	7	107	111	7
304	3	-2	16	6	0	12	1	-6	2	7	222	220	3
77	7	-1	16	6	0	19	1	-5	2	7	11	108	5
89	7	0	16	6	153	155	3	-4	2	7	25	16	25
125	6	1	16	6	0	31	1	-3	2	7	319	323	2
178	4	2	16	6	27	268	3	-2	2	7	137	132	3
152	5	3	16	6	3	19	30	-1	2	7	231	229	2
69	1	4	16	6	0	8	1	0	2	7	460	465	3
202	3	5	16	6	0	99	1	1	2	7	183	188	3
245	3	-6	17	6	72	95	12	2	2	7	489	498	4
51	1	-5	17	6	109	102	6	3	2	7	87	79	7
146	4	-4	17	6	73	68	10	4	2	7	273	279	3
78	5	-3	17	6	297	291	3	5	2	7	55	57	15
58	8	-2	17	6	242	240	3	6	2	7	53	75	53
186	3	-1	17	6	38	375	3	-8	3	7	3	1	30
148	4	0	17	6	77	78	5	-7	3	7	93	101	8
47	18	1	17	6	22	223	3	-6	3	7	0	8	1
54	17	2	17	6	54	48	14	-5	3	7	97	83	6
112	7	3	17	6	5	17	4	-4	3	7	122	115	4
4	18	4	17	6	0	56	1	-3	3	7	166	173	3
131	6	5	17	6	39	14	39	-2	3	7	162	167	3
210	4	-5	18	6	27	3	26	-1	3	7	470	479	4
74	9	-4	18	6	153	164	5	0	3	7	86	81	4
95	6	-3	18	6	45	51	18	1	3	7	180	182	3
150	4	-2	18	6	74	81	9	2	3	7	228	231	3
17	38	-1	18	6	34	24	34	3	3	7	167	161	4
422	4	0	18	6	42	0	42	4	3	7	143	143	5
31	9	1	18	6	49	87	48	5	3	7	85	82	9
331	3	2	18	6	0	9	1	6	3	7	48	38	20
56	8	3	18	6	71	79	11	-8	4	7	28	48	27
95	7	4	18	6	45	36	22	-7	4	7	215	212	4
225	3	-5	19	6	5	52	18	-6	4	7	38	31	28
30	1	-4	19	6	329	329	3	-5	4	7	151	151	4
115	7	-3	19	6	86	89	8	-4	4	7	33	34	33
102	7	-2	19	6	199	188	4	-3	4	7	142	142	4

Table 5b. Observed and calculated structure

h	k	l	10Fo	10Fc	10s	h	k	l	10Fo	10Fc	10s	h	k	l	10Fo	10Fc	10s
-2	4	7	216	208	2	4	10	7	0	11	1	1	18	7	65	41	11
-1	4	7	465	474	4	5	10	7	44	46	24	2	18	7	214	221	4
0	4	7	117	-21	6	6	10	7	113	110	8	3	18	7	86	78	9
1	4	7	363	368	3	-7	11	7	83	77	9	-4	19	7	38	54	38
2	4	7	140	-40	4	-6	11	7	163	171	5	-3	19	7	0	0	1
3	4	7	91	-01	7	-5	11	7	43	54	20	-2	19	7	0	1	1
4	4	7	105	96	6	-4	11	7	30	27	30	-1	19	7	45	19	44
5	4	7	142	-35	5	-3	11	7	113	123	5	0	19	7	31	46	31
6	4	7	12	9	11	-2	11	7	96	99	6	1	19	7	149	150	5
-7	5	7	26	5	26	-1	11	7	326	339	3	2	19	7	17	46	16
-6	5	7	0	58	1	0	11	7	92	93	4	3	19	7	12	11	12
-5	5	7	48	26	14	1	11	7	190	191	3	-4	20	7	39	57	39
-4	5	7	120	-19	5	2	11	7	138	137	5	-3	20	7	276	265	3
-3	5	7	25	29	25	3	11	7	64	58	10	-2	20	7	103	95	7
-2	5	7	86	-00	6	4	11	7	83	75	9	-1	20	7	147	145	5
-1	5	7	14	23	13	5	11	7	47	42	21	0	20	7	0	24	1
0	5	7	78	78	4	-7	12	7	162	165	5	1	20	7	68	55	11
1	5	7	242	247	2	-6	12	7	0	1	1	2	20	7	0	17	1
2	5	7	238	241	3	-5	12	7	201	199	4	-3	21	7	72	82	12
3	5	7	156	-46	4	-4	12	7	120	115	5	-2	21	7	38	30	38
4	5	7	23	5	23	-3	12	7	267	277	3	-1	21	7	232	225	4
5	5	7	60	73	14	-2	12	7	31	39	31	0	21	7	35	9	35
6	5	7	0	43	1	-1	12	7	181	184	3	1	21	7	0	15	1
-7	6	7	45	43	22	0	12	7	194	183	2	2	21	7	28	0	27
-6	6	7	273	279	3	1	12	7	267	262	3	-2	22	7	171	169	5
-5	6	7	0	6	1	2	12	7	180	177	4	-1	22	7	0	27	1
-4	6	7	443	451	4	3	12	7	233	223	3	0	22	7	154	156	4
-3	6	7	93	98	6	4	12	7	40	48	40	1	22	7	98	98	8
-2	6	7	590	592	5	5	12	7	167	158	5	-6	0	8	89	78	8
-1	6	7	14	38	13	-6	13	7	128	123	6	-4	0	8	146	147	4
0	6	7	130	-33	2	-5	13	7	0	81	1	-2	0	8	172	172	3
1	6	7	287	294	3	-4	13	7	0	10	1	0	0	8	410	410	2
2	6	7	0	34	1	-3	13	7	0	63	1	2	0	8	18	12	17
3	6	7	31	43	31	-2	13	7	217	224	3	4	0	8	223	221	4
4	6	7	239	231	3	-1	13	7	125	116	5	6	0	8	42	33	29
5	6	7	36	52	35	0	13	7	23	74	23	-7	1	8	177	177	4
6	6	7	150	-53	6	1	13	7	22	35	22	-6	1	8	121	116	6
-7	7	7	82	72	9	2	13	7	0	4	1	-5	1	8	263	268	3
-6	7	7	220	222	4	3	13	7	46	39	46	-4	1	8	301	301	2
-5	7	7	110	-17	6	4	13	7	46	1	19	-3	1	8	251	248	2
-4	7	7	117	98	5	5	13	7	93	86	9	-2	1	8	471	479	4
-3	7	7	0	12	1	-6	14	7	130	124	6	-1	1	8	139	141	4
-2	7	7	273	296	2	-5	14	7	0	67	1	0	1	8	111	105	3
-1	7	7	183	-73	3	-4	14	7	327	330	3	1	1	8	69	78	8
0	7	7	195	208	2	-3	14	7	44	105	43	2	1	8	0	10	1
1	7	7	0	16	1	-2	14	7	217	215	3	3	1	8	124	105	5
2	7	7	109	-16	5	-1	14	7	0	28	1	4	1	8	209	212	4
3	7	7	0	82	1	0	14	7	117	114	3	5	1	8	126	127	6

factors for $C_{14}H_{21}CrNO_3Si_2$.

h	k	l	10Fo	10Fc	10s	h	k	l	10Fo	10Fc	10s
6	4	8	28	37	27	-6	12	8	34	15	33
-7	5	8	59	63	14	-5	12	8	127	119	6
-6	5	8	110	96	6	-4	12	8	0	42	1
-5	5	8	163	157	4	-3	12	8	135	133	5
-4	5	8	0	13	1	-2	12	8	23	12	23
-3	5	8	316	316	3	-1	12	8	0	6	1
-2	5	8	115	112	5	0	12	8	0	15	1
-1	5	8	339	342	2	1	12	8	126	132	5
0	5	8	432	423	3	2	12	8	0	14	1
1	5	8	69	64	8	3	12	8	28	14	28
2	5	8	322	322	3	4	12	8	51	25	16
3	5	8	103	87	6	-6	13	8	153	145	5
4	5	8	15	44	15	-5	13	8	32	67	32
5	5	8	177	179	5	-4	13	8	269	271	3
-7	6	8	41	9	27	-3	13	8	230	225	3
-6	6	8	37	72	36	-2	13	8	151	157	4
-5	6	8	229	233	3	-1	13	8	133	143	5
-4	6	8	0	22	1	0	13	8	0	13	1
-3	6	8	109	106	5	1	13	8	114	115	6
-2	6	8	190	185	3	2	13	8	0	86	1
-1	6	8	49	47	11	3	13	8	219	227	4
0	6	8	39	34	11	4	13	8	136	115	6
1	6	8	43	25	42	-5	14	8	44	33	21
2	6	8	87	68	7	-4	14	8	41	36	23
3	6	8	0	16	1	-3	14	8	35	2	35
4	6	8	47	48	46	-2	14	8	79	73	8
5	6	8	0	2	1	-1	14	8	105	104	6
-7	7	8	0	44	1	0	14	8	45	45	17
-6	7	8	37	36	36	1	14	8	19	7	19
-5	7	8	0	15	1	2	14	8	132	144	6
-4	7	8	93	95	6	3	14	8	127	125	6
-3	7	8	202	204	3	4	14	8	57	56	16
-2	7	8	330	327	3	-5	15	8	153	155	5
-1	7	8	153	145	4	-4	15	8	83	74	9
0	7	8	223	217	2	-3	15	8	344	353	3
1	7	8	145	150	4	-2	15	8	20	30	20
2	7	8	140	133	5	-1	15	8	131	125	5
3	7	8	94	91	7	0	15	8	46	55	22
4	7	8	260	268	3	1	15	8	64	55	11
5	7	8	159	152	5	2	15	8	84	97	9
-7	8	8	0	42	1	3	15	8	23	51	23
-6	8	8	120	126	6	4	15	8	0	17	1
-5	8	8	104	111	7	-5	16	8	22	25	22
-4	8	8	218	218	3	-4	16	8	102	97	7
-3	8	8	74	66	8	-3	16	8	0	20	1
-2	8	8	91	82	6	-2	16	8	0	19	1
-1	8	8	180	184	3	-1	16	8	90	82	7
0	8	8	80	79	30	0	16	8	74	87	24

h	k	l	10Fo	10Fc	10s	h	k	l	10Fo	10Fc	10s	h	k	l	10Fo
4	7	7	57	51	_3	1	14	7	29	1	29	6	1	8	160
5	7	7	0	7	1	2	14	7	350	351	3	-7	2	8	78
6	7	7	0	9	1	3	14	7	18	49	17	-6	2	8	40
-7	8	7	139	150	6	4	14	7	269	260	3	-5	2	8	95
-6	8	7	62	52	_2	5	14	7	94	104	9	-4	2	8	87
-5	8	7	417	420	4	-6	15	7	42	50	27	-3	2	8	179
-4	8	7	79	83	8	-5	15	7	57	54	13	-2	2	8	10
-3	8	7	485	489	4	-4	15	7	135	130	5	-1	2	8	29
-2	8	7	0	35	1	-3	15	7	8_	71	8	0	2	8	12_
-1	8	7	341	346	3	-2	15	7	80	71	8	1	2	8	56
0	8	7	61	56	45	-1	15	7	125	126	5	2	2	8	0
1	8	7	222	232	3	0	15	7	28	9	28	3	2	8	0
2	8	7	145	149	4	1	15	7	0	4	1	4	2	8	43
3	8	7	97	81	6	2	15	7	17	72	17	5	2	8	0
4	8	7	20	57	_9	3	15	7	86	97	9	6	2	8	0
5	8	7	149	145	5	4	15	7	0	26	1	-7	3	8	165
6	8	7	39	56	38	-5	16	7	42	82	42	-6	3	8	333
-7	9	7	0	43	1	-4	16	7	97	98	7	-5	3	8	86
-6	9	7	43	53	22	-3	16	7	159	156	4	-4	3	8	195
-5	9	7	154	152	4	-2	16	7	98	102	7	-3	3	8	196
-4	9	7	84	79	7	-1	16	7	152	163	5	-2	3	8	108
-3	9	7	77	74	7	0	16	7	160	160	3	-1	3	8	275
-2	9	7	162	161	3	1	16	7	300	291	3	0	3	8	124
-1	9	7	186	190	3	2	16	7	44	30	43	1	3	8	412
0	9	7	194	190	2	3	16	7	225	221	4	2	3	8	176
1	9	7	111	109	5	4	16	7	8_	69	10	3	3	8	23_
2	9	7	258	260	3	-5	17	7	142	145	5	4	3	8	139
3	9	7	0	55	1	-4	17	7	0	50	1	5	3	8	80
4	9	7	20	10	20	-3	17	7	76	82	9	6	3	8	0
5	9	7	32	14	31	-2	17	7	230	230	3	-7	4	8	0
6	9	7	117	118	7	-1	17	7	9_	77	7	-6	4	8	57
-7	10	7	0	9	1	0	17	7	243	241	4	-5	4	8	43
-6	10	7	258	256	3	1	17	7	96	95	7	-4	4	8	153
-5	10	7	75	74	9	2	17	7	0	52	1	-3	4	8	129
-4	10	7	209	208	3	3	17	7	0	47	1	-2	4	8	93
-3	10	7	0	34	1	4	17	7	0	53	1	-1	4	8	274
-2	10	7	350	339	3	-5	18	7	42	33	24	0	4	8	53
-1	10	7	0	57	1	-4	18	7	87	100	9	1	4	8	52
0	10	7	371	383	2	-3	18	7	37	40	36	2	4	8	16
1	10	7	247	243	3	-2	18	7	122	117	6	3	4	8	173
2	10	7	155	151	4	-1	18	7	44	41	43	4	4	8	87
3	10	7	85	94	8	0	18	7	247	243	2	5	4	8	49

10Fc	10s	h	k	l	10Fo	10Fc	10s	h	k	l	10Fo	10Fc	10s
160	6	1	8	8	38	20	38	1	16	8	0	24	1
56	10	2	8	8	48	48	15	2	16	8	42	21	41
4	40	3	8	8	159	175	5	3	16	8	9	50	9
112	7	4	8	8	119	122	6	-4	17	8	100	101	7
95	7	5	8	8	112	100	7	-3	17	8	33	25	32
177	3	-7	9	8	129	101	6	-2	17	8	127	119	6
6	10	-6	9	8	112	111	7	-1	17	8	36	7	36
1	28	-5	9	8	0	26	1	0	17	8	236	228	2
123	3	-4	9	8	163	160	4	1	17	8	45	34	20
52	10	-3	9	8	38	42	21	2	17	8	192	186	4
32	1	-2	9	8	125	117	5	3	17	8	27	19	26
18	1	-1	9	8	329	329	3	-4	18	8	0	30	1
26	42	0	9	8	147	143	3	-3	18	8	33	7	33
33	1	1	9	8	439	446	4	-2	18	8	216	213	4
10	1	2	9	8	134	132	5	-1	18	8	0	51	1
160	5	3	9	8	322	325	3	0	18	8	84	76	6
335	3	4	9	8	142	140	5	1	18	8	66	78	12
89	7	5	9	8	46	10	20	2	18	8	57	54	15
191	3	-6	10	8	0	17	1	-3	19	8	25	51	24
187	3	-5	10	8	0	1	1	-2	19	8	170	161	5
108	5	-4	10	8	17	27	17	-1	19	8	177	173	4
283	2	-3	10	8	74	81	8	0	19	8	0	14	1
117	3	-2	10	8	148	145	4	1	19	8	248	247	4
412	4	-1	10	8	142	145	4	2	19	8	78	66	10
172	3	0	10	8	15	12	15	-2	20	8	57	24	15
234	3	1	10	8	0	11	1	-1	20	8	154	145	5
135	5	2	10	8	184	191	4	0	20	8	0	62	1
80	10	3	10	8	195	197	4	1	20	8	0	3	1
8	1	4	10	8	70	78	11	-7	0	9	69	78	13
44	1	5	10	8	0	35	1	-5	0	9	144	151	5
26	13	-6	11	8	0	12	1	-3	0	9	548	538	5
45	19	-5	11	8	200	202	4	-1	0	9	625	625	6
155	4	-4	11	8	58	60	12	1	0	9	226	228	3
135	4	-3	11	8	116	115	5	3	0	9	39	10	39
95	6	-2	11	8	158	155	4	5	0	9	67	65	13
290	2	-1	11	8	0	10	1	-7	1	9	8	8	7
44	12	0	11	8	326	336	10	-6	1	9	96	92	7
7	11	1	11	8	274	272	3	-5	1	9	58	63	12
81	15	2	11	8	376	373	3	-4	1	9	54	23	12
168	4	3	11	8	75	77	10	-3	1	9	182	184	4
94	8	4	11	8	148	154	5	-2	1	9	198	199	3
4	49	5	11	8	68	62	13	-1	1	9	124	127	5

Table 5b Observed and calculated structure

h	k	l	10Fo	10Fc	10s	h	k	l	10Fo	10Fc	10s	h	k	l	10Fo	10Fc	10s
0	1	9	146	-49	3	-5	8	9	142	146	5	0	16	9	66	56	66
1	1	9	184	-91	4	-4	8	9	62	64	12	1	16	9	295	291	3
2	1	9	46	58	46	-3	8	9	161	160	4	2	16	9	0	42	1
3	1	9	132	-35	6	-2	8	9	118	120	5	-3	17	9	41	59	26
4	1	9	0	65	1	-1	8	9	70	63	9	-2	17	9	23	12	23
5	1	9	135	-33	6	0	8	9	0	21	1	-1	17	9	125	119	6
-7	2	9	0	46	1	1	8	9	166	164	4	0	17	9	45	53	45
-6	2	9	140	-42	5	2	8	9	207	221	4	1	17	9	142	139	6
-5	2	9	44	4	43	3	8	9	265	260	3	-2	18	9	136	134	6
-4	2	9	384	385	3	4	8	9	33	69	32	-1	18	9	180	185	5
-3	2	9	86	-01	7	-6	9	9	44	47	23	0	18	9	180	174	3
-2	2	9	425	425	4	-5	9	9	100	89	7	1	18	9	0	30	1
-1	2	9	0	7	1	-4	9	9	167	159	4	-6	0	10	0	18	1
0	2	9	304	301	2	-3	9	9	0	67	1	-4	0	10	113	107	6
1	2	9	84	87	7	-2	9	9	40	3	19	-2	0	10	313	314	3
2	2	9	222	222	3	-1	9	9	37	37	36	0	0	10	55	69	34
3	2	9	0	76	1	0	9	9	284	287	2	2	0	10	190	192	4
4	2	9	118	-23	7	1	9	9	68	58	11	4	0	10	143	151	6
5	2	9	0	51	1	2	9	9	166	164	5	-6	1	10	74	72	11
-7	3	9	114	-02	7	3	9	9	0	2	1	-5	1	10	114	121	6
-6	3	9	76	72	10	4	9	9	51	29	50	-4	1	10	188	186	4
-5	3	9	74	43	9	-6	10	9	260	254	4	-3	1	10	149	136	4
-4	3	9	59	52	11	-5	10	9	42	2	42	-2	1	10	199	201	4
-3	3	9	43	4	42	-4	10	9	175	174	4	-1	1	10	171	171	4
-2	3	9	0	7	1	-3	10	9	102	90	6	0	1	10	221	221	3
-1	3	9	163	-63	4	-2	10	9	35	17	34	1	1	10	173	168	4
0	3	9	0	7	1	-1	10	9	94	84	7	2	1	10	0	54	1
1	3	9	103	-01	6	0	10	9	191	190	3	3	1	10	179	175	4
2	3	9	144	-38	5	1	10	9	17	16	17	4	1	10	31	46	31
3	3	9	0	91	1	2	10	9	369	374	3	-6	2	10	0	39	1
4	3	9	0	97	1	3	10	9	122	137	6	-5	2	10	35	39	35
5	3	9	0	57	1	4	10	9	225	226	4	-4	2	10	134	125	5
-6	4	9	146	-52	5	-5	11	9	0	69	1	-3	2	10	130	142	5
-5	4	9	227	226	3	-4	11	9	0	16	1	-2	2	10	24	27	24
-4	4	9	82	87	8	-3	11	9	0	54	1	-1	2	10	156	152	4
-3	4	9	216	221	3	-2	11	9	0	53	1	0	2	10	172	163	3
-2	4	9	122	-28	5	-1	11	9	163	158	4	1	2	10	231	225	3
-1	4	9	171	-81	4	0	11	9	201	198	3	2	2	10	95	101	8
0	4	9	51	67	23	1	11	9	90	73	8	3	2	10	155	158	5
1	4	9	246	245	3	2	11	9	48	28	47	4	2	10	63	69	14
2	4	9	34	26	33	3	11	9	125	133	6	-6	3	10	140	120	6
3	4	9	229	230	4	4	11	9	111	119	8	-5	3	10	227	222	3
4	4	9	54	43	16	-5	12	9	150	142	5	-4	3	10	160	153	4
5	4	9	82	79	10	-4	12	9	26	24	26	-3	3	10	257	262	3
-6	5	9	54	56	15	-3	12	9	259	256	3	-2	3	10	30	22	29
-5	5	9	108	-16	7	-2	12	9	0	37	1	-1	3	10	135	133	5
-4	5	9	43	47	18	-1	12	9	226	228	3	0	3	10	116	119	4
-3	5	9	182	-76	4	0	12	9	92	79	20	1	3	10	110	110	6

factors for $C_{14}H_{21}CrNO_3Si_2$.

h	k	l	10Fo	10Fc	10s	h	k	l	10Fo	10Fc	10s
2	6	10	0	21	1	0	1	11	56	69	55
3	6	10	0	25	1	1	1	11	96	97	8
4	6	10	0	25	1	2	1	11	144	142	5
-5	7	10	90	88	8	3	1	11	0	73	1
-4	7	10	87	73	8	-5	2	11	63	64	13
-3	7	10	221	221	4	-4	2	11	167	168	5
-2	7	10	230	233	3	-3	2	11	100	105	7
-1	7	10	211	214	4	-2	2	11	0	36	1
0	7	10	255	253	2	-1	2	11	48	48	48
1	7	10	0	75	1	0	2	11	0	64	1
2	7	10	45	61	45	1	2	11	130	134	6
3	7	10	33	33	32	2	2	11	41	29	27
-5	8	10	0	1	1	3	2	11	52	2	52
-4	8	10	181	171	4	-5	3	11	80	76	10
-3	8	10	58	53	13	-4	3	11	156	147	5
-2	8	10	146	133	5	-3	3	11	37	40	37
-1	8	10	47	39	46	-2	3	11	130	127	6
0	8	10	0	26	1	-1	3	11	71	61	10
1	8	10	126	115	6	0	3	11	178	178	3
2	8	10	0	67	1	1	3	11	121	112	6
3	8	10	105	108	7	2	3	11	145	146	5
-5	9	10	254	253	4	3	3	11	133	141	7
-4	9	10	19	69	18	-5	4	11	153	154	5
-3	9	10	192	192	4	-4	4	11	0	1	1
-2	9	10	162	159	4	-3	4	11	117	117	6
-1	9	10	22	46	21	-2	4	11	77	77	9
0	9	10	134	127	6	-1	4	11	90	83	7
1	9	10	114	121	7	0	4	11	0	14	1
2	9	10	0	30	1	1	4	11	46	54	20
3	9	10	116	108	7	2	4	11	145	143	5
-5	10	10	96	94	8	-4	5	11	47	45	18
-4	10	10	0	67	1	-3	5	11	135	140	6
-3	10	10	0	48	1	-2	5	11	94	91	7
-2	10	10	34	18	34	-1	5	11	128	125	5
-1	10	10	85	89	8	0	5	11	47	13	32
0	10	10	79	80	35	1	5	11	168	165	5
1	10	10	144	153	5	2	5	11	0	4	1
2	10	10	0	78	1	-4	6	11	0	7	1
3	10	10	48	46	47	-3	6	11	0	33	1
-4	11	10	168	160	5	-2	6	11	80	98	9
-3	11	10	0	27	1	-1	6	11	55	66	15
-2	11	10	159	154	5	0	6	11	241	239	2
-1	11	10	47	43	17	1	6	11	0	19	1
0	11	10	75	82	11	2	6	11	135	128	6
1	11	10	74	78	10	-4	7	11	98	105	8
2	11	10	60	61	14	-3	7	11	187	189	4
-4	12	10	120	123	7	-2	7	11	238	237	4
-3	12	10	178	187	4	-1	7	11	146	148	5

h	k	l	10Fo	10Fc	10s	h	k	l	10Fo	10Fc	10s	h	k	l	10Fo
-2	5	9	139	144	4	1	12	9	288	285	3	2	3	10	251
-1	5	9	0	5	1	2	12	9	0	54	1	3	3	10	64
0	5	9	0	15	1	3	12	9	207	210	4	4	3	10	182
1	5	9	132	129	5	-5	13	9	121	123	6	-6	4	10	158
2	5	9	19	18	18	-4	13	9	150	149	5	-5	4	10	130
3	5	9	0	38	1	-3	13	9	162	158	5	-4	4	10	50
4	5	9	19	44	18	-2	13	9	102	96	7	-3	4	10	0
5	5	9	51	52	20	-1	13	9	32	44	31	-2	4	10	42
-6	6	9	169	159	5	0	13	9	63	54	11	-1	4	10	182
-5	6	9	142	121	5	1	13	9	36	37	36	0	4	10	102
-4	6	9	117	110	6	2	13	9	0	28	1	1	4	10	0
-3	6	9	23	14	23	3	13	9	69	77	12	2	4	10	175
-2	6	9	170	177	4	-5	14	9	56	52	16	3	4	10	0
-1	6	9	224	230	3	-4	14	9	185	185	4	4	4	10	14
0	6	9	186	182	2	-3	14	9	42	41	41	-6	5	10	161
1	6	9	0	11	1	-2	14	9	406	409	4	-5	5	10	33
2	6	9	0	64	1	-1	14	9	150	144	5	-4	5	10	318
3	6	9	0	6	1	0	14	9	329	327	2	-3	5	10	25
4	6	9	198	202	4	1	14	9	0	30	1	-2	5	10	169
5	6	9	0	5	1	2	14	9	166	168	5	-1	5	10	229
-6	7	9	33	26	33	3	14	9	87	71	9	0	5	10	0
-5	7	9	0	28	1	-4	15	9	180	181	5	1	5	10	151
-4	7	9	54	32	13	-3	15	9	32	21	32	2	5	10	41
-3	7	9	24	17	23	-2	15	9	150	147	5	3	5	10	81
-2	7	9	152	153	4	-1	15	9	0	47	1	4	5	10	44
-1	7	9	86	82	7	0	15	9	0	36	1	-5	6	10	115
0	7	9	62	59	7	1	15	9	0	22	1	-4	6	10	0
1	7	9	102	102	6	2	15	9	0	15	1	-3	6	10	183
2	7	9	92	82	8	-4	16	9	0	12	1	-2	6	10	174
3	7	9	162	147	5	-3	16	9	128	134	6	-1	6	10	43
4	7	9	50	83	49	-2	16	9	0	5	1	0	6	10	32
-6	8	9	0	28	1	-1	16	9	242	236	3	1	6	10	48

10Fc	10s	h	k	l	10Fo	10Fc	10s	h	k	l	10Fo	10Fc	10s
255	4	-2	12	10	176	174	4	0	7	11	155	154	3
69	13	-1	12	10	19	52	18	1	7	11	44	16	22
175	5	0	12	10	164	169	3	2	7	11	54	69	18
150	5	1	12	10	202	201	4	-4	8	11	57	34	14
134	6	2	12	10	90	102	9	-3	8	11	60	38	13
29	16	-4	13	10	0	10	1	-2	8	11	0	49	1
51	1	-3	13	10	132	131	6	-1	8	11	186	189	4
25	42	-2	13	10	48	21	17	0	8	11	104	98	5
185	4	-1	13	10	151	151	5	1	8	11	184	189	5
99	4	0	13	10	157	155	5	2	8	11	20	70	19
55	1	1	13	10	95	108	8	-3	9	11	83	93	10
170	4	2	13	10	113	124	7	-2	9	11	108	109	7
7	1	-3	14	10	181	176	4	-1	9	11	134	136	6
24	14	-2	14	10	38	43	38	0	9	11	72	75	26
158	5	-1	14	10	194	194	4	1	9	11	0	27	1
18	32	0	14	10	30	37	29	-3	10	11	93	89	8
306	3	1	14	10	120	123	7	-2	10	11	137	131	5
42	25	-2	15	10	0	25	1	-1	10	11	38	59	38
172	4	-1	15	10	123	129	6	0	10	11	70	32	7
227	3	0	15	10	27	11	26	1	10	11	44	0	43
77	1	1	15	10	124	118	7	-3	11	11	165	163	5
154	5	-1	16	10	0	42	1	-2	11	11	0	96	1
53	25	-5	0	11	129	143	6	-1	11	11	144	145	5
73	9	-3	0	11	0	18	1	0	11	11	56	42	10
59	43	-1	0	11	109	109	6	1	11	11	91	84	9
104	6	1	0	11	0	39	1	-2	12	11	48	67	48
8	1	3	0	11	0	46	1	-1	12	11	81	89	10
182	4	-5	1	11	52	35	16	0	12	11	100	98	9
181	4	-4	1	11	0	66	1						
6	42	-3	1	11	152	161	5						
37	32	-2	1	11	0	13	1						
71	17	-1	1	11	102	101	7						

Structural parameters for

(η^6-pyridine)$Cr(CO)_3$

Table 1a Atomic coordinates (x 10^4) and equivalent isotropic displacement parameters (A^2 x 10^3) for $C_8H_5CrNO_3$ U(eq) is defined as one third of the trace of the orthogonalized U_{ij} tensor

	x	y	z	U(eq)
Cr(1)	2426(11)	260(16)	1842(11)	46(8)
C(1)	3195(8)	-996(13)	3392(9)	72(7)
O(1)	3663(7)	-1748(10)	4332(6)	108(6)
C(2)	1762(8)	-1801(13)	998(9)	65(6)
O(2)	1342(7)	-3102(9)	455(7)	88(5)
C(3)	870(8)	448(10)	2188(7)	53(5)
O(3)	-81(6)	523(8)	2406(6)	78(4)
N(11)	3484(8)	2774(10)	2508(7)	74(5)
C(11)	2309(10)	3059(11)	1456(11)	74(8)
C(12)	1975(8)	2201(12)	257(9)	70(6)
C(13)	2890(9)	1013(12)	120(8)	65(6)
C(14)	4084(8)	662(11)	1155(8)	57(6)
C(15)	4337(8)	1565(13)	2315(8)	69(6)
H(14)	4890	-17	1140	70
H(12)	1060	255	-530	80
H(15)	5170	1300	3210	79
H(13)	2660	190	-730	81
H(11)	1570	3790	1680	93

Table 2a Bond lengths [A] and angles [deg] for $C_9H_5CrNO_3$

Cr(1)-C(1)	1 875(10)
Cr(1)-C(2)	1 838(11)
Cr(1)-C(3)	1 857(8)
Cr(1)-N(11)	2 217(7)
Cr(1)-C(11)	2 178(8)
Cr(1)-C(12)	2 215(8)
Cr(1)-C(13)	2 224(7)
Cr(1)-C(14)	2 205(7)
Cr(1)-C(15)	2 165(8)
C(1)-O(1)	1 133(12)
C(2)-O(2)	1 165(13)
C(3)-O(3)	1 137(10)
N(11)-C(11)	1 383(14)
N(11)-C(15)	1 374(13)
C(11)-C(12)	1 406(15)
C(12)-C(13)	1 389(14)
C(13)-C(14)	1 396(12)
C(14)-C(15)	1 397(13)
C(1)-Cr(1)-C(2)	89 1(4)
C(1)-Cr(1)-C(3)	88 5(3)
C(1)-Cr(1)-N(11)	98 2(4)
C(1)-Cr(1)-C(11)	131 2(4)
C(1)-Cr(1)-C(12)	164 9(4)
C(1)-Cr(1)-C(13)	139 5(3)
C(1)-Cr(1)-C(14)	104 6(3)
C(1)-Cr(1)-C(15)	87 6(3)
C(2)-Cr(1)-C(3)	87 8(3)
C(2)-Cr(1)-N(11)	165 6(3)
C(2)-Cr(1)-C(11)	139 4(4)
C(2)-Cr(1)-C(12)	103 9(4)
C(2)-Cr(1)-C(13)	87 3(3)
C(2)-Cr(1)-C(14)	98 9(3)
C(2)-Cr(1)-C(15)	132 3(4)
C(3)-Cr(1)-N(11)	104.7(3)
C(3)-Cr(1)-C(11)	88 5(3)
C(3)-Cr(1)-C(12)	99 4(3)
C(3)-Cr(1)-C(13)	131 7(3)
C(3)-Cr(1)-C(14)	165 3(3)
C(3)-Cr(1)-C(15)	139 5(4)
N(11)-Cr(1)-C(11)	36 7(4)
N(11)-Cr(1)-C(12)	67 5(3)
N(11)-Cr(1)-C(13)	79 1(3)
N(11)-Cr(1)-C(14)	67 3(3)
N(11)-Cr(1)-C(15)	36 5(4)
C(11)-Cr(1)-C(12)	37 3(4)
C(11)-Cr(1)-C(13)	65 9(3)
C(11)-Cr(1)-C(14)	77 9(3)
C(11)-Cr(1)-C(15)	64 9(4)
C(12)-Cr(1)-C(13)	36 5(4)
C(12)-Cr(1)-C(14)	66 3(3)
C(12)-Cr(1)-C(15)	78 0(3)
C(13)-Cr(1)-C(14)	36 7(3)
C(13)-Cr(1)-C(15)	66 1(3)

C(14)-Cr(1)-C(15)	37 3(3)
Cr(1)-C(1)-O(1)	179 6(9)
Cr(1)-C(2)-O(2)	179 6(7)
Cr(1)-C(3)-O(3)	178 4(7)
Cr(1)-N(11)-C(11)	70 1(4)
Cr(1)-N(11)-C(15)	69 7(5)
C(11)-N(11)-C(15)	115 3(7)
Cr(1)-C(11)-N(11)	73 2(5)
Cr(1)-C(11)-C(12)	72 7(5)
N(11)-C(11)-C(12)	124 0(5)
Cr(1)-C(12)-C(11)	69 9(5)
Cr(1)-C(12)-Cr(13)	72 1(4)
C(11)-C(12)-Cr(13)	117 9(8)
Cr(1)-C(13)-C(12)	71 4(4)
Cr(1)-C(13)-C(14)	70 9(4)
C(12)-C(13)-C(14)	120 5(8)
Cr(1)-C(14)-C(13)	72 4(4)
Cr(1)-C(14)-C(15)	69 8(4)
C(13)-C(14)-C(15)	118 0(7)
Cr(1)-C(15)-N(11)	73 8(4)
Cr(1)-C(15)-C(14)	72 9(5)
N(11)-C(15)-C(14)	124 3(7)

Symmetry transformations used to generate equivalent atoms

Table 3a Anisotropic displacement parameters (A^2 x 10^3) for $C_8H_5CrNO_3$
The anisotropic displacement factor exponent takes the form
$-2\ pi^2\ [\ h^2\ a^{*2}\ U11 +\quad +\ 2\ h\ k\ a^*\ b^*\ U12\ ]$

	U11	U22	U33	U12	U13	U23
Cr(1)	46(1)	54(1)	45(1)	46(2)	24(2)	84(1)
C(1)	48(2)	99(2)	78(3)	10(6)	34(9)	12(2)
O(1)	94(9)	157(8)	75(6)	30(6)	34(6)	72(7)
C(2)	64(3)	71(2)	79(7)	11(9)	49(10)	20(2)
O(2)	103(6)	59(6)	116(6)	-10(6)	59(5)	-16(5)
C(3)	54(6)	60(9)	41(7)	0(6)	13(6)	4-(7)
O(3)	55(11)	108(9)	84(8)	-3(7)	42(8)	-14(9)
N(11)	72(3)	77(3)	79(5)	-15(8)	34(8)	-12(2)
C(11)	89(8)	45(9)	116(9)	7(8)	71(8)	11(8)
C(12)	65(7)	73(5)	71(8)	7(5)	23(7)	38(6)
C(13)	77(11)	81(13)	54(11)	-12(8)	46(9)	10(9)
C(14)	53(10)	71(8)	56(7)	-2(5)	31(7)	8(7)
C(15)	44(8)	91(9)	72(8)	-8(7)	21(6)	16(6)

Observed and calculated structural factors for

$(\eta^6$-pyridine)$Cr(CO)_3$

CR COMPLEX

Columns are 10Fo 10Fc 10000Sig, * for Insignificant

l	kFo	Fc	Sig
-10,	0,	l	
2	191	186	1475
4	22	28	1996
6	74	71	868
-10,	1,	l	
2	15	17	2479
3	149	154	905
4	87	94	598
5	260	270	1027
-9,	0,	l	
2	90	104	911
4	196	199	1345
6	150	165	1432
8	81	80	868
-9,	1,	l	
1	96	80	673
2	150	156	1012
3	151	145	997
4	6	13	1597*
5	8	6	4375*
6	52	65	675
7	148	149	938
8	10	9	5527*
-9,	2,	l	
1	33	34	963
2	46	47	736
3	28	34	1086
4	182	187	997
5	52	69	704
6	151	157	957
7	37	36	920
-9,	3,	l	
1	206	204	1058
2	20	25	1518
3	127	125	905
4	49	43	736
5	32	35	980
6	62	58	690
-8,	0,	l	
2	226	225	1258
9	57	60	720
-8,	2,	l	
1	75	70	552
2	271	272	905
3	71	75	552
4	133	129	798
5	29	36	905
6	6	5	1477*
7	10	21	1746*
8	107	113	765
-8,	3,	l	
1	25	25	1282
2	15	21	2330
3	105	104	734
4	51	43	659
5	210	202	966
6	119	112	822
7	106	107	751
-8,	4,	l	
1	139	139	905
2	229	221	1012
3	183	183	1027
4	60	54	659
5	41	43	827
6	64	62	659
-7,	0,	l	
2	264	268	1128
4	711	662	4295
6	284	292	1215
8	94	91	955
-7,	1,	l	
1	314	325	813
2	182	192	828
3	288	300	798
4	275	278	813
5	9	9	999
6	10	9	1955*
7	181	174	920
8	86	74	628
9	282	292	1012
2	81	83	583
3	196	189	905
4	99	85	706
5	48	52	673
6	75	75	567
7	146	146	926
8	57	56	675
-7,	4,	l	
1	22	24	1958
2	64	62	644
3	171	162	982
4	140	131	895
5	148	143	895
6	163	163	1027
7	99	90	704
-7,	5,	l	
1	168	158	1074
2	160	149	938
3	89	81	636
4	72	76	628
5	22	29	1346
-6,	0,	l	
2	380	391	998
4	95	109	955
6	526	555	1128
8	354	352	1258
10	259	247	1475
-6,	1,	l	
1	198	198	767
2	150	151	767
3	666	621	2792
4	54	62	506
5	406	435	767
6	96	83	659
7	191	200	890
8	51	56	659
9	24	21	1668
10	32	37	1050
-6,	2,	l	
1	174	178	708

l	kFo	Fc	Sig
4	294	295	828
5	331	333	859
6	107	101	778
7	66	61	583
8	121	125	890
9	45	51	843
	-6, 4, 1		
1	165	164	935
2	193	193	905
3	66	61	552
4	58	70	598
5	199	207	935
6	125	112	859
7	192	194	1012
8	242	234	1043
	-6, 5, 1		
1	45	38	751
2	93	92	628
3	132	127	843
4	179	166	997
5	117	109	827
6	98	89	690
	-5, 0, 1		
2	379	379	911
4	810	767	3644
6	96	92	998
8	78	82	781
10	180	182	1475
	-5, 1, 1		
1	598	565	2546
2	53	42	399
3	566	527	2577
4	200	222	706
5	165	166	767
6	40	42	598
7	325	337	828
8	152	147	935
9	240	250	951
10	5	8	2960*

4	252	251	1258
6	21	25	1692
8	271	286	1388
-8,	1,	l	
1	54	61	614
2	13	17	2201*
3	210	212	890
4	10	4	2144*
5	264	264	890
6	83	101	598
7	161	168	997
8	57	62	675

-7,	2,	l	
1	173	176	890
2	246	263	843
3	56	54	550
4	347	354	828
5	154	156	905
6	312	310	890
7	161	166	966
8	176	185	1012
9	118	127	798
-7,	3,	l	
1	326	330	890

2	265	285	767
3	6	12	3400*
4	15	1	1768
5	145	146	859
6	114	115	767
7	5	14	3001*
8	263	261	951
9	126	136	890
-6,	3,	l	
1	66	62	522
2	44	55	611
3	199	205	828

```
 1   138   141   767
 2   180   200   706
 3    15     7  1347
 4   364   381   736
 5   204   212   767
 6   236   249   798
 7     7    13  4014*
 8    24    19  1084
 9    57    68   675
10   148   154   920
    -5,   3, 1
 1   288   296   767
```

:R COMPLEX

Columns are 10Fo 10Fc 10000Sig, * for Insignificant

l	kFo	Fc	Sig	l	kFo	Fc	Sig	l	kFo	Fc	Sig
	-5, 3, l			3	121	132	706	5	292	308	675
2	224	222	767	4	353	356	675	6	226	226	736
3	64	63	460	5	87	84	598	7	456	472	767
4	116	115	706	6	188	186	798	8	142	142	905
5	260	273	828	7	34	31	765	9	276	277	951
6	189	192	874	8	301	309	890	10	6	19	1698*
7	275	276	890	9	45	55	767		-3, 2, l		
8	8	4	4336*	10	135	132	920	1	148	160	598
9	280	274	1012		-4, 3, l			2	55	30	399
	-5, 4, l			1	57	46	444	3	49	65	383
1	51	46	583	2	164	156	736	4	618	587	2485
2	176	171	859	3	684	651	2730	5	174	180	736
3	243	257	859	4	347	357	736	6	259	276	767
4	220	227	874	5	395	415	767	7	78	77	536
5	221	215	890	6	80	74	567	8	18	24	1396
6	184	183	951	7	123	115	767	9	34	28	935
7	22	16	1394	8	41	53	778	10	171	177	1074
8	19	14	1625	9	62	64	644		-3, 3, l		
	-5, 5, l				-4, 4, l			1	403	436	644
1	231	231	920	1	238	251	798	2	72	75	522
2	164	174	951	2	170	182	827	3	211	223	706
3	33	25	852	3	215	226	813	4	67	70	475
4	66	66	583	4	141	139	874	5	129	132	813
5	50	59	720	5	208	215	874	6	161	168	859
6	183	180	1027	6	158	147	951	7	293	296	874
7	155	153	1000	7	186	191	966	8	67	61	583
	-5, 6, l			8	250	250	1012	9	204	202	1012
1	5	16	3391*		-4, 5, l				-3, 4, l		
2	45	43	796	1	25	30	1072	1	264	276	751
3	143	141	874	2	199	192	905	2	382	397	736
4	131	126	905	3	102	100	706	3	247	258	767
5	118	103	813	4	285	283	905	4	341	352	798
	-4, 0, l			5	108	98	751	5	419	429	828
2	1246	1256	3124	6	172	172	1012	6	247	249	890
4	42	48	607	7	96	100	690	7	66	65	598
6	639	600	3948		-4, 6, l			8	28	24	1089
8	254	244	1215	1	184	183	997		-3, 5, l		
10	175	174	1475	2	155	151	1027	1	202	202	859

l	kFo	Fc	Sig
1	87	86	598
2	78	79	614
	-2, 0, 1		
2	487	456	2386
4	504	465	3080
6	414	426	998
8	396	394	1215
10	195	192	1475
	-2, 1, 1		
1	459	428	1718
2	437	405	1810
3	26	7	491
4	299	319	583
5	539	509	2485
6	208	202	736
7	31	10	763
8	19	12	1266
9	94	98	644
10	26	26	1212
	-2, 2, 1		
1	575	547	2025
2	53	46	383
3	220	228	583
4	243	248	644
5	61	67	430
6	380	401	736
7	195	190	828
8	324	331	890
9	81	86	567
10	121	117	828
	-2, 3, 1		
1	13	9	1018
2	108	108	690
3	626	607	2531
4	90	93	659
5	187	192	767
6	84	89	581
7	179	184	890
8	5	2	2500*

1	251	271	598
2	93	88	604
3	357	390	614
4	112	110	690
5	570	528	2623
6	210	208	767
7	42	45	628
8	60	60	567
9	142	149	982
10	19	22	1526
-4,	2,	1	
1	105	124	636
2	322	347	644
4	46	45	765
5	8	2	4513*
-3,	0,	1	
2	935	921	2733
4	813	788	3211
6	429	454	998
8	71	65	738
10	154	169	1475
-3,	1,	1	
1	454	432	1994
2	737	702	2025
3	467	426	2148
4	211	216	614
3	24	28	1011
4	22	26	1148
5	53	45	673
6	91	91	659
7	124	130	890
-3,	6,	1	
1	14	10	1793
2	103	105	767
3	146	141	895
4	128	136	859
5	119	113	890
6	4	8	2735*
-3,	7,	1	

```
9   143   143   890
   -2,   4, 1
1   129   142   767
2   259   266   736
3   126   132   798
4     6     1 3538*
5   165   178   859
6   117   117   798
7    46    38   720
8   153   159 1043
   -2,   5, 1
1     6     3 3499*
2   147   138   859
```

:R COMPLEX

Columns are 10Fo 10Fc 10000Sig, * for Insignificant

l	kFo	Fc	Sig
-2,	5,	l	
3	150	146	890
4	160	147	920
5	183	186	935
6	122	119	859
7	21	29	1359
-2,	6,	l	
1	165	162	951
2	163	166	951
3	38	30	828
4	134	132	859
5	26	27	1161
6	79	84	614
-2,	7,	l	
1	35	38	935
2	49	52	765
3	169	160	1104
-1,	0,	l	
2	984	992	2126
4	317	340	781
6	348	354	998
8	33	34	1215
10	56	53	998
-1,	1,	l	
1	946	1011	1473
2	64	61	444
3	254	266	522
4	567	536	2240
5	87	103	614
6	180	186	736
7	274	280	798
8	68	73	552
9	205	205	982
10	4	6	2689*
-1,	2,	l	
1	415	393	1917
2	258	255	522
3	58	61	399
4	309	336	644

l	kFo	Fc	Sig
8	55	52	675
9	98	98	673
-1,	4,	l	
1	4	8	2426*
2	273	287	706
3	196	203	767
4	228	232	798
5	150	157	890
6	188	194	890
7	36	36	859
8	60	68	659
-1,	5,	l	
1	126	122	859
2	178	180	859
3	74	71	536
4	46	38	659
5	106	102	778
6	21	29	1318
7	94	97	675
-1,	6,	l	
1	7	7	1693*
2	181	182	935
3	60	58	628
4	189	189	982
5	94	90	642
6	42	38	857
-1,	7,	l	
1	111	106	778
2	168	167	1074
3	28	25	1223
0,	0,	l	
2	719	701	1565
4	324	319	583
6	140	135	767
8	179	173	935
0,	1,	l	
1	521	513	1177
2	463	424	1403
3	708	681	1653

l	kFo	Fc	Sig
6	334	350	634
7	63	58	396
8	217	203	673
9	13	17	4907*
0,	3,	l	
1	478	474	1627
2	357	381	501
3	538	520	1801
4	274	299	576
5	284	285	626
6	177	183	607
7	115	124	567
8	8	28	1297
9	153	154	618
0,	4,	l	
0	377	399	706
1	585	562	2179
2	277	296	601
3	120	132	552
4	15	12	1465
5	62	61	391
6	105	96	517
7	8	3	1693*
8	125	129	651
0,	5,	l	
1	6	0	2585*
2	255	259	676
3	231	236	701
4	195	196	735
5	142	149	653
6	89	94	434
7	6	5	1516*
0,	6,	l	
0	146	159	951
1	207	211	651
2	62	62	423
3	88	85	444
4	51	50	504
5	23	20	974

l	kFo	Fc	Sig
2	637	617	1902
3	40	47	407
4	63	50	444
5	320	347	706
6	85	93	567
7	374	380	859
8	62	71	644
9	145	143	890
	1,	2, 1	
0	164	172	506
1	594	577	1994
2	834	829	2148
3	29	30	581
4	807	770	2608
5	368	389	736
6	291	304	828
7	15	12	1698
8	35	38	950
9	23	21	1473
	1,	3, 1	
0	234	258	614
1	577	558	2362
2	46	56	444
3	177	200	706
4	39	41	644
5	316	319	798
6	150	144	920
7	233	240	951
8	138	139	905
	1,	4, 1	
0	153	160	736
1	248	245	736
2	286	297	736
3	664	615	2945
4	318	330	828
5	156	152	920
6	122	124	828
7	42	42	828
	1,	5, 1	

6	67	68	488
7	110	112	767
8	15	22	1686
9	39	29	857
	-1,	3, l	
1	540	514	2316
2	21	8	709
3	263	278	659
4	21	19	843
5	91	92	655
6	19	14	1167
7	235	231	890

5	573	530	1828
6	122	115	569
7	130	123	629
8	24	19	808
9	34	45	656
	0,	2, l	
0	351	335	1841
1	290	318	401
2	785	789	1678
3	326	336	476
4	66	70	325
5	141	140	542

1	23	23	960
2	90	97	438
3	96	88	475
	1,	0, l	
0	30	12	304
2	930	953	2516
4	722	721	3384
6	277	279	1085
8	47	62	1041
	1,	1, l	
0	389	366	1442
1	994	1033	1626

```
1   108   117   751
2   102    98   717
3    26    28  1027
4     6     8  3290*
5    52    50   675
6   150   152   938
     1,   6, 1
0    43    37   736
1   179   181   951
2   120   117   828
3   182   188   997
4    95    95   675
```

:R COMPLEX

Columns are 10Fo 10Fc 10000Sig, * for Insignificant

l	kFo	Fc	Sig	l	kFo	Fc	Sig	l	kFo	Fc	Sig
	1,	6,	1								
5	208	203	1058	0	45	49	614	1	89	77	644
	1,	7,	1	1	156	156	859	2	117	124	791
0	132	138	890	2	191	182	890	3	117	112	767
1	71	66	644	3	231	232	905	4	223	218	905
2	188	180	1074	4	158	157	966	5	4	11	1961*
	2,	0,	1	5	80	83	567	6	17	10	1957
0	1054	1118	2256	6	81	86	614		3,	5,	1
2	539	510	2907		2,	6,	1	0	175	155	890
4	58	59	564	0	135	144	813	1	96	102	673
6	641	591	4382	1	70	64	567	2	89	83	614
8	207	219	1388	2	25	26	1134	3	25	32	1130
	2,	1,	1	3	75	67	583	4	41	41	813
0	250	252	460	4	22	20	1950	5	68	66	644
1	200	218	506		2,	7,	1		3,	6,	1
2	24	25	581	0	12	13	6335*	0	138	127	828
3	544	529	2377	1	35	31	980	1	26	22	1126
4	51	55	475		3,	0,	1	2	146	143	938
5	320	339	767	0	118	125	781	3	108	102	778
6	28	31	976	2	94	98	781		4,	0,	1
7	21	15	1349	4	170	180	1085	0	351	364	824
8	147	150	859	6	82	75	781	2	62	86	607
	2,	2,	1	8	149	152	1258	4	29	23	1128
0	135	152	552		3,	1,	1	6	266	259	1302
1	36	30	430	0	256	271	552		4,	1,	1
2	474	450	2347	1	251	278	583	0	112	111	659
3	55	67	399	2	17	16	843	1	383	413	644
4	335	355	736	3	9	9	5061*	2	100	97	644
5	109	114	736	4	112	127	675	3	271	293	736
6	335	334	859	5	189	201	828	4	45	53	598
7	142	147	907	6	78	84	536	5	274	266	874
8	229	225	1027	7	275	274	951	6	9	5	5458*
	2,	3,	1	8	32	40	1103	7	62	63	675
0	115	110	675		3,	2,	1		4,	2,	1
1	307	322	644	0	212	211	614	0	789	760	2516
2	270	286	675	1	4	7	2852*	1	256	272	706
3	405	407	736	2	331	339	675	2	292	305	736
4	270	285	782	3	22	18	896	3	90	111	644
5	328	333	828	4	311	310	767	4	21	22	1167
				5	156	165	874	5	19	23	1381

l	kFo	Fc	Sig
2	107	114	747
3	43	35	706
4	35	25	857
5	33	33	966
	4,	5, 1	
0	26	31	1025
1	174	175	935
2	41	30	767
3	121	121	874
4	58	58	690
	4,	6, 1	
0	102	100	734
1	120	110	840
2	83	79	598
	5,	0, 1	
0	305	314	955
2	469	483	1041
4	307	322	1215
6	181	172	1475
	5,	1, 1	
0	349	364	675
1	323	349	706
2	130	133	828
3	7	13	4284*
4	11	4	6084*
5	100	84	675
6	56	43	704
	5,	2, 1	
0	15	23	1313
1	79	72	536
2	345	357	798
3	189	192	874
4	230	224	920
5	58	50	659
6	98	91	659
	5,	3, 1	
0	225	236	798
1	275	272	798
2	168	174	890

7	22	26	1363
8	53	49	796
	2,	4, 1	
0	330	334	720
1	293	298	736
2	185	191	798
3	63	68	522
4	66	66	522
5	83	86	583
6	149	155	1012
7	182	184	1074
	2,	5, 1	

7	97	93	675
	3,	3, 1	
0	58	65	413
1	432	446	690
2	142	155	767
3	102	97	720
4	96	100	675
5	192	182	920
6	76	75	567
7	128	134	905
	3,	4, 1	
0	68	73	475

7	82	75	
	4,	3, 1	
0	55	53	
1	10	5	
2	169	168	
3	300	293	
4	88	71	
5	101	94	
6	77	71	
	4,	4, 1	
0	251	263	
1	215	205	

614	4	32	30	976
	5	120	122	840
475		5,	4, 1	
1418	0	94	103	706
828	1	232	237	890
828	2	156	154	951
624	3	45	39	751
717	4	154	150	945
583		5,	5, 1	
	0	108	100	791
798	1	83	88	567
828	2	43	44	813

CR COMPLEX

Columns are 10Fo 10Fc 10000Sig, * for Insignificant

l	kFo	Fc	Sig	l	kFo	Fc	Sig	l	kFo	Fc	Sig
	5, 5, 1				6, 3, 1			2	11	17	1994*
3	117	117	852	0	96	96	673	3	20	19	1407
	5, 6, 1			1	200	203	890	4	11	15	5594*
0	60	52	675	2	145	143	895		7, 2, 1		
1	41	39	888	3	277	276	951	0	18	13	1962
	6, 0, 1			4	13	3	7577*	1	5	21	3261*
0	269	273	1085		6, 4, 1			2	252	251	951
2	141	155	1258	0	178	180	951	3	59	59	675
4	133	137	1171	1	119	112	778	4	150	138	905
	6, 1, 1			2	47	50	767		7, 3, 1		
0	72	67	522	3	40	40	902	0	219	221	935
1	243	249	798		6, 5, 1			1	200	199	982
2	85	82	611	0	83	77	598	2	133	131	890
3	262	265	890	1	71	58	614	3	46	38	843
4	51	50	690	2	103	97	717		7, 4, 1		
5	170	156	1043		7, 0, 1			0	149	146	938
	6, 2, 1			0	59	53	781	1	102	103	704
0	416	430	798	2	270	267	1302	2	156	141	980
1	225	239	843	4	214	219	1475		7, 5, 1		
2	85	77	614		7, 1, 1			0	160	147	969
3	28	35	1055	0	97	93	675		8, 0, 1		
4	70	65	614	1	288	287	890	0	238	232	1302
5	11	6	6291*								

l	kFo	Fc	Sig
2	100	107	998
	8,	1, 1	
0	63	67	583
1	153	156	1012
2	57	55	675
3	240	234	1043
	8,	2, 1	
0	229	228	951
1	90	90	659
2	87	79	611
	8,	3, 1	
0	40	42	920
1	241	231	1027
	8,	4, 1	
0	175	167	1089
	9,	0, 1	
0	163	163	1475
	9,	1, 1	
0	25	24	1195
1	81	67	598
	9,	2, 1	
0	66	71	644